Essays in Demographic Economics: Three Perspectives on Population Decline

Dissertation zur Erlangung des Grades eines Doktors der Wirtschaftswissenschaft

eingereicht an der

Fakultät für Wirtschaftswissenschaften der Universität Regensburg

vorgelegt von Timon Manuel Hellwagner

Berichterstatter:

Prof. Dr. Enzo Weber, Universität Regensburg
Prof. Dr. Fabian Kindermann, Universität Regensburg

Tag der Disputation: 28. September 2026

Acknowledgments

Completing this dissertation would not have been possible without the support of many people.

First, I would like to thank Prof. Enzo Weber, not only for providing me with the opportunity to work on my dissertation under his supervision, but also for his continuous support during the demanding switch from a background in Geography to this dissertation in Economics. I would also like to thank Prof. Fabian Kindermann for his co-supervision, for his support, and for his insightful comments and suggestions.

Second, I would like to thank my colleagues in the MAKRO department at the Institute for Employment Research, especially Johann Fuchs, Tobias Hartl, Christian Schneemann, Doris Söhnlein, Susanne Wanger, Yasemin Yilmaz, and Johanna Zenk, for their support and valuable insights, for fruitful discussions, and for all the knowledge I have gained over the past couple of years. Similarly, I would also like to thank Philipp Deschermeier and Patrizio Vanella for providing me with the opportunity to gain valuable academic experience through joint projects early on in my doctoral studies.

Third, I am grateful for the financial support I received from the GradAB scholarship.

Finally, I would like to thank my family, especially my wife, Natascha, for her unconditional support during this challenging time. This dissertation would not have been possible without her.

Contents

Acknowledgments **iii**

Contents **v**

List of figures **ix**

List of tables **xiii**

1 Introduction **1**

1.1 Motivation 2

1.2 Contribution 9

1.2.1 Effects of Population Decline: A Historical Perspective on Labor Market Adjustments 9

1.2.2 Mitigation Potentials: A View on the Hidden Labor Force 10

1.2.3 Demographic Changes: A Stochastic Forecasting Model for Regional Migration 11

2 Labor Market Adjustments to Population Decline: A Historical Macroeconomic Perspective, 1875–2019 **13**

2.1 Introduction 13

2.2 Theoretical Perspectives: Reference Points 16

2.2.1 Population Decline and Economic Growth 16

2.2.2 Population Decline and Margins of Labor Supply and Demand . . 18

2.3 Population Decline and the Labor Market: Some Descriptive Statistics from a New Historical Dataset 20

2.3.1 Population Decline: Occurrence and Characteristics 20

2.3.2 Historical Labor Market Dataset: A Short Overview 22

2.3.3 The Labor Market in Times of Decline: Descriptive Evidence . . . 23

2.3.4 Towards an Empirical Framework 25

2.4 Econometric Strategy 25

2.4.1 Capturing Nonlinear Effects: Panel Smooth Transition VAR 26

2.4.2 Demographic Regimes: Transition Variable and Smoothing Parameters . . . 27
2.4.3 Identification of Structural Shocks by External Instruments . . . 29
2.4.4 Introducing a Suitable Instrument: Lagged Births . . . 30
2.4.5 Impulse Response Functions and Bootstrapping . . . 34
2.5 Results . . . 34
2.5.1 Regime-Dependent Effects of Structural Population Shocks . . . 34
2.5.2 Robustness . . . 44
2.6 Conclusion . . . 47
2.A Appendix A: Excluded Observations . . . 49
2.B Appendix B: Additional Impulse Response Functions . . . 50
2.C Appendix C: Identification . . . 52
2.D Appendix D: Robustness . . . 54
2.E Appendix E: Data Sources and Data Preparation . . . 62
2.E.1 Demographic Variables . . . 62
2.E.2 Labor Supply Variables . . . 66
2.E.3 Other Economic Variables . . . 74

3 Activation Potentials in Population Decline: Estimating Hidden Labor Force Rates by Dimensionality Reduction 79
3.1 Introduction . . . 79
3.2 Background . . . 82
3.3 Data . . . 85
3.4 Methods . . . 87
3.4.1 Data Preparation and Model . . . 87
3.4.2 PCA: Factors, Loadings, Interpretation . . . 89
3.4.3 Full-Employment Conditions & Hidden Labor Force Rates . . . 91
3.4.4 Baseline Calibration: Following the HLF Literature for Germany . 93
3.4.5 Sensitivity Calibration: Following Michaillat & Saez (2021, 2024b) 94
3.4.6 The Multiplier Effect of Full Employment: Quantification of Mitigation Potentials until 2035 . . . 95
3.5 Results . . . 97
3.5.1 Size and Structure of the HLF over Time . . . 97
3.5.2 Comparison to Existing Estimates . . . 99
3.5.3 Sensitivity Analysis . . . 102
3.5.4 Extension: Estimated HLFRs Among Those Aged 65–74 Years . . 103

3.5.5 Mitigating the Effects of Population Decline: Hidden Labor Force Activation until 2035 . . . 105
3.5.6 Limitations . . . 107
3.6 Conclusion . . . 108
3.A Appendix A: Additional Information on Data Sources, Data Preparation, and a Comparison to the LFS . . . 110
3.A.1 Labor Force Participation Rates, 1990–1996: Preparation Details . 110
3.A.2 Labor Force Participation Rates, 2011–2024: Sources & Preparation Details . . . 110
3.A.3 Visualization and Comparison to the LFS . . . 113
3.B Appendix B: Additional Results . . . 115
3.B.1 Supporting Figures for Main Text . . . 115
3.B.2 Alternative Calibration Procedure: Treating Remaining PCs as Zero 119

4 Parsimonious Stochastic Forecasting of International and Internal Migration on the NUTS-3 Level: An Outlook of Regional Depopulation Trends in Germany 121
4.1 Introduction . . . 121
4.2 (Regional) Migration Projections: An Illustrative Overview . . . 123
4.2.1 Flows, Rates and the Degree of Detail: Target Variables . . . 124
4.2.2 Consistency in Forecasts of Internal and International Migration . 125
4.2.3 Modeling Migration Processes and Determinants . . . 126
4.2.4 Incorporating Risk and Uncertainty . . . 128
4.2.5 Migration Forecasts for German Regions . . . 130
4.3 Data and Methods . . . 131
4.3.1 Data: Sources and Preparation . . . 133
4.3.2 Forecast Model . . . 134
4.4 Stochastic Forecast of Regional Migration Flows until 2040 . . . 139
4.5 Results . . . 143
4.5.1 Future Migration Flows among German Regions . . . 143
4.5.2 Migration Flows along the Urban-Rural Continuum . . . 146
4.5.3 Migration Flows Relative to District Population Size . . . 148
4.5.4 Probabilities of Migration-Induced Regional Depopulation . . . 148
4.6 Discussion and Conclusion . . . 151
4.A Appendix A: Model Selection . . . 155
4.A.1 Model 1: Gross Migration Flows, Naïve Model . . . 155

4.A.2 Models 2A and 2B: Gross Migration Flows, Observed Mean and Median Values . . . 155
4.A.3 Model 3: Net Migration Flows, Principal Component Analysis . . . 156
4.A.4 Model 4: Log-Gross Migration Flows, Principal Component Analysis 157
4.A.5 Model 5: Gross Migration Rates, Naïve Model . . . 158
4.A.6 Models 6A and 6B: Gross Migration Rates, Observed Mean and Median Values . . . 160
4.A.7 Model 7: Net Migration Rates, Principal Component Analysis . . . 160
4.A.8 Model 8: Log-Gross Migration Rates, Principal Component Analysis 162
4.A.9 Comparison of the Forecast Performance of the Candidate Models 162
4.B Appendix B: Inclusion of Territorial Reforms and Lack of Data in Germany since 1995 in the Model . . . 166
4.B.1 Approaches to Boundary Change Incorporation . . . 168
4.C Appendix C: Estimation of Age- and Sex-Specific Migration before 2002 . 168

5 Conclusion **171**

Bibliography **175**

List of Figures

1.1 Population by Age Groups among Selected Advanced Economies, 1800–2100 . . . 3
1.2 Labor Force Scenarios for Germany, 2012–2040 . . . 6
1.3 Cumulative Net Migration Rates across German Regions, 2013–2023 . . . 8

2.1 Distribution of Annual Working-Age Population Change Rates, Times of Growth and Decline . . . 21
2.2 Distribution of Annual Change Rates of the Variables in the Historical Dataset . . . 23
2.3 Stylized Evidence of Labor Market Dynamics Before and During Population Decline Periods . . . 24
2.4 Decline Probabilities Across the Countries in the Sample . . . 28
2.5 Positive Population Shock in Times of Growth: Impulse Response Functions . . . 35
2.6 Negative Population Shock in Times of Decline: Impulse Response Functions . . . 36
2.7 Positive Population Shock in Times of Growth: Additional Impulse Response Functions . . . 37
2.8 Negative Population Shock in Times of Decline: Additional Impulse Response Functions . . . 39
2A.1 Robustness Check: Shock Identification, Growth Regime . . . 52
2A.2 Robustness Check: Shock Identification, Decline Regime . . . 53
2A.3 Robustness Check: Sample Split, Linear . . . 54
2A.4 Robustness Check: Country Trends, Growth Regime . . . 55
2A.5 Robustness Check: Country Trends, Decline Regime . . . 55
2A.6 Robustness Check: World GDP, Growth Regime . . . 56
2A.7 Robustness Check: World GDP, Decline Regime . . . 56
2A.8 Robustness Check: World Population, Growth Regime . . . 57
2A.9 Robustness Check: World Population, Decline Regime . . . 57
2A.10 Robustness Check: Switching Point, Growth Regime . . . 58

2A.11 Robustness Check: Switching Point, Decline Regime 58
2A.12 Robustness Check: Smoothing Parameter, Growth Regime 59
2A.13 Robustness Check: Smoothing Parameter, Decline Regime 59
2A.14 Robustness Check: Age Structure, Growth Regime 60
2A.15 Robustness Check: Age Structure, Decline Regime 60
2A.16 Robustness Check: Depreciation Rates 61

3.1 Scores, Loadings, and Correlations of the First Principal Component . 90
3.2 Observed and Full-Employment Levels of the Unemployment Rate, 1991–2024 95
3.3 Total and Estimated Hidden Labor Force, 1991–2024 98
3.4 Total and Estimated Hidden Labor Force Rates by Sex and Age Group, 2024 98
3.5 Total and Estimated Hidden Labor Force Rates by Broad Age Groups, 1991–2024 99
3.6 Comparison of Total Hidden Labor Force and Total Hidden Labor Force Rates Across Sources 100
3.7 Estimated Hidden Labor Force, Baseline and Sensitivity Calibration, 1991–2024 103
3.8 Estimated Hidden Labor Force Rates by Sex and Age Group, Extended Model, 2024 104
3.9 Total Hidden Labor Force, Baseline and Extended Models, 1991–2024 . 104
3.10 Labor Market Flows and the Unemployment Rate in the Adjustment Scenario, 2024–2035 106
3A.1 Labor Force Participation Rates by Sex and Age Group, This Paper and LFS, 2024 114
3A.2 Explained Variance by Principal Component 115
3A.3 Principal Components 1–6, Scores, Loadings, and Correlations to External Indicators 116
3A.4 Population by Sex and Age, 2024 and 2035 117
3A.5 Total Hidden Labor Force Rates, Baseline Model and Fuchs & Weber (2021), 2005 117
3A.6 Estimated Hidden Labor Force, Lower and Higher Full-Employment Levels of the Unemployment Rate, 1991–2024 118
3A.7 Aggregate Participation Rates, 1991–2035 118
3A.8 Estimated Hidden Labor Force, Baseline and Alternative Calibration Procedures, 1991–2024 120

4.1 Loadings of the First Principal Component for Log-Inflows by Males . . 135
4.2 Loadings of the First Principal Component for Log-Inflows by Females 136
4.3 Loadings of the First Principal Component for Log-Outflows by Males . 137
4.4 Loadings of the First Principal Component for Log-Outflows by Females 138
4.5 Time Series of Principal Component 1 (Sign-Reversed) with Forecast . 140
4.6 Median Cumulative Net Migration in 2020–2040 by NUTS-3 Region and Age Group 144
4.7 Median Cumulative Net Migration in 2020–2040 by NUTS-3 Region and Age Group Divided by the Corresponding Population on December 31, 2019 149
4.8 Probability of Migration-Induced Depopulation Between 2019 and 2040 by District and Age Group 150
4A.1 Time Series (Sign-Reversed) of Principal Component 1 of Net Migration Model with Forecast 157
4A.2 Time Series (Sign-Reversed) of Principal Component 1 of the Log-Migration Model with Forecast 159
4A.3 Time Series (Sign-Reversed) of Principal Component 1 of the Log-Migration Rate Model with Forecast 161
4A.4 Time Series of Principal Component 1 of Male Shares in District Migration with Backcast 169
4A.5 Time Series of Principal Component 2 of Male Shares in District Migration with Backcast 170

List of Tables

2.1 Descriptive Statistics on Annual Working-Age Population Change Rates, 1875–2019 21

2A.1 Descriptive Overview of the Excluded Observations in the Identification Procedure 49

4.1 Explained Share of Variance by Principal Component 141

4.2 Median Cumulative Net Migration 2020–2040 by Age Group and Type of Region [in Thousands] 147

4A.1 Model Summaries with Forecast Accuracies 164

4A.2 Inclusion of Territorial Reforms and Lack of Data in Germany since 1995 in the Model 166

Chapter 1

Introduction

The sizes and structures of populations are continuously shifting. Such changes may carry profound economic implications, particularly in the labor market — for instance, because the size and the structure of a population are arguably the most pivotal determinants of the size and the structure of aggregate labor supply. As a prominent example, the secular decline in birth rates across many countries during the second half of the 20th century (Reher, 2015; Sánchez-Barricarte, 2018) and the subsequent commencement of pronounced population aging have drawn substantial attention in public discussions as well as in economic research (among many: Acemoğlu & Restrepo, 2017; Aksoy et al., 2019; Maestas et al., 2023). Recent population projections point to another downstream consequence of these structural changes: Across many countries, population decline is either impending or unfolding, in particular among those of working age (see, e.g., UN, 2024). These outlooks question or reverse stylized facts: As documented by Jones & Romer (2010), both economic and population growth have accelerated over centuries. Now, as the UN (2024) figures suggest, population growth does not only come to an end, but a secular decline in population size, in particular but not exclusively across advanced economies, is at least impending. Against this backdrop, the present thesis addresses population decline from different perspectives, aiming to contribute evidence to a yet rather sparse body of literature.

This introduction serves two purposes: First, it outlines the general motivation for a comprehensive analysis of population decline and its accompanying economic effects. Second, it provides a more granular view of the three chapters of this thesis and, for each of the chapters, summarizes scope, methods, and findings, as well as the contribution to the literature.

1.1 Motivation

Demographic changes have been a frequently discussed topic over decades and centuries, often with an inherent normative dimension (Schmalz, 2025). While in more recent years much of the debate has revolved around topics such as migration flows or population aging, the focus of debates in earlier times often concerned the implications of strong and enduring population growth with its accompanying effects. At least starting with the well-known essay by Malthus (1798), the idea of "overpopulation" has drawn widespread and long-lasting attention, impacting population policies up to the second half of the 20th century (Schmalz, 2025), although these Malthusian ideas did not remain undisputed (Boserup, 1965).

While the concerns about the effects of strong population growth gained momentum around the 1960s, for example, within the United Nations (Schmalz, 2025), a fundamental shift in fertility patterns across advanced economies occurred at the same time — the mid-century *baby booms* in many countries ended (Sánchez-Barricarte, 2018), often rather abruptly as *baby busts*. These swift decreases in total fertility rates have led to enduring below-replacement fertility regimes in most of the advanced economies since then (Reher, 2015).

Yet, as is well documented, a drop in fertility rates does not imply the immediate onset of population decline, due to the population momentum (Keyfitz, 1971; Bongaarts, 2009). Additionally, advanced economies have experienced decades of gains from net migration (Coleman, 2008). Consequently, despite below-replacement fertility rates, most advanced economies have experienced enduring population growth over decades, although this growth has been accompanied by population aging. Nevertheless, the fertility declines of the past cast their shadows, particularly from an economic point of view, as the large baby boom cohorts are now approaching retirement age.

Figure 1.1 illustrates this transformation for the aggregate of selected advanced economies graphically and compares the projected changes to the demographic development since the publication of Malthus's essay: Over most of the past two centuries, the total population has grown significantly. Yet, this development will likely be reversed in the upcoming decades. The UN (2024) projection data (medium variant) suggests that the total population of the advanced economies under consideration will enter a period of enduring stagnation in the near future.

This shift will not affect all age groups and countries to the same degree. By contrast, the projected stagnation period is accompanied by further population aging, with large increases among those aged 65 years or above, on the one hand, and with the working-age

Figure 1.1: Population by Age Groups among Selected Advanced Economies, 1800–2100

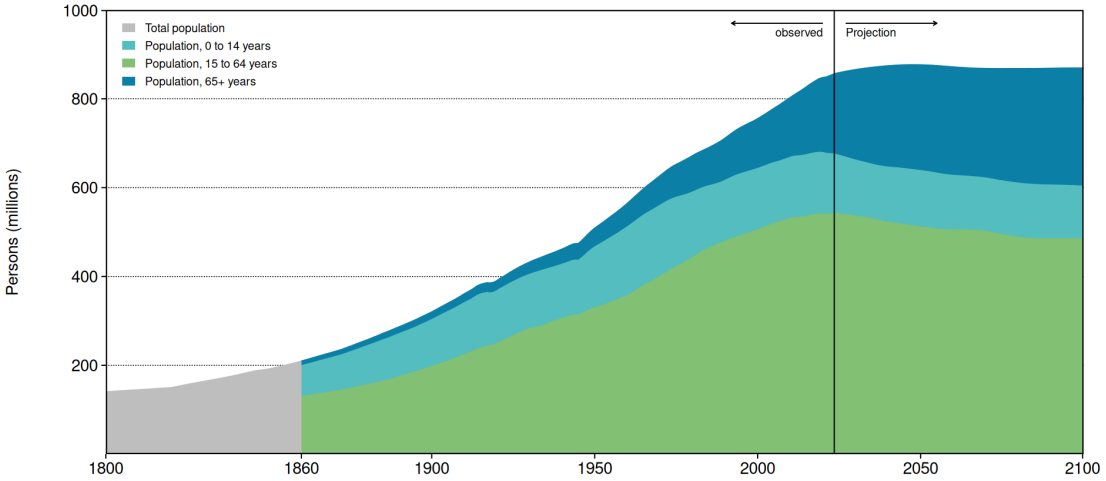

Notes: Data covers 16 countries, see appendix of Chapter 2. Sources: 1800–1820 from Gapminder (2015b); 1820–1860 from Bolt & van Zanden (2020), with linear interpolation of missing observations across countries; 1860–1950: see appendix of Chapter 2; 1950–2100: UN (2024). Observations are chain-linked using overlapping years. Author's own computations and illustration.

population (15–64 years) entering a period of secular decline from 2025 onward, on the other hand. Between 2024 and 2050, the working-age population is projected to decline by about 5.6 percent, which corresponds to a decrease by 30 million persons. Between 2024 and 2100, the projected decline amounts to 10.6 percent (57 million persons).

Across countries, the most well-known case is probably Japan, where the working-age population has entered a regime of decline in the mid-1990s, with a decrease of the population aged 15–64 years by 14.5 million persons (16.5 percent) until 2023. According to the UN (2024) data, other countries such as Italy or Germany have entered a regime of working-age population more recently, but the projected declines in the upcoming decades are strong, implying annual decreases by more than one percent. By contrast, countries such as the United States are projected to enter a regime of working-age population stagnation, rather than decline — however, compared to high growth rates in the past, this is also a significant transformation.

Overall, these projections call for attention, given that in economic models, the population is typically a crucial input factor, and the underlying assumption is typically a constant growth rate. Now, as Figure 1.1 displays, declines in the working-age population are a crucial facet of the impending transformations, and, per definition, it is this share of the total population which constitutes labor supply.

Studies dealing with population decline are few and far between, and have seen a rise only in more recent years. An early approach is Ritschl (1985), who analyzes the Solow model and discusses the stability of the steady state under conditions of population

decline. In a more recent contribution, Sasaki (2019) also investigates the Solow model and demonstrates that, if the elasticity of substitution is less than unity, economic growth under conditions of population decline is given by the rate of technological progress. In ideas-based growth models, findings differ, given that the population size is a crucial driver for economic growth. As outlined by Jones (2022), if output is produced using the stock of knowledge A and people N, so $Y = f(A, N)$, (exogenously given) population decline has unpleasant implications: Eventually, living standards stagnate for a vanishing number of people, thus economic growth comes to an end. Jones (2022) refers to this outcome as the *Empty Planet* result. Suggesting an augmentation of this mechanism by implementing an endogenous fertility decision, Jones (2022) shows that if equilibrium fertility is negative, the economy may transition to the opposite of the Empty Planet, the *Expanding Cosmos*, with enduring economic growth by switching to an optimal allocation soon enough; if not, economic growth ends.

Other recent contributions challenge these findings. For instance, Strulik (2024) presents an overlapping generations model and shows that, if one includes human capital as an input factor for both goods and ideas as well as an education decision by parents, economic growth and the growth of ideas can be maintained even when the population continues to decline. Other approaches, such as Bucci (2023) or Boikos et al. (2023), present similar findings.

These examples demonstrate that there has been a rising number of contributions from a theoretical point of view in recent years. By contrast, empirical evidence on the effects of population decline remains sparse. Lianos et al. (2023) rely on data for mostly Eastern European countries to estimate the effects of population decline on economic growth between 2000 and 2020, and their findings point to a possible co-existence of both — yet, the decline observed in the countries of their dataset differs from the long-term, fertility-driven decline that is discussed in the literature, as it is mainly caused by negative net migration in the wake of the political upheavals in many Eastern European countries in the 1990s (Lianos et al., 2023). Siskova et al. (2023) provide empirical evidence along the lines of theoretical models, indicating that fertility decline is partly compensated by increases in education and health investments. This limited number of contributions which investigate the economic effects of population decline calls for attention.

However, while questions discussed in the growth literature concern the implications of population decline for long-run economic growth, it also creates policy-relevant economic challenges with a more immediate reference period. For example, the decline in the working-age population may induce demographically driven labor shortages (e.g.,

OECD, 2024, 2025). In the case of Germany, projections expect a shortage of more than 0.5 million skilled workers before 2030, strongly driven by the retirement of the large cohorts of the 1960s (Zika et al., 2025). Notably, this does not only apply to the national level; the literature has also pointed to distinct regional differences in future labor supply and demand, and the role of demographic changes therein (for the case of Germany: Schneemann et al., 2025).

Closely related, another example concerns the effects of population aging and decline for social security systems (e.g., Bodnár & Nerlich, 2022). This applies in particular to countries in which population aging and decline are projected to intensify comparatively strongly in the near future; again, this is the case in Germany. As of 2024, Germany was the EU country which had the largest share of persons aged 60–64 years in the working-age population,[1] with a projected increase of the old-age dependency ratio from 0.36 percent in 2024 to 0.5 percent in 2035 (UN, 2024). While this development, due to the prevailing fertility regime, was already underway and foreseeable decades ago (e.g., Börsch-Supan & Schnabel, 1998), the expected increases in old-age dependency have been partially cushioned by positive net migration, in particular during the 2010s (see BiB, 2026a, for migration figures).

For these issues, an apparent starting point is to perpetuate the mitigating effect that also positive net migration implies: increasing the size of the labor force. This is well-known and has already been addressed in earlier contributions that address the sustainability of fiscal policies and social security systems (e.g., Storesletten 2000; for a more recent, policy-oriented perspective: European Commission 2024), aside of further alternatives such as pension reforms — an illustrative overview for the example of the Austrian pension system, including an analysis of the redistributive implications of such reforms, is presented by Sánchez-Romero et al. (2024).

To increase the size of the labor force, the two components of labor supply changes (Fuchs, 2015) can be addressed: changes in demography and changes in behavior. More formally, the change of the labor force L between t and $t+n$ can be written as

$$L_{t+n} - L_t = \sum_{s}^{S} \sum_{a}^{A} \Big(\overbrace{l_{s,a,t} \left(P_{s,a,t+n} - P_{s,a,t} \right)}^{Demography} + \overbrace{P_{s,a,t} \left(l_{s,a,t+n} - l_{s,a,t} \right)}^{Behavior} + \underbrace{\left(l_{s,a,t+n} - l_{s,a,t} \right) \left(P_{s,a,t+n} - P_{s,a,t} \right)}_{Interaction} \Big), \tag{1.1}$$

[1] According to the population figures as of 1 January 2024 (Eurostat, 2026b).

where P is the population and l is the labor force participation rate, both by sex s and age a.

Put differently, in the presence of enduring structural downward pressure due to low fertility in the past, increases in labor force participation as well as gains by net migration, can contribute to maintaining the level of labor supply during upcoming decades. The leverage of both components can be shown by comparing deterministic projections. Figure 1.2 illustrates the future development of labor supply for the example of Germany according to four scenarios for the period 2012–2040. The black solid line displays the observed labor force up to 2024. The blue and turquoise solid lines display the future labor force in scenarios with annual net migration of 400,000 and 200,000 persons, respectively, coupled with rising participation rates. The turquoise and yellow dotted lines display the results of scenarios with annual net migration of 200,000 and 0 persons, respectively, coupled with constant participation rates. The comparison reveals: In the absence of adjustments due to rising participation or net migration, overall labor supply is projected to decline strongly by 13.9 percent until 2040 — while this is an unrealistic scenario, it is the benchmark indicating the downward pressure by demographic change. An annual net migration of 200,000 persons, which is close to the long-term mean in Germany (compare figures from BiB, 2026a), contributes to mitigate parts of this transformation

Figure 1.2: Labor Force Scenarios for Germany, 2012–2040

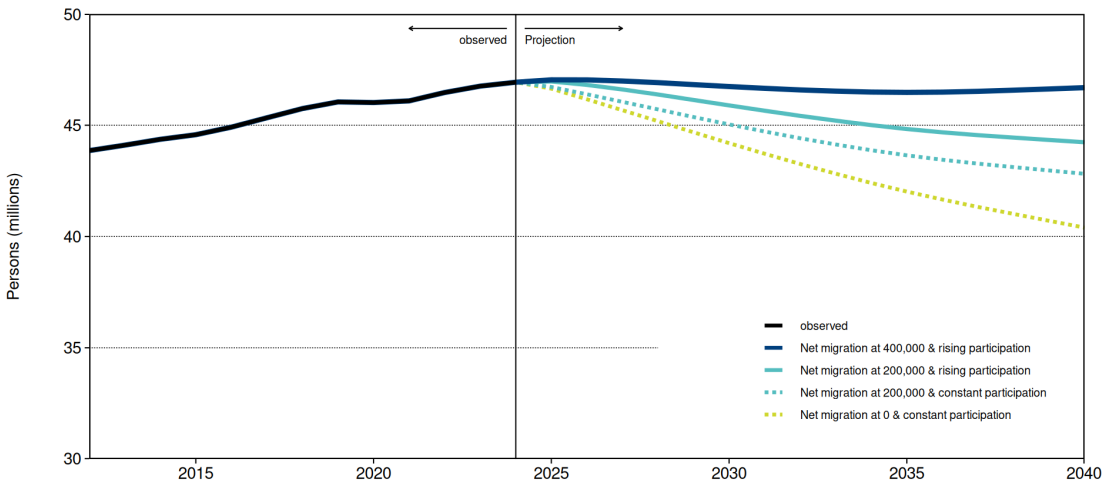

Notes: Net migration calculated by assuming constant emigration at the level of 2024 and correspondingly adjusted immigration figures. Structures of migration flows by sex and age are set to the mean of 2012–2024. Survival rates are assumed to be constant to the last observed values. Sources: Population until 2024 from Destatis (2025h) and sent by Destatis on request. Migration data by sex and age from Destatis (2026d). Mortality data from Destatis (2026b). Participation rates as introduced in the appendix of Chapter 3. Projection of participation rates rely on the recent update of Hellwagner et al. (2023), implementation analogously to the projection exercise presented in Chapter 3. Author's own computations and illustration.

(−8.8 percent in 2040), and even a combination with rising participation still projects a considerable decline (−5.8 percent in 2040). Only the combination of strong net migration, here at 400,000 persons per year, and rising participation offer the possibility to stabilize the size of the aggregate labor force in Germany.

The comparison of the different projections in Figure 1.2 shows that both demographic changes as well as changes in the participation behavior, and their interaction, offer substantial mitigation potentials in view of population decline. Increases at the extensive margin of labor supply are a frequently discussed topic with regards to the implications of demographic changes for social security systems — a prominent and effective example are increases in the retirement age (recent empirical evidence in the case of Germany: Geyer et al. 2020; Riphahn & Schrader 2023; see also Fehr et al. 2012 for a simulation analysis of the labor supply effects of different pension reforms in Germany). Other approaches suggest reforms in the pension system which incentivize labor supply in earlier periods of the working-life cycle (Kindermann & Püschel, 2024). Moreover, another channel at the extensive margin are inflows into and outflows from the labor force due to business cycle changes — in the literature, this is often conceptualized as *discouraged worker effect* (Long, 1953, 1958); if conditions worsen and finding a job becomes more difficult, individuals exit from the labor market. Sometimes, this group of potential additional labor supply is denoted as *hidden labor force*. Indeed, survey results point to substantial activation potentials — for example, results for Germany presented by Destatis (2025a) suggest a hidden labor force of at least 1.3 million persons in 2024. However, reasons for inactivity such as discouragement are not well defined and surveys responses indicate labor supply intentions rather than realized labor market entries — thus, neither the conditions for labor market entries nor a quantification of corresponding activation potentials are straightforward to derive.

In the case of gains from net migration, the literature has already seen various contributions, which model the determinants of country-to-country migration, often using gravity-models (Beine et al., 2016), thereby being able to quantify the inherent uncertainty in forecasting exercises (e.g., Hellwagner et al., 2023). On the regional level, not only international but also internal region-to-region migrations shape the demographic structure. However, the size of net migration, and thus its impact on regional populations, differs strongly across regions, as Figure 1.3 illustrates for the example of NUTS-3 regions in Germany. During the period 2013–2023, some regions have seen substantial increases due to net migration (dark blue areas), for example close to Berlin, whereas other regions in Eastern Germany have seen only minor increases (light blue areas). Nevertheless, contrary to the national level, existing regional population projection approaches

Figure 1.3: Cumulative Net Migration Rates across German Regions, 2013–2023

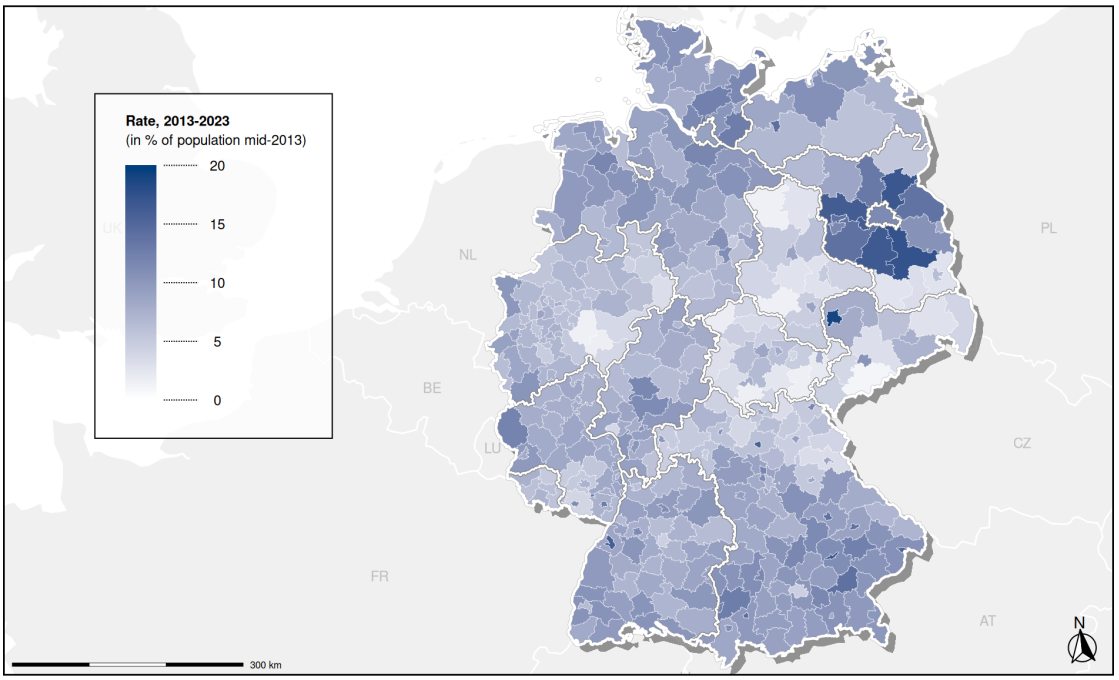

Sources: Migration and population data from BBSR (2026). Shapefiles from BKG (2026) and Eurostat (2026a). Author's own computations and illustration.

often do neither explicitly model migration processes nor the inherent uncertainty but rely on deterministic assumptions (Maretzke et al., 2021), as done in the illustrative example in Figure 1.2. However, an accurate assessment of future demographic changes is of key importance, as outlined, calling for methodological advances in migration forecasting on the regional level.

This section has provided an overview that highlights a number of essential perspectives for a better understanding of the impending population decline and its implications: First, empirical perspectives which expand our knowledge of the economic effects of population decline. Second, perspectives which examine and quantify mitigation potentials to population decline — here, the labor market entry of the hidden labor force offers a suitable starting point. Third, in view of the age structures across many countries, declines in the working-age population appear inevitable — yet, demographic processes remain subject to uncertainty, particularly at the regional level. This calls for suitable modeling approaches to capture this inherent uncertainty in demographic forecasts, in particular for migration dynamics. This thesis seeks to contribute to each of these three perspectives.

1.2 Contribution

1.2.1 Effects of Population Decline: A Historical Perspective on Labor Market Adjustments

The second chapter, *Labor Market Adjustments to Population Decline: A Historical Macroeconomic Perspective, 1875-2019*, is joint work with Enzo Weber (University of Regensburg and Institute for Employment Research). In this paper, we address the first perspective — the economic effects of population decline.

Given the rare occurrence of (working-age) population decline observations across advanced economies in the more recent past, this is a demanding task. We exploit cross-country variation using a newly created historical dataset. This connects well to a series of other recent contributions which rely on country-level panel data variation over more than one century (e.g., Bergeaud et al., 2016; Jordà et al., 2017).

Our dataset covers seven countries (Denmark, Germany, Netherlands, Norway, Sweden, United Kingdom, United States) from 1875 until 2019 and, due to data availability constraints, another nine countries (Australia, Austria, Belgium, Finland, France, Italy, Japan, New Zealand, Switzerland) from 1900 until 2019. It offers information on core demographic and economic variables: population by age groups, real GDP, real wages, real investment, employment, unemployment, labor force participation, and average annual hours worked. Additionally, the dataset covers data on births starting as early as 1815 for some countries as well as information on cohort mortality. We compile the data from two kinds of sources: On the one hand, we rely on existing data collections, such as the International Historical Statistics (Mitchell, 2013), Maddison's Historical Statistics (Bolt & van Zanden, 2020), the Macrohistory Database (Jordà et al., 2017), or the Long-Term Productivity Database (Bergeaud et al., 2016). On the other hand, as those existing collections do not offer coverage for some variables in our dataset and exhibit missing observations for others, we also rely on data from a large number of national sources. As a result, our newly compiled dataset combines information from more than 100 individual sources. We provide a detailed overview of data sources and preparation steps in the appendix of the second chapter.

In our econometric framework, we combine established approaches from the literature. On the one hand, we augment a panel VAR (see Canova & Ciccarelli 2013 for a comprehensive survey, and Aksoy et al. 2019 for a recent application) by a smooth-transition structure (González et al., 2005), which resembles the idea that macroeconomic interdependencies are regime-dependent — in our application, this translates into differences of these interdependencies during periods of population growth versus periods of popula-

tion decline. On the other hand, we identify population growth and decline shocks using external instruments (Stock & Watson, 2018), in our case using lagged fertility data.

The results suggest differences between regimes and novel insights: Population decline passes through to the labor market more quickly compared to population growth. Subsequently, regime-dependent adjustments unfold: Labor force participation increases stronger in response to a population decline shock compared to the decrease following a population growth shock. By contrast, while the unemployment rate increases in response to population growth, we find no significant changes in response to population decline. Moreover, the capital-labor ratio changes in response to population shocks. Thus, while our results also point to negative effects on productivity, as indicated by recent contributions, the findings of our paper suggest that negative effects for economic growth are mitigated by increases in labor force participation and the capital-labor ratio.

The contribution of this paper is twofold. On the one hand, we address the substantial undercoverage of the economic implications of population decline. We do so by providing estimates for the labor market effects of exogenous population growth and population decline shocks using historical data. The latter, on the other hand, constitutes a (partially) novel compilation of demographic and economic data for 16 advanced economies, expanding the database also for future approaches. We document the underlying sources in the appendix of the second chapter in detail.

1.2.2 Mitigation Potentials: A View on the Hidden Labor Force

The third chapter, *Activation Potentials in Population Decline: Estimating Hidden Labor Force Rates by Dimensionality Reduction*, is joint work with Enzo Weber. In this paper, we examine the activation potentials among the hidden labor force for mitigating the effects of population decline.

Thus, in the paper, we address the second perspective, and in doing so, we introduce a framework to estimate hidden labor force rates, and apply our approach to German data for the period 1990–2024. Initially, we identify a latent labor market tightness factor from a matrix of employment and unemployment rates by sex and age. Then, we simulate counterfactual states of full-employment using an endogenous calibration exercise and derive hidden labor force rates.

The results suggest considerable potentials for additional labor supply: In 2024, the hidden labor force in Germany was 1.13 million (among those aged 15–64 years) to 1.47 million persons (among those aged 15–74 years), and its activation would have increased the labor force by 2.4 to 3.1 percent. Thereby, hidden labor force rates are larger among younger persons, as well as among persons close to retirement, but lower in prime age.

We link our results to recent discussions on efficient full-employment conditions and find that these activation potentials are not only feasible, but also efficient. Defining the underlying mechanism as the multiplier effect of unemployment reduction for employment following from the additional activation of the hidden labor force. Eventually, we combine our framework with a population projection until 2035 (based upon a recent update of Hellwagner et al., 2023) and obtain encouraging results from a policy perspective: By activating the hidden labor force, employment decline in Germany could be offset until 2032.

This paper contributes to the literature by offering a parsimonious modeling framework for the hidden labor force, accounting for the interaction of the demographic structure and labor force participation rates, which can easily be linked to other use cases and population projections. Moreover, as a minor contribution, we introduce a data preparation procedure for labor force participation rates by sex and age, which account for the growing divergence of the German Labor Force Survey and the employment estimates within the German national accounts (Körner & Marder-Puch, 2015; Destatis, 2025b), offering a promising database for future approaches. We document the preparation in the appendix of the third chapter.

1.2.3 Demographic Changes: A Stochastic Forecasting Model for Regional Migration

The fourth chapter, *Parsimonious Stochastic Forecasting of International and Internal Migration on the NUTS-3 Level: An Outlook of Regional Depopulation Trends in Germany*, is joint work with Patrizio Vanella (aQua Institute and University of Rostock) and Philipp Deschermeier (German Economic Institute), and has been published in the *Vienna Yearbook of Population Research*, volume 21, pages 361–415 (DOI: 10.1553/p-5pn2-fmn8). In this paper, we address the third perspective, specifically, the paramount role of migration dynamics on the regional level.

Using migration data for German regions by sex and age groups for the period 1995–2019, we evaluate the predictive performance of various model specifications in pseudo-out-of-sample forecasts, use the best-performing model, and draw on a Monte Carlo simulation to present a stochastic forecast of sex- and age-specific regional migration flows across German regions until 2040. Additionally, we quantify the probability of migration-induced regional population decline.

The results suggest that well-known age-specific migration patterns along the urban-rural continuum, such as education-driven migration by younger persons, are likely to

persist. Consequently, it is also this age group where the probability of migration-induced population decline is high for many regions in Germany.

This paper contributes to the literature by developing a stochastic forecasting framework for regional migration flows and quantifying regional differences in migration-induced population decline probabilities. Moreover, in the Online Supplement (available from 10.1553/p-5pn2-fmn8), we provide the data used in our paper, including a backcast for migration flows before 2002, for usage in future approaches.

Chapter 2

Labor Market Adjustments to Population Decline

A Historical Macroeconomic Perspective, 1875–2019

2.1 Introduction

A hitherto stylized fact, the perpetual growth of the population, is questioned in the short to the medium and the long term by a range of demographic forecasts across countries (e.g., UN, 2019). In the years and decades to come, depending on the scenario under consideration, advanced economies will face a stagnation and, sooner or later, a secular decline of their populations. The decline is expected to be more pronounced among those of working age, which is particularly relevant from an economic perspective.[1]

Given the issue's contemporary and future relevance across countries as well as the importance of demography for economic growth in general and the labor market in particular, questions about the economic implications of population decline emerge. Ultimately, the expected developments may challenge other supposedly stylized facts as well, such as the ever-accelerating growth of GDP (per capita) (Jones & Romer, 2010) or the constant labor share in national income (Kaldor, 1961).

However, despite its occurrence or imminence in most advanced economies, there is substantial undercoverage among theoretical and empirical research on the economic implications of population decline, in general as well as with regard to the labor market. In formal economic modeling, most approaches assume a growing, or at least stagnant,

[1] As we focus on working-age population (15–64 years) from here onward, we use the terms working-age population and population interchangeably.

population (Jones, 2022). On the contrary, population decline and the accompanying implications have hardly been discussed as yet. In the existing literature, there have been some attempts to investigate the effects of demographic changes in Ramsey-type models (Brida & Accinelli, 2007; Kajanovičová et al., 2020), Solow-type models (Sasaki, 2019), or endogenous and semi-endogenous growth models (Christiaans, 2011; Jones, 2022; Sasaki & Hoshida, 2017). Among empirical studies, the undercoverage is even more distinct and may be explained by the fact that there have been comparatively few periods of population decline across advanced economies in the recent past, hampering the reliable identification of its effects. Consequently, existing macroeconomic research on the demography-economy nexus focuses on a variety of different issues: a multitude of empirical studies analyze the effects of population growth (see Headey & Hodge 2009 for a comprehensive meta-study) on economic growth, while others investigate the consequences of population aging (e.g., Acemoğlu & Restrepo, 2017, 2022; Börsch-Supan, 2008) or changing mortality, fertility, and human capital patterns (for many: Barro, 1991, 1998; Barro & Lee, 1994; Bloom & Williamson, 1998; Hall & Jones, 1999; Galor & Mountford, 2008). From a more conceptual perspective, both the secular stagnation debate (Eggertsson et al., 2019) and the unified growth theory (Cervellati et al., 2017), among others, have addressed the role of demography for long-term economic development. But as in theory, population decline has not yet drawn widespread attention in the empirical literature.

Importantly, sparse contributions, such as the one more recently by Jones (2022), suggest that the economic effects of growth and decline in the population do not need to follow symmetrical paths. Yet, whether this applies to labor market issues as well — such as the behavior of wages, the capital utilization of firms, or the elasticity of labor supply when the population is declining — has hardly been addressed so far, neither in theory nor in empirics. To provide an empirically substantiated starting and orientation point for both policy and future research, such as the incorporation of labor market adjustments to population decline in formal modeling, we examine the effects of population decline on the labor market from a historical macroeconomic perspective.

Operationalizing our analysis consists of three key components. First, the occurrence of periods of actual population decline and the availability of labor market data do not necessarily coincide. As noted above, for most advanced economies, population shrinkage appears to be a rather new phenomenon. However, if we take a more historical perspective, even back to the second half of the 19th century, we are able to identify several periods of decline and low population growth, distributed across countries. On the one hand, this suggests to empirically investigate population decline and its macroeconomic

implications in a historical cross-country framework. On the other hand, economic data availability proves to be sparse in the very long run. To this end, we compiled a new historical dataset from a large number national and international sources. We collected information on population, births, mortality, real GDP, real wages, real investment, employment, unemployment, labor force participation, and hours worked for 16 countries from more than 100 sources, providing an annual coverage for seven countries from 1875–2019 and for nine from 1900. Second, the estimation must adequately address possible nonlinear interdependencies of macroeconomic variables conditional on the prevailing demographic regime. To account for this, we specify a panel smooth-transition VAR, thereby contributing to growing bodies of literature that rely on, first, cross-country settings (e.g., Aksoy et al., 2019), and second, regime-dependent methods (e.g., Auerbach & Gorodnichenko, 2012) in analyzing dynamic interdependencies of macroeconomic aggregates. Third, tracing possibly nonlinear responses to population decline requires an appropriate identification of the structural population shock. By relying on external instruments, or proxy variables, we follow another strand of recent research (e.g., Gertler & Karadi, 2015; Mertens & Ravn, 2013; Stock & Watson, 2018). Drawing on lagged births data as an instrument for working-age population inflows and outflows, we identify the contemporaneous effects of a structural population shock in times of population growth and decline, and trace the corresponding impact of the structural shock using orthogonal impulse response functions.

Our findings indicate differences in the effects of population changes and corresponding adjustments across regimes. In general, population changes pass through to the labor market more quickly in times of decline, translating, inter alia, into a swifter decline in employment and disinvestment compared to times of growth. In the medium to long term, regime-specific adjustment processes unfold. In periods of population decline, labor force participation increases as a response to the initially quick reduction of labor supply, likewise disinvestment tendencies decelerate. By contrast, the effects of population growth unfold lagged but steadily. Notably, we do not find decreases in unemployment or any significant changes of wages as a shortage indicator in times of population decline. Thus, while population decline tends to depress total factor productivity, as also discussed by the literature, our findings indicate that corresponding negative effects for economic growth are mitigated by increases in participation and capital intensity.

The remainder of the paper is structured as follows. In Section 2.2, we provide an illustrative overview of the role of population and labor force size in theoretical models to motivate the empirical investigation in this paper. Subsequently, and complementary to the survey on theoretical considerations, we provide some descriptive statistics on

population decline in the past, introduce our historical dataset, and offer stylized evidence on trajectories of labor market variables during periods of decline in Section 2.3. Based upon these two parts, Section 2.4 outlines a suitable nonlinear econometric strategy to identify (possibly) asymmetric effects of population changes during times of growth and decline. The corresponding results are presented and discussed in Section 2.5. The last section concludes.

2.2 Theoretical Perspectives: Reference Points

In general, considerations on the economic effects of population decline depart from the fact that even in the simplest production function, $Y = f(K, L)$, the supplied amount of labor L is a crucial input determining economic growth. Yet, the literature analyzing the economic effects of population decline remains limited. A view across different approaches that investigate the population-economy nexus offers some reference points to guide our empirical investigation of the economic effects of population decline.

2.2.1 Population Decline and Economic Growth

In a typical, generic macroeconomic growth model (see standard textbooks, such as Romer 2019), the population consists of a given number of households N with an identical number of household members H_t, growing at a constant rate $g > 0$ over time:

$$H_t = H_0 e^{gt}. \tag{2.1}$$

Here, each member of each household inelastically supplies one unit of labor, thus at each point t in time

$$P_t = NH_t = L_t, \tag{2.2}$$

i.e., the population size equals the size of the labor force, and the growth rate of the population is identical to the growth rate of the labor supply. In the simplest case, firms, using the given labor as well as capital as inputs, being subject to common factor prices and a given level of technology A_t, produce according to the identical production function. Consequently, total output results as $Y_t = f(K_t, A_t L_t)$.

If in this setting, the elasticity of substitution σ is zero, then capital and labor are perfect complements — thus, ceteris paribus, a decrease in labor causes a decrease in output. Yet, those effects may already differ when assuming a production function subject to $\sigma > 0$ (Arrow et al., 1961). Here, depending on the value of σ, a decrease

in labor may be mitigated by capital deepening and, thus, maintaining the output level even in the event of population decline.

The majority of macroeconomic research is still in rather early stages when it comes to analyzing the effects of population decline — only selected approaches deviate from the standard assumption of a constantly growing L_t and analyze the corresponding effects. Some have investigated the effects of population changes in a Malthusian framework. For instance, Voigtländer & Voth (2013) develop a model to show that the population decline in Europe caused by the Black Death explains a substantial part of increases in income per capita. Similarly, Young (2005) analyzes the effect of the AIDS epidemic on per capita consumption in South Africa, finding an increasing effect.

Yet, the imminent population decline across advanced economies is different from epidemic-induced declines, often suggesting transition periods from high growth to low growth, stagnation, and eventually decline (UN, 2019). In this context, authors have investigated the effects of changes in the population growth rate in Ramsey-type growth models, for example when population growth is logistic (Brida & Accinelli, 2007). Sasaki (2019) analyzes the consequences of negative population growth on the long run growth rate of per capita output using a Solow-type growth model. He demonstrates that, if in such a setting the elasticity of substitution is less than unity, economic growth exclusively depends on the rate of technological progress. Christiaans (2011) as well as Sasaki & Hoshida (2017) use semi-endogenous growth models to investigate the effects of population decline on output per capita. The results suggest varying responses of economic growth to negative population growth, inter alia depending on the assumed depreciation rate of capital. Sasaki (2023) uses a Solow growth model with automation capital and shows that the population decline and economic growth can coincide. Notably, the results indicate that the absolute value of population decline may play an important role.

In a more recent contribution, Jones (2022) demonstrates that, in the case of population decline, endogenous and semi-endogenous growth models lead to stagnating living standards and knowledge. The underlying mechanism resembles the established endogenous growth literature (among many: Romer, 1986b, 1990), in which ideas determine economic growth, and depend themselves on the population size (for a discussion, see Dinopoulos & Thompson, 1999). But by taking one step further and endogenizing fertility, Jones (2022) shows that economic growth can only be resumed if the economy switches to an optimal allocation soon enough. Other recent contributions challenge the stagnation scenario. Strulik (2024) augments the model of Jones (2022) by endogenous education components and human capital as an input factor of production. Similarly, Boikos et al. (2023) build an R&D-based growth model with human capital accumulation,

and Bucci (2023) uses an endogenous growth model with human capital accumulation. In these theoretical settings, economic growth and population decline may coexist. Also, Elgin & Tumen (2012) elaborate on findings along this line.

Thus, the questions whether population decline and economic growth can coexist, and whether population decline negatively affects TFP, have not been fully resolved yet. Hypotheses on these issues serve as a first reference point for our empirical investigation. Similarly, the role of capital, as the other factor input, and the question to which extent capital adjustment may unfold in response to population decline, serve as another.

2.2.2 Population Decline and Margins of Labor Supply and Demand

Even though L_t is arguably closely connected to the size of the population P_t, both are not identical. Descriptive empirical evidence shows that neither participation rates are 100 percent nor working hours are evenly distributed across individuals and time (OECD, 2022).

However, in economic research, questions concerning causes and effects of changes in the size and composition of L are often addressed separately, by different parts of the literature and model families, and are not necessarily linked to population decline. The insights delivered by the contributions surveyed above are substantial, but hardly deviate from the assumption of $P_t = L_t$. Yet, if labor supply side dynamics are more complex than the inelasticity assumption in Equation (2.2) suggests, actual labor supply should rather be understood as

$$a_t h_t P_t = L_t, \tag{2.3}$$

where a_t is the labor force participation rate (extensive margin) and h_t are the average hours worked (intensive margin) at time t. Important adjustment mechanisms to demographic changes may unfold through these channels. Existing (micro- and macroeconomic) empirical and theoretical approaches have addressed them in different settings and have also investigated interactions of changing labor supply with the labor demand (firm) side.

It is conceivable that demographic shrinkage could be offset by rising labor supply that comes as a reaction to higher wages. That hinges on labor supply elasticities. The idea is based on an individual's (a household's) utility function, $U = f(c, l)$, encompassing consumption c — which, in the absence of non-labor income, is solely determined by the wage rate and the supplied hours of work — and leisure l. Approaches have analyzed elasticities of hours and participation in different settings, often suggesting positive effects of wage increases. This applies in particular, but not exclusively, on the extensive margin (among many: Ashenfelter et al. 2010; Bargain et al. 2014; Blundell et al. 2013; Chetty

2012; Evers et al. 2008; Keane & Rogerson 2012; for a discussion on the variation in estimates of labor supply elasticities, see Bargain & Peichl 2016).

Logically, a relevant question is in how far population decline triggers wage growth. In view of labor supply decline, one may postulate an increase of wages as a shortage indicator. This assumption can be traced back, for example, to the literature on the wage curve, discussing a linear connection between higher unemployment and lower wages (Blanchflower & Oswald, 1995), with the former usually perceived as a sign of underutilized labor supply. Results from Voigtländer & Voth (2013) and Young (2005) for epidemic population declines also support the role of the shortage channel.

But of course, population decline may affect the economy beyond labor supply, thus triggering further adjustment processes. These can involve the capital and labor demand side, too. The standard law of labor demand suggests that rising wages reduce a firm's labor demand, depending on mediating factors such as substitutability (Hamermesh 1993; for a detailed survey on labor demand elasticities, see Lichter et al. 2015, for example). In a recent contribution, Bossler & Popp (2026) augment the law of labor demand by hiring costs. They demonstrate that not only rising wages but also general labor market tightness reduces the labor demand of firms, rather than increasing it, as searching becomes costlier. These findings suggest that even if a slack labor market reduces wages, a tight labor market does not necessarily cause rising wages. Thus, ex ante, the effects of population decline on labor supply and wages are unclear. The above considerations serve as a third reference point for the empirical analysis.

The brief illustrative overview demonstrates that from the existing body of theoretical literature, the economic effects of changes in the population size are difficult to derive and may depend on the interaction of a series of relevant factors, such as wages or hours worked,[2] and this interaction may itself be state-dependent. This calls for empirical evidence on the causal effects of population shrinkage in order to learn about the potential future path of many economies and to inform further theory development.

[2]Of course, numerous contributions have documented factors impacting both the supply and demand of labor beyond wages as the single determinant — such as the institutional setting and policies, for example in fostering or hampering female labor force participation (among many: Costa 2000; Cipollone et al. 2014; for an exemplary survey, see Abraham & Kearney 2020).

2.3 Population Decline and the Labor Market: Some Descriptive Statistics from a New Historical Dataset

2.3.1 Population Decline: Occurrence and Characteristics

The undercoverage of population decline in (economic) research, as outlined above, is accompanied by similarly sparse descriptive statistics on the nature of population decline in the past; that is, the frequency of its occurrence, magnitude, distribution, and duration. A view on the historical data for annual working-age population change among selected advanced economies from 1875 to 2019 in Table 2.1 provides insights.

First, the vast majority of years during the past one and a half centuries have been years of population growth: 154 of 2096 observations, or 7.3 percent, were decline years. Over the whole period covered, the median annual change of the working-age population was 0.85 percent, with 0.92 in growth years and −0.26 in decline years, and with the strongest increases in overseas migration destinations in the 19th century as well as the strongest decrease during Japan's ongoing decline since the 1990s. For all observations, the interquartile range goes from 0.38 to 1.30 percent, illustrated in Figure 2.1. Among growth observations, our data has an interquartile range from 0.48 to 1.33 percent, and among decline observations from −0.45 to −0.10 percent.

Second, population decline tends to occur consecutively, forming periods of shrinkage rather than single years. In the historical data, we are able to identify 34 periods of consecutive decline,[3] whereby the median length was three years. The median *peak-to-through* (compare Reinhart & Rogoff 2014 on GDP changes in the course of financial crises) magnitude, that is, the median cumulative decline in a shrinkage period, was −0.48 percent.

Third, occurrence differs across countries. Some have never faced working-age population decline in non-war years (Australia, New Zealand, United States), whereas others have repeatedly undergone shrinkage periods, although with differing duration and magnitude. Japan has experienced the most non-war years (25) of working-age population shrinkage, followed by Austria and Italy (22) as well as Germany (21) with some shorter sequences distributed across the whole observation period. Also, the underlying drivers of population decline differ, ranging from overseas emigration in the late 19th century, inter alia due to economic reasons such as wage differentials (Hatton & Williamson, 1998), to below-replacement fertility over decades in more recent time. Later, we use

[3]Notably, for this illustrative purpose, we define a period to be one or more years of consecutive decline. A period starts whenever there is a decline of the population and there has not been a decline in the preceding two years, avoiding to count one period of decline as two due to very low growth in between. We exclude those periods that started during war years.

Table 2.1: Descriptive Statistics on Annual Working-Age Population Change Rates, 1875–2019

	All years						Growth years		Decline years	
	Obs.	Median	Mean	Min	Max	SD	Obs.	Median	Obs.	Median
1875–2019	2096	0.85	0.90	−1.40	10.63	0.77	1942	0.92	154	−0.26
1875–1969	1296	1.05	1.10	−1.10	10.63	0.80	1238	1.08	58	−0.21
1970–2019	800	0.54	0.59	−1.40	3.40	0.60	704	0.62	96	−0.30

Notes: Figures in this table encompass working-age population data from the 16 countries covered by the historical dataset over the period 1874–2019 but exclude observations in war years (1914–1919 and 1939–1946). For information on data sources, see Appendix 2.E. Author's own computations.

an instrument based on lagged births in order to avoid endogeneity stemming from any such contemporaneous shocks.

Notably, there has been more pronounced growth in the years before 1970 compared to those afterwards, vividly demonstrating the secular decline of population growth in the very long run. By contrast, population decline observations have been much more similar over time, whereby 43 of the 96 decline observations after 1970 have occurred since 2010. And notably, the median of the decline observations in the past (−0.26 percent) is remarkably close to the median of projected decline observations in the same countries between 2019 and 2040 according to the UN (2019) projections (−0.23 percent).

Over the decades and across advanced economies, persons aged 15–64 years account for almost the entire workforce (see, e.g., ILO, 1977a,b; OECD, 2022), and these age brackets are widely used to define working age. Importantly, one may argue, against the backdrop of the ongoing population aging across advanced economies, that this definition

Figure 2.1: Distribution of Annual Working-Age Population Change Rates, Times of Growth and Decline

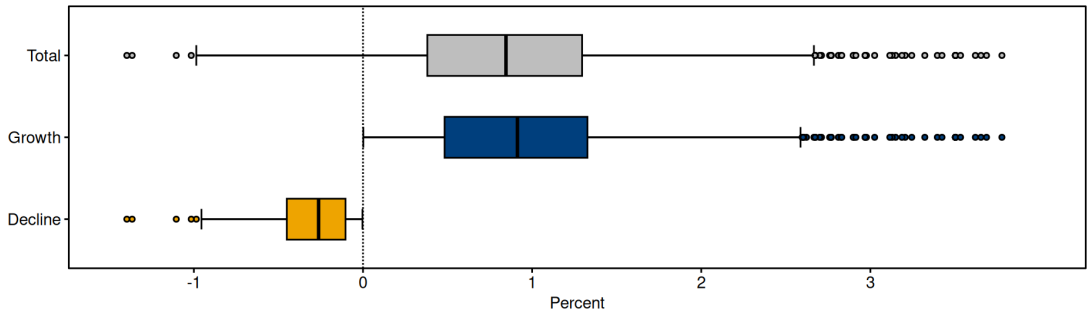

Notes: Observations included correspond to Table 2.1. Whiskers indicate 1.5 IQR. Outliers among the growth observations that are larger than 4 percent are not displayed for illustrative purposes. Boxplots indicate data for annual changes in percent. For information on data sources, see Appendix 2.E. Author's own computations and illustration.

should also encompass persons aged 65–69 years, given rising participation rates. But in the historical setting of out paper, including those aged 65–69 years is not feasible due to limited availability beyond the more recent past, as coverage for one half of our sample starts only in the 1990s or 2000s. Second, despite recent increases, participation rates in this age group are also still low — the median of the 2010s was at 19.2 percent (OECD, 2024). Jointly, these points render a definition of working age as those aged 15–64 years not only necessary but also justified.

2.3.2 Historical Labor Market Dataset: A Short Overview

A substantial share of the empirical literature using macroeconomic aggregates in (dynamic) panel models draws on time series starting in the 1960s, 1970s, or later, in particular in a cross-country perspective, with varying frequencies (e.g., Aksoy et al. 2019; Antonakakis et al. 2017; Canova et al. 2007; Comunale 2022; among others). Additionally, also labor market statistics across countries, most importantly information on unemployment, such as those delivered by the OECD, start around the mid-1960s or later, indicating this period as a somewhat natural starting point for empirical analyses. Yet, as noted above, striving to cover a sufficient set of periods of population decline, we exploit observations as early as 1875.

Such an exploration of historical economic dynamics across countries is a notoriously difficult task, particularly when focused on labor market issues. Well-known data collections such as the International Historical Statistics (Mitchell, 2013) or Maddison's Historical Statistics (Bolt & van Zanden, 2020) and their respective predecessors, among others, have settled the path for comparative historical economic research for decades. However, the availability of annual data in the very long run remained limited to selected variables. We have seen substantial improvements in recent years by compilations such as the Macrohistory Database (Jordà et al., 2017) or the Long-Term Productivity Database (Bergeaud et al., 2016), both starting in the second half of the 19th century, covering a variety of advanced economies, and broadening the range of macroeconomic indicators. But the availability of annual information on variables such as unemployment is still strongly limited.

Based upon this finding, and in order to operationalize an analysis of macroeconomic labor market adjustments to population decline, we compiled a new historical annual labor market dataset, stemming from extensive data acquisition efforts. On the one hand, we draw both on existing macroeconomic and demographic databases, such as those quoted above, the Human Mortality Database (HMD, 2023) or various OECD statistics. On the other hand, and more importantly, we rely on a vast number of

Figure 2.2: Distribution of Annual Change Rates of the Variables in the Historical Dataset

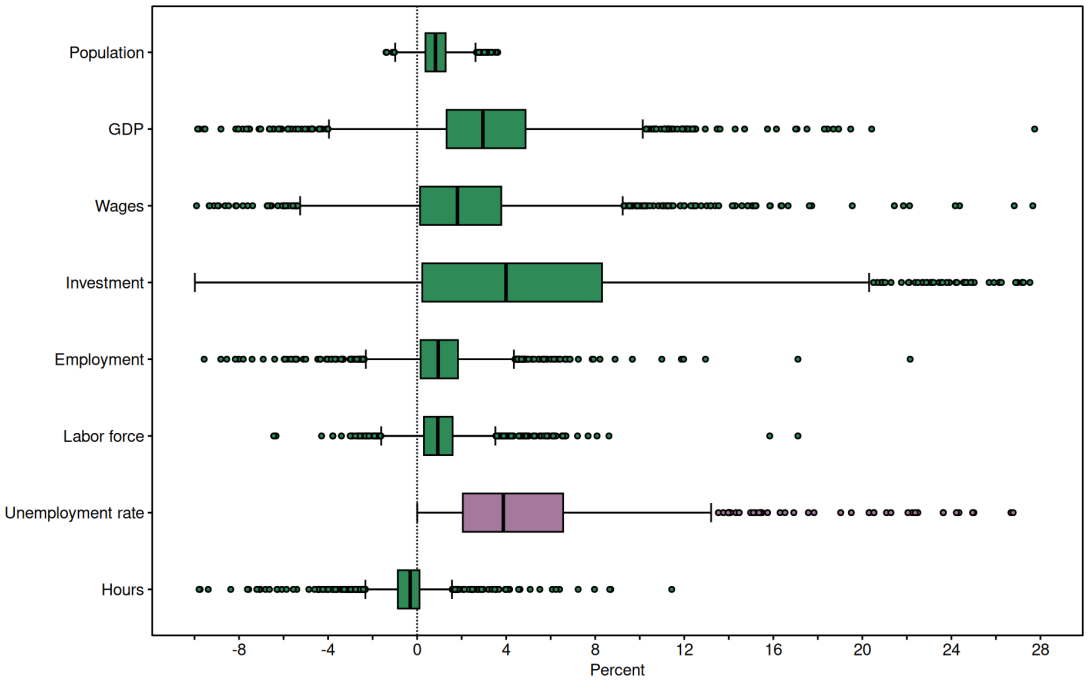

Notes: Observations included correspond to Table 2.1. Whiskers indicate 1.5 IQR. Outliers above 30 percent and below −10 percent have been excluded for presentation. Green colored boxplots indicate data for annual changes in percent, the purple colored boxplot indicates the unemployment rate in percent of the labor force. For information on data sources, see Appendix 2.E. Author's own computations and illustration.

individual (national) data sources and collections. Overall, the compilation combines information from more than 100 different sources.

The historical dataset covers 16 advanced economies, seven of which starting from 1875 (Denmark, Germany, Netherlands, Norway, Sweden, United Kingdom, United States) and nine starting from 1900 (Australia, Austria, Belgium, Finland, France, Italy, Japan, New Zealand, Switzerland) due to limited data availability. The collection contains annual information on demographic and economic variables until 2019, which are population by age groups, births, mortality, real GDP, real wages, real investment, total employment, the unemployment rate, labor force participation, and average annual hours worked. Figure 2.2 provides a broad and descriptive overview of selected variables.

2.3.3 The Labor Market in Times of Decline: Descriptive Evidence

Given that decline usually persists over several years, one may also assume that adjustment processes unfold over a longer time span. In Figure 2.3, the dynamics of working-age population as well as of the labor market variables in advance of and during periods of

Figure 2.3: Stylized Evidence of Labor Market Dynamics Before and During Population Decline Periods

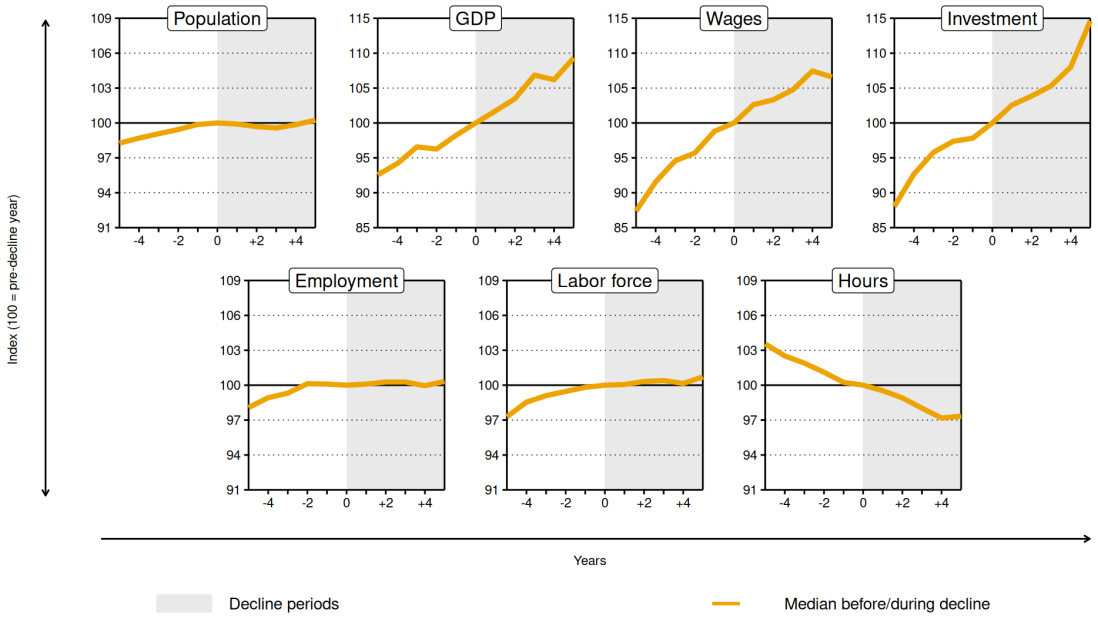

Notes: For information on data sources, see Appendix 2.E. Author's own computations and illustration.

population decline are displayed as solid orange lines,[4] with the levels being indexed to the last year before the decline started. The displayed dynamics are those of annual median values, covering six years prior to the decline period and five years of the decline period itself (gray background).[5]

Notably, population growth rates had already been low prior to the respective decline. This implies the intuitively appealing fact that population decline is generally preceded low growth, respectively, stagnation. In other words, switches between a regime of strong, or at least average, population growth and a shrinkage regime take place generally more slowly than quickly. Moreover, the dynamics of labor market variables exhibit differences. For example, wages and hours worked closely stick to the pre-decline trend, indicating limited effects of population decline. On the other hand, there is low employment and labor force growth prior to the decline mirroring low population growth rates, followed by very similar patterns once decline occurs, suggesting a more pronounced effect for these variables.

Obviously, these findings are stylized, neither causal relations nor dynamic interdependencies of the examined macroeconomic aggregates are appropriately mirrored. Put

[4]Since we include the labor force rather than unemployment in the estimation outlined below, we display the labor force here as well.

[5]Notably, we display the median values of all periods; that is, both those that have ended earlier than five years and those that have ended later than the displayed horizon.

differently, descriptive evidence as shown in Figure 2.3 does not allow the inference of the causal effects of population decline on labor market variables of interest, and it also does not consider how distinct and enduring a particular decline period has been.

2.3.4 Towards an Empirical Framework

The short analysis in this section implies there are four directions that an empirical analysis aiming to carve out possibly nonlinear macroeconomic effects of population decline needs to follow. First, a suitable empirical strategy must identify the causal effect of positive, respectively, negative population changes, distinguishing it from other shocks in the economy, and clearly examine the dynamic adjustment process over time that may differ in times of growth and decline. Second, simply distinguishing population growth and decline into two separate regimes does not account for empirically observed demographic developments. Rather, choosing an estimation setting that allows the impact of population changes to differ continuously from high to low growth to decline takes the existence of population stagnation before and after periods of decline into account. Third, the sparse occurrence of population decline calls for a cross-country perspective. Identifying nonlinear effects of population changes in growth and decline periods using an econometric model requires a sufficient number of observations for both, which is clearly not given when focusing on an individual economy. Even for countries that experienced comparatively many years of decline, a dynamic analysis including more than two or three variables with a sufficient number of lags quickly depletes its degrees of freedom for decline periods. Fourth, even in a cross-country perspective, there have been only few observations in the more recent past, calling to exploit the full variation of population changes not only across countries but also over time, whenever reliable labor market data exist. Below, we propose an estimation framework addressing the mentioned necessities.

2.4 Econometric Strategy

As outlined, we exploit the time-series variation from multiple countries to identify possibly differing effects of population growth and decline, using an empirical strategy that permits the analysis of dynamic interdependencies conditional on the demographic regime. We draw on and expand different strands of the literature and introduce a suitable external instrument to identify the effects of a structural population shock in the economy. We divide this section into a series of subsections on nonlinear dynamic modeling, regime specification, shock identification, instruments, and impulse responses.

2.4.1 Capturing Nonlinear Effects: Panel Smooth Transition VAR

We start by specifying a panel VAR, and in doing so, we contribute to a growing body of literature making use of panel VARs in macroeconomics (e.g., Aksoy et al., 2019). Applying a vector autoregressive structure allows the flexible analysis of macroeconomic interdependencies without a priori imposing assumptions on the directions of effects (Canova & Ciccarelli, 2013). Drawing on this literature, we specify our model in its linear version as

$$Y_{i,t} = \mu_i + \delta_t + AY_{i,t-1} + EX_{i,t} + u_{i,t}, \tag{2.4}$$

with $i = 1, \ldots, I$ and $t = 1, \ldots, T$; I and T being the panel and time dimensions, respectively. $Y_{i,t}$ is the vector of endogenous variables, μ_i and δ_t denote country- and time-fixed effects, respectively, and $X_{i,t}$ represents country-year dummy variables to capture the effects of war, post-war, and interwar periods.[6] A and E are coefficient matrices. $Y_{i,t}$ comprises seven variables: the working-age population, real GDP, real wages, real investment, employment, the labor force, and average annual hours worked. All variables are included in log levels. Notably, given the inclusion of $Y_{i,t}$ in levels, when allowing for a sufficient lag length, the VAR is able to capture level relations and flexibly form quasi-differences in the presence of unit roots (see, e.g., Sims et al. 1990; more recently Weber & Weigand 2018).

Since the focus of the present paper is on the analysis of potentially different effects of population decline compared to population growth, and the descriptive evidence suggests a continuous rather than a threshold modeling approach, we combine our panel VAR with a nonlinear smooth-transition structure. This follows a strand of literature using common vector autoregressive models and nonlinear extensions to account for regime-wise interdependencies of macroeconomic variables (e.g., Auerbach & Gorodnichenko, 2012). Thus, our linear model in Equation (2.4) is modified as follows:

$$Y_{i,t} = \mu_i + \delta_t + [1 - P(q_{i,t})]GY_{i,t-1} + [P(q_{i,t})]DY_{i,t-1} + EX_{i,t} + u_{i,t}, \tag{2.5}$$

where G and D are matrices holding the regime-dependent coefficients of the endogenous variables, and $P(q_{i,t})$ refers to the probability of experiencing population decline. This probability is given as

$$P(q_{i,t}) = \frac{exp[-\gamma(q_{i,t} - \kappa)]}{1 + exp[-\gamma(q_{i,t} - \kappa)]}, \tag{2.6}$$

[6] This vector of dummy variables eliminates the effects of all observations from 1914 to 1922 as well as from 1929 to 1949, and is basically equal to removing those observations from the panel dataset completely. We keep these observations and eliminate the corresponding effects using dummy variables instead of excluding them in order to find regime weights as well as easily carry out the residual resampling. We additionally include a dummy for the German hyperinflation in 1923.

where $q_{i,t}$ is the transition variable, γ defines the smoothness of the transition, and κ is a location parameter defining the value of $q_{i,t}$ at which the regime-switch occurs.

By using the framework in Equation (2.5), we exploit the effects of varying population growth and decline rates within countries over time, while the differences between countries, such as their sizes or other fixed effects, are accounted for by the inclusion of μ_i.

2.4.2 Demographic Regimes: Transition Variable and Smoothing Parameters

Given the scope of the paper, the transition variable $q_{i,t}$ incorporates information on the prevailing demographic regime, that is, population growth rates. However, from a conceptual perspective, the selection of an appropriate transition variable is not straightforward. Moreover, the smoothing and location parameters γ and κ are not predefined either. In the literature (e.g., Auerbach & Gorodnichenko, 2012; Gehrke & Hochmuth, 2021), authors tend to select a transition variable, define a switching point κ, and then calibrate γ such that the share of observations with probability $\geq 1 - \tau$ is close or equal to τ, which is the share of observation in the regime of interest, e.g., years of population decline.

The selection of a transition variable mainly translates into the question of which period of population change is relevant to depict a demographic regime under which a labor market operates. To answer this question, we use the trend of annual population growth rates as delivered by the HP filter ($\lambda = 100$) as our transition variable. To avoid the common bias of the HP filter at the ends of the sample, we use population growth rates from 1860 to 2025, using data sources as outlined in Appendix 2.E.

For the switching point, the literature tends to define $\kappa = 0$, which, in case of the usual z-standardization of the transition variable, implies a switch at the mean. In our case, the plausibility of this switching point (0.63 percent) is disputable, as it implies that the majority of the years after 1970 is closer to the decline than the growth regime (compare Table 2.1), i.e., working-age population decline has been more likely than growth. This contrasts the narrative that extensive working-age population decline is a rather recent phenomenon. To find a more suitable switching point, we rely on the distribution of the (original) annual population change rates in our dataset. We define $\kappa = Q_1^{G,z}$, which is the lower quartile of growth observations across all years in the panel (0.48 percent) after the z-standardization of $q_{i,t}$. In the robustness section, we address this choice.

Eventually, for calibrating γ, we follow the standard procedure in the literature as outlined above. The share of population decline observation in the observations across

Figure 2.4: Decline Probabilities Across the Countries in the Sample

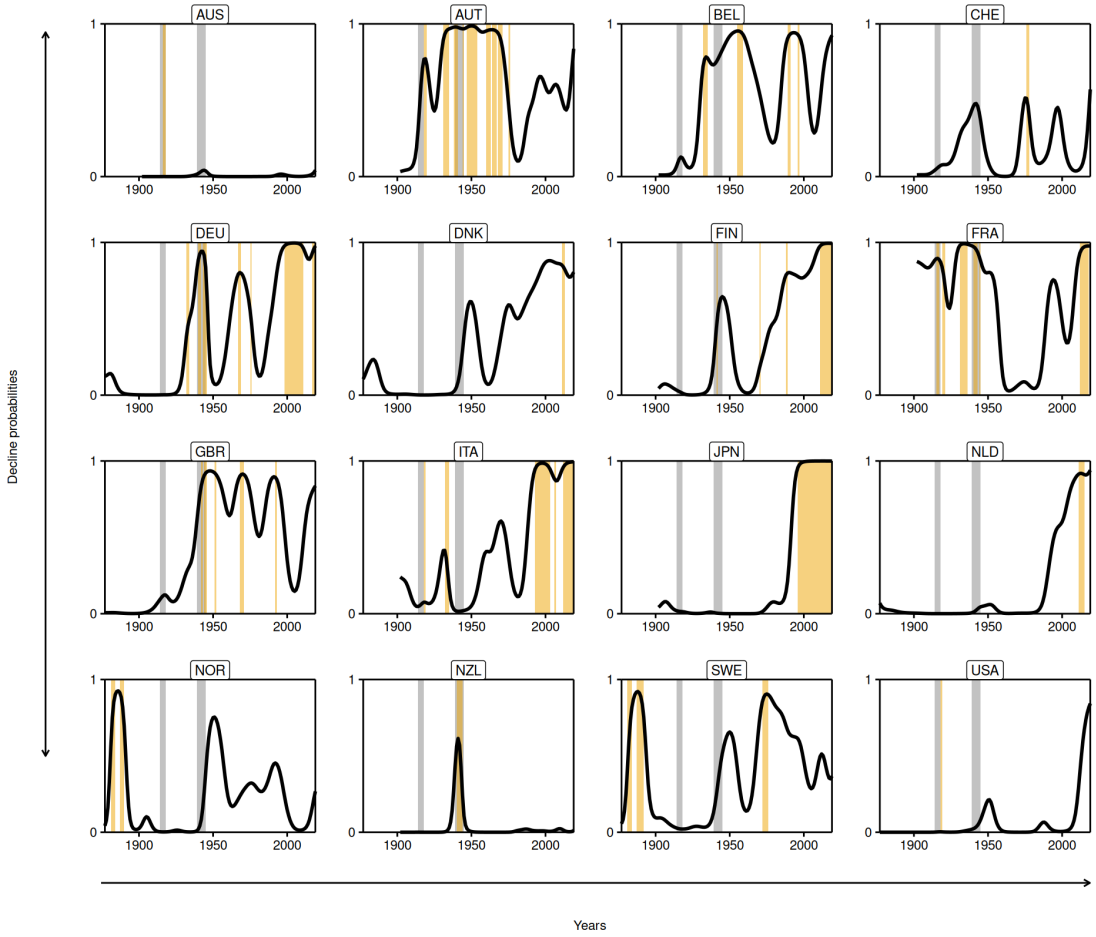

Notes: Shaded areas indicate war (gray) and decline (orange) years. Author's own computations and illustration.

all countries in the final panel is 8.7 percent. In accordance with the literature, and to ensure a sufficient number of observations in each regime, we calibrate to the original share of decline observations. We set γ such that $Pr[P(q_{i,t}) \geq 0.913] \approx 0.087$. This calibration exercise yields $\gamma = 3.81$. Figure 2.4 illustrates the distribution of the decline probabilities stemming from this specification across the countries in our panel. As intended, the calibration exercise creates decline probabilities coinciding with actual decline observations and allows for smooth changes from and to periods of growth.

Having distributed growth and decline weights across all observations in the sample, we are able to estimate the model equations-wise by OLS. We check for the appropriate lag length by relying on the BIC, and arrive at a lag length of $p = 2$. Notably, by using the HP filter to smooth annual change rates, we capture only sufficiently long periods as decline (growth) periods. Single decline (growth) years in between enduring periods of

growth (decline) do not trigger regime changes. As a consequence, the median duration of periods where $Pr[P(q_{i,t}) \geq 0.913]$ is eight years. Thereby, as Figure 2.4 displays, more than 80 percent of overall decline observations entering our estimation are located in periods of at least eight years; thus, the results presented below reflect more than mere short-lived fluctuations.

2.4.3 Identification of Structural Shocks by External Instruments

However, to trace possibly asymmetric labor market adjustments to population changes over time, we do not only estimate the reduced form, but we need to identify corresponding structural population shocks. Evidently, working-age population can be endogenous to economic variables, for example to push and pull factors driving migration decisions. Indeed, estimations ignoring simultaneity in Appendix 2.C demonstrate the importance of introducing instruments in the identification strategy.

In recent years, shock identification using external instruments has found widespread application (Gertler & Karadi, 2015; Stock & Watson, 2018). This approach exploits the well-known fact that the reduced form innovations $u_{i,t}$ are a linear combination of structural shocks $\epsilon_{i,t}$:

$$u_{i,t} = S\epsilon_{i,t}. \tag{2.7}$$

Analyses drawing on identification by external instruments refrain from identifying the full matrix S by imposing restrictions but rather focus only on the shock of interest, that is, only identify the corresponding column s. To identify the structural shock of interest $\epsilon^s_{i,t}$ — the population shock — appropriately, a suitable instrument $z_{i,t}$ must satisfy the well-known conditions

$$E(\epsilon^s_{i,t} z_{i,t}) \neq 0, \tag{2.8}$$

$$E(\epsilon^{-s}_{i,t} z_{i,t}) = 0. \tag{2.9}$$

While Equation (2.8) states that $z_{i,t}$ must be relevant, i.e., correlated with the population shock, equation (2.9) requires the instrument to be exogenous to the remaining unidentified shocks $\epsilon^{-s}_{i,t}$ (Gertler & Karadi, 2015).

The contemporaneous effect of a structural shock is estimated by two-stage least squares (2SLS). In the first-stage regression, we isolate the structural shock; that is, we regress the residuals of the equation of interest, here of the population equation, $\hat{u}^1_{i,t}$, on the instrument. In the second stage, we identify the contemporaneous impact of the structural shock by regressing the residuals of all of our j equations — with $j = 1, \ldots, 7$, — of the reduced-form estimation on the fitted values of the first stage. Notably,

in the second stage, we weight the RHS by the respective regime probabilities. More formally, the regime-dependent contemporaneous impact is given by

$$\hat{u}^1_{i,t} = \alpha + \omega z_{i,t} + v_{i,t}, \tag{2.10}$$

$$\hat{u}^j_{i,t} = \beta^j + \theta^j_G[1 - P(q_{i,t})]\hat{s}_{i,t} + \theta^j_D[P(q_{i,t})]\hat{s}_{i,t} + r^j_{i,t}, \tag{2.11}$$

where $\hat{s}_{i,t} \coloneqq \hat{\hat{u}}^1_{i,t}$ is the estimated population shock in country i at time t, i.e., the fitted value obtained by estimating Equation (2.10), ω is the coefficient from the first stage, and θ^j_G and θ^j_D hold the regime-dependent coefficients of interest from the second stage. Importantly, by construction, this identification strategy scales the contemporaneous effects to a structural shock of 1 percent.[7] Yet, before estimating these regime-dependent contemporaneous effects of a structural population shock as outlined, we need to find a valid instrument, meeting both the relevancy and exogeneity conditions.

2.4.4 Introducing a Suitable Instrument: Lagged Births

In the historical context of our paper, the availability of suitable instruments is highly limited. In particular, this applies to economic indicators, but less so for demographic data. To unravel how we may exploit the variation in external demographic data to identify structural shocks, we start from the basic observation that the development of a population can be written as $f(B, D, M)$, thus as a function of the three demographic components: births, deaths, and migration (Shryock & Siegel, 1976). Given our dataset starts in 1875, migration data is difficult, and for some countries impossible, to obtain, but information on natural population change — births and deaths — can be easily retrieved. However, as we strive to estimate the impact of a structural shock in the working-age population (15–64 years), the role of births differs from the role in the total population: The development of a working-age population can rather be written as $f(I, O, D, M)$, i.e., inflows into and outflows from the age group instead of births determine the size. Since we define the working-age population to be those aged 15–64 years, inflows in period t are persons aged 14 years in period $t-1$ and outflows in period t are persons aged 64 years in period $t-1$.

Notably, documenting annual births has a long tradition and corresponding time series are available starting from the early 19th century, and, by definition, a birth cohort always corresponds to a single age-year cohort in a given population. This observation suggests that inflows and outflows should be approximated by using lagged births data

[7] This applies to the linear case. When identifying the contemporaneous effect in a nonlinear framework, as in Equation (2.11), this coefficient may be different from 1. In our case, these differences are small. Thus, we manually scale the contemporaneous effects accordingly.

since, arguably, births lagged 15 and 65 years are an instrument that satisfies both conditions stated in Equations (2.8) and (2.9).

Despite the time lags, endogeneity concerns may arise. The literature has shown that births respond to current economic conditions (Sobotka et al., 2011), and economic conditions of today also likely predict future economic conditions. Doepke et al. (2015) describe a well-known example: During World War II, female labor force participation rates in the United States increased, and the effect lasted beyond the end of the war. Due to this persistence, younger women who entered the labor market after the war faced increased competition — and more often opted for having children. In turn, this has likely driven larger investments in infrastructure.

Yet, we argue that this endogeneity channel does not raise concerns in our use case. First, an economic shock can have permanent and transitory effects. This is well known and applies to all non-stationary variables. But even if an economic shock in the past has changed the level of births permanently, this does not apply to its differences — which is the source of variation that we seek to exploit. Second, this assumption is mirrored by the data — the autocorrelation of the instrument vanishes rapidly. Again, this indicates that the variation on which we are identifying is independent of past economic shocks, even if the level has changed permanently. Third, beyond econometric considerations, the literature has shown that the length of business cycles varies across countries and time (Jordà et al., 2017), but it is, on average, substantially shorter than the time lags of births as used above. This rules out any interference in our identification due transitory effects of economic shocks. Fourth, following Equation (2.9), the instrument must be uncorrelated with the shocks, not with the variables themselves. Logically, while lagged births are allowed to be linked to the level of today's economic magnitudes, uncorrelatedness is only required for the new innovations.

While these arguments support the validity of the instrument, using information on lagged fertility as an instrument to identify demographic changes has already some precedents in the literature. Among others, Jaimovich & Siu (2009) use such data as an instrument for the age structure of the labor force and analyze corresponding effects on output volatility. In a recent contribution, Maestas et al. (2023) analyze the effect of population aging on economic growth, the labor force, and productivity. To address endogeneity issues, they use data on lagged age structure as an instrument for the contemporaneous shares, weighted by corresponding survival probabilities. In this paper, we combine and augment these existing approaches from the literature.

We start by acknowledging that the suitability of using births to identify a structural shock must take into account the interaction with the other two components of

demographic changes, mortality and migration. Consequently, we conduct a series of preparatory steps.

First, mortality patterns have changed substantially over the past two centuries (Davenport, 2021). Correspondingly, the probability of a person reaching 15 and 65 years of age has been vastly different in the 19th century compared to the 20th and 21st century. An intuitive way of correcting for these changes and simultaneously relying on a variable of widespread availability is to weight births in a given year with some information on the life expectancy of newborns in the same year. However, life expectancy is typically calculated by using period mortality, that is, using the age-specific death rates in the same year or reference period (see, e.g., Anderton et al., 1997; Shryock & Siegel, 1976). But this does not account for the impact that drastic events have on age-specific death rates, such as the effect of wars on the mortality of those who have already entered working age, as well as for general improvements in health care and longevity over centuries. Consequently, we weight births lagged 15 and 65 years, denoted as $B_{i,t-15}$ and $B_{i,t-65}$, with the corresponding cohort survival rate, if available,[8] denoted as $m_{i,t}^{15}$ and $m_{i,t}^{65}$, thus $\tilde{B}_{i,t-15} = B_{i,t-15} * m_{i,t}^{15}$ and $\tilde{B}_{i,t-65} = B_{i,t-65} * m_{i,t}^{65}$.

Second, the contribution of fertility to population growth, here the contribution of inflows into and outflows from the working-age population, depends on the population size at a given point in time. Put differently, the same birth cohort might contribute to population change in vastly different ways when entering and exiting working age not only due to mortality, as it may also differ substantially when the in-between change of the population size was large, e.g., due to strong migration dynamics. We account for this by dividing births by the population level one year prior to the longest lag p in the VAR. More formally, this is

$$\tilde{b}_{i,t} = \frac{\tilde{B}_{i,t-15} - \tilde{B}_{i,t-65}}{P_{i,t-(p+1)}}. \tag{2.12}$$

By doing so, we combine information on births lagged 15 and 65 years in a single instrument to exploit the joint explanatory power. In the robustness section, we control for the age structure in the working-age population to ensure that the identified effects stem from a population shock rather than from changes in the age structure.

Third, the model proposed in Equation (2.5) encompasses the contribution of the natural component to overall working-age population growth. Now, in striving to isolate the structural population shock in the residuals of the population equation by using lagged births as an instrument, we essentially address those innovations in the natural

[8] Again, we document all data sources and adjustment steps in Appendix 2.E in detail.

component of population change that have remained unexplained by the model. Put differently, rather than resembling the natural population change component already included in the VAR, an appropriate instrument should approximate only the idiosyncratic changes of innovations in this component. To this end, before using it as an instrument, we filter $\tilde{b}_{i,t}$ by an autoregressive structure, with π being the corresponding coefficient, by country ($\tilde{\mu}_i$) and year fixed-effects ($\tilde{\delta}_t$), and by country-year dummy variables ($X_{i,t}$) — all of this analogous to Equation (2.5):

$$\tilde{b}_{i,t} = \tilde{\mu}_i + \tilde{\delta}_t + \pi \tilde{b}_{i,t-1} + \eta' X_{i,t} + e_{i,t}. \tag{2.13}$$

Since recorded births are flow data, we use only one lag to resemble the level structure as included in the VAR. Having estimated Equation (2.13), we compute $\hat{e}_{i,t}$ and define $z_{i,t} \coloneqq \hat{e}_{i,t}$, i.e., the residuals stemming from this filtering step serve as the instrument in our identification strategy.

We plug $z_{i,t}$ into the first-stage equation (2.10) and retrieve the corresponding fitted values. This isolates the structural population shock in the population equation residuals from the initial reduced-form estimation, as outlined above. Using the isolated shock in the second-stage equation (2.11), we obtain θ_G^j and θ_D^j, which are the contemporaneous effects of a structural population shock on the jth variable in the model — in times of population growth and times of population decline, respectively.

Eventually, more general questions concerning instrument strength and data quality emerge. We can test for the former: In the first-stage estimation, we obtain an F statistic (HAC) of 163.1, demonstrating sufficient strength. Importantly, while both components of the instrument, births lagged 15 as well as 65 years, show sufficient strength, the combination of both yields the best fit, and is also consistent with instrumenting both inflows and outflows rather than only one of those two. Moreover, the F statistic suggests that using information on lagged fertility as outlined provides a strong instrument for current, exogenous population changes — even if there have been strong demographic, possibly interfering events such as pandemics (Spanish Flu) or large-scale migration flows (Blanc & Wacziarg, 2025).

The answer to concerns on data quality is more nuanced: In the identification step, we exploit the information from all reduced-form residuals for which there are available data for births. Notably, this is the case for 90.6 percent of the observations. For the remaining 9.4 percent, estimated data exist. In Appendix 2.A, we outline in detail across which countries and periods these estimated data points are distributed. Importantly, we include all observations, based on estimated or observed births data, only in the filtering Equation (2.13) — in order to the estimate the trend correctly and equivalent

to the VAR structure. Still, we rely on the subsample of the 90.6 percent observations based on actual, observed births to identify the shock.

2.4.5 Impulse Response Functions and Bootstrapping

By stacking all θ_G^j and θ_D^j coefficients into two vectors and using the estimated coefficient matrices from the reduced-form estimation, G and D, we are able to derive orthogonal impulse response functions and trace the effects of a structural population shock in times of population growth and in times of population decline. Importantly, by deriving orthogonal impulse response functions, we implicitly assume that the estimated system stays in the respective regime. Hence, as argued by Auerbach & Gorodnichenko (2012), the model is linear for each regime, and the corresponding impulse response functions do not depend on history (for details on impulse response functions and history dependence in the context of nonlinear multivariate models, see Koop et al. 1996).

From the impulse responses of the log level of the endogenous variables, we can derive the reactions of further ratios and variables of interest: the labor force participation rate, the employment rate in the labor force, GDP per capita, productivity, the capital stock, and, consequently, the capital-labor ratio. In Appendix 2.B, we outline in detail how we obtain these reactions.

We construct 68 percent confidence intervals by applying recursive cross-sectional residual resampling with $5,000$ draws. Following and building upon Jentsch & Lunsford (2022), we preserve the covariance of the structural population shock, the instruments, and also the regime weights by resampling them simultaneously. We choose the block length to be equal to the lag length of the model, which corresponds to a block length of three.

In the robustness section, we address frequent questions appearing both in panel models and historical settings, such as cross-sectional dependence or parameter constancy, and demonstrate that our findings remain valid when explicitly accounting for those factors.

2.5 Results

2.5.1 Regime-Dependent Effects of Structural Population Shocks

In this subsection, we report and analyze the impulse response functions to positive, respectively, negative population shocks. Thereby, we address three varieties of (possible) asymmetries of these responses across regimes: in magnitude, in sign, and in timing. First, we present the results for the growth regime. Then, we do the same for the decline

regime, and additionally include the mirrored point estimate from the growth regime. The latter enables a quick comparison in terms of symmetry, that is, what would the impulse response look like if it were symmetrical to the growth regime.

In Figure 2.5, the blue solid lines represent the impulse response functions of the point estimates of the level variables included in the baseline specification to a positive population shock in times of population growth. Since we include all variables in logs, the results can be interpreted as elasticities. Thus, the impulse response functions indicate the percent change of the respective variable to a 1 percent population shock. The blue shaded areas indicate corresponding 68 percent confidence intervals. The plots permit the analysis of the effects over a horizon of up to ten years after the shock, i.e., from the short to the medium and long term.

As Figure 2.5 illustrates, the impulse response of the population variable to its own shock grows by up to 4 percent after ten years. This extent is important as it sets the benchmark to which the reaction of the other variables must be compared. It mirrors that population growth is persistent.

The trajectories of the other impulse responses indicate that economic reactions to population shocks in periods of growth take time. Put differently, in periods of growth, population changes do not translate into economic reactions straightaway. However, the responses of GDP, of investment, and of the extensive margin of labor supply —

Figure 2.5: Positive Population Shock in Times of Growth: Impulse Response Functions

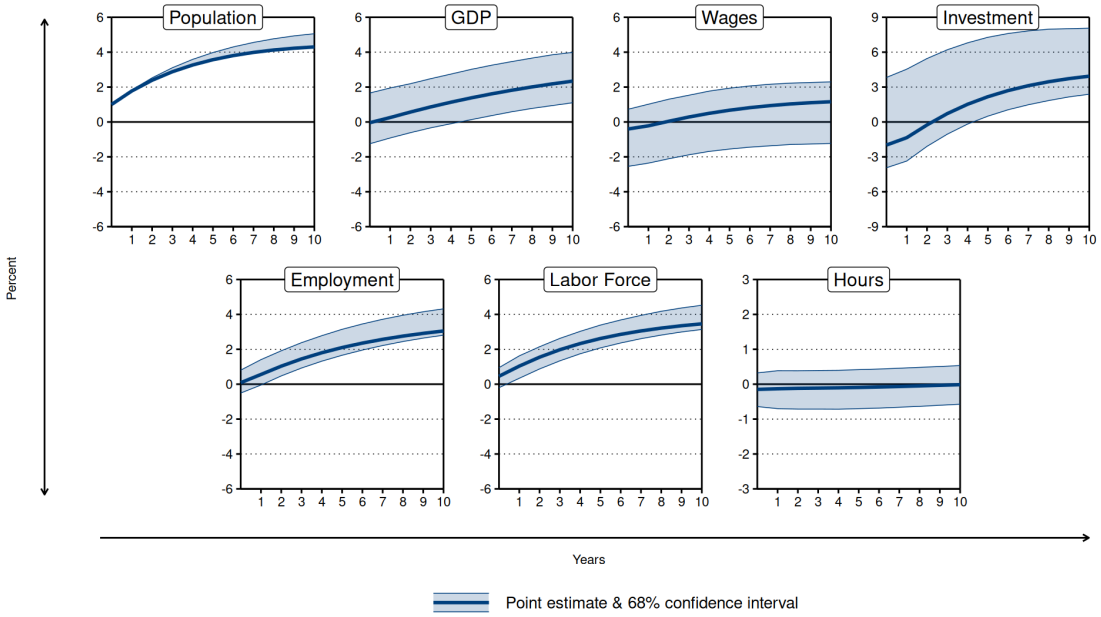

Notes: Author's own computations and illustration.

employment and the labor force — grow and become significant. By contrast, as the plot indicates, we do not find any significant effects on real wages or on average annual hours worked.

Below, Figure 2.6 offers the complementary analysis for the decline regime. The solid orange line indicates the impulse response functions of the point estimates of the level variables included in the baseline specification to a negative population shock of 1 percent in times of population decline. The orange shaded areas indicate the corresponding 68 percent confidence intervals. The blue line indicates the mirrored point estimate from the growth regime, as given in Figure 2.5.

As Figure 2.6 shows, the impulse response of the population variable is less pronounced in the long term compared to the growth regime, flattening out at about 3.3 percent after ten years. Again, this is the benchmark to which the other results must be compared before drawing conclusions across regimes.

Contrary to the growth regime, population changes translate more swiftly into the economy in times of decline. In the short term, this becomes visible in the point estimates of GDP, investment, and employment. Unlike population growth, population decline quickly passes through to the labor market. But in the medium to long term, the initial differences disappear or reverse. The effect on total GDP after ten years is similar in both regimes. The impulse responses for investment, employment, and the labor force flatten

Figure 2.6: Negative Population Shock in Times of Decline: Impulse Response Functions

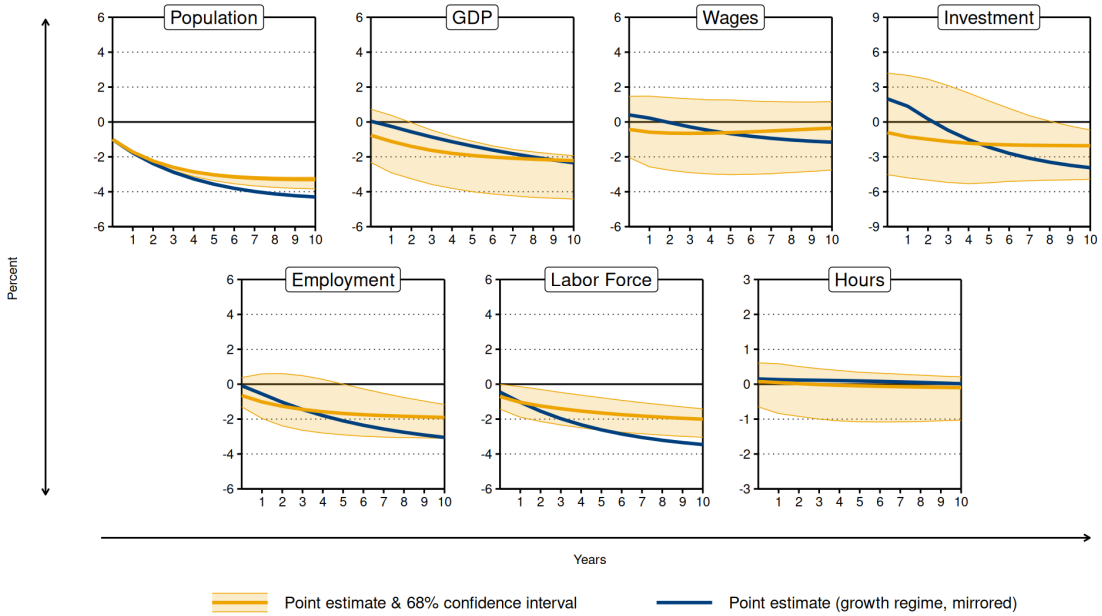

Notes: Author's own computations and illustration.

our more quickly — both in comparison to the growth regime but also in comparison to the trajectory of the population in the decline regime. These results suggest that economies have proven to be successful in cushioning the adverse effects of population decline on labor supply. Since this avoids further losses in the production factor labor, for the complementary production factor capital it also counteracts disinvestment tendencies, as mirrored in the corresponding impulse response. As in the growth regime, we do not find any significant changes of real wages or average annual hours worked.

So far, the analysis has focused on the results as straightforwardly provided by the baseline model. By deriving a series of additional impulse response functions, we are able to quantify these results in the form of well-known indicators, such as the labor force participation rate. Figures 2.7 and 2.8 allow for corresponding analyses. For the depreciation rate, we assume 4.6 percent (e.g., ECB, 2006). We discuss variations of this deprecation rate in the next section.

As Figure 2.7 shows, a positive population shock in times of population growth causes GDP per capita to decline. The point estimate of the short-term effect indicates a pronounced but insignificant decline. After ten years, the effect arrives at a significant 2 percent decline. Importantly, this impulse response is calculated using the population variable in the model, which is the working-age population. Thus, the effect should

Figure 2.7: Positive Population Shock in Times of Growth: Additional Impulse Response Functions

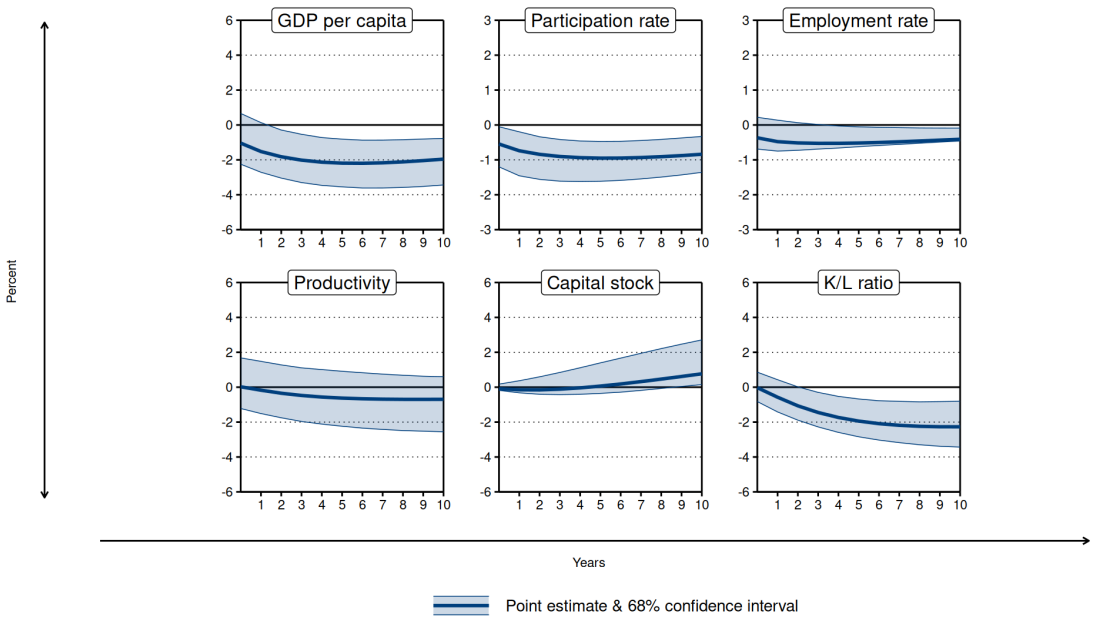

Notes: Impulse response functions for the capital stock and the capital-labor ratio are calculated by assuming a depreciation rate of 4.6 percent. For further information on the derivation of the additional impulse response functions, see Appendix 2.B. Author's own computations and illustration.

rather be interpreted as GDP per capita of those of working age. The effect on GDP per capita measured using the total population depends on the ratio of those of working age to those of non-working age and, even more importantly, on the changes in the non-working-age population following the shock. Quantifying these effects is beyond the scope of this paper.

There are two possible explanations for this decline in output per capita. One is that labor does not increase as strongly as the population, that is, proportionally fewer people contribute to production. Looking at the level effects in Figure 2.5, this effect appears to be evident and is quantified in Figure 2.7, where the labor force participation rate declines significantly by 0.8 percent in the long term. Moreover, the employment rate in the labor force declines significantly by 0.4 percent after ten years. Put differently, following a positive population shock in times of population growth, people participate less in the labor market, and those participating are less often in employment — i.e., the unemployment rate increases.

Another possible explanation is changes in productivity. The impulse response function for productivity — output per hour worked — suggests an effect close to zero in the short term, and subsequently a moderate decline by 0.7 percent, which is, however, not statistically significant. A certain decrease in productivity would be explained by a lower capital-labor ratio. Indeed, the capital stock increases only with a lag. As a consequence, we observe only an incomplete adjustment of the capital side after ten years according to the results of our model — which implies a lower capital-labor ratio. In fact, in a back-of-the-envelope calculation, when assuming a stylized Cobb-Douglas production function and an output elasticity of one quarter (see Vollrath 2024 for a recent contribution on reasonable ranges of capital elasticities), an isolated change in the capital-labor ratio of -2.3 percent would reduce productivity by 0.6 percent — which is very close to the model results.

In Figure 2.8, the derived impulse response functions for the decline regime are visualized, again with the mirrored response from the growth regime as the blue line. The increase in GDP per capita is not as pronounced as the response in the growth regime would suggest, arriving at around 1.1 percent after ten years, and not reaching statistical significance.

Again, there are two possible drivers for changes in GDP per capita: increasing employment participation or productivity. In Figure 2.8, the regime differences in the labor supply reaction in terms of participation and employment are well illustrated. The labor force participation quickly overtakes the mirrored response from the growth regime. After ten years, we see a substantial and significant increase of the labor force

Figure 2.8: Negative Population Shock in Times of Decline: Additional Impulse Response Functions

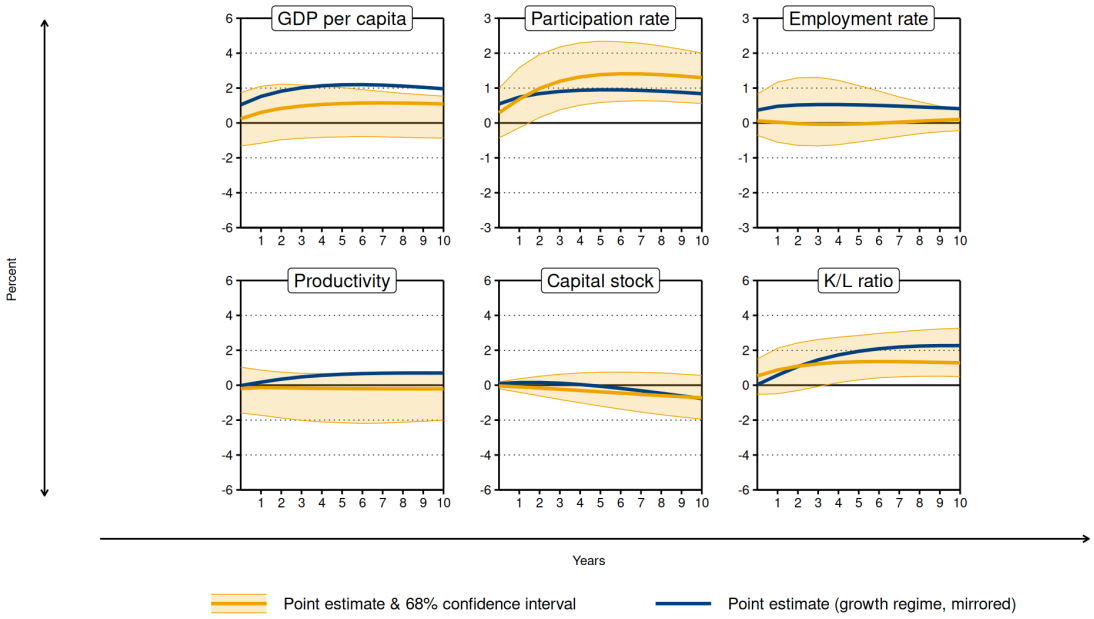

Notes: Impulse response functions for the capital stock and the capital-labor ratio are calculated by assuming a depreciation rate of 4.6 percent. For further information on the derivation of the additional impulse response functions, see Appendix 2.B. Author's own calculations and illustration.

participation rate in times of decline by 1.3 percent, which is about 0.5 percentage points larger compared to the mirrored response from the growth regime.

In order to dig more into the underlying processes, sex-specific results may be of particular relevance. The period under analysis has seen substantial increases in female labor force participation and these increases likely also served as an adjustment margin in times of shortages, for instance documented for World War II by Goldin (1991). While our data does not allow to disentangle sex-specific patterns due to data limitations in the historical context, a look on corresponding descriptive data (OECD, 2024) for more recent observations reveals participation effects for both, women and men: In decline years, participation rates of females grew annually by a median of 0.5 percentage points (compared to 0.35 among all observations), and rates of males exhibited a median annual growth of 0.16 percentage points in decline periods (compared to -0.01 among all observations). Similarly, the OECD (2025) data also reveals labor supply effects across education levels: In more recent decline years, participation rates grew from 0.11 (tertiary) to 0.14 (below upper secondary) and 0.22 (upper secondary) percentage points, compared to increases between 0.05 and 0.07 percentage points among all observations. These descriptive data suggest that the labor supply effects observed in our model re-

sults occur across the board rather than being driven only by specific socio-demographic groups.

Moreover, as outlined above, in times of growth, the unemployment rate rises as the labor force grows more strongly compared to employment. But in times of decline, by contrast, we observe much more similar changes of employment and the labor force. As a result, as Figure 2.8 visualizes, the employment rate remains roughly stable throughout the analyzed horizon, thus we find no evidence for any significant changes in the unemployment rate in times of decline.

Eventually, while productivity declines moderately in the growth regime, we observe no increase in periods of population decline. Furthermore, since neither unemployment nor hours worked change noticeably, this implies that the observed rise in GDP per capita in periods of decline is mainly driven by changes at the extensive margin, i.e., increasing labor force participation.

Discussion: A View on the Existing Literature

The productivity decline by 0.2 percent can be related to the literature. Recent approaches such as Jones (2022) seek to model the endogenous dynamics leading to population decline and analyze, as a consequence of population decline, the implications for economic growth in the long run. Jones (2022) shows that in a regime of persistent population decline, the diminishing number of people eventually leads to stagnating GDP per capita and productivity, as outlined above.

While we do not consider the long-run or steady-state dynamics of the economy analogously to theoretical models, the effects we are analyzing can be compared since they are conditional on the prevailing regime, i.e., on enduring population decline. Consequently, we use the way ideas evolve according to Jones (2022, see Table 1) and the calibration therein in a back-of-the-envelope calculation and compare two scenarios:[9] First, a scenario with a constant negative population growth rate, set to -0.5 percent, as done by Jones (2022). Second, a scenario with additional exogenously induced population decline as given by the impulse response of the population from our baseline specification. By comparing the trajectories of knowledge in both cases, we observe that, compared to the first scenario, the additional population decline lowers productivity by about 0.4 percent after ten years.

This exceeds the productivity reaction as observed in our model. However if labor supply decreases and, at the same time, the capital stock does not fall proportionately,

[9] Jones assumes 2 percent annual TFP growth. This calibration suits our empirical data well, as we observe a median annual productivity change of 2.2 percent (only years that entered the estimation).

then the capital-labor ratio increases, as outlined above. When assuming a stylized Cobb-Douglas production function and an output elasticity of capital of one quarter as above, a 1.3 percent increase in the capital-labor ratio, as given by our results, would imply an increase of productivity by 0.3 percent. Logically, the fact that productivity instead decreases by 0.2 percent implies a negative effect on total factor productivity of 0.5 percent. Therefore, the effect derived from Jones (2022) is compatible with our results. Moreover, this channel is also mirrored by descriptive data on patent applications for more recent observations. According to World Bank (2025) data starting in the early 1980s, per capita patent applications by residents fell by an annual median of 0.25 percent. However, there are differences between regimes: applications fell only by 0.12 percent in growth years, but by 0.55 percent in decline years.

Recent contributions have also pointed to another, productivity-increasing factor in times of population decline: the role of education decisions (Strulik, 2024). Again, a comprehensive empirical inclusion of this channel into our model is not feasible due to the lack of data. But for the period 1950–2010, quinquennial data by Barro & Lee (2013) on incomplete tertiary education rates among those aged 20–34 years exist, allowing for a descriptive analysis of the interpolated annual changes during periods of decline as in Figure 2.3. Thereby, we interpret rising incomplete tertiary education rates as a proxy for rising tertiary enrollment rates, and thus as a proxy for decisions for further investment in education. We find that this rate grows by an annual median of 0.26 percentage points in periods of decline, but only by 0.15 percentage points among all observations.

Although this descriptive evidence suggests that education is, in fact, increasing stronger in times of population decline, the effect on overall productivity within the 10-year horizon of our model may be limited: Based upon the Barro & Lee (2013) data on population and enrollment rates by age and assuming a college wage premium of 50 percent as a proxy for productivity (for variation in U.S. college wage premium over time, see Autor et al. 2020, among others), we can derive that an increase in tertiary education completion rates among persons 20–34 years old by 1 percentage point increases overall labor productivity by 0.1 percent. While this calculation does not encompass education decisions at younger or older ages, and assumes that the age structure of the labor force is the same as in the population aged 15–64 years, it still points towards a limited education-induced increase in productivity due to population shrinkage.

Despite the pronounced TFP decline, in Figure 2.8 we find an insignificant but clearly positive reaction of GDP per capita. This is explained by the combination of rising capital intensity and rising labor force participation. These mechanisms, that are absent in standard models, jointly offset possibly negative productivity effects due to a decreasing

population size. Logically, these margins should be part of theoretical considerations on the odds of GDP stagnation.

Other results discussed above have yet not been addressed explicitly in the context of population decline, but in the related literature. An established strand analyzes the wage and unemployment effects of shrinking cohort sizes. Another strand investigates the effects of emigration. If flexibility of labor demand is limited, shrinking cohort sizes may decrease crowding out effects and thus improve the labor market outcomes (Easterlin, 1961). However, for firms, smaller youth entry cohorts may also lower the incentive to create new jobs (Shimer, 2001), besides labor supply also aggregate demand effects have to be taken into account (Macunovich, 1999) and the cohort effects may change over time (Zimmermann, 1991). Similarly, other studies have found that emigration may increase the wages of stayers (e.g., Biavaschi, 2013; Dustmann et al., 2015). While the overall evidence is not unambiguous, even if one comes from the hypothesis that labor market outcomes deteriorate with cohort size (such as Berger, 1985; Brunello, 2010; Foote, 2007; Garloff et al., 2013) or are linked to emigration, the view of our study differs in one important aspect: the cohort shifts and emigration dynamics in the recent decades analyzed in the literature usually do not represent actual (working-age) population shrinkage, which is our focus. Evidently, the overall decline of the working-age population goes beyond cohort shrinkage or emigration, and thus we find distinct adjustment channels: no wage and unemployment reaction, but higher labor force participation and capital deepening. Importantly, rising participation does not come about through wage increases, as would be the case when thinking of conventional labor supply elasticities. Evidently, contraction in the labor market affects the extensive margin directly via other channels.

Limitations: Historical Context, Data Quality, and Future Population Declines

Breaking new ground with historical and comparative datasets is subject to a trade-off between the value of additional insights and measurement uncertainty. While we are confident that our investments in data quality are enough for the former to outweigh the latter, results and conclusions are subject to limitations. First and foremost, this can be attributed to the historicity of the data used. Both the quality of measurement of labor market indicators as well as underlying concepts and definitions (see, e.g., Romer 1986a or Piore 1987) have changed over time, which complicates, for example, the comparison of unemployment dynamics between the late 19th and the early 21st century. Moreover, for example, one key limitation in interpreting the absence of effects on wages is the data

quality: Most historical wage series focus on urban unskilled laborers. In the literature, some argue that these wage series resemble overall wages in the economy quite well (e.g., Allen, 2001). Still, given that urban unskilled laborers have represented only one part of the labor force, there are conceivable limitations in the interpretation.

Similarly, overall economic and social structures have changed. Put differently, economies and their labor markets have evolved strongly over the past 140 years, for example with regard to sectoral structure (among others, Herrendorf et al., 2014) or, in recent decades, due to automation (Carbonero et al., 2020) — and the same applies to social norms and values (e.g., Fernández, 2013; Humphries & Sarasúa, 2012). While our dataset offers clear advantages for estimating effects that would otherwise be hard to measure, it is, due to the long time span, also subject to such transformations. We address potential interference of these changes over time for our estimation results in the upcoming robustness section.

Eventually, the external validity of our study is naturally linked to the range and the duration of population decline rates as observed in the past. On the one hand, as insights from theoretical models indicate (e.g., Sasaki, 2023), the size of population decline might play a role. The median of the decline observations in the sample is -0.26 percent, with an interquartile range from -0.45 to -0.10 percent, and with only few observations exceeding the -1 percent threshold (Figure 2.1). The value of -0.26 percent is close to the median of the projected annual changes in the aggregate of advanced economies until 2040, as mentioned above. Still, there are countries where the projection suggests the median of the annual changes to be close to or even exceeding -1 percent (e.g., Italy, Japan, or Germany).

On the other hand, observed decline periods in the past appear to be shorter compared to projected decline periods in future, questioning in how far our findings are relevant for the shrinkage that advanced economies are facing. Yet, projected population changes are usually derived from deterministic frameworks (e.g., UN, 2019) and, importantly, driven by constant or smoothly evolving migration flows; this disregards fluctuations in migration patterns and other demographic factors, and thus overestimates the endurance of future decline periods. In other words, the future will not be as homogeneous as long-term projection models make it appear. Against this backdrop, we are confident that relying on a smooth-transition specification is not only suitable to analyze past population changes, but also provides plausible insights for the demographic future. Additionally, we address this issue in the upcoming robustness section by varying the smoothing parameter of regime probabilities above, yielding and implying longer periods of decline among the observations in the past.

2.5.2 Robustness

We check the plausibility of our results by applying a series of robustness checks, thereby addressing apparent and frequently discussed factors we have not explicitly accounted for in our baseline specification. In each case, the corresponding plots can be found in Appendix 2.D.

First, the data underlying our estimation covers a long period in which large-scale social, technological, and economic changes have occurred. This raises questions as to whether the "nature" of macroeconomic interdependencies might have changed over time and, as a consequence, questions the **parameter constancy assumption** embodied in our baseline specification. We use a straightforward approach to demonstrate the robustness of our findings by splitting the sample in 1950 — which is the first post-war observation in our setting — and estimating a separate linear model for 1950–2019.[10] The results are shown in Figure 2A.3. The trajectories of the derived impulse responses are remarkably similar for both samples, with remaining differences mostly stemming from contemporaneous effects. Based upon this analysis, we argue that the assumption of parameter constancy is reasonable, thus our results appear to be robust.

Second, in a similar vein, social, technological, and economic differences do not only exist in time, but also across countries. In the case of migration, for example, the strongly changing patterns for the countries in our panel are well documented — over the course of the past 140 years as well as between countries (Ferrie & Hatton, 2015). In the baseline model, we account for time-invariant unobserved heterogeneity by the inclusion of μ_i. Now, we evaluate whether our model is also robust to the inclusion of **country-specific trends**. We allow for the changes in trends by including separate country-specific trends for the pre-war (linear), the interwar (linear), as well as the post-war period (logarithmic). The functional form of the time trends was chosen after visual inspection of the data, which is supported by fit measures. Figures 2A.4 and 2A.5 display the impulse responses that resemble the baseline findings in most cases. This is reassuring in view of the high flexibility of deterministics that we allowed for. A moderate deviation is given by the flat GDP per capita response in times of decline, compared to an insignificant increase in the baseline. This is connected to a somewhat weaker capital response.

Third, advanced economies, and thus their labor markets, are anything but entities independent from each other — a fact that necessarily needs to be accounted for in a given empirical strategy. However, as argued by Pedroni (1999) and others, a common way to account for **cross-sectional dependence** is to demean over the cross-section,

[10] Estimating nonlinear models for these subsamples is not feasible due to the lack of a sufficient number of decline observations.

as done by introducing δ_t in the estimation above. Another way to account for cross-sectional dependence, and in doing so a robustness check, is to introduce an additional continuous regressor, such as world GDP (less a country's own; e.g., Comunale 2022). We test the robustness of our specification accordingly, calculating world GDP from GDP per capita and population data from Bolt & van Zanden (2020), and include the growth rate of the contemporaneous period as an exogenous predictor. Figures 2A.6 and 2A.7 present the results. For both regimes, the impulse responses are very similar to those of the baseline specification. Similarly, populations across countries are not independent from each other, but connected by migration flows. This raises the question of another adjustment channel: When a country enters population decline, the adverse consequences may be mitigated by increasing immigration from other countries. Yet, this mitigation potential may vanish if these sending countries enter population decline as well. Again, we check the robustness of our findings accordingly, here by including the growth rate of the aggregate working-age population of all other countries in our sample. Figures 2A.8 and 2A.9 display the results, which are also very similar to the baseline. Based upon these findings, we conclude that our results are robust in terms of unaccounted cross-sectional dependence.

Fourth, in distributing growth and decline probabilities across the panel, we imposed **parameter assumptions** on the transition function. In order to investigate whether imposing different assumptions alters our results, we conduct two robustness checks. First, rather than assuming $\kappa = Q_1^{G,z}$, we set $\kappa = Q_1^z$, which is the lower quartile across all observations, growth and decline, and corresponds to a value of 0.38 percent. Figures 2A.10 and 2A.11 show the results. While the results for the growth regime for this robustness check are very similar to those of the baseline specification, the decline regime shows some differences. While the findings for the labor force participation rate are robust, the robustness check suggests a slight increase in unemployment. However, the confidence interval of the baseline specification is wide. Moreover, the robustness check suggests some differences in productivity, possibly driven by a longer-lasting increase in the capital-labor ratio. Nevertheless, the main results, that the labor supply reaction is more pronounced compared to the growth regime as well as a different effect on unemployment in the long run, still hold. Second, rather than using $\lambda = 100$, we impose $\lambda = 200$ in order to evaluate the effect of using a different smoothing parameter. Figures 2A.12 and 2A.13 display the corresponding results, which show only minor differences to the baseline results. Overall, these results indicate robustness towards potential misspecification of the transition function.

Fifth, the effects of **population aging** on the economy and the labor market have already drawn widespread attention in the literature (among many: Acemoğlu & Restrepo, 2017; Aksoy et al., 2019; Börsch-Supan, 2008). In our baseline specification, we do not explicitly control for any age structure underlying the included working-age population. However, since we include year effects in our baseline specification and changes in the age structure exhibit strong similarities across advanced economies (see, e.g., Reher 2015 for a discussion on population aging across countries due to *baby booms* and *busts*), we argue that most of these effects have already been captured. Still, to strengthen our argumentation and to account for possible effects stemming from country-specific variations in demographic trends such as boom-and-bust cycles, we conduct another robustness check by explicitly including information on age structure. Following Aksoy et al. (2019), we include contemporaneous shares of age groups as exogenous predictors.[11] Figures 2A.14 and 2A.15 present the results. The results show only very slight differences compared to the baseline specification. This confirms the expectation that age structure effects are no important disregarded factor.

Eventually, we evaluate the sensitivity of the results for the capital-labor ratio to **changed depreciation rates** by assuming lower (2.5 percent) and higher (7 percent) values. We find these comparison values by following the assumptions of Xiao et al. (2021) for depreciation rates over time in low- and high-income countries. In Figure 2A.16, we visualize the effects for both the growth and the decline regime simultaneously. The comparison of the results from the point estimates indicate only minor differences — with more pronounced changes for the 2.5 percent depreciation rate and less pronounced effects for the 7 percent depreciation rate case. But importantly, in the case of the 7 percent depreciation rate, only some intermediate years in both regimes indicate significant effects, the long-run effect is insignificant. Thus, the sensitivity analysis demonstrates that the significance of the effects of population changes on the capital-labor ratio are dependent upon the assumed depreciation rate. Put differently, the finding on significant long-run changes in the capital-labor ratio as a consequence of population shocks does not necessarily hold. Still, the point estimates suggest large effects, irrespective of the assumed depreciation rate.

[11] Yet, as we are using lagged births as instruments, we already account for the implied change in the age structure due to inflows and outflows. To address the corresponding endogeneity issue, we include the shares of ten-year age groups among those aged 20–59 years as a proxy. In doing so, we only include information on age structure that is independent of inflows and outflows due to lagged births — and control for the effects of the accompanying heterogeneity.

2.6 Conclusion

According to recent projections, most advanced economies will face population decline in the years and decades to come, providing a challenging demographic context in the short to the medium and long term. Notably, decline patterns are expected to be particularly pronounced among those of working age. Although a decreasing population may have profound economic implications, above all in the labor market, there is still little theoretical and empirical evidence on this issue. We contribute to this sparse body of literature by focusing on the latter and compile a new historical dataset using more than 100 individual sources, containing information on demographics (population, births, mortality) and labor market variables (real GDP, real investment, real wages, employment, unemployment, participation rates, hours worked) to analyze the labor market effects of population decline from a macroeconomic point of view.

Notably, this research objective does not only call for combining information from several countries, but also for identifying causal effects of population changes and differentiating between times of demographic growth and decline. Tailoring our modeling approach to these requirements, we combine a reduced form panel model with an instrumental variable approach and a smooth-transition specification. We identify structural population shocks in the reduced-form residuals using lagged births as external instruments for working-age population inflows and outflows, and derive regime-dependent orthogonal impulse response functions to trace the effects of positive (negative) population shocks in the labor market in times of population growth (decline).

So far, the existing literature has relied on theoretical models to analyze the economic effects of population decline. Empirically, the effects have, as yet, been unclear, and our paper addresses this gap. The results resemble the conclusion that maintaining economic growth is generally feasible and add additional insights: We find that population changes pass through to the labor market more quickly in times of decline compared to times of growth. Subsequently, regime-dependent adjustment processes unfold. Labor force participation increases as a response to the decline in labor supply, and in the long term it does so more strongly than it shrinks in times of growth. This rise in overall labor force participation likely plays a crucial role for further observed patterns, for example in decelerating initially swift disinvestment tendencies in times of population decline. By contrast, we find no significant changes in the unemployment rate as a response to population decline. Similarly, despite declining labor supply, we do not find any significant changes of wages as a shortage indicator over time. Eventually, while both our results and the existing economic literature on population decline point to negative

effects on productivity, the findings of this paper suggest that corresponding negative effects for economic growth are mitigated by increases in participation and the capital-labor ratio.

Thus, the paper suggests that incorporating elastic labor supply into future model-based approaches that analyze the effects of population decline may enhance the resulting insights. Importantly, two properties should be considered: First, increases in participation are limited, eventually by the population size. Second, adjustments along the participation dimension may take time, as our results suggest. Similar results exist for other interventions. For example, there is evidence that active labor market policies (ALMPs) increase labor force participation rates (Escudero, 2018) — but short-term effects of ALMPs are substantially smaller than medium- to long-term effects (Card et al. 2018 for ALMPs targeting persons inside the labor force).

Furthermore, and despite some caveats for the interpretation of the results as discussed in Section 2.5, the paper offers additional contributions, both to the academic literature as well as in a broader policy perspective. Regarding the academic literature, the further contribution is threefold: Data relatedly, the paper offers a (partially) novel compilation of historical labor market data, providing both a suitable database for future research projects as well as a suitable starting point to improve existing, or create new, historical datasets. Methodically, it expands the existing body of literature by combining a proxy SVAR identification strategy with a nonlinear reduced form panel model. Substantively, it proposes to use, and implements, lagged births as a suitable instrument for the identification of population shocks. Jointly, these contributions permit, for the first time, the conducting of a comprehensive empirical analysis of the labor market effects of population decline from a macroeconomic perspective.

However, also in the broader policy context, the results bear importance. In light of the imminent population decline across advanced economies and corresponding discussions concerning labor supply shortages, findings such as increasing labor force participation in response to population decline are of crucial importance — and indicate that adjustments are feasible. This point must be qualified in its translation into policy. Clearly, the activation of individuals outside of the labor force is limited beyond a certain point; this applies, in particular, to demographic groups that already exhibit high participation rates. Therefore, adjustment is likely to become more critical the more the existing potential is exhausted. Furthermore, the systematic responses to demographic shocks as measured in the model based on empirical data include the political reactions that have appeared in the past. Therefore, if policymakers want to change the outcome, their measures would have to go beyond the typical reactions of the past.

2.A Appendix A: Excluded Observations

As outlined in the main text, we exclude a number of observations from the identification of the structural population shocks. In the table below, we provide information on country, period, and reason for each case. Additionally, we also indicate how many observations are effectively lost — that is, have not already been excluded due to, e.g., being a war year.

Table 2A.1: Descriptive Overview of the Excluded Observations in the Identification Procedure

Country	**Years**	**Reason**	**Obs. excl.**
AUS	1900–1916	For this period, only estimated annual data from Gapminder (2015a) is available for outflows.	12
AUT	1954–1955	The inflows in this period are strongly driven by the unprecedented increase in births in Austria following the annexation by Germany in 1939. We categorize these observations as outliers.	2
AUT	2004–2005	The outflows in this period are strongly driven by the unprecedented increase in births in Austria following the annexation by Germany in 1939. We categorize these observations as outliers.	2
DEU	1875–1883	For this period, only estimated annual data from Gapminder (2015a) is available for outflows.	7
GBR	1875–1907	As above, Gapminder (2015a).	31
ITA	1900–1928	As above, Gapminder (2015a).	18
JPN	1900–1939	As above, Gapminder (2015a).	18
JPN	1959–1963	As above, Gapminder (2015a).	5
JPN	2009–2013	As above, Gapminder (2015a).	5
NZL	1900–1921	As above, Gapminder (2015a).	12
USA	1900–1921	As above, Gapminder (2015a).	37

Author's own computations.

2.B Appendix B: Additional Impulse Response Functions

With our econometric strategy, we are able to compute impulse response functions to a structural population shock for each of the seven endogenous variables in our model. Moreover, we may obtain the impulse response functions to an additional series of relevant labor market indicators (Figures 2.7 and 2.8) by linking the coefficients of the main results (Figures 2.5 and 2.6) to each other. Below, a detailed outline of the calculation of each of these additional impulse response functions is given.

Let GDP_t and POP_t be the estimated elasticities of a structural population shock on real GDP and on the working-age population at time t. Then, the elasticity for GDP per capita in the same period, $GDPpc_t$, is given by

$$GDPpc_t = GDP_t - POP_t. \tag{2A.1}$$

Let LF_t be the estimated elasticity of a structural population shock on the labor force at time t. Then, the elasticity for the labor force participation rate in the same period, $LFPR_t$, is given by

$$LFPR_t = LF_t - POP_t. \tag{2A.2}$$

Let EMP_t be the estimated elasticity of a structural population shock on employment at time t. Then, the elasticity for the employment rate in the labor force in the same period, ER_t, is given by

$$ER_t = EMP_t - LF_t. \tag{2A.3}$$

Let AVH_t be the estimated elasticity of a structural population shock on average hours worked at time t. Then, the elasticity for productivity in the same period, $PROD_t$, is given by

$$PROD_t = GDP_t - (EMP_t + AVH_t). \tag{2A.4}$$

Let INV_0 be the estimated elasticity of a structural population shock on investment in period 0 and let ϑ be the annual depreciation rate. Departing from a steady-state assumption, that is, in the absence of the structural population shock there would be no changes in the variables under consideration, then the ratio of annual investment to the capital stock is equal to ϑ. This assumption allows the derivation of the contemporaneous effect of a structural population shock on the capital stock CAP_0 as

$$CAP_0 = INV_0 * \vartheta. \tag{2A.5}$$

Subsequently, from period t onward, with in this case $t = 1, \ldots, H$, and H is equal to the chosen horizon length for computing the impulse response functions, the effect is given by

$$CAP_t = CAP_{t-1} - CAP_{t-1} * \vartheta + INV_t * \vartheta. \tag{2A.6}$$

Eventually, the elasticity for the capital-labor ratio at time t, KLR_t, is given by

$$KLR_t = CAP_t - (EMP_t + AVH_t). \tag{2A.7}$$

2.C Appendix C: Identification

The identification of structural population shocks is of key importance for our analysis. We do this in order to ensure that we estimate the causal effect of a population change and avoid biased results due to endogeneity. Possible sources of bias range from GDP and wages to employment, among others, all of which can be assumed to possibly exert effects on population, for example as push and pull factors driving migration dynamics.

Below, we illustrate the results of an identification without instruments. We follow the common identification strategy and impose a lower triangular matrix. In doing so, we assume that the population shock affects all variables in the model in the same period, but not vice versa. We implement the identification of regime-dependent shocks by regressing the residuals of each equation on the residuals of the population equation, weighted by the corresponding regime probabilities. Figure 2A.1 and Figure 2A.2 visualize the results of this specification. As illustrated, this identification strategy appears to capture an additional correlation between population and the other variables in the model. In particular, for GDP, employment, and investment we see far stronger contemporaneous effects. As noted above, observing an additional strong correlation between population and these variables is consistent with typical push-pull frameworks. Particularly, given that reverse causality of economic variables on population is positive, the figures display

Figure 2A.1: Robustness Check: Shock Identification, Growth Regime

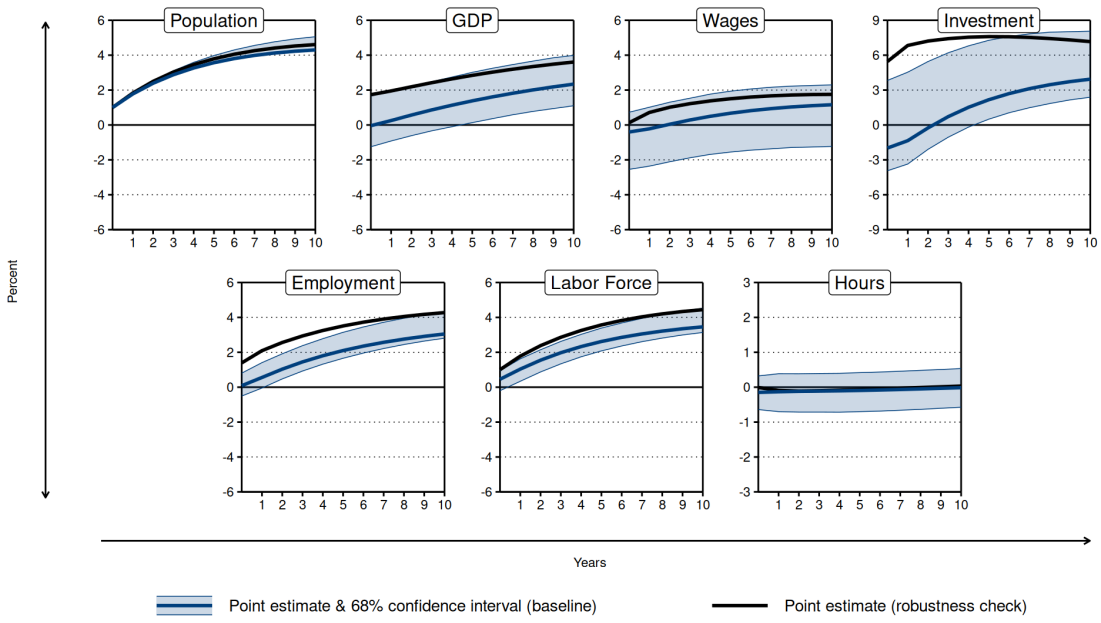

Notes: Author's own calculations and illustration.

Figure 2A.2: Robustness Check: Shock Identification, Decline Regime

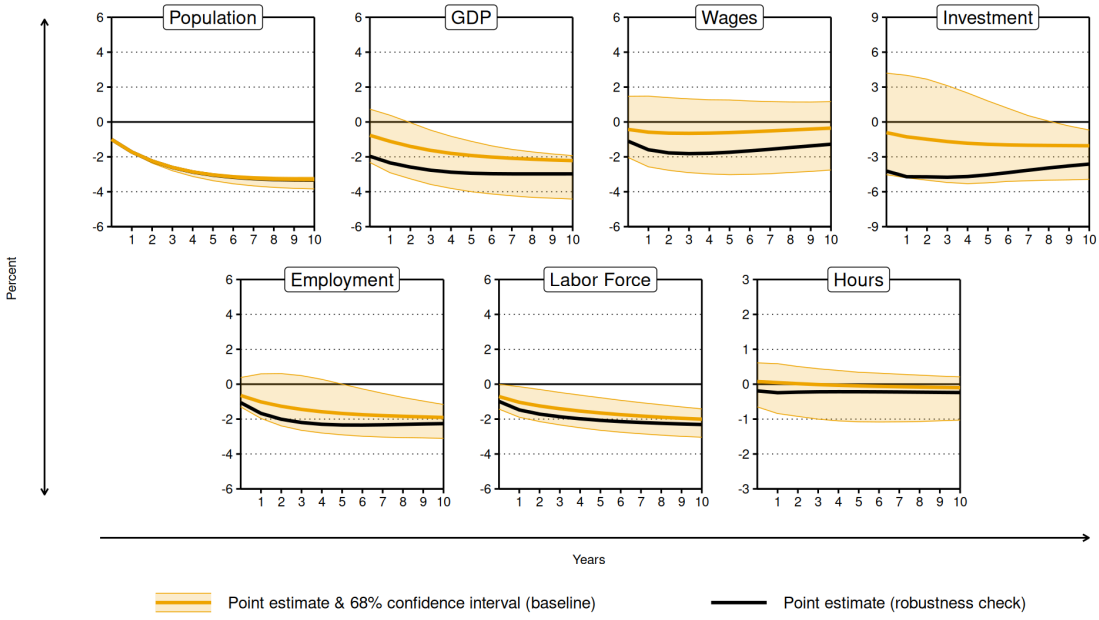

Notes: Author's own calculations and illustration.

exactly the bias one expect when ignoring simultaneity. Moreover, as an example, the supposedly strong effects of population on GDP cannot necessarily be reconciled with existing evidence (e.g., Headey & Hodge, 2009). Thus, the results based solely on a lower triangular matrix in comparison to our baseline results underpin the need for an instrument-based identification strategy.

2.D Appendix D: Robustness

Figure 2A.3: Robustness Check: Sample Split, Linear

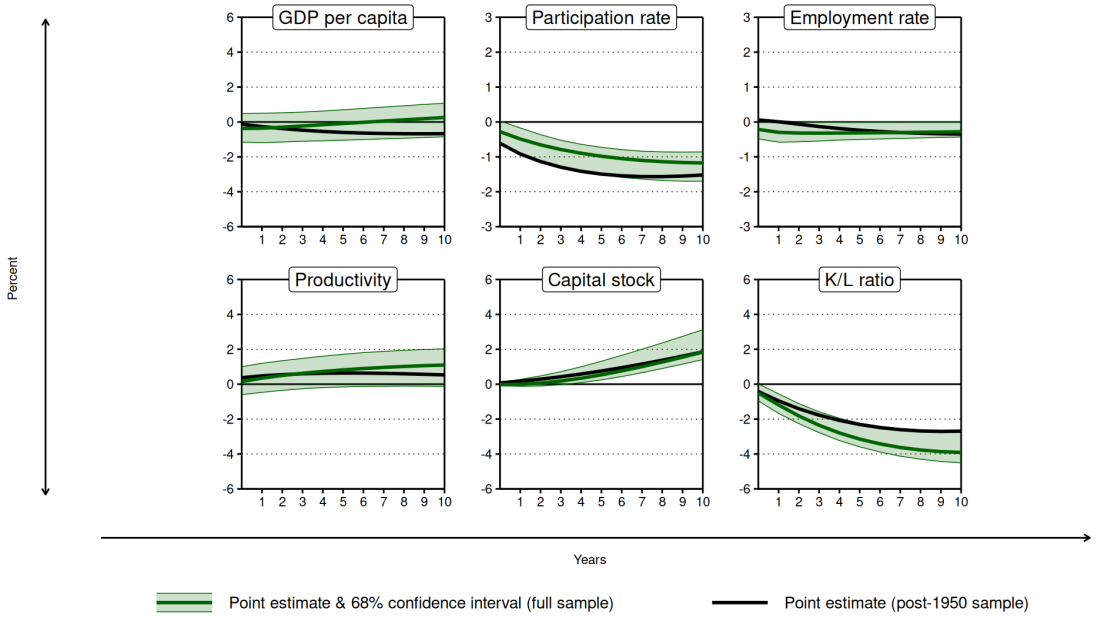

Notes: Impulse response functions for the capital stock and the capital-labor ratio are calculated by assuming a depreciation rate of 4.6 percent. For further information on the derivation of the additional impulse response functions, see Appendix 2.B. Author's own calculations and illustration.

Figure 2A.4: Robustness Check: Country Trends, Growth Regime

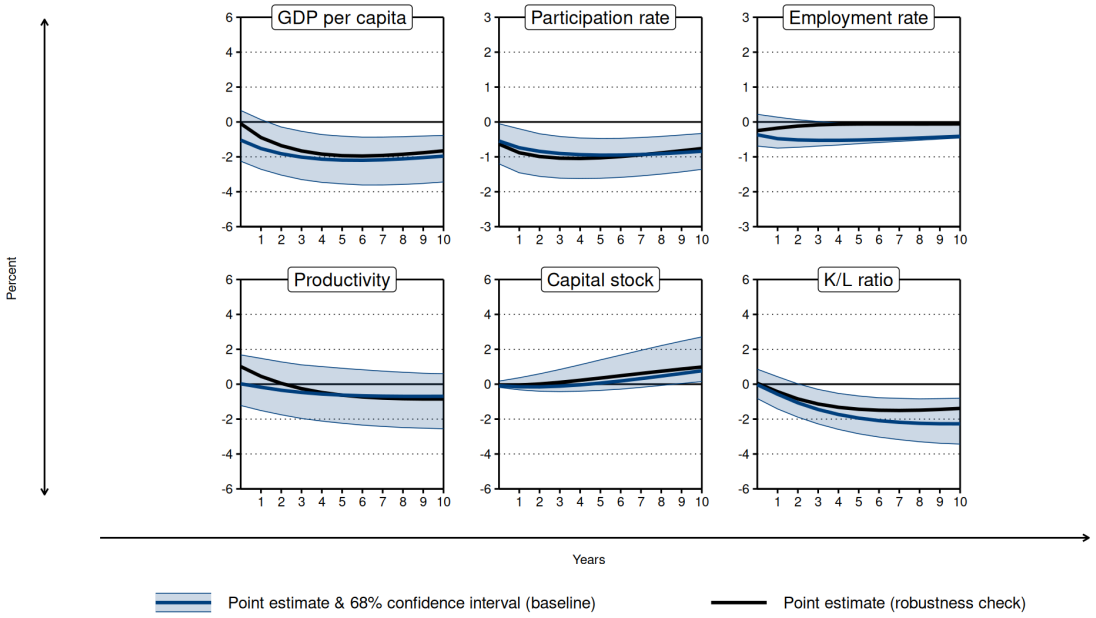

Notes: Impulse response functions for the capital stock and the capital-labor ratio are calculated by assuming a depreciation rate of 4.6 percent. For further information on the derivation of the additional impulse response functions, see Appendix 2.B. Author's own calculations and illustration.

Figure 2A.5: Robustness Check: Country Trends, Decline Regime

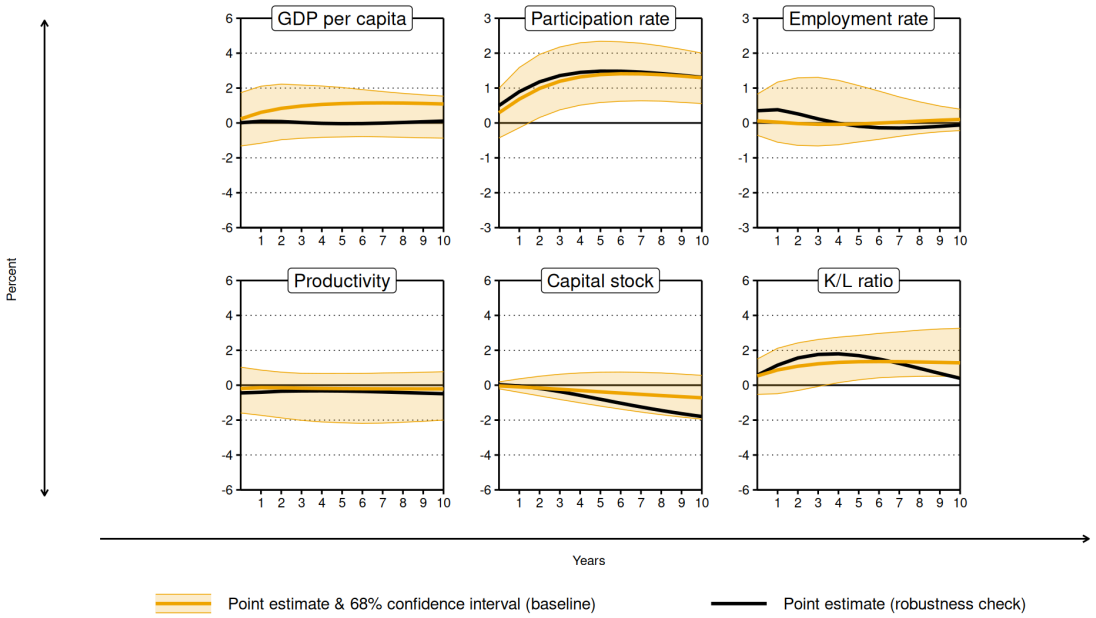

Notes: Impulse response functions for the capital stock and the capital-labor ratio are calculated by assuming a depreciation rate of 4.6 percent. For further information on the derivation of the additional impulse response functions, see Appendix 2.B. Author's own calculations and illustration.

Figure 2A.6: Robustness Check: World GDP, Growth Regime

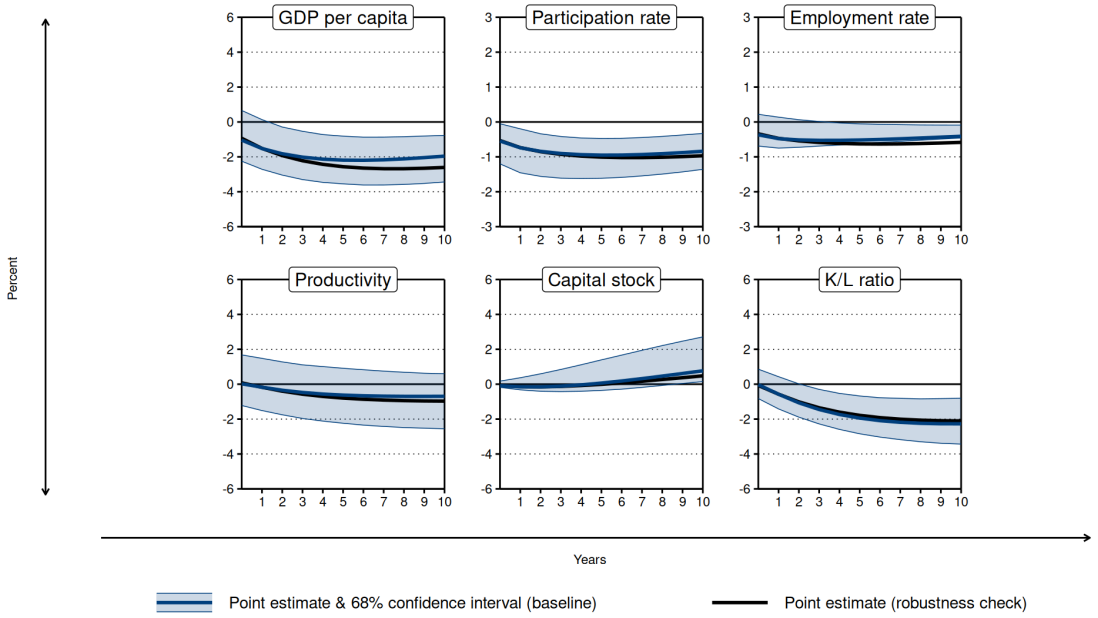

Notes: Impulse response functions for the capital stock and the capital-labor ratio are calculated by assuming a depreciation rate of 4.6 percent. For further information on the derivation of the additional impulse response functions, see Appendix 2.B. Author's own calculations and illustration.

Figure 2A.7: Robustness Check: World GDP, Decline Regime

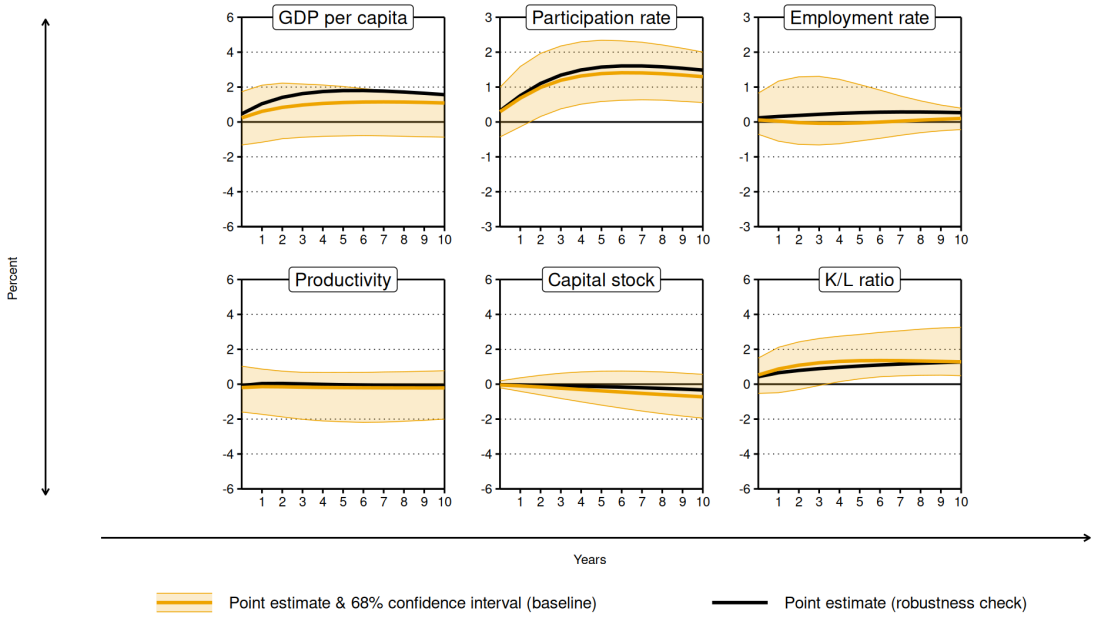

Notes: Impulse response functions for the capital stock and the capital-labor ratio are calculated by assuming a depreciation rate of 4.6 percent. For further information on the derivation of the additional impulse response functions, see Appendix 2.B. Author's own calculations and illustration.

Figure 2A.8: Robustness Check: World Population, Growth Regime

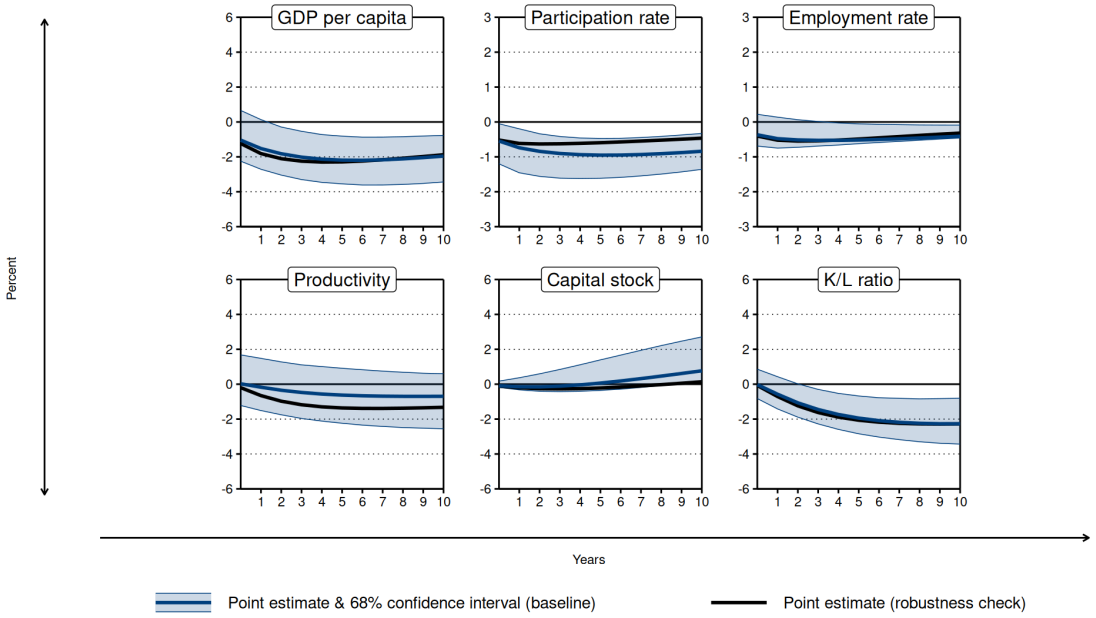

Notes: Impulse response functions for the capital stock and the capital-labor ratio are calculated by assuming a depreciation rate of 4.6 percent. For further information on the derivation of the additional impulse response functions, see Appendix 2.B. Author's own calculations and illustration.

Figure 2A.9: Robustness Check: World Population, Decline Regime

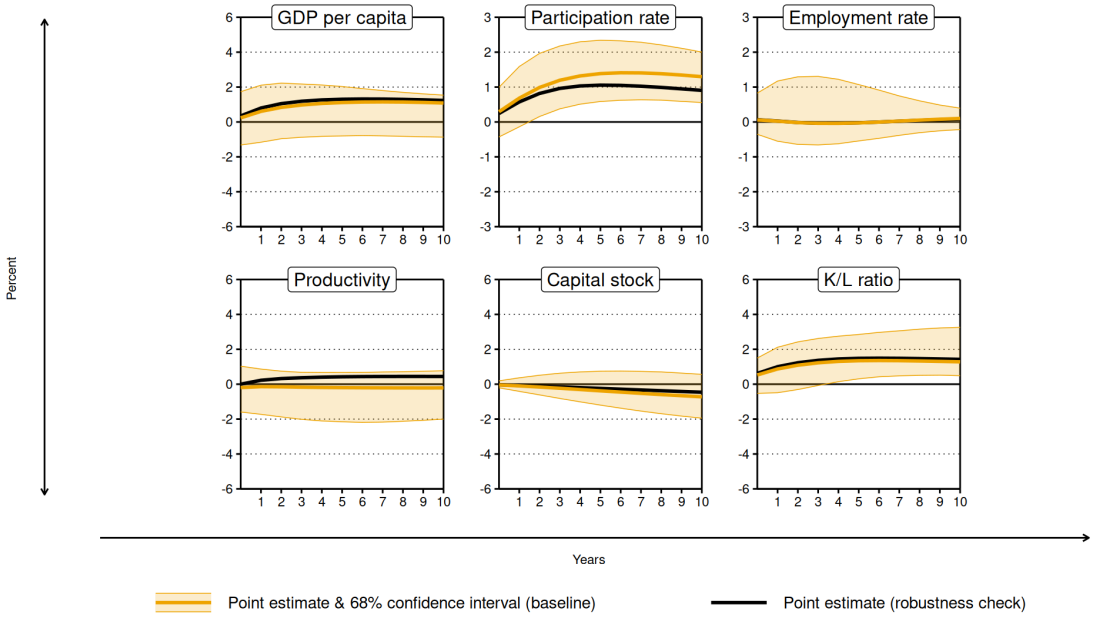

Notes: Impulse response functions for the capital stock and the capital-labor ratio are calculated by assuming a depreciation rate of 4.6 percent. For further information on the derivation of the additional impulse response functions, see Appendix 2.B. Author's own calculations and illustration.

Figure 2A.10: Robustness Check: Switching Point, Growth Regime

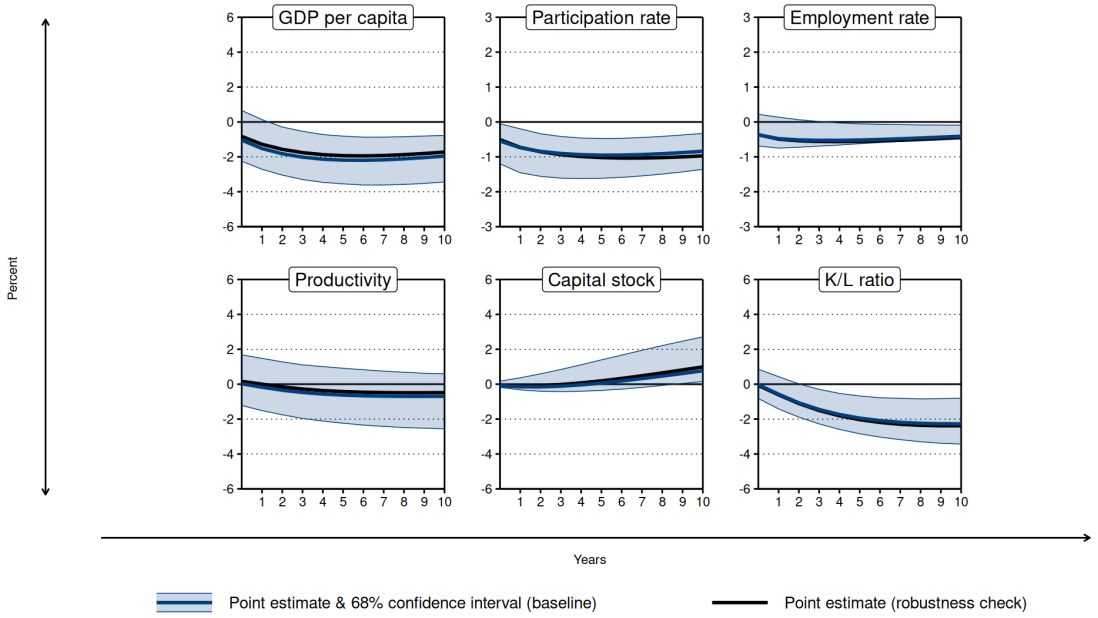

Notes: Impulse response functions for the capital stock and the capital-labor ratio are calculated by assuming a depreciation rate of 4.6 percent. For further information on the derivation of the additional impulse response functions, see Appendix 2.B. Author's own calculations and illustration.

Figure 2A.11: Robustness Check: Switching Point, Decline Regime

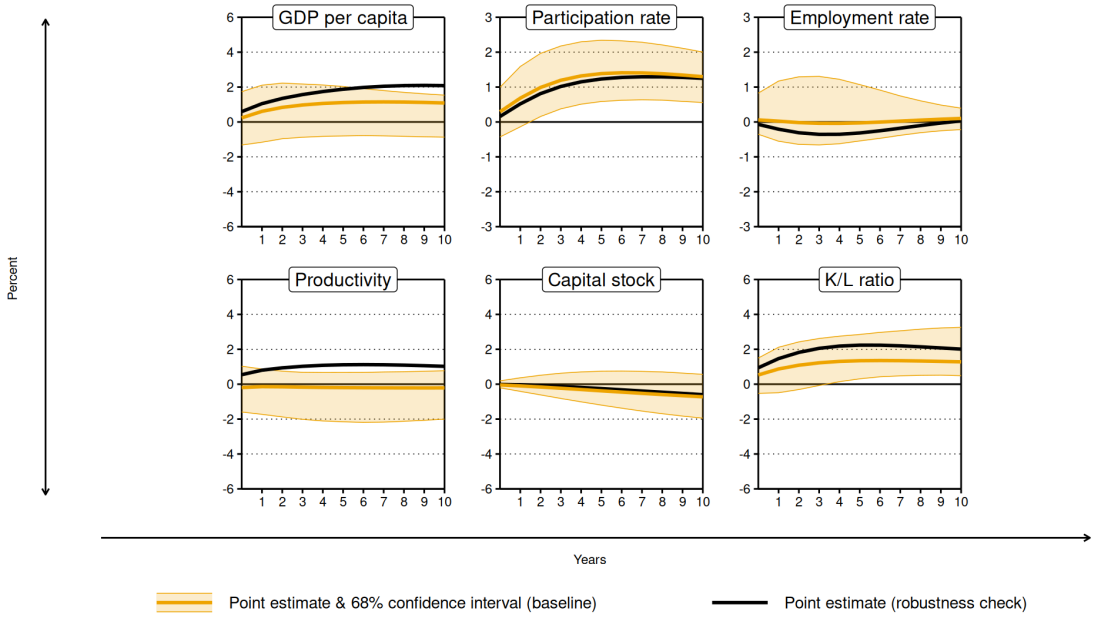

Notes: Impulse response functions for the capital stock and the capital-labor ratio are calculated by assuming a depreciation rate of 4.6 percent. For further information on the derivation of the additional impulse response functions, see Appendix 2.B. Author's own calculations and illustration.

Figure 2A.12: Robustness Check: Smoothing Parameter, Growth Regime

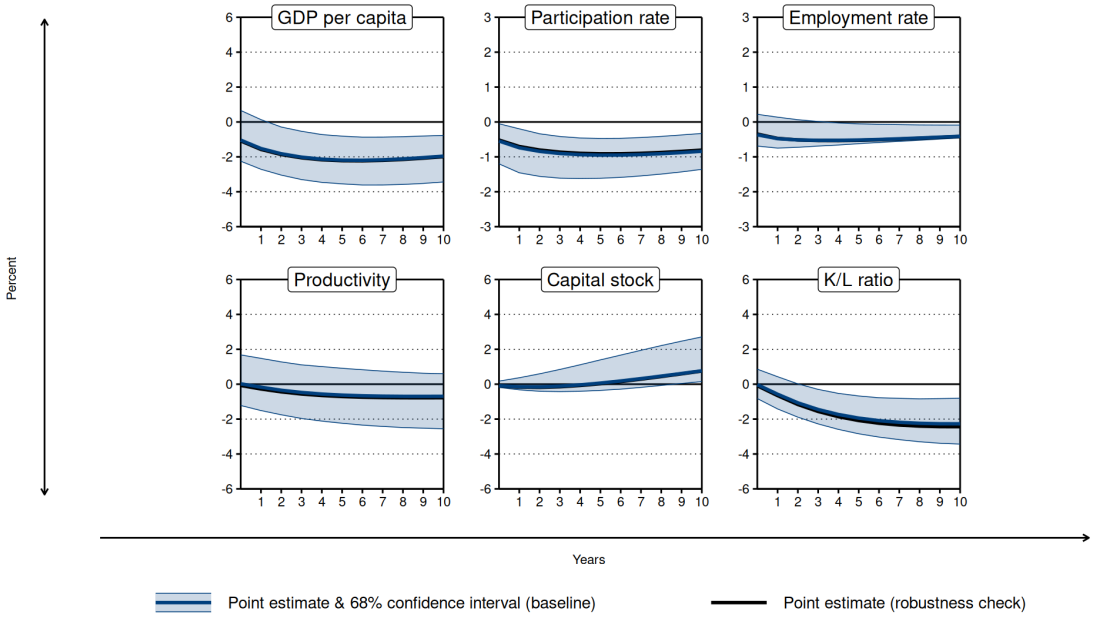

Notes: Impulse response functions for the capital stock and the capital-labor ratio are calculated by assuming a depreciation rate of 4.6 percent. For further information on the derivation of the additional impulse response functions, see Appendix 2.B. Author's own calculations and illustration.

Figure 2A.13: Robustness Check: Smoothing Parameter, Decline Regime

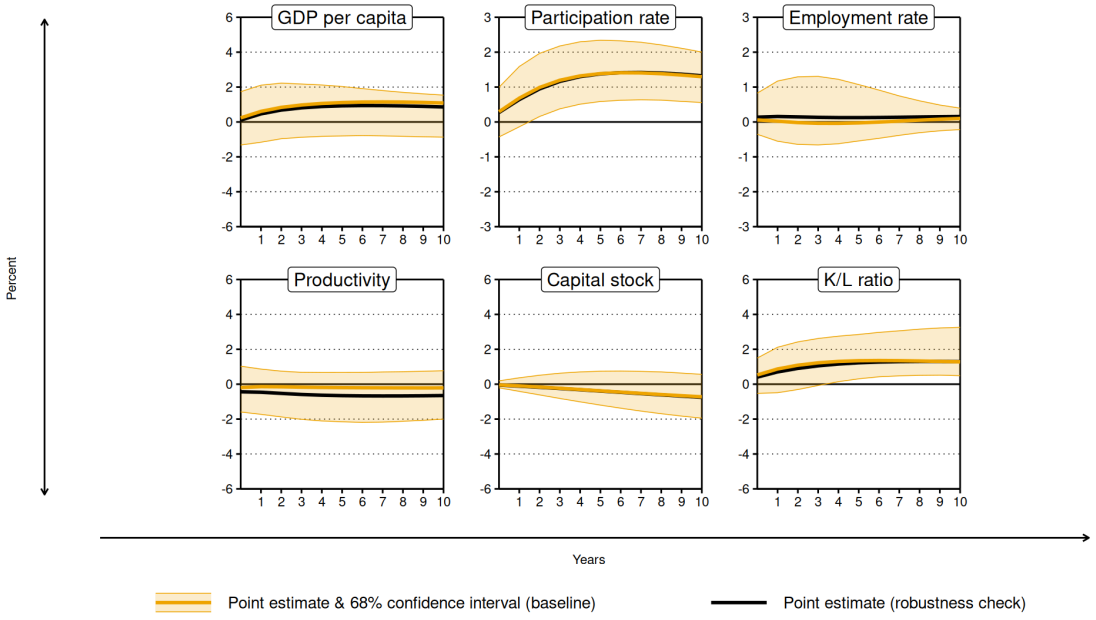

Notes: Impulse response functions for the capital stock and the capital-labor ratio are calculated by assuming a depreciation rate of 4.6 percent. For further information on the derivation of the additional impulse response functions, see Appendix 2.B. Author's own calculations and illustration.

Figure 2A.14: Robustness Check: Age Structure, Growth Regime

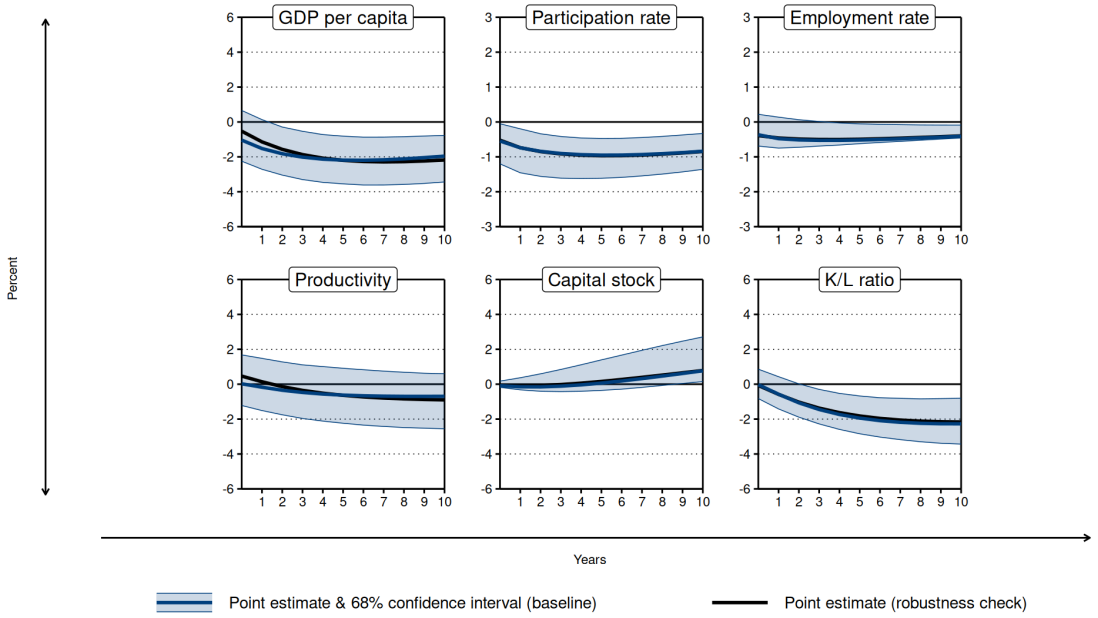

Notes: Impulse response functions for the capital stock and the capital-labor ratio are calculated by assuming a depreciation rate of 4.6 percent. For further information on the derivation of the additional impulse response functions, see Appendix 2.B. Author's own calculations and illustration.

Figure 2A.15: Robustness Check: Age Structure, Decline Regime

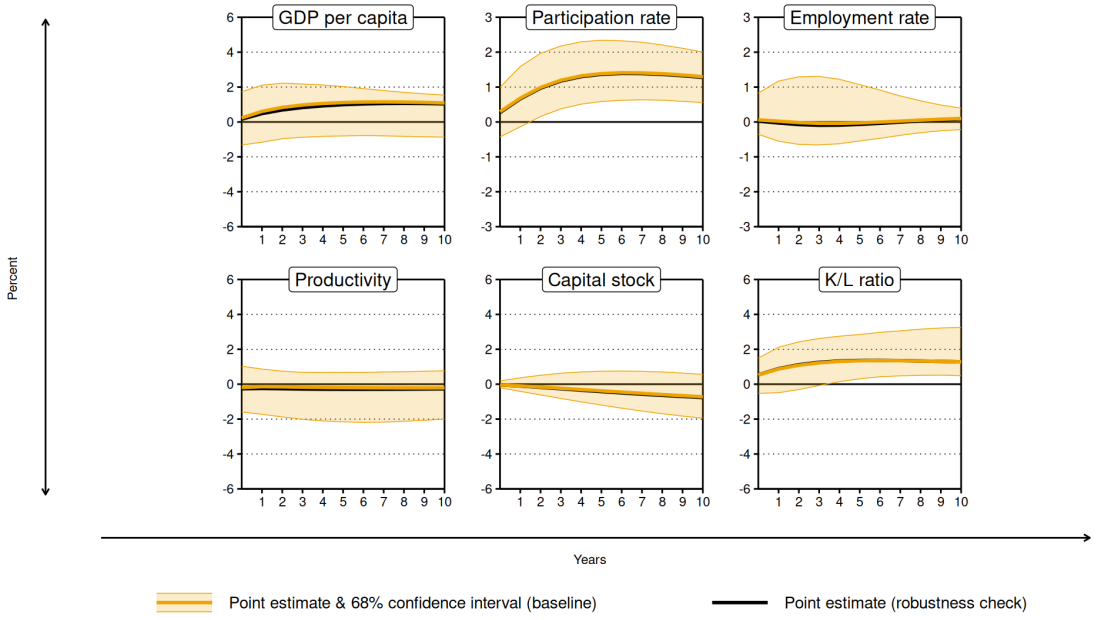

Notes: Impulse response functions for the capital stock and the capital-labor ratio are calculated by assuming a depreciation rate of 4.6 percent. For further information on the derivation of the additional impulse response functions, see Appendix 2.B. Author's own calculations and illustration.

Figure 2A.16: Robustness Check: Depreciation Rates

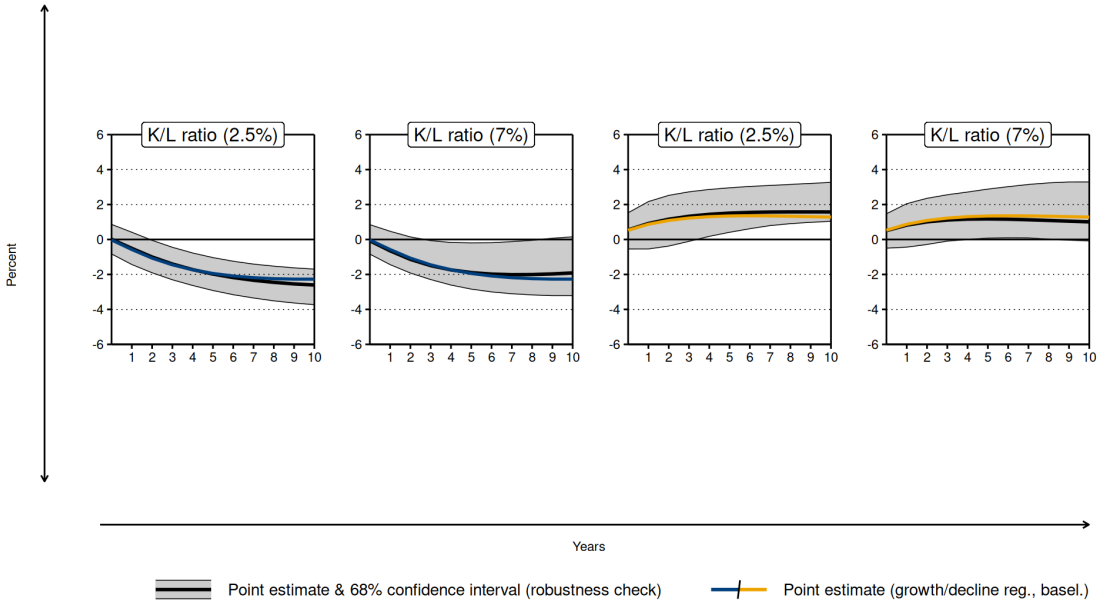

Notes: For further information on the derivation of the additional impulse response functions, see Appendix 2.B. Author's own calculations and illustration.

2.E Appendix E: Data Sources and Data Preparation

Note: Unless otherwise indicated, we chain-link time series using overlapping years.

2.E.1 Demographic Variables

Population by age. Population by broad age groups (0–14 years, 15–64 years, 65 years and above) at mid-year. For population data that is only available for another date, we follow the Human Mortality Database (HMD, 2023) methodology and estimate the population as of mid-year by linear interpolation.

Australia 1860–1901: Gapminder (2015b), data for total population | 1901–1921: Smith (2009), data taken from Hyndman (2017) | 1921–2019: HMD (2023) | 2019–2025: UN (2019)

Austria 1860–1870: Bolt & van Zanden (2020), data for total population | 1870–1914: Ediev & Gisser (2007) | 1914–1923: Bolt & van Zanden (2020), data for total population, as well as shares by age groups in 1914 and 1923 from Ediev & Gisser (2007). In between, we use information on births to obtain annual variation — see detailed explanation of construction of these series in the text for Germany below (1911–1950 period). For more fine-grained age groups, we linearly interpolate the shares. | 1923–1940: Ediev & Gisser (2007) | 1940–1947: Bolt & van Zanden (2020), data for total population, as well as shares by age groups in 1940 from Ediev & Gisser (2007), and in 1947 from HMD (2023). In between, we use information on births to obtain annual variation. | 1947–2019: HMD (2023) | 2019–2025: UN (2019)

Belgium 1860–1914: HMD (2023) | 1914–1919: Bolt & van Zanden (2020), data for total population, as well as shares by age groups in 1914 and 1923 from HMD (2023). In between, we use information on births to obtain annual variation. | 1919–2019: HMD (2023) | 2019–2025: UN (2019)

Denmark 1860–2019: HMD (2020) | 2019–2025: UN (2019)

Finland 1860–1866: Bolt & van Zanden (2020), data for total population | 1866–1878: Statistics Finland (2020), data is given for 31st December, we assume the data to be representative for 1st January of the subsequent year — this procedure follows the literature (e.g., Klüsener et al., 2018) | 1878–2019: HMD (2023) | 2019–2025: UN (2019)

France 1860–2016: HMD (2023)| 2019–2025: UN (2019)

Germany 1860–1872: Bolt & van Zanden (2020), data for total population | 1872–1911: Lösch (1936), data largely taken from the Gesis database, but we apply some adjustments (error correction) using the original source. The data is given for 31st December, we assume 1st January. | 1911–1950: Since the data for the total population by Bolt & van Zanden (2020) contains level breaks, we use information from Destatis (1972) for the population on the territory of the FRG in 1910, 1939, and 1946 to the scale their series. Then, we use information on population shares by broad age groups at census dates in 1910 from Lösch (1936), in 1919, 1925, 1933, 1939, and 1946 from Franzmann (2015), and in 1950 from Sensch (2004), original source is Rothenbacher (2002). Using these shares as well as the scaled annual series for the total population from Bolt & van Zanden (2020), we obtain "reference figures" for age groups at census dates. To obtain

annual variation between census dates, we use information on births. For those below the age of 15, we add births in the same year as inflows and subtract births lagged 15 years as outflows. For those aged 15–64 years, we add births lagged 15 years as inflows and subtract births lagged 65 years as outflows. For those aged 65 years and above, we add births lagged 65 years as inflows. We apply this procedure for each intercensal period and scale the obtained series by their respective deviation from the subsequent reference figure. We apply the resulting shares for age groups to the scaled annual series as outlined above to ensure consistency. Information on lagged births is subject to the same adjustment for cohort mortality as outlined in the main text. For more fine-grained age groups, we linearly interpolate the respective shares, using the same sources as outlined. | 1950–1951: Bolt & van Zanden (2020), data for total population | 1951–1956: Destatis (2023), data refers to East and West Germany | 1956–2019: HMD (2023), up to 1990 for West Germany. We calculate the relation of the age shares for all of Germany and West Germany in 1990 and interpolate its deviation back to 1956. We scale the population shares for West Germany by the resulting series and obtain population figures by age group by multiplication with the chain-linked overall working-age population. | 2019–2025: UN (2019)

Italy 1860–1872: Bolt & van Zanden (2020), data for total population | 1872–2019: HMD (2023) | 2019–2025: UN (2019)

Japan 1860–1872: Bolt & van Zanden (2020), data for total population | 1872–1920: Umemura et al. (1988), data taken from RCISSS (2016). In this source, only age-specific data for those aged 60 years and above is available. To separate the age groups 15–64 years from those 65 years and above, we linearly interpolate the respective shares at census dates in 1884, 1893, 1903, 1913, and 1920 as given by Mitchell (2013). The data is given for 31st December, we assume 1st January. | 1920–1940: Statistics Japan (2021) | 1940–1947: Bolt & van Zanden (2020), data for total population, as well as the shares by age groups in 1940 from Statistics Japan (2021) and 1947 as outlined in the following. In between, we use information on births to obtain annual variation. | 1947–2019: Statistics Japan (2021), data is for 1st October, we interpolate to mid-year values. HMD (2023) for 1996–1999, 2001–2004, and 2011–2014 due to breaks after census dates. | 2019–2025: UN (2019)

Netherlands 1860–2019: HMD (2023) | 2019–2025: UN (2019)

Norway 1860–2019: HMD (2023) | 2019–2025: UN (2019)

New Zealand 1860–1871: Bolt & van Zanden (2020), data for total population in Australia | 1871–1901: Bolt & van Zanden (2020), data for total population | 1901–1948: HMD (2023), data for non-Māori population | 1948–2019: HMD (2023) | 2019–2025: UN (2019)

Sweden 1860–2019: HMD (2023) | 2019–2025: UN (2019)

Switzerland 1860–1861: Bolt & van Zanden (2020), data for total population | 1861–1875: BFS (2023), data is given for 31st December, we assume 1st January | 1875–2019: HMD (2023) | 2019–2025: UN (2019)

United Kingdom 1860–1922: HMD (2023), data refer to England, Wales, and Scotland | 1922–2019: HMD (2023) | 2019–2025: UN (2019)

United States 1860–1900: We apply several data preparation steps in order to derive annual series that approximate population by age as closely as possible: We gather data on population

by single age years at census dates in 1880 and 1890 from U.S. Bureau of the Census (1883) and U.S. Bureau of the Census (1895), and for 1900 from U.S. Bureau of the Census (2000). For 1880 and 1890, we smooth the shares of single age years by a centered five-year moving average to cope with age heaping. Additionally, we obtain shares for the 1870 census as follows: We use shares for five-year age groups as given by Mitchell (2013) and obtain the ratio of these shares between 1870 and 1880. We treat these ratios to be representative for the youngest cohort in each age group and linearly interpolate to derive shares for each individual cohort. We then scale the 1880 shares of single age years accordingly and obtain a distribution for 1870. Additionally, we use births data as outlined below. We interpolate cohort shares between census dates and use births to introduce new cohorts. We calculate the ratio of births to population aged 0 years in the census and linearly interpolate this share to scale the entry of new cohorts. Moreover, we scale the resulting overall population in each year by the series given by HSUS (2023). Also, before 1870, we assume all age groups to follow the relative changes of this series. | 1900–1948: U.S. Bureau of the Census (2000) | 1948–2019: HMD (2023) | 2019–2025: UN (2019)

Live births per year.

Australia 1835–1850: Gapminder (2015a) | 1850–1860: births rates from Mitchell (2013) and total population from Bolt & van Zanden (2020) | 1860–2004: HMD (2023)

Austria 1835–1871: Butschek (1992) | 1871–2004: HMD (2023)

Belgium 1835–1840: birth rates from Mitchell (2013) and total population from Bolt & van Zanden (2020) | 1840–2004: HMD (2023)

Denmark 1810–1835: Abildgren (2017), birth rates and population figures | 1835–2004: HMD (2023)

Finland 1835–2004: Statistics Finland (2023)

France 1835–2004: HMD (2023)

Germany 1810–1817: Gapminder (2015a) | 1817–1976: Sensch (2004); we scale this series for 1943 and earlier with the ratio of births according on the territory of the FRG to Destatis (1972) and fill the gaps in 1944 and 1945 as follows: For 1944, we use the relative change in the TFR according to BiB (2023). For 1945, we used the relative change according to Destatis (1972). | 1976–1990: HMD (2023), sum of the births for West Germany and East Germany | 1990–2004: HMD (2023)

Italy 1835–1862: Gapminder (2015a) | 1862–2004: HMD (2023)

Japan 1835–1873: Gapminder (2015a) | 1873–2004: HMD (2023), except for 1941–1943, where we use births derived using the birth rates from Mitchell (2013) and the total population from Bolt & van Zanden (2020) as well as for 1944–1946, where we use Gapminder (2015a).

Netherlands 1810–1850: Smits et al. (2000). | 1850–2004: HMD (2023)

New Zealand 1835–1855: Gapminder (2015a) | 1855–1943: Statistics New Zealand (2002) | 1948–2004: HMD (2023)

Norway 1810–1846: birth rates from Mitchell (2013) and the total population from Bolt & van Zanden (2020). Population data for 1810–1820 derived using the average annual growth rate of 1820–1830. | 1846–2004: HMD (2023)

Sweden 1810–2004: HMD (2023)
Switzerland 1835–1871: HSSO (2022d) | 1871–2004: HMD (2023)
United Kingdom 1810–1841: Gapminder (2015a) | 1841–1855: HMD (2023), data for England and Wales | 1855–1922: HMD (2023), England, Wales, and Scotland | 1922–2004: HMD (2023)
United States 1810–1855: Gapminder (2015a) | 1855–1909: birth rates from Mitchell (2013) and the total population from Bolt & van Zanden (2020) | 1909–1933: NCHS (2023) | 1933–2004: HMD (2023)

Cohort mortality up to 15 and 65 years of age. Available data sources do not cover all years in the sample, thus we augment cohort mortality rates by centered period death rates (by single age years) or use other data preparation methods outlined in detail below.
Australia 1835–1849: We assume the value of 1850. | 1850–1921: We use the ratio of UK cohort mortality in 1850 and 1921, chain-link, and linearly interpolate. | 1921–1986: HMD (2020) | 1986–2001: HMD (2020), centered period death rates | 2002–2004: value of 2001
Austria 1835–1947: Ediev & Gisser (2007), centered period death rates; for missing observations in 1940–1946, we use the relative changes in period death rates as in World War I. | 1947–1987: HMD (2020) | 1987–2002: HMD (2020), centered period death rates | 2003–2004: value of 2002
Belgium 1835–1840: value of 1841 | 1841–1919: HMD (2020), centered period death rates; for 1913–1918, we use the variation in the French period death rates. | 1919–1988: HMD (2020) | 1988–2003: HMD (2020), centered period death rates | 2004: value of 2003
Denmark 1810–1835: value of 1835 | 1835–1989: HMD (2020) | 1989–2004: HMD (2020), centered period death rates
Finland 1835–1878: We use the ratio of Swedish cohort mortality in 1835 and 1878, chain-link, and linearly interpolate in between. | 1878–1988: HMD (2020) | 1988–2004: HMD (2020), centered period death rates
France 1835–1987: HMD (2020) | 1987–2002: HMD (2020), centered period death rates | 2003–2004: value of 2002
Germany 1810–1818: value of 1819 | 1819–1871: We use the variation in Austrian centered period mortality for 1819–1871 according to Ediev & Gisser (2007). | 1871–2004: Destatis (2017)
Italy 1835–1871: value of 1872 | 1872–1987: HMD (2020) | 1987–2004: We use the relative changes in the centered period death rates from HMD (2020). | 2004: value of 2003
Japan 1835–1849: value of 1850 | 1850–1947: We use the ratio of UK cohort mortality in 1850 and 1947, chain-link, and linearly interpolate in between. | 1947–1988: HMD (2020) | 1988–2003: HMD (2020), centered period death rates | 2004: value of 2003
Netherlands 1810–1849: value of 1850 | 1850–1986: HMD (2020) | 1986–2001: HMD (2020), centered period death rates | 2002–2004: value of 2001
New Zealand 1835–1840: value of 1841 | 1841–1901: We use the ratio of UK cohort mortality in 1841 and 1901, chain-link, and linearly interpolate. | 1901–1943: HMD (2020), cohort mortality rates for the non-Māori population | 1948–1983: HMD (2020) | 1943–1948: HMD (2020), centered period death rates for the non-Māori population | 1983–1998: HMD (2020), centered period death rates | 1999–2004: value of 1998

Norway 1810–1845: value of 1846 | 1846–1988: HMD (2020) | 1988–2003: HMD (2020), centered period death rates | 2004: value of 2003
Sweden 1810–1988: HMD (2020) | 1988–2003: HMD (2020), centered period death rates | 2004: value of 2003
Switzerland 1835–1876: We use the ratio of Austrian centered period mortality rates in 1819 and 1876 according to Ediev & Gisser (2007), chain-link, and linearly interpolate. | 1876–1896: HMD (2020), centered period death rates | 1896–1986: HMD (2020) | 1986–2002: HMD (2020), centered period death rates | 2003–2004: value of 2002
United Kingdom 1810–1840: value of 1841 | 1841–1922: HMD (2020), cohort death rates for England and Wales | 1922–1986: HMD (2020) | 1986–2001: HMD (2020), centered period death rates | 2002–2004: value of 2001
United States 1810–1849: value of 1850 | 1850–1933: We use the ratio of UK cohort mortality in 1850 and 1933, chain-link, and linearly interpolate. | 1933–1987: HMD (2020) | 1987–2002: HMD (2020), centered period death rates | 2003–2004: value of 2002

2.E.2 Labor Supply Variables

In the model, we include information on employment and the labor force. Doing the latter inevitably requires information on unemployment. Moreover, aiming to analyze the effects of changes in a given population, here aged 15–64 years, the labor supply variables should be consistent with this age group definition. To address these requirements, we combine information on total employment, unemployment rates, and labor force participation rates by age from a large number of sources and conduct extensive data preparation. Below, we describe the process and the underlying sources in detail. Importantly, as indicated in each case below, for some observations the derivation of the (un-)employment value can only be understood by simultaneously referring to the detailed information on the sources and data preparation description of the respective other part of the labor force.

Employment.
Australia 1900–1950: Withers et al. (1985) | 1950–1978: Feenstra et al. (2015) | 1978–2019: First, we obtain level figures for the labor force aged 15–64 years by multiplying participation rates from OECD (2022) and the population aged 15–64 years as stated above. Then, second, we derive employment figures by subtracting those unemployed according to the unemployment rate as outlined below.
Austria 1900–1950: Butschek (1992), with linear interpolation for 1914–1915 and with replacement of the value in 1913 by the ratio of employment in 1913 and 1924 according to WIFO (1965) | 1950–1994: Feenstra et al. (2015) | 1994–2019: OECD (2022), see procedure for Australia. We chain-link the break in the series in 2004 by using information on total employment from Feenstra et al. (2015).
Belgium 1900–1913: Maddison (1982), labor force for 1900 and 1913 with linear interpolation; we obtain employment figures by subtracting unemployment as outlined below. | 1913–1924: Bergeaud et al. (2016) | 1924–1938 and 1950: Maddison (1964), labor force, combined with the

unemployment rate as outlined below | 1938–1946: Maddison (1964), labor force for 1938, and for 1946 as outlined below, with linear interpolation, combined with the unemployment rate as outlined below | 1946–1950: Clark (1957), labor force, combined with the unemployment rate as outlined below | 1950–2002: Feenstra et al. (2015) | 2002–2019: OECD (2022), see procedure for Australia

Denmark 1875–1900: Abildgren (2017), labor force, combined with the unemployment rate as outlined below | 1900–1950: Abildgren (2017) | 1950–2002: Feenstra et al. (2015) | 2002–2019: OECD (2022), see procedure for Australia

Finland 1900–1950: Statistics Finland, unemployment levels and rate, data sent on request | 1950–1970: Feenstra et al. (2015) | 1970–2019: OECD (2022), see procedure for Australia

France 1900–1950: Villa (1993), with firm employment only for 1914–1918 and 1940–1945 | 1950–2003: Feenstra et al. (2015) | 2003–2019: OECD (2022), see procedure for Australia

Germany 1875–1939: Hoffmann (1965) and Sommariva & Tullio (1987), data obtained from Rahlf (2015) and Sommariva & Tullio (1987), with linear interpolation for 1876–1877. For 1918–1919, we use the information on population given in Sommariva & Tullio (1987) and the data on total population as outlined above to cope with the boundary break. | 1939–1945: Sommariva & Tullio (1987), original source is Hoffmann (1965). We scale the data point in 1939 using data on population as outlined above and on labor force participation in 1939 and 1950 as well as on unemployment in both years as outlined below. In doing so, we are able to account for the structural break due to boundary changes. | 1946–1950: Available sources for this period suggest contradictory employment patterns (e.g., Sommariva & Tullio, 1987; Clark, 1957). We derive relative changes in total employment as follows: We use information on unemployment in levels and in rates from Mitchell (2013) to find employment data for 1948–1950. Additionally, we use information on the relative changes in employment from BMA (1950) for 1946 and 1948. For 1947–1948, we use information on the labor force from Abelshauser (1975) and for unemployment from Galenson & Zellner (1957). | 1950–1970: Bundesbank (2023) | 1970–2019: OECD (2022), see procedure for Australia. We chain-link the break in 1990-1991 by using information on total employment from Bundesbank (2020).

Italy 1900–1950: Giordano & Zollino (2016) | 1950–1970: Feenstra et al. (2015) | 1970–2019: OECD (2022), see procedure for Australia

Japan 1900–1920: Umemura et al. (1988), labor force (the number of gainful workers, Japanese only, mid-year) aged 15 years and above, data obtained from RCISSS (2016), combined with unemployment as outlined below | 1920–1940: Umemura et al. (1988), labor force figures (the number of gainful workers, 1st October) aged 15 years and above, data obtained from RCISSS (2016) and JSPS (2023), combined with unemployment as outlined below | 1940–1950: Pilat (2002), data taken from van Leeuwen (2007) | 1950–1968: Feenstra et al. (2015) | 1968–2019: OECD (2022), see procedure for Australia

Netherlands 1875–1950: CBS (2014) | 1950–1987: Feenstra et al. (2015) | 1987–2019: OECD (2022), see procedure for Australia

New Zealand 1900–1921: Bergeaud et al. (2016) | 1921–1939: Rankin (1994), with linear interpolation to mid-year values | 1939–1950: Bergeaud et al. (2016) | 1950–1986: Feenstra et al. (2015) | 1986–2019: OECD (2022), see procedure for Australia
Norway 1875–1900: Total employment derived as the residual figures from the labor force and unemployment rate as outlined below. | 1900–1950: SSB (2020) | 1950–1970: Feenstra et al. (2015) | 1970–2019: OECD (2022), see procedure for Australia
Sweden 1875–1950: Krantz & Schön (2007) and Schön & Krantz (2012) | 1950–1960: Feenstra et al. (2015) | 1960–2019: OECD (2022), see procedure for Australia
Switzerland 1900–1913: HSSO (2022c), with chain-linkage of the break in 1912–1913 using the growth rate from 1911–1912 | 1913–1950: HSSO (2022f) | 1950–1956: Feenstra et al. (2015) | 1956–1987: Since Swiss population data are available for the *de jure* population only with a lag (see, e.g., HMD, 2023, for further information), the large inflow of foreign workers around 1960 (see, e.g., Clark, 1983) is only mirrored in the employment, but not in the population statistics. To avoid inconsistency with the central variable of interest, the population, we adjust the employment series accordingly. We create an appropriate series by removing those persons in employment with foreign citizenship who are not counted in the *de jure* population according to HSSO (2022b). For 1972–1973, we use Feenstra et al. (2015). | 1987–2010: Feenstra et al. (2015) | 2010–2019: OECD (2022), see procedure for Australia
United Kingdom 1875–1950: Bank of England (2017) | 1950–2004: Feenstra et al. (2015) | 2004–2019: OECD (2022), see procedure for Australia
United States 1875–1900: Vernon (1994) | 1900–1947: U.S. Bureau of the Census (1975), calculated by subtracting unemployed persons from total labor force, series D1-10 | 1947–1950: U.S. Bureau of the Census (1975), calculated by subtracting unemployed persons from total labor force, series D11-25 | 1950–1960: Feenstra et al. (2015) | 1960–2019: OECD (2022), see procedure for Australia

Unemployment rate in the labor force. For later years, we use OECD (2022) for the unemployment rate among those aged 15–64 years. For earlier years, often age-specific information is unavailable. Thus, we use various sources for the unemployment rate in the total labor force and assume that the relative changes in these unemployment rates are the same as for those aged 15–64 years.
Australia 1900–1963: Withers et al. (1985) | 1964–1966: OECD (2016) | 1966–2019: OECD (2022)
Austria 1900–1977: Butschek (1992), with linear interpolation for 1914–1915 and 1917. For 1942–1945, we assume the level of 1941. | 1978–1994: OECD (2016) | 1994–2019: OECD (2022)
Belgium 1900–1903: Galenson & Zellner (1957), data for trade union members in Ghent and taken from Sensch (2014) | 1903–1912: Galenson & Zellner (1957), data for trade union members and data taken from Sensch (2014) | 1913: Maddison (1964) | 1914–1919: We apply linear interpolation. | 1920–1939: Goossens et al. (1988) | 1940–1944: We apply linear interpolation. | 1945–1949: We derive the unemployment rate by using labor force figures from Clark (1957), scaled by the interpolated ratio to Maddison (1964) labor force figures in 1938 and 1950, and

unemployment in levels from Mitchell (2013), with linear interpolation for 1945. | 1950–1959: Maddison (1982) | 1960–1983: OECD (2016) | 1983–2019: OECD (2022)

Denmark 1875–1899: Abildgren (2005) | 1900–1960: Abildgren (2017) | 1960–1968: OECD (2005), with scaling of its values by obtaining ratios to the preceding and the subsequent sources in 1960 and 1969 and linearly interpolate this ratio in between. | 1969–1982: OECD (2016) | 1983–2019: OECD (2022)

Finland 1900–1920: Tiainen (1994), multiplied by the ratio of this series and Grytten (2008) series in 1920. The Tiainen data was sent on request by Statistics Finland. | 1920–1938: Grytten (2008) | 1938–1950: Tiainen (1994), scaled by its ratios to the preceding series in 1938, the subsequent series in 1950 as well as their interpolation | 1950–1959: Maddison (1982) | 1960–1963: OECD (2016) | 1963–2019: OECD (2022)

France 1900–1950: We apply a three-step procedure: (1) We obtain the unemployment rate using unemployment figures and total employment from Villa (1993). (2) We take the quinquennial census unemployment rates from Galenson & Zellner (1957) as benchmark values. (3) We obtain the ratios of the census rates and the rates from Villa (1993) in (1), linearly interpolate between these observations, and scale the series in (1) to obtain unemployment figures for this period. | 1950–1960: Maddison (1982) | 1960–1975: OECD (2016) | 1975–2019: OECD (2022)

Germany 1875–1887: We use the ratio of the labor force to employment figures for benchmark years from Clark (1957) and scale the employment series as outlined above accordingly. For 1887, we obtain a benchmark value by using the same employment series and information on unemployment as outlined below. We linearly interpolate the labor force in the missing years and obtain unemployment figures by subtracting employment as outlined above. For 1875–1877, we assume the value of 1877. | 1887–1914: Kuczynski (1962) and Kuczynski (1967), modified by Pierenkemper (1987), and tabulated by Hohls (1991), data taken from Sensch (2016) | 1915–1921: Mitchell (2013) | 1922–1939: Petzina et al. (1978), data taken from Sensch (2016) | 1940–1945: The series of the unemployment rate by Petzina et al. (1978) shows a value of 0.5 percent for 1939. We follow the analysis of Kosche & Bach (1991), who suggest that the labor shortage intensified after 1940, additionally to large numbers of forced labor and recruited foreign workers, and assume that there was negligible unemployment during these times. Therefore, we assume a value of 0.5 percent throughout this period. | 1946–1949: We assume the value of Petzina et al. (1978) for 1949. | 1950–1970: BA (2020), data for West Germany | 1970–2019: OECD (2022)

Italy 1900–1913: Clark (1957), scaled by the 1913 ratio to Maddison (1964). We assume the value of 1901 for 1900. | 1913: Maddison (1964) | 1914–1928: Clark (1957), scaled by the ratios to Maddison (1964) in 1913 and 1929 as well as their interpolation | 1929–1938: Maddison (1982), except for 1935–1936 for which we use the same source and procedure as for 1914–1928. | 1939–1945: We use the same source and procedure as for 1914–1928. | 1946–1949: Mitchell (2013), data on unemployment levels, and employment levels as outlined. We scale the resulting unemployment rate by its 1950 ratio to the subsequent source. | 1950–1959: Maddison (1982) | 1960–1970: OECD (2016) | 1970–2019: OECD (2022)

Japan 1900–1912: value of 1913 | 1913–1929: Clark (1957), with linear interpolation for 1914–1918. In using this series, we see a spike in the unemployment rate the early 1920s, which is

in accordance with the literature (e.g., Kase, 2004). | 1929–1939: Kato (2008) | 1940–1946: We apply linear interpolation. | 1947–1950: UN (1951) | 1950–1960: Maddison (1982) | 1960–1968: OECD (2016) | 1968–2019: OECD (2022)

Netherlands 1875–1960: CBS (2014) | 1960–1971: OECD (2016) | 1971–2019: OECD (2022)

New Zealand 1900–1920: We apply a three-step procedure: (1) We retrieve the unemployment rate for 1901, 1906, 1911, and 1916 (consolidated series) from Statistics New Zealand (2002). (2) We obtain the number of unemployed assisted into employment from Martin (1996), taken from Statistics New Zealand (2002), and linearly interpolate to end-of-year values. (3) We obtain the ratios of, on the one hand, unemployment levels in benchmark years 1901, 1906, 1911, 1916, and for 1921 from Rankin (1994) — prepared as outlined below — using the rate in (1) and employment levels as outlined above, and, on the other hand, the level figures as given in (2). We linearly interpolate these ratios and use the results to scale the figures in (2). Using the scaled figures and employment, we find the unemployment rate between benchmark years. For 1900, we assume the value of 1901. | 1921–1939: Rankin (1994), with interpolation to mid-year values | 1940–1951: Mitchell (2013), data for unemployment levels, and labor force figures as outlined above. We scale this unemployment rate by its ratios to the preceding series in 1940, the subsequent series in 1951, as well as their interpolation. | 1951–1960: Rankin (1993), with interpolation to mid-year values | 1960–1986: OECD (2016) | 1986–2019: OECD (2022)

Norway 1875–1902: We apply a four-step procedure: (1) We obtain labor force figures from Central Bureau of Central Bureau of Statistics of Norway (1966) for 1875, 1880, 1885, 1890, 1895, and 1900, as well as from the same source for 1877, 1887, 1899 by relating total GDP to GDP per person of the labor force provided therein. We linearly interpolate the remaining missing observations. (2) We obtain level figures for males seeking public relief from Central Bureau of Statistics of Norway (1968). Due to the break in the series, we scale figures from 1886 onward with the ratio of 1885 to 1886. We use this variable as a proxy for the true unemployment level. (3) We backward extend the subsequent absolute unemployment figures using these data. We additionally scale these figures by a five-year moving average of the Swedish unemployment rate as outlined below, mirroring the close connection of both countries at that time, amplifying the dynamics underlying the figures of those seeking public relief. (4) We obtain the unemployment rate by calculating the ratio of (3) and (1). | 1903: We calculate a value for 1904 by multiplying the unemployment rate in 1904 using the 1903-to-1904-ratio of the seven-months-average of union unemployment from NOS (1949). | 1904–1920: Grytten (1994) | 1920–1939: Grytten (2008) | 1939–1949: We apply a four-step procedure: (1) We use unemployment levels given in SSB (1945) for 1939 and 1941, SSB (1950) for 1946–1949, and we linearly interpolate the levels for missing observations in 1940 and in 1942–1946. (2) We use the total employment figures from the source indicated above and the unemployed levels in (1) to derive a series for the unemployment rate. (3) We scale this series by the ratio to Grytten (2008) in 1939, to the ratio to the chain-linked unemployment rate from Galenson & Zellner (1957) in 1950 — whereby we use the value of Maddison (1982) as a benchmark — as well as to the interpolation of these ratios. | 1950–1960: Maddison (1982) | 1960–1972: OECD (2016) | 1972–2019: OECD (2022)

Sweden 1875–1911: Clark (1957) | 1911–1920: Molinder (2018) and Bengtsson & Molinder (2017) | 1920–1938: Grytten (2008) | 1939–1960: Molinder (2018) and Bengtsson & Molinder (2017) | 1960–1963: OECD (2016) | 1963–2019: OECD (2022)
Switzerland 1900–1913: We use the ratio of job seekers in the city of Zurich from HSSO (2022e), chain-linked to the unemployment level in 1913, to employed persons to derive information on unemployment dynamics. | 1913–1974: HSSO (2022f) | 1975–1991: OECD (2016) | 1991–2019: OECD (2022)
United Kingdom 1875–1970: Bank of England (2017) | 1971–1984: OECD (2016) | 1984–2019: OECD (2022)
United States 1875–1899: Vernon (1994) | 1900–1959: Weir (1992), data taken from Ramey & Francis (2009) | 1960–2019: OECD (2022)

Labor force participation rate of those aged 15–64 years. We introduce benchmark values (BV) for labor force participation rates and use these BV to scale employment and unemployment levels as outlined above. This is associated with both advantages and disadvantages. One advantage is that the final series delivers more accurate patterns of age-specific participation rates over time. For example, the PWT series for total employment in Austria after 1950 (Feenstra et al., 2015) uses the same relative changes as employment in Butschek (1992). Notably, employment in Butschek (1992) encompasses only dependent employees but not those being self-employed and suggest a strong increase of employment after World War II. Treating the series as representative for overall employment among working age in Austria, this would lead to low levels of participation rates among those of working age in 1950 — far below the figures suggested by ILO (1977a) and others. At the same time, the series for self-employment in Austria by Butschek (1974) for the period 1961–1971 shows that the number of those being self-employed declined by more than a quarter within ten years, suggesting that at least some of the increase in dependent employment may be driven by the decline of self-employment. Thus, introducing benchmark values accounts for this shortcoming. By contrast, the disadvantage that this procedure implies is that, by construction, some annual change rates are amplified while others are attenuated. If the original change rates are very close to zero, some may flip signs. In the course of preparing the dataset as outlined, we have evaluated the impact of introducing benchmarks and found that the annual change rates of our adjusted series are still very strongly correlated to the original change rates.

Having obtained BV, we calculate the ratio of these BV to the labor force participation rates derived from the unadjusted data on total employment and unemployment as outlined above. In between the benchmark years, we linearly interpolate the ratio and use the resulting series to scale the unadjusted data on total employment and unemployment.
Australia 1900–1950: BV for 1911 from ABS (1917), for 1921 from ABS (1925), and for 1933 ABS (1937), as well as for 1900 by using the 1900-to-1911-ratio from New Zealand, and for 1950 from ILO (1977a). | 1950–1978: BV for 1950, 1955, 1960, and 1965 from ILO (1977a). For 1978, we assume a ratio of 1.

Austria 1900–1950: BV for 1910 from K.K. Statistische Zentralkommission (1916), encompasses those aged 11–70 years, and from ILO (1977a) for 1950. | 1950–1994: BV for 1950, 1955, 1960, 1965, and 1970 from ILO (1977a). For 1994, we assume a ratio of 1.
Belgium 1950–2002: BV for 1950, 1955, 1960, 1965, and 1970 from ILO (1977a). For 2002, we assume a ratio of 1.
Denmark 1950–2002: BV for 1955, 1960, 1965, and 1970 from ILO (1977a). For 2002, we assume a ratio of 1.
Finland 1950–1970: BV for 1950 from ILO (1977a). For 1970, we assume a ratio of 1.
France 1900–1950: BV for 1906, 1911, 1921, 1931, and 1946 from Maruani & Meron (2012) and for 1950 from ILO (1977a). | 1950–2003: BV for 1950, 1955, 1960, and 1965 from ILO (1977a). For 2003, we assume a ratio of 1.
Germany 1895–1950: BV for 1895, 1907, 1925, 1933, and 1939 from Long (1958) and for 1950 from ILO (1977a). | 1950–1990: BV for 1950, 1955, 1960, 1965, and 1970 from ILO (1977a). For 1978, we assume a ratio of 1.
Italy 1901–1950: BV for 1901 from Fuà (1976) and for 1950 from ILO (1977a). | 1950–1970: BV for 1950 from ILO (1977a). For 1970, we assume a ratio of 1.
Japan 1920–1950: BV for 1920 by combining age-group-specific rates from Umemura (1962) and population by Statistics Japan (2021), as well as for 1950 from ILO (1977b). | 1950–1968: BV for 1950, 1955, 1960, and 1965 from ILO (1977b). For 1968, we assume a ratio of 1.
Netherlands 1950–1987: BV for 1950, 1955, 1960, 1965, and 1970 from ILO (1977a). For 1987, we assume a ratio of 1.
New Zealand 1901–1950: BV for 1901, 1906, 1911, 1921, 1926, 1936, and 1945 from Long (1958) and for 1950 from ILO (1977a). | 1950–1970: BV for 1950, 1955, 1960, and 1965 from ILO (1977a). For 1970, we assume a ratio of 1.
Norway 1950–1970: BV for 1950, 1955, 1960, and 1965 from ILO (1977a). For 1970, we assume a ratio of 1.
United Kingdom 1911–1950: BV for 1911, 1921, 1931, and 1939 from Long (1958), encompasses those aged 14–64 years, and for 1950 from ILO (1977a). | 1950–2004: BV for 1950, 1955, 1960, 1965, and 1970 from ILO (1977a). For 2004, we assume a ratio of 1.
United States 1890–1950: BV for 1890, 1900, 1910, 1920, 1930, and 1940 from Long (1958) and for 1950 from ILO (1977a). | 1950–1960: BV for 1950 from ILO (1977a) for 1950. For 1960, we assume a ratio of 1.

Average annual hours worked. For 1950–2019, we rely on Feenstra et al. (2015) for all countries wherever data are available. Before 1950, data resembling annual hours worked are sparse. Thus, for the period before 1950, and if not stated explicitly otherwise, we use the benchmark estimates for average annual hours worked by Huberman & Minns (2007) and combine them with the variation from other sources, as similarly done by others, e.g., Bergeaud et al. (2016).
Australia 1900–1950: Gilmore (2021), average working week in manufacturing | 1950–2019: Feenstra et al. (2015)

Austria We obtain benchmark values by using information from Maddison (1982), scaled by the bias of the Maddison estimates compared to the Huberman & Minns (2007) estimates for Germany: 1900–1929: We use the values for 1900 and 1929 from Gilmore (2021) as a reference point and use the variation of German average annual hours worked in between. | 1929–1950: Gilmore (2021), average working week in manufacturing, with linear interpolation for 1938–1946 | 1950–2019: Feenstra et al. (2015)

Belgium 1900–1913: Gilmore (2021), average working week in manufacturing in France | 1913–1939: Gilmore (2021), average working week in manufacturing, with linear interpolation for 1921 | 1939–1950: Gilmore (2021), average working week in manufacturing in France | 1950–2019: Feenstra et al. (2015)

Denmark 1875–1929: Gilmore (2021), average working week in manufacturing, combined with Abildgren (2017), agreed annual working time | 1929–1950: Abildgren (2017), agreed annual working time | 1950–2019: Feenstra et al. (2015)

Finland 1900–1950: Bergeaud et al. (2016), hours worked, data sent on request | 1950–2019: Feenstra et al. (2015)

France 1900–1919: Villa (1993), average working week in industry, with linear interpolation for 1914–1918 | 1919–1939: Villa (1993), average working week | 1940–1945: Villa (1993), average working week in industry | 1946–1950: Villa (1993), average working week | 1950–2019: Feenstra et al. (2015)

Germany 1875–1950: Schröder (1980), Meinert (1958), and BMAS (2012), average weekly working hours in the industry, data taken from Sensch (2015), with linear interpolation for the years 1915–1918, 1925, and 1945–1949 | 1950–2019: Feenstra et al. (2015)

Italy 1900–1913: Huberman & Minns (2007), with linear interpolation | 1913–1920: Clark (1957), average annual hours worked | 1921–1927: Gilmore (2021), average weekly hours worked in manufacturing, scaled by the interpolated ratio to Clark (1957) figures in 1920 and 1928 | 1928–1950: Clark (1957), average annual hours worked | 1950–2019: Feenstra et al. (2015)

Japan Here, we do not use benchmark estimates but rely on the relative changes of the following sources: 1900–1905: value of 1906 | 1906–1918: Rōdō Undō Shiryō Iinkai (1959), hours series, derived by multiplying days worked per year and hours worked per year, and scaled by overlapping information with Clark (1957) in 1913 | 1918–1927: Clark (1957), average annual hours worked | 1927–1950: Gilmore (2021), average weekly working hours in manufacturing, with linear interpolation for 1946 | 1950–2019: Feenstra et al. (2015)

Netherlands 1875–1913: Gilmore (2021), average weekly working hours in manufacturing, assuming 1902–1903 to be constant | 1913–1939: Clark (1957), average annual working hours | 1939–1950: Gilmore (2021), average weekly working hours in manufacturing | 1950–2019: Feenstra et al. (2015)

New Zealand 1900–1970: Bergeaud et al. (2016), hours worked, data sent on request | 1970–2019: Feenstra et al. (2015)

Norway Here, we do not use benchmark estimates but rely on the relative changes of the following sources: 1900–1937: We use the average variation in the series as outlined for Denmark above and for Sweden below; for 1908–1910 we only use relative changes from Denmark. |

1937–1950: Gilmore (2021), average weekly working hours in manufacturing | 1950–2019: Feenstra et al. (2015)
Sweden 1875–1938: Clark (1957), average annual working hours, except for 1900–1913, where we assume constant hours, following Bergeaud et al. (2016) | 1938–1950: Gilmore (2021), average weekly working hours in manufacturing up to 1952, with linear interpolation for the years 1947–1952 | 1950–2019: Feenstra et al. (2015)
Switzerland 1900–1950: Gilmore (2021), average working week in manufacturing | 1950–2019: Feenstra et al. (2015)
United Kingdom 1875–1950: Bank of England (2017), average weekly working hours | 1950–2019: Feenstra et al. (2015)
United States 1875–1890: Huberman & Minns (2007), with linear interpolation | 1890–1919: HSUS (2023), average weekly hours in manufacturing | 1919–1950: HSUS (2023), average weekly hours of production or non-supervisory workers on private payrolls in manufacturing | 1950–2019: Feenstra et al. (2015)

2.E.3 Other Economic Variables

Real gross domestic product. We derive a series for real GDP by multiplying total population, derived as described above, with a given real GDP per capita value. For 1950–2019, we use GDP per capita values that result from dividing real GDP by total population from PWT 10.01 national accounts data Feenstra et al. (2015). Before 1950, we use the relative changes in the real GDP per capita series by (Bolt & van Zanden, 2020). The only exception is Germany, where we use the relative changes in real GDP per capita from Bundesbank (2023) for the period 1950–1991.

Real wage, hourly. Deriving a consistent dataset for real wages across space and time is a difficult task. We combine a multitude of sources to derive series for real wages that (1) approximate hourly real wages as closely as possible and (2) are consistent within a country. The latter implies that our series do not allow to conduct PPP analyses across countries. This shortcoming reflects the fact that PPP-adjusted wages across space and time are a complex research field in its own (e.g., de Zwart et al., 2014). Below, we specify the frequency which the used wages indicators refer to. If this frequency is anything else than hourly, we divide accordingly by information delivered by our average annual hours worked (AVH) time series. For example, to adjust weekly wages, we divide them by (AVH/52), which approximates average weekly hours worked. We do not account for the changing nature of working days and weeks across space and time, which is beyond the scope of this paper (for a discussion, see Huberman & Minns, 2007).
Australia 1900–1900: Jordà et al. (2017), weekly nominal wages, deflated using the CPI series from the same source | 1990–2019: OECD (2021), average annual real wages
Austria 1900–1912: Cvrcek (2013), nominal wages in Vienna, deflated by the CPI series from Hubmann et al. (2020) | 1912–1924: We assume the same wage developments as in Germany. | 1924–1937: WIFO (1965), sum of all wages as the share in nominal GDP, divided by the total annual hours worked using employment and hour worked time series as outlined above and below,

deflated by the CPI series from Hubmann et al. (2020) | 1937–1948: We use the ratio of German real wages between 1937 and 1948, and linearly interpolate. | 1948–1950: same procedure as for 1924–1937 | 1950–1958: WIFO (1958), monthly nominal wages, deflated using the CPI series from the same source | 1958–1990: OECD (2019), hourly nominal earnings in manufacturing, deflated using the CPI series from Hubmann et al. (2020) | 1990–2019: OECD (2021), average annual real wages

Belgium 1900–1938: Williamson (1995), annual real wages, with linear interpolation of missing years in 1915–1919 | 1938–1947: Jordà et al. (2017), hourly nominal wages, deflated using the CPI series from the same source, with linear interpolation of missing observations in 1942–1946 | 1947–1959: Williamson (1995), daily real wages | 1959–1990: Jordà et al. (2017), weekly nominal wages, deflated using the CPI series from the same source | 1990–2019: OECD (2021), annual real wages

Denmark 1875–1990: Jordà et al. (2017), hourly nominal wages, deflated using the CPI series from the same source | 1990–2019: OECD (2021), average annual real wages

Finland 1900–1913: Heikkinen (1997), daily real wages in manufacturing | 1913–1914: Hjerppe (1989), nominal wages, deflated using the CPI series from Jordà et al. (2017) | 1914–1950: Jordà et al. (2017), nominal wages, deflated using the CPI series from the same source, frequency unclear | 1950–1990: Jordà et al. (2017), hourly nominal wages, deflated using the CPI series from the same source | 1990–2019: OECD (2021), average annual real wages

France 1900–1938: Jordà et al. (2017), nominal wages, deflated using the CPI series from the same source, frequency unclear | 1938–1939: Williamson (1995), daily real wages | 1939–1948: Jordà et al. (2017), hourly nominal wages, deflated using the CPI series from the same source | 1948–1990: Jordà et al. (2017), weekly nominal wages, deflated using the CPI series from the same source | 1990–2019: OECD (2021), average annual real wages

Germany 1875–1914: Jordà et al. (2017), annual nominal wages, deflated using the CPI series from the same source | 1914–1918: Williamson (1995), real wages, frequency unclear | 1918–1924: Pierenkemper (1984), weekly real wages, data taken from Sensch (2012) | 1924–1991: Jordà et al. (2017), annual nominal wages, deflated using the CPI series from the same source | 1991–2019: OECD (2021), average annual real wages

Italy 1900–1914: Jordà et al. (2017), hourly nominal wages, deflated using the CPI series from the same source | 1914–1943: Jordà et al. (2017), daily nominal wages, deflated using the CPI series from the same source | 1943–1950: Williamson (1995), daily real wages | 1950–1990: Jordà et al. (2017), weekly nominal wages, deflated using the CPI series from the same source | 1990–2019: OECD (2021), average annual real wages

Japan 1900–1945: Jordà et al. (2017), nominal daily wages, deflated using the CPI series from the same source | 1945–1947: Mitchell (2013), nominal hourly wages, deflated by the CPI series from Jordà et al. (2017) | 1947–1950: Available data sources for this period indicate stark differences in the development of real wages — for example, for 1949–1950 ranging from a 10 percent decline to a 36 percent increase (see van Leeuwen, 2007; ILO, 1952, among others). These differences appear to be attributed to using wages either in agriculture or in industry. To avoid using biased change rates for the period under consideration due to relying on one or another, we use changes in both

agriculture and manufacturing weighted by the share of agriculture in overall employment. All relevant data — agricultural and manufacturing wages, the CPI, and the share in employment in 1950 — are taken from ILO (1952). | 1950–1957: Mitchell (2013), hourly nominal wages, deflated using the CPI series from Jordà et al. (2017) | 1957–1990: Jordà et al. (2017), nominal weekly wages, deflated using the CPI series from the same source | 1990–2019: OECD (2021), average annual real wages

Netherlands 1875–1913: Jordà et al. (2017), nominal wages, deflated using the CPI series from the same source, frequency unclear | 1913–1948: Jordà et al. (2017), daily nominal wages, deflated using the CPI series from the same source | 1948–1990: Jordà et al. (2017), weekly nominal wages, deflated using the CPI series from the same source | 1990–2019: OECD (2021), average annual real wages

New Zealand 1900–1940: Greasley & Oxley (2004), real wages | 1940–1985: Statistics New Zealand (2002), weekly real earnings | 1985–1990: Mitchell (2013), hourly nominal wages, deflated using the CPI series from OECD (2020) | 1990–2019: OECD (2021), average annual real wages

Norway 1875–1990: Jordà et al. (2017), annual nominal wages, deflated using the CPI series from the same source | 1990–2019: OECD (2021), average annual real wages

Switzerland 1900–1990: Jordà et al. (2017), hourly nominal wages, deflated using the CPI series from the same source | 1990–2019: OECD (2021), average annual real wages

Sweden 1875–1949: Prado (2010), hourly earnings of males, deflated using the CPI series from Jordà et al. (2017) | 1949–1990: Jordà et al. (2017), weekly nominal wages, deflated using the CPI series from the same source | 1990–2019: OECD (2021), average annual real wages

United Kingdom 1875–1990: Jordà et al. (2017), annual nominal earnings, deflated using the CPI series from the same source | 1990–2019: OECD (2021), average annual real wages

United States 1875–1890: Jordà et al. (2017), annual nominal wages, deflated using the CPI series from the same source | 1890–1990: Jordà et al. (2017), hourly nominal earnings, deflated using the CPI series from the same source | 1990–2019: OECD (2021), average annual real wages

Real investment. We collect data on real investment for the period 1960–2019 for all countries from IMF (2021). Before 1960, we use the relative changes from various sources. We use data on gross fixed capital formation, if available, and on gross capital formation else. Eventually, we scale the series by using the ratio of real investment to real GDP from IMF (2021) in 2019, multiplied by the real GDP series as outlined above, as the benchmark value.

Australia 1900–1960: Butlin (1977), real total fixed investment, with linear interpolation of the data to 31st December. For 1900–1901, we assume the same change rate as for 1901–1902. | 1960–2019: IMF (2021)

Austria 1900–1913: Due to the absence of an investment series for that period, we use the relative changes in the real fixed capital stock from Schulze (2005). | 1913–1924: Handler et al. (1968), real gross fixed capital formation | 1924–1937: WIFO (1965), real gross fixed capital formation | 1937–1948: Handler et al. (1968), real gross fixed capital formation | 1948–1960: WIFO (1965), real gross fixed capital formation | 1960–2019: IMF (2021)

Belgium 1900–1960: van Meerten (2003), gross fixed capital formation, deflated by the CPI series from Jordà et al. (2017) | 1960–2019: IMF (2021)
Denmark 1900–1960: Abildgren (2017), real gross capital formation | 1960–2019: IMF (2021)
Finland 1900–1960: Hjerppe (1989), nominal gross fixed capital formation, deflated by the GDP deflator from the same source | 1960–2021: IMF (2021)
France 1900–1920: Villa (1993), nominal gross capital formation, deflated by the CPI series from Jordà et al. (2017) | 1920–1935: Nominal gross fixed capital formation, derived by multiplying the share of gross fixed capital formation in GDP from van Meerten (2003) with nominal GDP from Villa (1993), deflated by the CPI series from Jordà et al. (2017). | 1935–1960: Maddison (1994), real non-residential gross investment | 1960–2019: IMF (2021)
Germany 1875–1913: Nominal gross capital formation, derived by multiplying the share of gross capital formation in GDP and nominal GDP from Jordà et al. (2017), deflated by the CPI series from the same source. | 1913–1920: We assume real investment to follow real GDP. | 1920–1960: Maddison (1994), real non-residential gross investment | 1960–1991: Bundesbank (2023), real gross fixed capital formation | 1991–2019: IMF (2021)
Italy 1900–1960: Baffigi (2011), real gross fixed capital formation | 1960–2019: IMF (2021)
Japan 1900–1960: Maddison (1994), real non-residential gross investment | 1960–2019: IMF (2021)
Netherlands 1875–1913: Smits et al. (2000), real gross fixed capital formation | 1913–1960: Groote et al. (1996), real gross fixed capital formation | 1960–2019: IMF (2021)
New Zealand 1900–1914: Statistics New Zealand (2002), nominal gross capital formation, deflated by using the five-year moving average of the Australian CPI series from Jordà et al. (2017), and chain-link to the subsequent source for New Zealand from BIS (2022) | 1914–1960: Statistics New Zealand (2002), nominal gross capital formation, deflated using the CPI series from BIS (2022) | 1960–2019: IMF (2021)
Norway 1875–1960: Grytten (2004), real gross capital formation, updated by Norges Bank (2018) | 1960–2019: IMF (2021)
Sweden 1875–1960: Krantz & Schön (2007) and Schön & Krantz (2012), real gross fixed capital formation | 1960–2019: IMF (2021)
Switzerland 1900–1948: HSSO (2022a), real gross capital formation | 1948–1960: We use the relative changes in nominal gross capital formation, derived by multiplying the share of gross capital formation in GDP from Jordà et al. (2017) and nominal GDP from BFS (2022), deflated by the CPI series from Jordà et al. (2017). | 1960–2019: IMF (2021)
United Kingdom 1875–1960: Maddison (1994), real non-residential gross investment | 1960–2019: IMF (2021)
United States 1875–1960: Maddison (1994), real non-residential gross investment | 1960–2019: IMF (2021)

Chapter 3

Activation Potentials in Population Decline

Estimating Hidden Labor Force Rates by Dimensionality Reduction

3.1 Introduction

Labor shortages have increasingly gained attention in recent years (Causa et al., 2025) and may have various reasons (Duval et al., 2022). Thereby, the secular decline in birth rates during the second half of the 20th century across advanced economies plays a crucial role. This applies in particular to Germany, where fertility rates, after having peaked in the mid-1960s, quickly and permanently dropped below the replacement level in the early 1970s (BiB, 2026b). The long shadow of this marked demographic turning point will become virulent in the near future, as the retirement of the large cohorts of the mid-1960s is approaching. This raises a multitude of questions, concerning the overall labor market effects (Hellwagner & Weber, 2024), but in particular concerning the accompanying downward pressure on labor supply, as a range of medium- to long-term projections and forecasts expect pronounced labor supply decline in Germany (among others: Destatis, 2020; Hellwagner et al., 2023; Kubis & Schneider, 2024; Zika et al., 2025).

In this context, the activation of the hidden labor force (e.g., Destatis, 2025a; Holst & Schupp, 2000; Rengers & Fuchs, 2022) — also referred to as, for example, *potential labor force* (ILO, 2013, 2025), *potential additional labor force* (Eurostat, 2025b), or *hidden unemployment* (Armstrong, 1999) — emerges as one among several levers to address and

mitigate labor shortages in general and the effects of demographically induced labor supply declines in particular.

While the labor force encompasses those being either employed or unemployed, the definition of the hidden labor force (henceforth: HLF) is more vague. According to the ILO (2013, page 18), it encompasses "all persons of working age who, during the short reference period, were neither in employment nor in unemployment", but who can be classified as either unavailable jobseekers or available potential jobseekers. While persons in the former group actively seek employment, but are currently not available to take up work, persons in the latter group are currently available, want to work, but are not actively seeking employment (ILO, 2013). Similarly, Eurostat (2025b) defines those two groups of the HLF as persons seeking work but not immediately available and persons available to work but not seeking. The German Federal Statistical Office (Destatis) categorizes those two groups as HLF-A and HLF-B. Additionally, Destatis also publishes statistics on the HLF-C, encompassing also persons who have a general desire to work but are neither actively seeking employment nor currently available to take up work (Rengers & Fuchs, 2022).

Data on the HLF and its subgroups are of core importance, informing policy makers not only about the size and the demographic structure of the additionally activatable labor force, but often also about the reasons for inactivity. Corresponding figures are often derived from the Labor Force Survey (LFS).[1] For example, in the case of Germany, the LFS data suggest that in 2024 the sum of HLF-A and HLF-B was 1.3 million persons, with about 0.38 million persons in HLF-A and 0.93 million persons in HLF-B (Destatis, 2025a). Given an overall labor force of more than 47 million persons in 2024 (Destatis, 2025e), a HLF of 1.3 million persons points towards substantial activation potentials for the German labor market. While among those in HLF-A — the unavailable jobseekers — the LFS results show that education, care obligations, or health issues are among the main reasons for current non-availability (Destatis, 2025d), among those in HLF-B — the available potential jobseekers — the LFS results indicate that also discouragement plays an important role (Destatis, 2025c). Additionally, the LFS figures for 2024 also show a HLF-C of 1.8 million persons (Destatis, 2025a).

These are important insights but inherit some caveats. First, while survey results provide insights on *intended* labor supply, conditional on the fulfillment of corresponding preconditions, these figures do not necessarily mirror *feasible* additional labor supply. For example, stated reasons for inactivity such as discouragement are not well defined and, consequently, neither the conditions for labor market entries nor quantifying correspond-

[1] In Germany, the LFS is part of the German Microcensus since 1968 (GESIS, 2025). In this paper, we use both terms interchangeably.

ing activation potentials are straightforward to derive. In response to this, approaches have been developed in the literature, often estimating the effects of changes in labor market indicators on participation rates by using aggregate time-series data (e.g., using German data, Fuchs & Weber, 2021; Provenzano, 2017). Then, by combining the coefficient estimates with counterfactual scenarios of the labor market indicators — sometimes referred to as *full-employment conditions* — researchers derive the size and the structure of the HLF. Yet, existing estimation approaches require complex systems of equations (Provenzano, 2017), sometimes with a multitude of assumptions of full-employment conditions across many labor market indicators (Fuchs & Weber, 2010, 2021). Second, while estimates of the hidden labor force provide an order of magnitude of the *feasible* additional labor supply under some defined full-employment conditions, this does not necessarily correspond to the *efficient* additional labor supply from a policy perspective. The latter relates to insights from search-and-matching models which suggest that if the labor market becomes very tight, for example due to a switch to full-employment conditions, search may become inefficiently costly. This has also been addressed in a recent discussion on the efficient level of the unemployment rate (Michaillat & Saez, 2021, 2024b).

We address and incorporate these issues in our data preparation and empirical strategy, and illustrate our approach using data on the German labor market for the period 1990–2024. We do so based upon two considerations: On the one hand, in Germany, the share of those aged 60–64 years among the working-age population[2] is the highest across all EU countries[3], and thus the question of available levers to address the impending, demographically induced labor supply decline is the most relevant. On the other hand, in the case of Germany, there are not only survey results on the HLF, but also earlier estimation approaches, allowing us to compare our results against these benchmarks.

The paper offers several contributions: First, we introduce a parsimonious approach to estimate the size and the structure of the HLF. While existing approaches in the literature often model and tailor complex systems of individual equations for labor force participation rates across sex and age, we reduce dimensionality by applying a single Principal Component Analysis (PCA) to the matrix of employment and unemployment rates by sex and age, and simulate full-employment conditions by calibrating the resulting labor market tightness component accordingly. Second, beyond parsimony, this also reduces the impact of modeling choices, such as varying regressors across individual equations; this is particularly relevant when labor market indicators, upon which full-employment conditions are based, differ. Third, our paper exploits variation in realized

[2]The population aged 15–64 years.
[3]According to the population figures as of 1 January 2024 (Eurostat, 2026b).

labor supply, offering a consistent estimation approach that is easily transferable to other use cases. This contrasts with available survey-based HLF figures, which mirror labor supply intentions and which are subject to possible divergence between intended and realized behavior, effects of the concrete survey setting on declared intentions, or structural breaks due to changes in the questionnaires. Fourth, using corresponding data to illustrate our approach, we provide consistent estimates on the size and the structure of the HLF in Germany for 1991–2024. A comparison to the findings of earlier, more complex approaches suggest clear similarities, underpinning the suitability of our parsimonious approach. Fifth, we link our framework to a population and participation projection for Germany. By doing so, we are able to analyze the extent to which an activation of the HLF can contribute to maintaining the employment level in the future despite population aging and decline. Again, this application is easily transferable to other use cases.

We find considerable activation potentials, both in the past and in the future, with distinct heterogeneity across demographic groups. According to our model, the HLF among those aged 15–64 (15–74) years in Germany was 1.13 (1.47) million persons in 2024. Its activation would have increased the labor force in Germany by 2.4 (3.1) percent. While our results suggest higher HLF rates among younger persons and among those close to or in retirement, we find lower rates among persons of prime age. This aligns well with earlier approaches in the literature. By linking our model to recent discussions on efficient full-employment conditions, we find that the activation potentials suggested by our empirical approach are not only feasible, but also efficient. Moreover, defining the mechanism implied by our framework as a *multiplier effect* of unemployment reduction for employment, which follows from the additional activation of the HLF, and combining our approach with a population projection, we find that this channel can plausibly serve as an important building block to stabilize aggregate labor supply in Germany in the upcoming years. Our results suggest that until 2032, even the entire decline in aggregate employment could be offset via this multiplier effect.

3.2 Background

In the past decades, the Beveridge curve (Beveridge, 1944) has become a leading macroeconomic framework to analyze the labor market (Blanchard & Diamond, 1989; Elsby et al., 2015), illustrating the inverse relationship between unemployment and vacancies that has been observed across countries and decades, although subject to horizontal shifts (Jackman et al., 1990; Nickell et al., 2003). While shifts of the Beveridge curve occur due to structural changes such as in matching efficiency (Elsby et al., 2015) or the separation

rate (Klinger & Weber, 2016), movements along the Beveridge curve typically indicate cyclical changes in labor market tightness — the ratio of vacancies and unemployment changes.

For our paper, these movements along the Beveridge curve offer an intuitive starting point, as they connect well to the core observation that underlies existing approaches seeking to estimate the extent of the HLF; that is, unemployment exhibits distinct cyclicality — it decreases in economic upswings and increases in economic downturns. This fuels the idea that, at least in economic downturns, the unemployment rate is above its minimum, and thus the labor market is inefficiently slack. This difference of the unemployment from some feasible minimum may be called *unemployment gap* (Michaillat & Saez, 2021) and is simply given by $u - u^*$, where u is the observed unemployment rate and u^* is the minimum under full-employment conditions (for a comprehensive recent survey on full-employment concepts, see Lichtenberger et al., 2025).

The Beveridge framework and the observation of unemployment cyclicality directly link to the core assumption of HLF estimation approaches: By closing the unemployment gap — which is equivalent to switching to full-employment conditions — not only the unemployed enter employment, but the prevailing of full-employment conditions also fosters the labor market entry of previously inactive, *hidden* persons (Fuchs & Weber, 2021). The latter is often connected to the *discouraged worker effect* (DWE), which dates back to the seminal work of Long (1953, 1958). The DWE suggests that during an economic downturn, the job finding expectations worsen, which discourages unemployed job seekers from further searching (Dagsvik et al., 2013) — consequently, they exit the labor force. Numerous studies have found evidence for the DWE across countries, both using micro-level (e.g., Bloemen, 2005; Blundell et al., 1998; Dagsvik et al., 2013, 2025) and macro-level data (e.g., Emerson, 2011; Fuchs & Weber, 2021; Österholm, 2010; Provenzano, 2017). By contrast, the concept of the *added worker effect* (AWE) assumes that the labor force participation rate exhibits also some counter-cyclicality. The idea of the AWE dates back to the Great Depression (Woytinsky, 1940) and postulates that, from a household (and single-breadwinner) perspective, if the breadwinner loses his or her job, the spouse joins the labor force in order to replace the lost household income. Evidence suggests that the DWE and the AWE can co-exist (Lee & Parasnis, 2014).

For Germany, existing approaches have also found evidence for both. Fuchs & Weber (2013) use a trend-cycle decomposition of the aggregate unemployment rate in Germany and estimate the effects of both components on the labor force participation rates by sex and broad age groups. Their results suggest clear evidence for a DWE, in particular among the elderly, but also evidence for the simultaneous existence of an AWE, most

notably among young and middle-aged women. Fuchs & Weber (2017) elaborate on the role of short- and long-term unemployment. Other approaches using German data, such as Fuchs & Weber (2010, 2021) or Provenzano (2017), use a different empirical strategy and employ panel models or systems of single equations to estimate the DWE/AWE by sex, age groups, and citizenship. Similar to Fuchs & Weber (2013), the approach by Provenzano (2017) suggests that, first, there is a substantial DWE, in particular among the older workforce, but also among the younger age groups, and second, that there is evidence for an AWE among middle-aged women. The approach by Fuchs & Weber (2021) provides a net estimate of the DWE and the AWE, where the DWE is larger for all demographic groups, also with larger rates among the younger and the older age groups.

Having estimated these effects, both Provenzano (2017) and Fuchs & Weber (2021) use their coefficient estimates to derive the size of the HLF in Germany, that is, calculating the number of workers that could enter the labor market if the economy switches to full-employment conditions. Thereby, characterizing full-employment conditions is crucial. Fuchs & Weber (2021) follow earlier approaches in the literature (Armstrong, 1999) and rely on regional benchmarking to find, for instance, a feasible minimum (full-employment) level of the unemployment rate. This approach is appealing and intuitive, as it offers a quick and transparent way to derive the size of the HLF and inform policy makers accordingly. But doing so requires a sound knowledge of the full-employment level of the regressor under consideration and insights from the search-and-matching literature point towards some caveats.

From these models (Pissarides, 1985; Elsby et al., 2015), we know that if unemployment decreases, vacancies become more difficult to fill, and thus recruitment becomes costlier. Consequently, a stark decline in the unemployment rate implies a stark increase in labor market tightness, with accompanying side effects. Bossler & Popp (2026) present findings along this line for Germany: According to their results, the rising labor market tightness in Germany between 2012 and 2019 has decreased firms' labor demand; in the absence of a rise in labor market tightness, an additional 1.1 million jobs could have been created during that period. In the context of HLF estimation approaches, this points to the necessity of a critical evaluation: Even if a full-employment level of the unemployment rate, as often defined by contributions in the literature, may be *feasible*, one might ask whether it is also *efficient*, as search becomes inefficiently costly.

Recently, Michaillat & Saez (2021, 2024b) have conceptualized this as *Beveridgean unemployment gap*, formalized some of these considerations, and introduced a full-employment measure respectively a measure of the efficient level of the unemployment rate, that is,

the social planner's solution to maximize welfare given the unemployment and the vacancy rate. Let u be the observed unemployment rate (unemployed divided by the labor force), v be the observed vacancy rate (vacancies divided by the labor force), ε be the Beveridge elasticity, ζ be the value from nonwork, and κ be the recruiting costs, then u^* is given by

$$u^* = \left(\frac{\kappa\varepsilon}{1-\zeta} \cdot \frac{v}{u^{-\varepsilon}} \right)^{1/(1+\varepsilon)}, \tag{3.1}$$

where time subscripts are dropped for simplicity. If $u > u^*$, the labor market is inefficiently slack, and if $u < u^*$, the labor market is inefficiently tight. For calculating u^*, knowledge of ε, ζ, and κ is necessary. As shown by Michaillat & Saez (2024b), if $\varepsilon = 1$, $\zeta = 0$, and $\kappa = 1$, Equation 3.1 reduces to

$$u^* = \sqrt{uv}, \tag{3.2}$$

which is a simple and intuitive rule for the efficient level of the unemployment rate from a labor market policy perspective. Thus, while in the HLF literature, the unemployment gap is often derived by calculating the difference of the observed unemployment rate from some defined full-employment level, for example based on regional benchmarking, Michaillat & Saez (2021, 2024b) introduce a measure of the unemployment gap that is conceptually consistent with search-and-matching frameworks. The combination of both allows to evaluate not only the feasibility but also the efficiency of the activation of the HLF in empirical applications.

However, recent contributions have also pointed towards some caveats here: As noted by Hobijn (2024), outward shifts of the Beveridge curve due to policy changes — for example as a consequence of unemployment insurance extensions — might imply a rather spurious increase in u^*. Moreover, Hobijn (2024) also notes that the underlying Beveridge curve in $u^* = \sqrt{uv}$ assumes an elasticity of the matching function of about one-half, which is not necessarily always and everywhere the case. Despite these concerns, the measure proposed by Michaillat & Saez (2021, 2024b) provides the first and only possibility to compare an empirically substantiated full-employment level of unemployment to a level that is underpinned by economic theory. Thus, we also address this concept in our analysis below.

3.3 Data

We use data sources that provide disaggregated information by sex and age over time. For the period 1990–2011, we use data on employment, unemployment, and the population

from the LFS. For 2001–2011, the data were sent by Destatis on request, for 1990–2001 we use data from the Destatis (2016) website. For the year 2005, we additionally retrieve data from the Federal Employment Agency (FEA) and from the Microcensus Scientific Use File to address the change in the mode of collection — from data collection only at a set timeframe, usually in April or May of each year, to a collection during the entire year (GESIS, 2025). For the period 2011–2024, we prepare employment and unemployment figures from a variety of different sources in order to account for the increasing divergence of the labor forces figures of the LFS and of the German national accounts in recent years Destatis (2025b). We relate these figures to the census-adjusted population data from (Destatis, 2025h) and to recent population figures sent by Destatis on request. In Appendix 3.A, we provide a detailed description of all preparation steps and of the underlying data sources. Eventually, this preparation strategy allows us to derive employment and unemployment rates by sex and five-year age groups (15–64 years) throughout the period 1990–2024.

Importantly, in the case of Germany, definitions and availability of unemployment data in the LFS have changed over time. Before 1996, those classified as unemployed encompassed both *immediately available job seekers* (IAJS) and *non-immediately available job seekers* (NAJS). While the former correspond to the ILO definition of unemployment, that is, non-employed job-seeking persons who are available to take up work within a short time frame, the latter encompass non-employed job-seeking persons who are not available to take up work within this short time frame (ILO, 2013; Rengers, 2004). This group of NAJS are usually largely categorized as a subgroup of the HLF (Fuchs & Weber, 2021; ILO, 2025). In the case of Germany, the size of the group of NAJS before 1996 is known in total (Fuchs & Weber, 2021), but there is no information by sex and age. To be able to use data from 1990 onward, we prepare sex- and age-specific unemployment rates that include NAJS throughout the observation period, despite conceptual differences to the ILO concept. This follows earlier approaches in the literature (e.g., Fuchs & Weber, 2021). Thus, due to the particularities of the German LFS, our data on unemployment by sex and age already include information on some *observable HLF*, i.e., the group of NAJS, which we distinguish below from an *estimated HLF* that our model delivers. We refer to the sum of both as *total HLF*.

Additionally, we use aggregate data on vacancies from the Job Vacancy Survey (Bossler et al., 2020) and from the FEA (2025b) for 2007 and earlier years, on the labor force according to the German national accounts from Destatis (2026a), on the job finding rate from Parker & Weber (forth.), and on unemployment (domestic concept)

from the FEA (2025a), with the latter also referred to as "registered unemployment", differing from the ILO definition (see Destatis, 2026c, for further information).

3.4 Methods

We apply PCA to identify a latent labor market tightness factor in the data. The application of PCA to analyze high-dimensional, correlated economic and demographic data is well established in empirical research (Hellwagner et al., 2023; McCracken & Ng, 2016; Vanella et al., 2022, 2023, and others). The underlying idea is that variables under consideration, such as labor force participation rates, are driven by a few underlying factors, which we use to derive labor force participation rates under full-employment conditions.

3.4.1 Data Preparation and Model

To do so, let $P_{s,a,t}$ be the population of sex s and in age group a, with $a = 1, \ldots, A$, where $A = 10$ corresponds to the overall number of five-year age groups covering the working-age population (15–64 years) in year t. Let L be the labor force, E be the employed individuals, and U be the unemployed individuals; then the labor force participation rate for any given group $l_{s,a,t}$ can be written as

$$l_{s,a,t} = \frac{L_{s,a,t}}{P_{s,a,t}} = \frac{E_{s,a,t}}{P_{s,a,t}} + \frac{U_{s,a,t}}{P_{s,a,t}} = e_{s,a,t} + u_{s,a,t}, \tag{3.3}$$

where $e_{s,a,t}$ and $u_{s,a,t}$ are the corresponding employment and unemployment rates *in the population*. In our case, as outlined, the unemployed encompass both those who are immediately available ($U_{s,a,t,I}$) and those who are not immediately available ($U_{s,a,t,N}$), thus $U_{s,a,t} = U_{s,a,t,I} + U_{s,a,t,N}$ and $u_{s,a,t} = u_{s,a,t,I} + u_{s,a,t,N}$. Moreover, we denote the unemployment rate *in the labor force*, which is the most common indicator in labor market statistics, as $\tilde{u}_t = \frac{U_t}{L_t}$.

As also outlined above, approaches in the literature usually model sex- and age-specific participation rates, often using single-equation (Fuchs & Weber, 2021) or panel models (Provenzano, 2017). In this paper, we pursue a different approach. We neither model participation rates nor do we estimate a complex system of equations, but we rather stack the two separate $T \times (A \cdot S)$ matrices of the employment and unemployment rates into a single matrix and apply PCA. Put differently, we apply PCA to a matrix consisting of 40 columns, due to the inclusion of sex-specific employment and unemployment rates for ten age groups, and 34 rows, due to the observation period 1990–2024 being subject to differencing as outlined below.

There are two reasons for this strategy. First, by using only a single PCA model, our empirical framework is more parsimonious compared to complex systems in the literature. It reduces dimensionality and identifies a small number of relevant components, or factors (F_t), to explain the large number of our $A \cdot S \cdot 2$ original time series — rather than modeling and tailoring each series and model individually. Second, from a more conceptual perspective, modeling disaggregated information on employment and unemployment allows us to determine full-employment conditions *endogenously*, that is, by calibrating the aggregate unemployment rate to a given full-employment level.

The latter is a nuanced but conceptually appealing merit of our framework. Existing approaches exploit the correlation of participation rates by sex and age with *external* full-employment indicators such as the aggregate unemployment rate, often lagged by one period to avoid endogeneity. Our nonparametric approach differs, as we use a contemporaneous factor identified from the data to calibrate employment and unemployment rates simultaneously, thereby ruling out any similar endogeneity concerns. Moreover, our approach simulates identical counterfactual full-employment conditions for all groups and accounts for the inherent demographic structure of the population — both are not ensured by existing approaches in the literature. We return to our calibration exercise below in more detail.

We apply two additional preparation steps before conducting the PCA: On the one hand, we logit-transform all rates. In the literature, this is often done to ensure that estimated participation rates do not exceed the natural boundaries $[0, 1]$. The same logic applies to employment and unemployment rates. On the other hand, we use first differences of the logit-transformed data. This ensures consistency. To provide more intuition here, assume that a given employment rate $e_{s,a,t}$ evolves according to the static factor model representation $e_{s,a,t} = \Lambda F_t + \epsilon_t$. Both F_t and ϵ_t can be $I(0)$ or $I(1)$. If ϵ_t is $I(1)$, applying PCA to the data in levels may yield inconsistent results (Bai & Ng, 2008). Using first differences addresses this issue and has already been applied in the literature (Vanella et al., 2022). We denote the resulting time series of first differences as $\Delta e_{s,a,t}$ and $\Delta u_{s,a,t}$, and apply z-standardization.

Then, we apply singular value decomposition and derive the kth principal component $f_{k,t}$ as

$$f_{k,t} = \sum_{s=1}^{S} \sum_{a=1}^{A} \lambda^{e}_{k,s,a} \Delta e_{s,a,t} + \sum_{s=1}^{S} \sum_{a=1}^{A} \lambda^{u}_{k,s,a} \Delta u_{s,a,t}, \tag{3.4}$$

where $\lambda^{e}_{k,s,a}$ and $\lambda^{u}_{k,s,a}$ are the factor loadings for the first differences of the employment and unemployment rates, respectively. For a more general overview on PCA, see Jolliffe (2002).

3.4.2 PCA: Factors, Loadings, Interpretation

Each principal component derived from the data is initially of purely statistical origin. Assigning economic meaning to those principal components is the decisive part of the subsequent analysis. Typically, the individual contributions of the derived PCs in explaining the variation in the underlying data differ strongly, and thus retaining and analyzing only a small number of components — those with the highest shares of explained variance — is sufficient (Jolliffe, 2002). While plotting the individual contributions of components offers an intuitive way to graphically determine the number of PCs to retain (Cattell, 1966), more formal approaches have been developed and applied in the literature. While the Kaiser-Guttman criterion (KGC) may be the most familiar (Guttman, 1954; Kaiser, 1960), the literature has pointed out that the KGC tends to overestimate the number of PCs to retain (Zwick & Velicer, 1986). Among others, an early adaptation of the KGC is the adjusted criterion by Horn (1965).

In our case, the first PC explains by far the largest share of the overall variance (56 percent), while the subsequent components explain less than ten percent each. Figure 3A.2 in the appendix illustrates these marked differences graphically. Still, the KGC suggests to retain six components, but the adaptation of Horn — aligning with the graphical findings — suggests to retain only the first PC.

Yet, in the literature, approaches do not only rely on the share of explained variance, but also evaluate whether PCs, and the corresponding loadings, provide clear interpretations (Vanella et al., 2022). In this paper, we aim to evaluate the changes in labor market participation across sex and age groups in counterfactual states of full employment. Thus, we are interested in PCs informing us about changes in the labor market that resemble movements along the Beveridge curve, as outlined above. We evaluate PCs 1–6 by inspecting the course of the component scores over time, the factor loadings of employment ($\lambda^{e}_{k,s,a}$) and unemployment rates ($\lambda^{u}_{k,s,a}$) by sex and age group, and check whether the PCs correlate with changes in aggregate external indicators — the vacancy rate, the job finding rate, and the aggregate unemployment rate.

By doing so, we find that the first PC does not only exhibit by far the largest share of explained variance, but is the only to provide a clear interpretation, as illustrated in Figure 3.1: The component score fluctuates between positive and negative values over time, with upward spikes in recession years (SVR, 2025) such as 1993, 2003, or 2020. An increase in the component score, which is shown in plot a), is associated with declines in employment rates (blue) across all groups, and simultaneously with increases in unemployment rates (red) across all groups, both shown in plot b). Put differently, an increase in the first PC can be interpreted as a decrease in labor market tightness —

Figure 3.1: Scores, Loadings, and Correlations of the First Principal Component

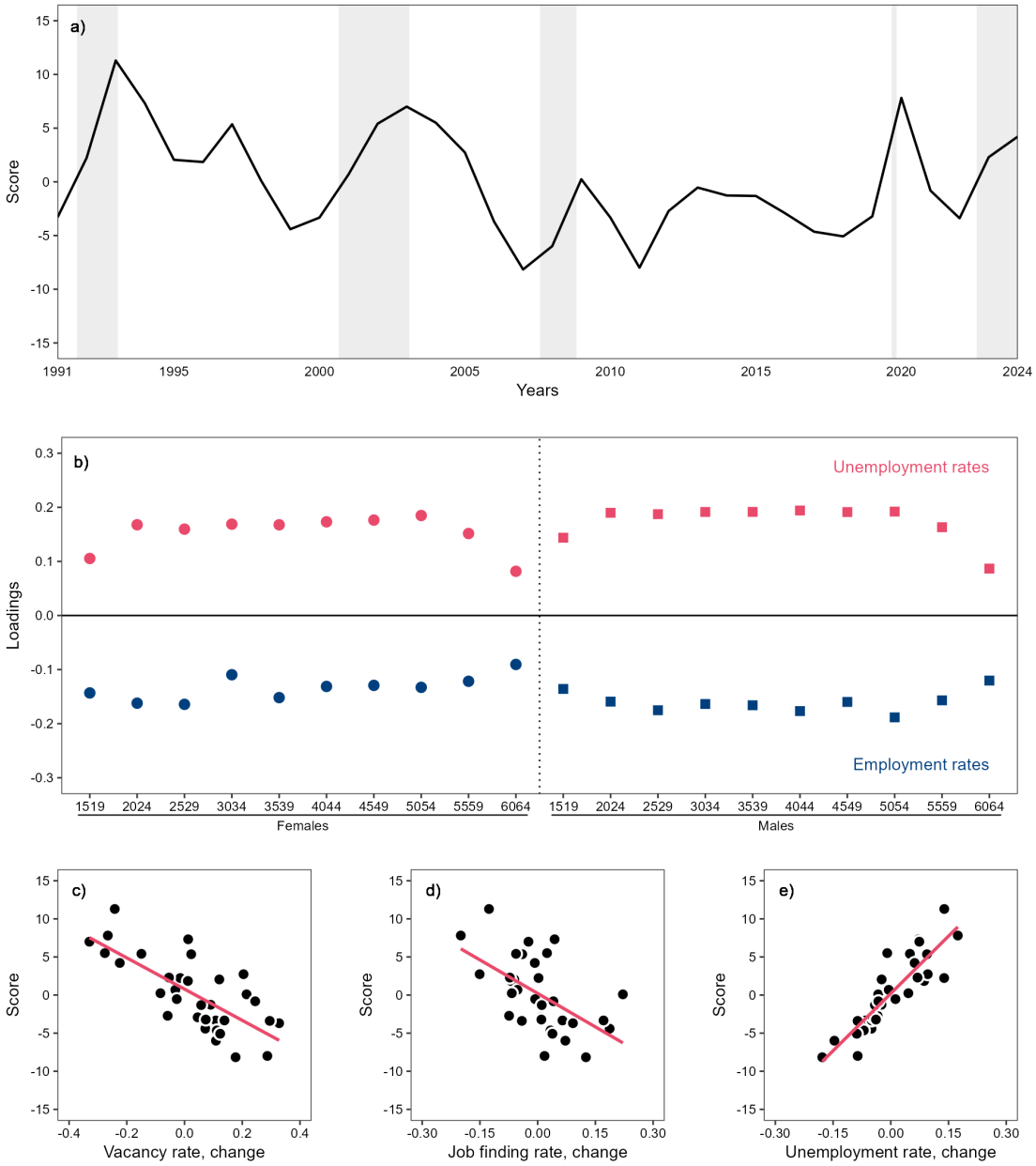

Notes: Gray rectangles in the background indicate recession periods according to SVR (2025) and based on more recent monthly GDP growth rates from Destatis (2025j). Reading example for the horizontal axis in plot b): 1519 = persons aged 15–19 years. External variables in plots c) to e) are shown as log changes. See text for sources other than author's estimates. Author's own computations and illustration.

employment rates fall, unemployment rates rise. As noted, this mechanism applies to all age groups, for both men and women, yet with different magnitudes as the factor loadings suggest.

The interpretation as a *Beveridge factor* gains additional support by evaluating the correlations with external indicators: Plot c) displays the correlation of the first PC with annual changes of the aggregate vacancy rate, that is, vacancies divided by the labor force. If the Beveridge factor increases, we expect to see decreases in the vacancy rate, as labor demand decreases, and vice versa. Here, we find the expected correlation pattern, exhibiting satisfactory strength (-0.73) — an increase in the first PC is associated with a decrease in the vacancy rate. Plot d) in the middle displays the correlation with the job finding rate; here, we expect to see a decline of the job finding rate as it becomes more difficult to exit unemployment when labor demand declines. Indeed, we find the expected pattern with a correlation coefficient of -0.56. Plot e) on the right-hand side displays the correlation with annual changes in the aggregate unemployment rate (domestic concept), and serves as a double-check: Doing so rules out that our results are driven by either changes in the group of $U_{t,N}$ or by data issues, such as structural breaks in the LFS time series. Here, the correlation is particularly strong (0.88).

These findings strengthen our argument to interpret the first PC as movements along the Beveridge curve:[4] Increases in the component score are associated with rising unemployment rates and falling employment rates, accompanied by decreases in the vacancy rate and the job finding rate — all of which are expected patterns when labor market tightness decreases.

3.4.3 Full-Employment Conditions & Hidden Labor Force Rates

Using the first PC, we seek to endogenously determine employment and unemployment rates, and thus their respective sums — the labor force participation rates — under full-employment conditions. In the literature, full-employment conditions are often operationalized by assuming a decrease of the unemployment rate (in the labor force) to a given level. In this paper, we implement this idea by calibrating the first PC such that the aggregate unemployment rate approximates its full-employment level.

Let $\tilde{u}_t^*$ be the aggregate unemployment rate in the labor force under full-employment conditions, and let $e_{s,a,t}^*$ and $u_{s,a,t}^*$ be the employment and unemployment rates in the

[4] By contrast, for PCs 2–6, we do neither find a sufficient amount of explained variance nor do we find courses, loadings, or correlations that align with a similar Beveridge curve interpretation as for the first PC. We plot PCs 1–6 in Figure 3A.3.

population by sex and age group under full-employment conditions. We calibrate the first PC by using a grid search such that

$$\frac{\sum_{s=1}^{S}\sum_{a=1}^{A} u^*_{s,a,t} P_{s,a,t}}{\sum_{s=1}^{S}\sum_{a=1}^{A}\left(e^*_{s,a,t}+u^*_{s,a,t}\right) P_{s,a,t}} \approx \tilde{u}^*_t, \tag{3.5}$$

with

$$e^*_{s,a,t} = \frac{exp\left(\sum_{k=1}^{K} \lambda^e_{k,s,a} f^*_{k,t} + e_{s,a,t-1}\right)}{1 + exp\left(\sum_{k=1}^{K} \lambda^e_{k,s,a} f^*_{k,t} + e_{s,a,t-1}\right)}, \tag{3.6}$$

where $\lambda^e_{k,s,a}$ are the loadings from the PCA above, $f^*_{1,t}$ is the calibrated value for the first PC, all other PCs, $f^*_{2,t}, \ldots, f^*_{40,t}$, are assumed to follow their observed courses,[5] and $e_{s,a,t-1}$ are the observed, logit-transformed levels of the employment rates in $t-1$.[6] To derive $u^*_{s,a,t}$, we proceed analogously as in Equation (3.6).

Then, we obtain the corresponding labor force participation rates, $l^*_{s,a,t}$, as follows:

$$l^*_{s,a,t} = e^*_{s,a,t} + u^*_{s,a,t}. \tag{3.7}$$

Now, to derive hidden labor force rates (HLFRs), we compare $l^*_{s,a,t}$ to its baseline, $l_{s,a,t}$, interpreting the differences between both as the HLFRs. Eventually, we derive the estimated HLFRs $\hat{h}_{s,a,t}$ by

$$\hat{h}_{s,a,t} = l^*_{s,a,t} - l_{s,a,t} = \left(e^*_{s,a,t} + u^*_{s,a,t}\right) - \left(e_{s,a,t} + u_{s,a,t}\right). \tag{3.8}$$

From a conceptual point of view, this framework allows an interpretation of differences in changes in labor market tightness. While $e_{s,a,t}$ and $u_{s,a,t}$, provide insights how employment and unemployment rates have changed in reality (inter alia due to observed movements along the Beveridge curve), our calibration for $f^*_{1,t}$, with resulting $e^*_{s,a,t}$ and $u^*_{s,a,t}$, provide a counterfactual interpretation; that is, how employment and unemployment rates would have changed if labor market tightness had increased sufficiently strong to reach full-employment conditions. The differences of both are the HLFRs.

While the calibration is straightforward, the corresponding results heavily depend on the assumption for $\tilde{u}^*_t$. To impose these assumptions, we rely on two perspectives outlined below. Moreover, in doing so, we need to take account of the particularities of the data in our model. First, while we use employment and unemployment data consistent with the ILO definition, discussions in HLF literature with focus on Germany

[5] In Figure 3A.8, we provide results for an alternative calibration procedure where PCs $f^*_{2,t}, \ldots, f^*_{40,t}$ are assumed to be zero.

[6] For readability, we do not explicitly include the backwards transformation of the z-standardization here.

rely on the unemployment rate following the domestic concept defined in the Social Code. To translate a full-employment level of the unemployment rate according to the domestic concept into a level consistent with our data, we assume a proportional decline. Second, our unemployment data inevitably includes $U_{t,N}$, that is, persons who are searching but who are not available to take up a job. To account for this, we subtract $U_{t,N}$ both from the numerator and the denominator in our calibration strategy. Implicitly, this requires the assumption that the increase in labor market tightness does not change their availability and thus do not foster their labor market entry, but it ensures conceptual consistency with earlier approaches (Fuchs & Weber, 2021; Provenzano, 2017) as well as with the framework by Michaillat & Saez (2021, 2024b), and also excludes any interference of structural breaks in the LFS time series.

3.4.4 Baseline Calibration: Following the HLF Literature for Germany

For our baseline calibration exercise, we again reach out to the existing literature: In the case of Germany, Fuchs & Weber (2010) assume an unemployment rate of 2.5 percent (domestic concept) to be the full-employment level (prior to the Hartz reforms and 3.5 percent afterwards), derived by a descriptive analysis of past values of the unemployment rate across business cycles and German regions. Similarly, Provenzano (2017) uses 2.5 percent as the full-employment level and Weber (2014), based upon historical labor market data, also argues that the full-employment level may lie between 2 and 3 percent (domestic concept). In a more recent paper, Fuchs & Weber (2021) assume a level of 3.2 percent, derived by regional benchmarking across Federal States. Importantly, in this case, the unemployment rate is calculated by using the labor force without self-employment in the denominator — by construction, this increases the level of the unemployment rate. Using the total labor force in the denominator as well as more recent annual (monthly) data, the benchmarking strategy by Fuchs & Weber (2021) would suggest a level of 2.8 (2.6) percent. Against the backdrop of all these earlier contributions, we assume that full-employment conditions correspond to an unemployment rate (domestic concept) of 2.75 percent.[7]

We translate this benchmark to our data as follows: For readability, let $\tilde{u}_t^{FEA}$ be the unemployment rate derived by relating the unemployed according to the domestic concept from the FEA to the labor force given by the national accounts,[8] and let $\tilde{u}_{t,I}$ be

[7] This implies that the minimum decline in the unemployment rate required to arrive at full-employment conditions is 50 percent, as the unemployment rate (domestic concept) was at 5.5 percent in 2019, which was the lowest value since 1991.

[8] Notably, the unemployment rate as published by the FEA is calculated using a figure for the total labor force in the denominator that deviates from the national accounts (for further information, see

the unemployment rate in the labor force given by our data as before. Then, using this measure, we calculate the full-employment level of the unemployment rate, $\tilde{u}^*_{t,I}$, as

$$\tilde{u}^*_{t,I} = \frac{0.0275}{\tilde{u}^{FEA}_t}\tilde{u}_{t,I}, \tag{3.9}$$

and doing so also slightly changes, due to the exclusion of $U_{t,N}$, the calibration idea as introduced in Equation (3.5), to

$$\frac{-U_{t,N} + \sum_{s=1}^{S}\sum_{a=1}^{A} u^*_{s,a,t}P_{s,a,t}}{-U_{t,N} + \sum_{s=1}^{S}\sum_{a=1}^{A}\left(e^*_{s,a,t} + u^*_{s,a,t}\right)P_{s,a,t}} \approx \tilde{u}^*_{t,I}. \tag{3.10}$$

In Figure 3.2, $\tilde{u}^*_{t,I}$ is shown as the black dotted line, which indicates a non-constant, but slowly moving full-employment level of the unemployment rate. In the upcoming section, we simulate a decline of the aggregate unemployment rate in our data from the solid to the black dotted line.

3.4.5 Sensitivity Calibration: Following Michaillat & Saez (2021, 2024b)

To address the sensitivity of our results to differences in feasibility and efficiency assumptions, we apply another calibration exercise. Let $\tilde{v}^{JVS}_t$ be the vacancy rate derived by relating vacancies from the Job Vacancy Survey (and FEA for earlier years, see data section) to the labor force given by the national accounts. Then, we find $\tilde{u}^*_{t,I}$ by

$$\tilde{u}^*_{t,I} = \frac{\sqrt{\tilde{u}^{FEA}_t\tilde{v}^{JVS}_t}}{\tilde{u}^{FEA}_t}\tilde{u}_{t,I}. \tag{3.11}$$

However, there is uncertainty whether, for Germany, Equation (3.1) reduces to Equation (3.2), since Michaillat & Saez (2021, 2024b) derive the formula using evidence for the United States, where the assumptions $\varepsilon = 1$, $\zeta = 0$, and $\kappa = 1$ plausibly hold. Moreover, these parameters may also vary over decades. To address this, as in Michaillat & Saez (2024b), we allow the parameters to vary within a set range — with $\varepsilon \in [0.75, 1.25]$, $\zeta \in [-0.25, 0.25]$, and $\kappa \in [0.75, 1.25]$ — and calculate upper and lower bounds. This range of possible combinations and resulting levels of $\tilde{u}^*_{t,I}$ is shown as shaded area in Figure 3.2.

Thus, while the black dotted line displays the level of the unemployment rate under full-employment conditions that is supposed to be feasible, the shaded area gives the range of levels that are supposed to be efficient, following recent conceptual contributions

FEA, 2025a). However, the resulting differences are small: In 2024, the unemployment rate given by the FEA was 6.0 percent, our calculation gives 5.9 percent.

Figure 3.2: Observed and Full-Employment Levels of the Unemployment Rate, 1991–2024

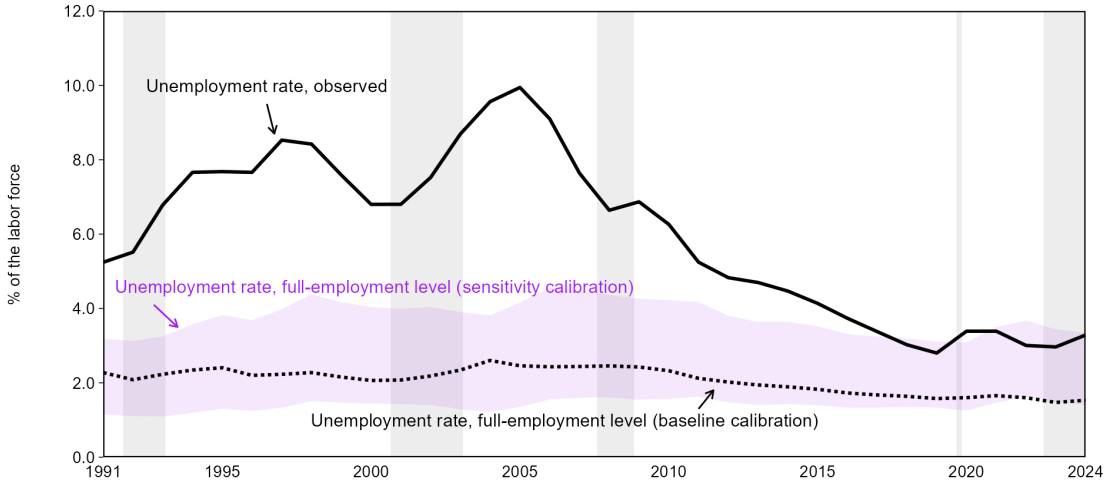

Notes: Gray rectangles in the background indicate recession periods according to SVR (2025) and based on more recent monthly GDP growth rates from Destatis (2025j). See text for sources other than author's estimates. Author's own computations and illustration.

in the literature. The comparison reveals that the black dotted line mostly lies within the shaded area. This provides conceptual support for our baseline calibration strategy. We return to a more detailed discussion in the results section, in particular with regards to the years following the Covid-19 pandemic.

Eventually, both calibration exercises deliver estimated HLFRs, $\hat{h}_{s,a,t}$. However, in the literature (e.g., Fuchs & Weber, 2021) as well as in the LFS results, $U_{t,N}$ are also defined as HLF — since those persons, although currently unavailable, are job-seeking and could be activated for the labor market under suitable conditions, such as available care options, as outlined above. Thus, by combining both the estimated HLFRs as well as the observed rates $u_{s,a,t,N}$, we are able to compare our findings to both the LFS results as well as to other existing estimation approaches in the literature. We calculate the total HLFRs $h_{s,a,t}$ as

$$h_{s,a,t} = \hat{h}_{s,a,t} + u_{s,a,t,N}. \tag{3.12}$$

3.4.6 The Multiplier Effect of Full Employment: Quantification of Mitigation Potentials until 2035

To address the effects of demographic change and quantify mitigation potentials from the HLF, we link our model to a population and labor supply projection, delivering projection data until 2035. We choose the projection horizon until 2035 as this period covers the gradual exit of the large mid-1960s cohorts from age groups with high labor

force participation rates, and is thus the most interesting from a demographic perspective. Eventually, this linkage allows us to quantify to which extent an activation of the HLF is able to counteract declines in aggregate labor supply as a consequence of population aging and decline, and thus to maintain the aggregate employment level at its size of the year 2024.

For this purpose, we rely on the updated projection model by Hellwagner et al. (2023). This model is tailored to Germany, offering readily usable population data. Moreover, it provides a projection method for full-employment participation rates — which is a resulting measure of our model, allowing us to easily apply the participation projection framework to our data. In the appendix, Figure 3A.4 displays the sex- and age-structure resulting from the population projection for the year 2035. Moreover, using projection values for $l^*_{s,a,t}$ implies using projection values for labor force participation under full-employment conditions. This allows us to interpret the projected changes as driven by factors *other than* movements along the Beveridge curve.

Thus, we now calibrate the first PC in projection year t such that aggregate employment remains constant at the level of 2024. We denote the resulting score as $f^\star_{1,t}$. Then, we find the corresponding sex- and age-specific employment rates $e^\star_{s,a,t}$ by[9]

$$\sum_{s=1}^{S}\sum_{a=1}^{A}\left(\left(\hat{\beta}_{s,a}f^\star_{1,t}+e^\star_{s,a,t-1}\right)+\Delta\dot{e}_{s,a,t}\right)P_{s,a,t}=\sum_{s=1}^{S}\sum_{a=1}^{A}e^\star_{s,a,t}P_{s,a,t}\approx\sum_{s=1}^{S}\sum_{a=1}^{A}E_{s,a,2024}, \tag{3.13}$$

where we obtain $\hat{\beta}_{s,a}$ from linear regressions of the original first differences of the logits ($\Delta e_{s,a,t}$) on the first PC, and where $e^\star_{s,a,t-1}$ are the level of the employment rates in the previous projection year.[10] Using the calibrated values for $f^\star_{1,t}$, we can also derive $u^\star_{s,a,t}$.

In this setting, all other components are treated as zero. The latter is a conceptually plausible assumption due to the inclusion of $\Delta\dot{e}_{s,a,t}$ and $\Delta\dot{u}_{s,a,t}$, capturing the important variation in participation behavior over time which does not represent changes in participation behavior induced by movements along the Beveridge curve. We find $\Delta\dot{e}_{s,a,t}$ and $\Delta\dot{u}_{s,a,t}$ by exploiting the variation in projected changes of $l^*_{s,a,t}$ given by the framework of Hellwagner et al. (2023) as follows:

$$\Delta\dot{e}_{s,a,t}=\left(\frac{e^\star_{s,a,t-1}}{e^\star_{s,a,t-1}+u^\star_{s,a,t-1}}\right)\Delta l^*_{s,a,t}, \tag{3.14}$$

$$\Delta\dot{u}_{s,a,t}=\left(\frac{u^\star_{s,a,t-1}}{e^\star_{s,a,t-1}+u^\star_{s,a,t-1}}\right)\Delta l^*_{s,a,t}, \tag{3.15}$$

[9] For readability, we do not explicitly include any exponentiation of logit-transformed data here.

[10] Naturally, for the first period in the projection, $e^\star_{s,a,t-1}$ equals the observed levels in 2024, $e_{s,a,2024}$.

which, notably, implies that we assume $u^{\star}_{s,a,t,N}$ to remain at the 2024 values throughout the period until 2035.

As a consequence, our projection framework is a stepwise one-year-ahead procedure which accounts not only for changes in employment, unemployment, and participation driven by movements along the Beveridge curve, but also for changes in the size and structure of the population due to the inclusion of the population projection as well as for general trends in sex- and age-specific labor force participation patterns over time due to the inclusion of the participation projection. Moreover, since this procedure delivers values for unemployment, we can derive the resulting aggregate unemployment rate in the labor force, $\tilde{u}^{\star}_{t}$.

The latter offers a more intuitive interpretation: Which size of a decline in the unemployment rate is required to maintain the employment level at its value of 2024? Conceptually, this quantification exploits a *multiplier effect*: An increase (decrease) in labor market tightness (the unemployment rate) implies not only people moving from unemployment into employment but also activates people from outside of the labor force — the hidden labor force. In the results section, we quantify both channels.

3.5 Results

3.5.1 Size and Structure of the HLF over Time

Figure 3.3 displays the aggregate HLF for the period 1991–2024. The black dotted line displays the estimated HLF according to our model, the solid black line displays the total HLF defined as the sum of the estimated HLF and observable HLF. We derive the level of the HLF by linking the estimated and total HLFRs to the population figures from Klüsener et al. (2018),[11] Destatis (2025h), and to the population figures for more recent years sent by Destatis on request. Doing so accounts for census adjustments in the past.

The model estimates a larger HLF during the first half of the observation period, with an estimated average of 1.27 million persons between 1991 and 2005, peaking at 1.45 million persons in 1996. The estimated HLF entered an enduring decline in subsequent years, with a minimum of 0.58 million persons in 2022. The total HLF mirrored these developments. In 2024, the estimated HLF was at 0.72 million persons, the total HLF was at 1.13 million persons.

Thereby, the distribution of the HLF across demographic groups varies. Figure 3.4 provides corresponding disaggregated insights and displays the HLFRs by sex and age group for the year 2024. Again, the black dotted line shows the estimated HLFRs and

[11] Data downloaded from the Human Mortality Database: www.mortality.org (5 November 2025).

Figure 3.3: Total and Estimated Hidden Labor Force, 1991–2024

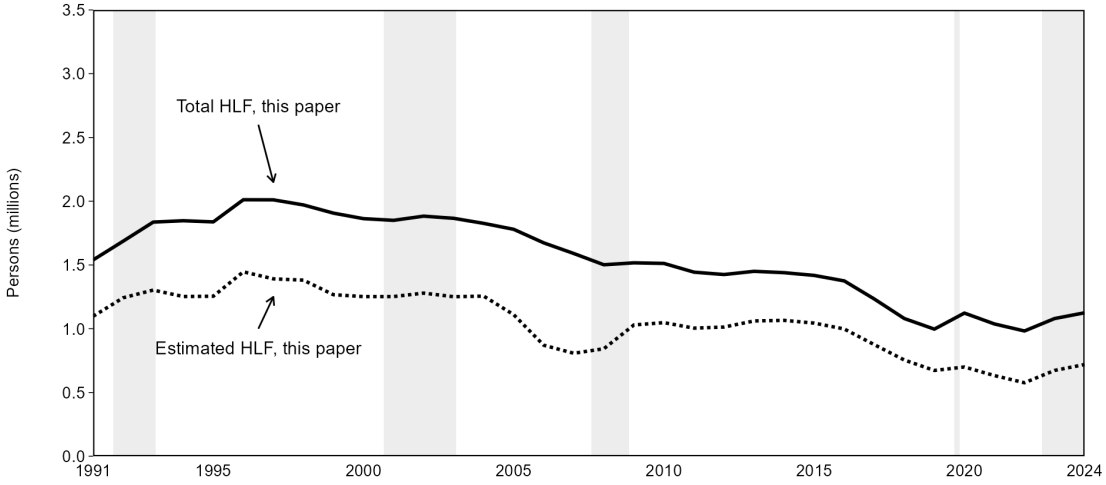

Notes: Gray rectangles in the background indicate recession periods according to SVR (2025) and based on more recent monthly GDP growth rates from Destatis (2025j). HLF = hidden labor force. Author's own computations and illustration.

the solid black line indicates the total HLFRs. The results indicate for both males and females larger HLFRs among younger persons. According to our model, lower HLFRs can be found among those of prime age, whereas HLFRs are increasing towards retirement age, yet still below the level of younger persons. Across all demographic groups, the largest total (estimated) HLFR in 2024 is that of females aged 15–19 years with 5.8 (4.7) percent, the lowest total (estimated) HLFR is that of females aged 45–49 years with 0.7

Figure 3.4: Total and Estimated Hidden Labor Force Rates by Sex and Age Group, 2024

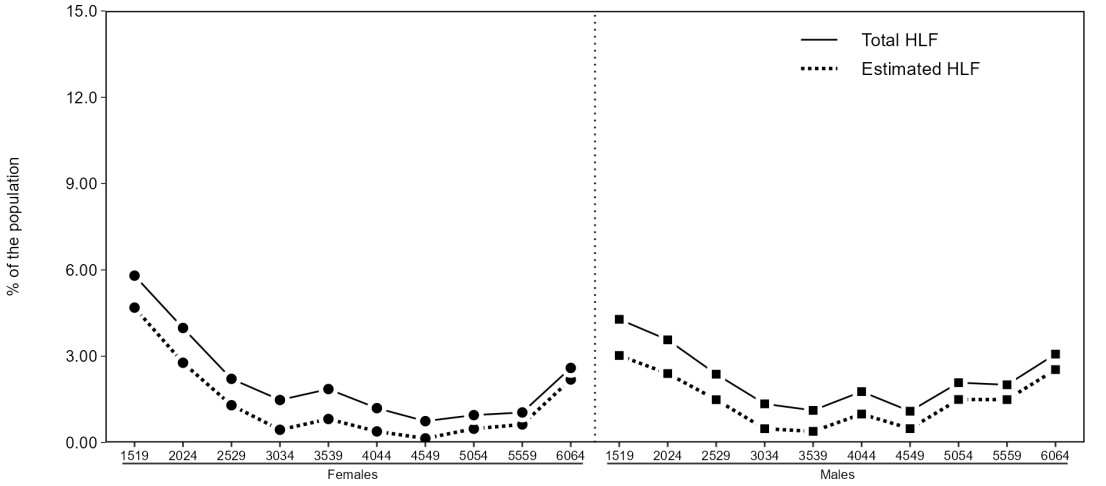

Notes: HLF = hidden labor force. Reading example for the horizontal axis: 1519 = persons aged 15–19 years. Author's own computations and illustration.

Figure 3.5: Total and Estimated Hidden Labor Force Rates by Broad Age Groups, 1991–2024

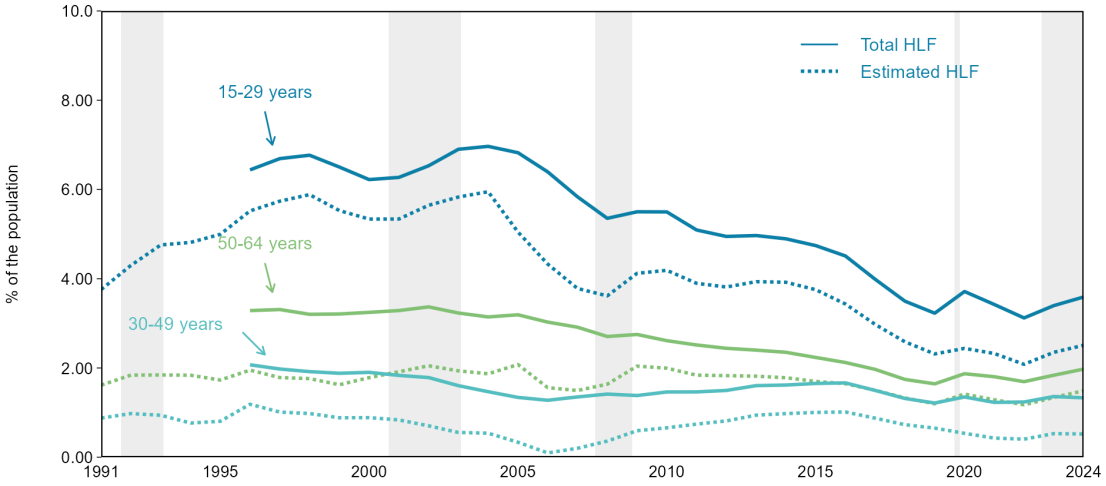

Notes: Gray rectangles in the background indicate recession periods according to SVR (2025) and based on more recent monthly GDP growth rates from Destatis (2025j). HLF = hidden labor force. Author's own computations and illustration.

(0.1) percent. The total (estimated) HLFR in the overall population aged 15–64 years in 2024 is 2.1 (1.4) percent.

Figure 3.5 displays HLFRs by broad age groups over time, again with the dotted lines for estimation results and the solid lines for total HLFRs. For younger and older persons, the HLFRs are not only larger from a cross-sectional perspective, but exhibit also larger fluctuations over time; the decline during the past decade can be seen among younger and older persons, but less so among those of prime age.

3.5.2 Comparison to Existing Estimates

We check the plausibility of our results by comparing them, on the one hand, to survey results from the LFS and, on the other hand, to the existing estimates by Fuchs & Weber (2021). While our approach covers those aged 15–64 years, resembling earlier contributions (Fuchs & Weber, 2021; Provenzano, 2017), the LFS holds evidence for persons aged 15–74 years — but among those aged 60 years and older, the HLFRs in the LFS are small. We provide a corresponding extension of our approach to older age groups below.

Figure 3.6 allows a comparison of the size of the HLF according to the different sources over time in the upper plot a).[12] As before, the black solid line is the total HLF according to the framework introduced in this paper. The yellow solid lines are the HLF

[12]Since the publication of the results by Fuchs & Weber (2021) and (some) of the LFS data, population figures in Germany have been revised (Destatis, 2025h). In the subsequent comparison, we do not

Figure 3.6: Comparison of Total Hidden Labor Force and Total Hidden Labor Force Rates Across Sources

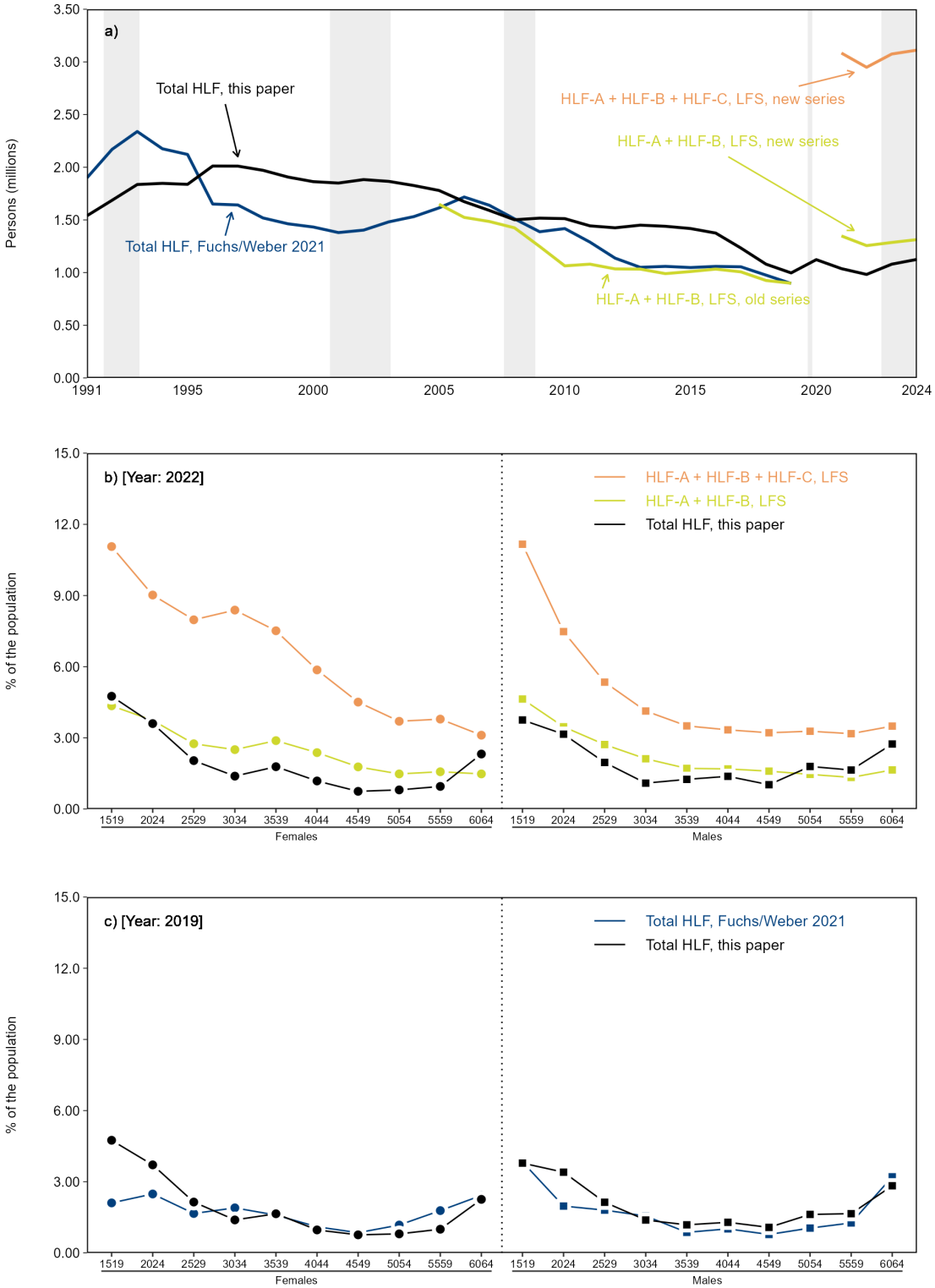

Notes: Gray rectangles in the background indicate recession periods according to SVR (2025) and based on more recent monthly GDP growth rates from Destatis (2025j). See text for sources other than author's estimates. HLF = hidden labor force. LFS = Labor Force Survey. Reading example for the horizontal axis in plots b) and c): 1519 = persons aged 15–19 years. Author's own computations and illustration.

as given by the LFS (Eurostat, 2026c), including HLF-A and HLF-B. The orange solid line additionally includes HLF-C. There was a structural break in the LFS time series around 2020 (see Destatis, 2025f, for further information). The blue solid line is the total HLF from Fuchs & Weber (2021); conceptually, their interpretation is identical to our model, that is, encompassing both the estimation-based and the NAJS-based HLF. Yet, it differs with regard to the empirical model and the underlying full-employment assumptions.

An important explanation for the differences in the HLF size compared to Fuchs & Weber (2021) is the modeling strategy: They use a large number of individual models, with varying external full-employment indicators and also varying full-employment levels over time. By contrast, we use a single model, identify a latent labor market tightness factor, and calibrate full-employment conditions endogenously.

While there are still conceptual similarities of our approach to Fuchs & Weber (2021), the conceptual differences to the LFS figures are larger. There, the data is based on survey responses and indicate persons who are either currently not actively looking for a job or, despite looking for a job, are not immediately available — with underlying reasons being manifold and may not diminish due to rising labor market tightness. This may cause larger differences of the LFS results to our model, not only with regard to the size of the HLF, but also concerning its demographic structure.

The latter becomes visible when comparing the HLFRs by sex and age across sources in Figure 3.6. For the LFS, shown in plot b), we retrieved HLFRs for the year 2022 from the Microcensus Scientific Use File, and for Fuchs & Weber (2021) we use their most recent estimate in 2019 in plot c).[13] Our results resemble some findings of the sex- and age-specific HLFRs from the LFS (HLF-A+HLF-B), in particular the high HLFRs among younger persons, but indicate comparatively lower HLFRs among prime-age and higher HLFRs among persons close to retirement; all of this for both men and women. We document more similarities when comparing our model results to those of Fuchs & Weber (2021) in plot c). Here, we analyze the HLFRs by source for the year 2019. Like the more complex, single-equations-based approach by Fuchs & Weber (2021), our model tends to deliver slightly u-shaped HLFRs, with larger rates among younger persons and those close to retirement, but lower rates for those of prime age. Larger differences in 2019 are only visible among younger females. Importantly, the estimates differ more strongly for earlier years (see Figure 3A.5 in the Appendix 3.B).

account for this revision, or for other minor differences in the underlying population data compared to our approach, but present the original results from those two sources.

[13] Fuchs & Weber (2021) use data on labor force participation by sex, age, and — additionally — citizenship. To compare our results to their estimates, we combine the HLFRs as well as the population by citizenship as given in their paper accordingly.

Notably, while the LFS series suffers from the structural break in 2020, this is ruled out in our approach up to the scale of $U_{t,N}$, which is based upon LFS data as well and which exhibits an increase by roughly 100,000 persons from 2019 to 2021. Beyond that, our model suggests only small changes in the level of the HLF. By contrast, the total increase of HLF-A and HLF-B from the LFS during the same period was approximately 450,000 persons. Against this backdrop, our approach provides a consistent measure for the HLF over time and can also be used to assess the HLF during the structural break and before.[14]

3.5.3 Sensitivity Analysis

The sensitivity of the model results to different full-employment assumptions are illustrated in Figure 3.7 by comparing the baseline results (black dotted line) to the sensitivity calibration exercises (shaded area). For most years, our baseline calibration exercise clearly coincides with the range of plausible efficiency levels, as the black dotted line lies within the shaded area. From a policy perspective, this is encouraging, as it suggests that the substantial activation potentials implied by the baseline calibration are not only feasible but also efficient. Only for recent years, in the aftermath of the Covid-19 pandemic, we observe some signs of slight divergence.[15] As noted above, recent contributions (Hobijn, 2024) pointed towards possible issues in the derivation of u^* as introduced by Michaillat & Saez (2021, 2024b) — such a mechanism could also play role here, as, for example, the outward shift of the Beveridge curve in recent years (SVR, 2024) may have increased the level of u^* and, vice versa, decreased the estimated HLF. Yet, we argue, that this mechanism is informative as it calls for policies to shift the Beveridge curve back inwards. In the case of the outward shift of the Beveridge curve after the pandemic, beyond institutional factors (Weber, 2026), recent evidence suggests that in particular the mismatch in the labor market for unskilled and semi-skilled workers has increased (Bauer, 2024). For example, as Bauer (2024) argues, policies that aim at improving qualification levels of the unemployed in order to align demand and supply across requirement levels are important. This does not only decrease current mismatch in the labor market but also sets the conditions for an efficient activation of the feasible HLF.

[14] While our paper exploits realized labor supply over time, survey responses represent labor supply intentions — which not necessarily translate into realized actions. Moreover, surveyed intentions may differ depending on the concrete survey settings. For example, in Germany, the Microcensus and the Socio-Economic Panel (SOEP) both measure underemployment, but provide vastly different figures, even after accounting for differences such as survey design (see Rengers et al., 2017, for a detailed analysis).

[15] Notably, this divergence is larger (smaller) when assuming lower (higher) full-employment levels compared to the baseline calibration exercise. Figure 3A.6 in Appendix 3.B provides the results when assuming unemployment rates of 2.5 percent and 3 percent rather than 2.75 percent.

Figure 3.7: Estimated Hidden Labor Force, Baseline and Sensitivity Calibration, 1991–2024

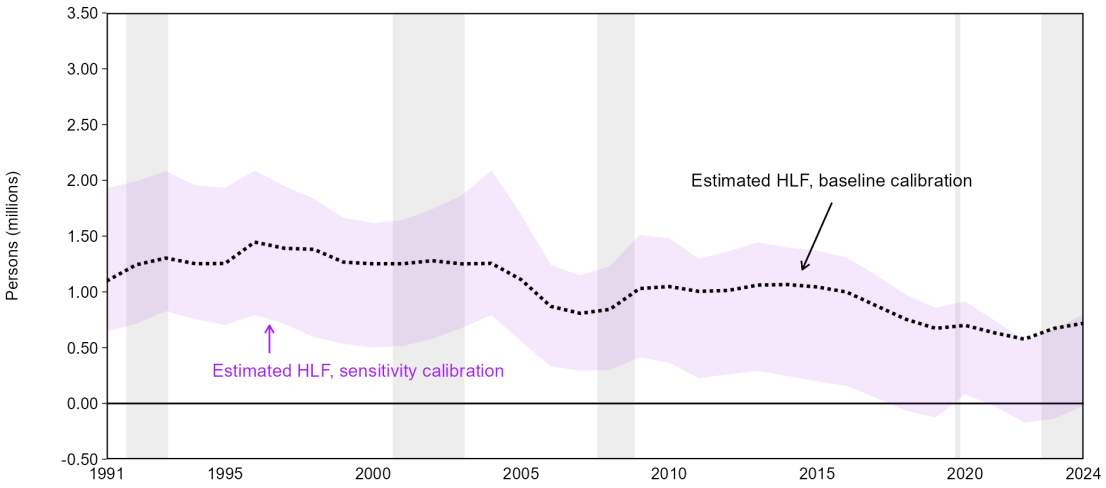

Notes: Gray rectangles in the background indicate recession periods according to SVR (2025) and based on more recent monthly GDP growth rates from Destatis (2025j). HLF = hidden labor force. Author's own computations and illustration.

3.5.4 Extension: Estimated HLFRs Among Those Aged 65–74 Years

In our baseline model, we use data on employment and unemployment rates by sex and age groups among those of working age. This resembles earlier estimation approaches in the literature (Fuchs & Weber, 2021; Provenzano, 2017), yet disregards the growing labor market participation among persons beyond 65 years of age (Walwei, 2024). Also, the HLF as given by the LFS includes persons 15–74 years of age (Destatis, 2025a).

To account for this, we extend the model by including the labor market participation rates of those aged 65–69 years as well as those aged 70–74 years by sex. The data sources are identical to the data used in the baseline model. However, in the extension, we only include participation rates, since unemployment rates in the case of those beyond 65 years of age are either nonexistent or unavailable due to very low case figures. Thus, participation rates for these age groups are essentially employment rates.

Using the same calibration as in the baseline specification, we derive corresponding HLFRs by sex and age, plotted for the year 2024 in Figure 3.8, where the light blue dotted line illustrates the results.

The differences among those aged 15–64 years compared to the baseline model are negligible. For the newly added groups of persons aged 65–69 years and 70–74 years, we find substantial HLFRs. In 2024, the estimated rates for females (males) aged 65–69 years are 3.7 (3.9) percent, for those aged 70–74 years the rates are slightly lower with 2.8 (3.3) percent.

Figure 3.8: Estimated Hidden Labor Force Rates by Sex and Age Group, Extended Model, 2024

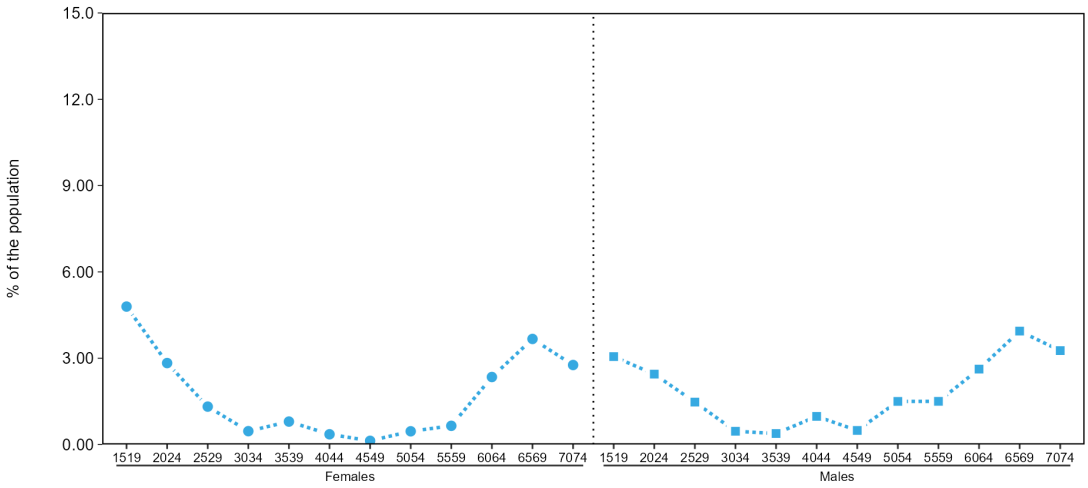

Notes: Reading example for the horizontal axis: 1519 = persons aged 15–19 years. Author's own computations and illustration.

For 2024, this translates into 0.33 million persons in the HLF that have not been captured by the baseline model and reflects a growing HLF among the elderly as illustrated by Figure 3.9. These figures appear high, yet international comparisons show that in Germany, participation rates among persons aged 65 years and above lag behind those in other countries (Walwei, 2024), and the extent of these gaps can be reconciled well with our findings.

Figure 3.9: Total Hidden Labor Force, Baseline and Extended Models, 1991–2024

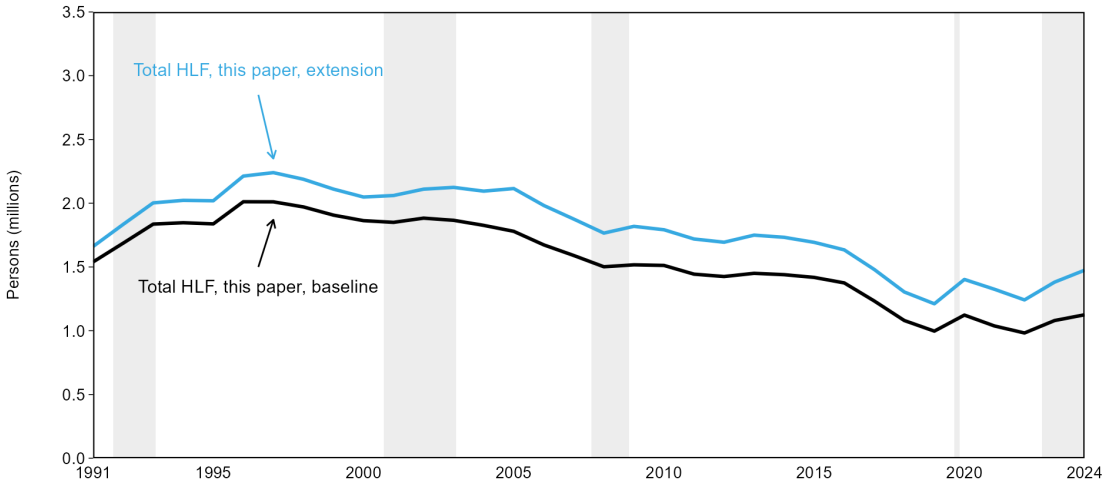

Notes: Gray rectangles in the background indicate recession periods according to SVR (2025) and based on more recent monthly GDP growth rates from Destatis (2025j). HLF = hidden labor force. Author's own computations and illustration.

3.5.5 Mitigating the Effects of Population Decline: Hidden Labor Force Activation until 2035

Against the backdrop of population aging and decline, our HLF estimates suggest substantial mitigation potentials. Yet, quantifying these potentials requires a closer look, in particular concerning the interaction of participation patterns with future changes in the demographic structure.

In Figure 3.10, we display the results of the projection framework introduced in Equations (3.13) to (3.15). In the upper plot a), we display the implied flows into employment in the adjustment scenario, resulting from the introduced stepwise year-on-year calibration of the first PC such that aggregate employment remains at its level in 2024. As shown by the stacked bars, the adjustment scenario exploits a multiplier effect: If labor market tightness increases, we observe both persons moving from outside of the labor force into employment (I-E flows; HLF activation), but also from unemployment into employment (U-E flows). We decompose to which extents both channels contribute to maintain aggregate employment at its 2024 level, with U-E flows as light pink and I-E flows as darker pink areas in plot a). Thereby, the annual activation from the HLF is larger, with an average of 150,000 persons per year between 2026 and 2035, compared to an annual average of 95,000 persons from unemployment. While both channels contribute to a similar extent during the first years, the contribution of the activation from the HLF increases over time.

Of course, in reality declines in the unemployment rate are limited. In Figure 3.10, the lower plot b) addresses this issue and visualizes the level of the unemployment rate which results from the calibration exercise. Put differently, plot b) shows the level of the unemployment rate which is necessary to maintain aggregate employment at its 2024 level; this level is visualized as the black solid line. Between 2026 and 2035, the mean annual decline in the unemployment rate necessary to maintain the employment level is 0.2 percentage points.[16]

The comparison with the horizontal line in the background suggests that the declines in the unemployment rate until 2032 are feasible when compared to the full-employment level of the unemployment rate as of 2024. In other words, our results suggest that the activation of the HLF can serve as an important building block to mitigate demographically induced declines in labor supply for some of the upcoming years — in our application, given the population and participation projections, until 2032 — but may

[16] Due to the proportional increases introduced by Equations (3.14) and (3.15), the unemployment rate in the non-adjustment scenario is always very close to the unemployment rate in the respective previous year. Changes in the demographic structure cause minor differences.

Figure 3.10: Labor Market Flows and the Unemployment Rate in the Adjustment Scenario, 2024–2035

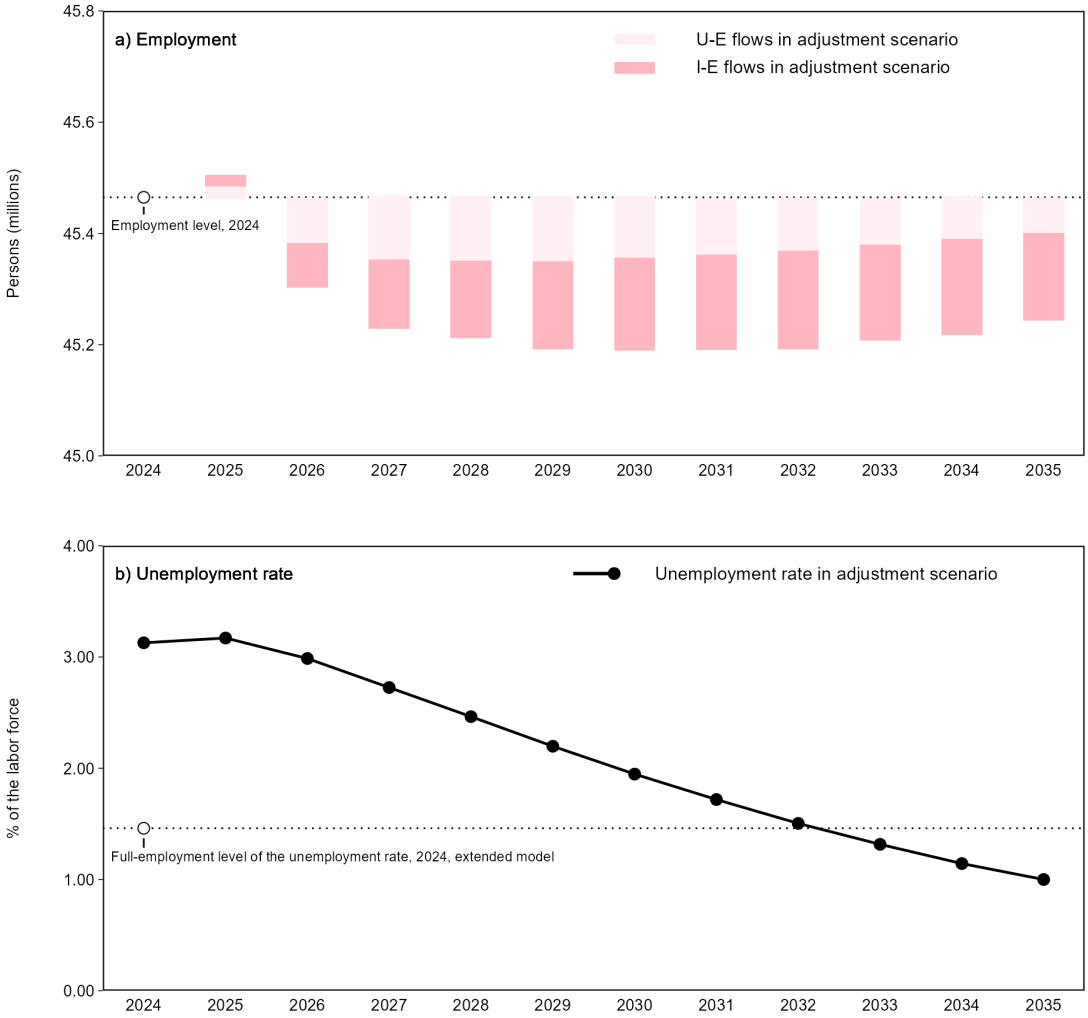

Notes: Author's own computations and illustration.

not be sufficient in view of the whole order of magnitude of the impending demographic change.[17]

Still, we argue that from a policy perspective, our findings are encouraging. First, in view of the impact of the impending demographic change, maintaining the employment level until 2032 would already be noteworthy.[18] Second, this framework is based upon the underlying population projection by Hellwagner et al. (2023), subject to a compara-

[17]Notably, this is also mirrored in the aggregate participation rate resulting from our projection and calibration strategy. As shown in Figure 3A.7 in Appendix 3.B, the aggregate participation rate exceeds the projected aggregate full-employment participation rate after 2032.

[18]In the absence of the calibration channel, thus if employment rates would only develop as a result of Equation (3.14), aggregate employment in 2032 would be 1.7 million persons lower compared to 2024.

tively low net migration which could increase due to a decline in unemployment.[19] Put differently, the combination of participation increases due to HLF activation, on the one hand, with a moderately higher net migration than implied by the underlying population projection, on the other hand, emerges as a promising path to stabilize aggregate labor supply in Germany in the upcoming years.[20] Third, rather than requiring an immediate and strong decline in the unemployment rate, the calibrated annual declines in the unemployment rate according to our model are limited.

3.5.6 Limitations

Despite notable plausibility in comparison to other existing estimates and survey results, our approach still exhibits some limitations.

We split the labor force participation rates into employment and unemployment rates in order to calibrate full-employment conditions endogenously. This modeling strategy is accompanied by two implications. First, despite applying a logit transformation to the data, the sum of employment and unemployment rates under full-employment conditions can exceed the value of one. In our application, this does not happen, and the largest value of labor force participation rates under full-employment conditions is 0.984. Applications that encounter this issue might rely on other, yet possibly less intuitive data preparation steps, such as isometric log ratios. Second, the size of the HLFRs by age and sex does not only depend on the necessary change in the labor demand factor between $t-1$ and t to achieve full-employment conditions in t, but also on the level of sex- and age-specific employment and unemployment rates in $t-1$. As a consequence, estimated sex- and age-specific HLFRs may become negative for some or all groups in some or all years. In our baseline application, this happens to some estimated HLFRs of women aged 40–59 years during the early- and mid-2000s, when the group-specific unemployment rates were particularly high and the modeled declines in unemployment rates (in the population) exceed increases of the employment rates (in the population).

Moreover, in any approach estimating participation rates under full-employment conditions, benchmarking the latter is decisive. While contributions in the literature offer some definitions, translating these into specific levels for the unemployment rate is still up for debate. This relates to both the feasibility of realizing a defined unemployment

[19] In their projection, the net migration drops below the level of 200,000 persons from 2026 onward. Compared to the observed net migration to Germany over the past decades, this is a rather low value.

[20] By contrast, other approaches suggest the necessity of a substantially higher annual net migration of 400,000 to maintain the overall labor supply level, yet do not discuss HLF activation (e.g., Fuchs et al., 2021b).

rate,[21] but also to the accompanying effects, that is, both the question of an efficient level of the unemployment rate (Michaillat & Saez, 2021) as well as possible trade-offs between rising labor supply and rising inflation. Numerous contributions have addressed the trade-off between unemployment and inflation (as a recent example Crump et al., 2019), advocating the non-accelerating inflation rate of unemployment (NAIRU) as a pivotal policy benchmark. Thereby, the NAIRU suggests a way smaller (or negative) unemployment gap than HLF estimation approaches (AMECO, 2026), implying substantially smaller to no efficient activation potentials. In this paper, we do not address this issue. In another recent contribution, Michaillat & Saez (2024a) present a framework which suggests that inflation is on target whenever the labor market is efficient. For future research, this offers promising starting points.

3.6 Conclusion

Labor shortages have increasingly gained attention in recent years, particularly in Germany, where the drop to below-replacement fertility in the 1970s is heralding impending declines in labor supply in the near future. Among others, the labor market entry of yet inactive persons may offer substantial mitigation potentials. However, the extent to which additional labor market entries are feasible is often either unclear or requires complex empirical approaches. In this paper, we address these issues by introducing a parsimonious empirical framework to estimate hidden labor force rates by sex and age. We apply PCA to a matrix of employment and unemployment rates by demographic groups, covering the period 1990–2024, and use an endogenous calibration exercise to derive the levels of labor force participation rates under full-employment conditions.

Our results suggest that in 2024, the hidden labor force in Germany among those aged 15–64 (15–74) years was 1.13 (1.47) million persons. If all of these persons entered the labor market, the labor force in Germany would have increased by 2.4 (3.1) percent. Thus, against the backdrop of a demographically induced labor supply decline, the hidden labor force offers considerable activation and mitigation potentials. Thereby, our model results suggest differences across demographic groups. While we find higher hidden labor force rate among younger persons and among those close to retirement, we find lower rates among those in prime age. This aligns well with the findings of earlier

[21] Notably, from a policy perspective, this paper offers an approach to quantify feasible and efficient additional labor supply in Germany, but the model does not provide any policy insights beyond these estimates. Thus, it does not allow to provide additional insights into the mechanism or policy requirements to achieve full employment (for an overview: Lichtenberger et al., 2025). Similarly, the model addresses only the extensive margin of labor supply, while unused labor supply may also be activated at the intensive margin (see Destatis, 2025i, for recent evidence on involuntary part-time work in Germany).

estimation approaches in the literature. By contrast, compared to survey results, our findings suggest lower hidden labor force rates among those in prime age and markedly higher hidden labor force rates among those close to retirement age. Importantly, the size of the hidden labor force in our model strongly depends on the imposed assumption of full-employment conditions, that is, at which level of the aggregate unemployment rate one perceives a state of full employment to be achieved. We link our results to a recent and ongoing discussion on efficient full-employment conditions and find that the activation potentials suggested by our empirical approach are not only feasible, but also efficient.

Eventually, we define and exploit the multiplier effect of unemployment reduction for employment, which follows from the additional activation of the HLF. We do so by combining our empirical framework with a population and participation projection for Germany, allowing us to evaluate, against the backdrop of expected demographically induced labor supply declines in the future, to which extent this multiplier effect offers mitigation potentials. We find that unemployment reduction and the accompanying activation of the hidden labor force can serve as an important building block to counteract impending declines in aggregate employment. Until 2032, even the entire decline could be offset via this channel.

3.A Appendix A: Additional Information on Data Sources, Data Preparation, and a Comparison to the LFS

3.A.1 Labor Force Participation Rates, 1990–1996: Preparation Details

As outlined in the main text, we use data from the Destatis website for the period 1990–2001. For the years 1990–1996, we rely on data for West Germany in order to exclude any interference driven by the German reunification. In 1996, we chain-link to the data for Germany.

3.A.2 Labor Force Participation Rates, 2011–2024: Sources & Preparation Details

In Germany, two sources quantify overall labor supply: the LFS and the employment estimates within the German national accounts (EENA). While the LFS allows to disentangle labor supply by sex and age, the EENA publishes only an aggregate figure. Moreover, as well documented in the literature (Körner & Marder-Puch, 2015), the figures of overall employment in Germany differ strongly between both sources, with the EENA usually delivering a larger figure. In 2024, this difference amounted to 3.1 million persons, with the EENA finding a total employment of 45.8 million persons (Destatis, 2025b).

Inevitably, if the LFS underestimates labor supply, the corresponding labor force participation rates tend to be too low — and, vice versa, the remaining capacity for increases is too high. In order to avoid overestimating activation potentials, we collect data from various sources to construct labor force participation rates by sex and five-year age groups for the period 2011–2024 that are consistent with the German national accounts.

As in the main text, for sex s and age group a, the labor force participation rate l in year t is given by $l_{s,a,t} = \frac{L_{s,a,t}}{P_{s,a,t}}$, where L is the mean annual labor force and P is the corresponding mean annual population. For the latter, we use population data by Klüsener et al. (2018),[22] Destatis (2025h) as well as for more recent years from population data sent by Destatis on request, and calculate the mean annual population from the original data by linear interpolation.

To calculate L by sex and age, we rely on several data sources to address all components appropriately. For simplicity, assume the following notation: dependent employ-

[22] Data downloaded from the Human Mortality Database: www.mortality.org (5 November 2025).

ment excluding civil servants ($DE_{s,a,t}$), self-employment ($SE_{s,a,t}$), contributing family workers ($CF_{s,a,t}$), civil servants ($CS_{s,a,t}$), unemployment according to the ILO definition ($U_{s,a,t,I}$), additional estimates ($AD_{s,a,t}$), and out-commuters ($OC_{s,a,t}$).

Thereby, we strive to find annual participation rates by sex and age, $l_{s,a,t}$, which mirror an aggregate labor force that corresponds to the benchmark figures of the EENA, thus to ensure:

$$\sum_{s=1}^{S}\sum_{a=1}^{A} l_{s,a,t}P_{s,a,t} = E_t + U_t = L_t^{EENA} + OC_t, \tag{3A.1}$$

where OC_t are the out-commuters to other countries. We return to this subgroup below. Notably, all of these data refer to the labor force resident in Germany, that is, excluding incoming commuters.

Dependent Employment Excluding Civil Servants

For dependent employment, we use detailed statistics by the FEA. These statistics cover all dependent employees in Germany, excluding civil servants, and are available by sex and age. Given the nature of its collection as a register database, the FEA statistics are assumed to be of high quality. For 2024, the FEA statistics holds more than 39 million dependent employees, which accounts for the major part of L_t^{EENA}.

Self-Employment, Contributing Family Workers, Civil Servants, and Unemployment

For self-employment, contributing family workers, civil servants, and unemployment, we apply different preparation steps. Using the aggregate figures of those components from the EENA, we find the structure by sex and age by relying on the LFS (sent by Destatis on request), and additionally for civil servants on the Statistics of Public Employees (for the 2022 data: Destatis, 2025g). We adjust the size of each sex- and age-specific group of these components except unemployment by relying on information for secondary dependent employment from the Microcensus Scientific Use Files, in order to avoid double-counting of those that have already been captured by $DE_{s,a,t}$. In 2024, the unadjusted sum of self-employed, contributing family workers, and civil servants amounted to 5.8 million persons, which accounts for a minor part of L_t^{EENA}.

Additional Estimates

Now, summing across all those components, we obtain labor force figures which are, for each year of the period 2011–2024, still smaller than the corresponding benchmark

figures, L_t^{EENA}. As documented in the EENA manual (AKETR, 2016), the difference is due to estimated additional employment. We account for this in two steps.

First, as stated in AKETR (2016), a substantial share of the additional estimates is due to undocumented employment in NACE sector T,[23] that is, employment in households. From 2011 to 2024, the difference between documented employment in T according to the FEA statistics and the final, additional estimation-including EENA figures for NACE T varies between roughly 600,000 to more than 700,000 persons. We distribute these differences across sex and age according to the observed employment patterns from the FEA statistics. This resembles a data preparation approach in Wanger et al. (2019). For readability, we denote these groups as AD_t^{HH}.

Second, the remaining difference is smaller, varying between 100,000 to 400,000 persons over the observation period. Since we do not have any precise information on the distribution of these persons across economic sectors, we choose a different approach, and distribute the remaining difference according to the structure of inactive persons I_t. More formally, we calculate

$$I_{s,a,t} = P_{s,a,t} - DE_{s,a,t} - SE_{s,a,t} - CF_{s,a,t} - CS_{s,a,t} - U_{s,a,t} - AD_{s,a,t}^{HH} - OC_{s,a,t}, \quad \text{(3A.2)}$$

and derive the remaining additional labor force by sex and age $AD_{s,a,t}^{OTHER}$ as

$$AD_{s,a,t}^{OTHER} = \frac{I_{s,a,t} w_{s,a,t}}{\sum_{s=1}^{S} \sum_{a=1}^{A} I_{s,a,t} w_{s,a,t}} AD_t, \quad \text{(3A.3)}$$

where $w_{s,a,t}$ are sex- and age-specific weights that capture the sex- and age-specific participation rates, as prepared up to this point, and the respective differences to the LFS rates. This allows to distribute the remaining, not-yet assigned labor force across the remaining inactive persons, but includes information on sex- and age-specific participation patterns as well as structural information from the LFS. In any case, the impact of this step is rather small, as less than one percent of the labor force is calculated and distributed this way.

Out-Commuters

Eventually, compared to LFS data, the EENA and its implicitly underlying participation rates do not include out-commuters. As before, this may lead to biased results as the remaining capacity for increases is too large. Addressing this issue, we add out-commuters by sex and age $OC_{s,a,t}$ to our participation rates by combining the aggregate

[23] NACE ist the statistical classification of economic activities as used by Eurostat.

number of out-commuters from Eurostat (2025a) with information on its structure from the Microcensus Scientific Use Files as well as from BFS (2025).

Observed HLF

Eventually, we also add the observed HLF, $U_{s,a,t,N}$, (see main text for further information) to the newly prepared participation rates as this is conceptually consistent with the data that enter our model for earlier years. We do not apply any additional data preparation steps here but use the rates as given by the LFS.

Thus, the sex- and age-specific participation rates for the population resident in Germany, adjusted to the labor force size of the German national accounts and including the observable HLF, are given by:

$$l_{s,a,t} = \frac{\left(DE_{s,a,t} + SE_{s,a,t} + CF_{s,a,t} + CS_{s,a,t} + U_{s,a,t,I} + U_{s,a,t,N} + AD^{HH}_{s,a,t} + AD^{OTHER}_{s,a,t} + OC_{s,a,t}\right)}{P_{s,a,t}}. \tag{3A.4}$$

3.A.3 Visualization and Comparison to the LFS

In Figure 3A.1, we visualize and compare the participation rates including observed HLF (solid black line), derived by the preparation strategy introduced above, to the corresponding participation rates including observed HLFRs from the LFS (dashed black line) for the year 2024. Across sex and age, the newly prepared labor force participation rates are larger than given by the LFS, mirroring the larger labor force size of the German national accounts. These differences tend to be larger for younger and older age groups compared to prime age, and also for women compared to men; both findings can be well reconciled with previous analyses (Fuchs & Weber, 2005).

Figure 3A.1: Labor Force Participation Rates by Sex and Age Group, This Paper and LFS, 2024

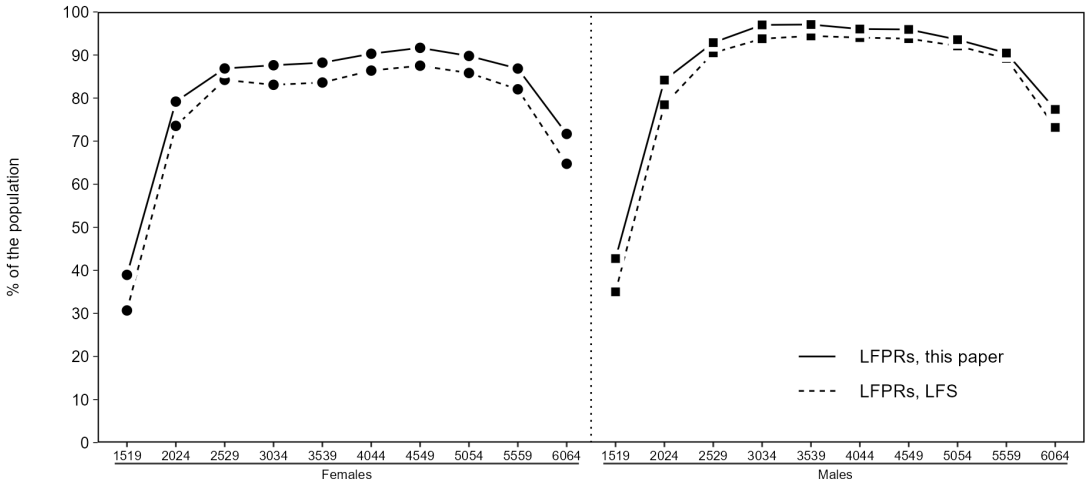

Notes: LFPR = labor force participation rates. LFS = Labor Force Survey. Reading example for the horizontal axis: 1519 = persons aged 15–19 years. Author's own computations and illustration.

3.B Appendix B: Additional Results

3.B.1 Supporting Figures for Main Text

Figure 3A.2: Explained Variance by Principal Component

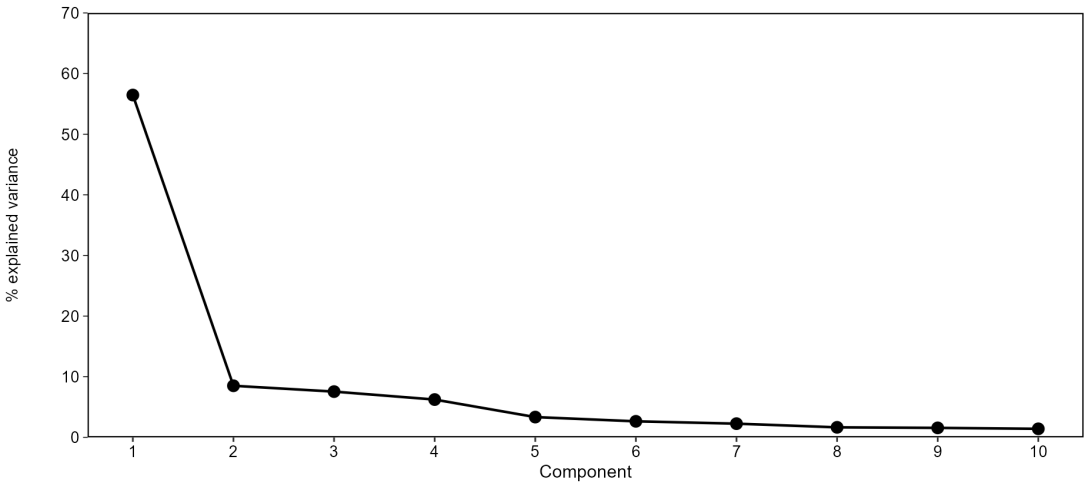

Notes: Author's own computations and illustration.

Figure 3A.3: Principal Components 1–6, Scores, Loadings, and Correlations to External Indicators

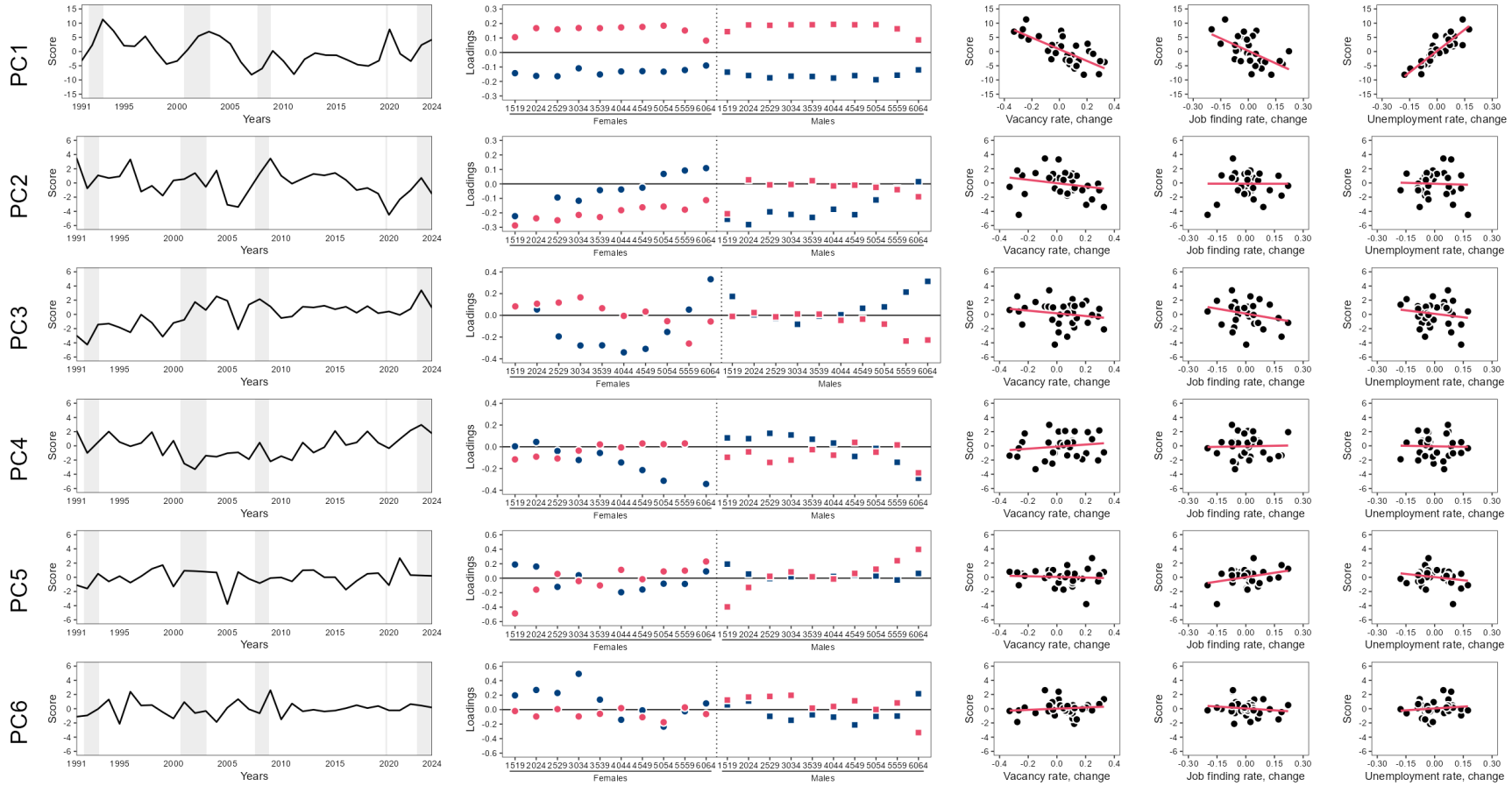

Notes: Gray rectangles in the background indicate recession periods according to SVR (2025) and based on more recent monthly GDP growth rates from Destatis (2025j). See main text for underlying sources of the external indicators. Reading example for the horizontal axis of the plots in the second column: 1519 = persons aged 15–19 years. Author's own computations and illustration.

Figure 3A.4: Population by Sex and Age, 2024 and 2035

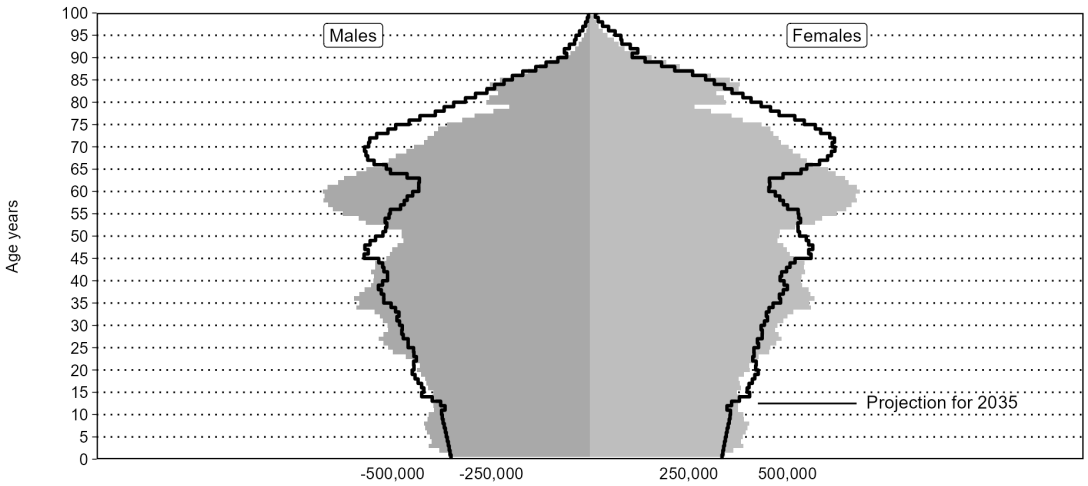

Sources: Data for 2024 sent by Destatis on request. Projection data from Hellwagner et al. (2023). Data refers to the end-of-year population. Notes: Author's own computations and illustration.

Figure 3A.5: Total Hidden Labor Force Rates, Baseline Model and Fuchs & Weber (2021), 2005

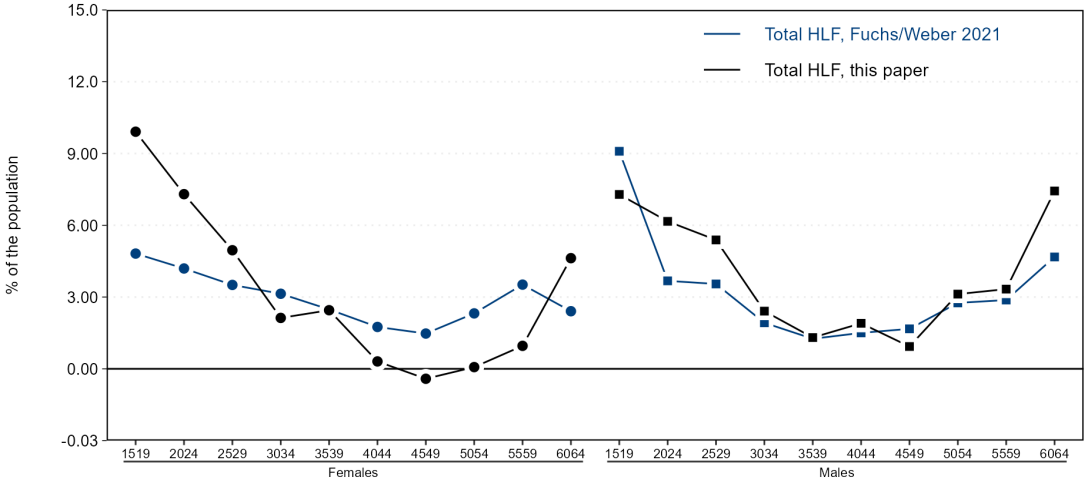

Notes: HLF = hidden labor force. Reading example for the horizontal axis: 1519 = persons aged 15–19 years. Author's own computations and illustration.

Figure 3A.6: Estimated Hidden Labor Force, Lower and Higher Full-Employment Levels of the Unemployment Rate, 1991–2024

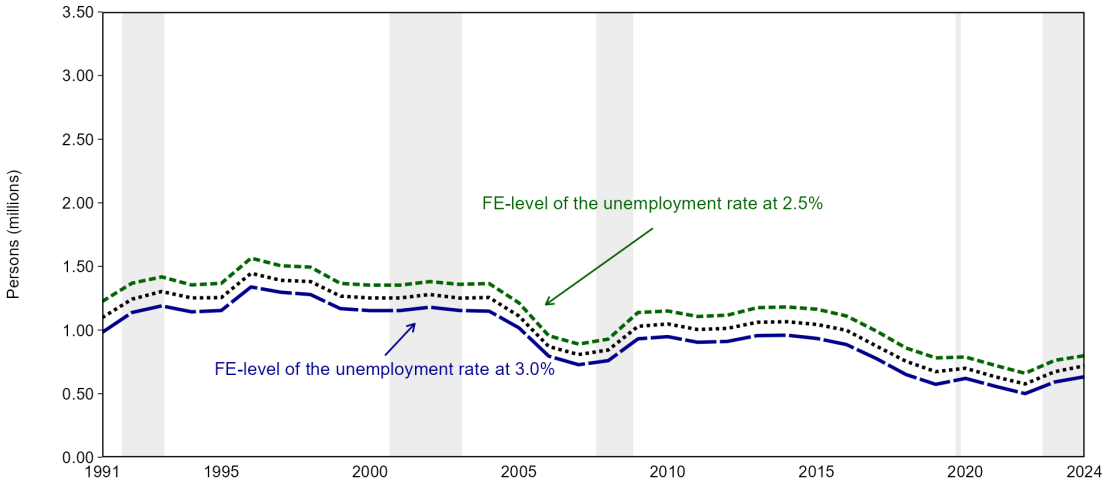

Notes: Gray rectangles in the background indicate recession periods according to SVR (2025) and based on more recent monthly GDP growth rates from Destatis (2025j). HLF = hidden labor force. FE = full employment. Author's own computations and illustration.

Figure 3A.7: Aggregate Participation Rates, 1991–2035

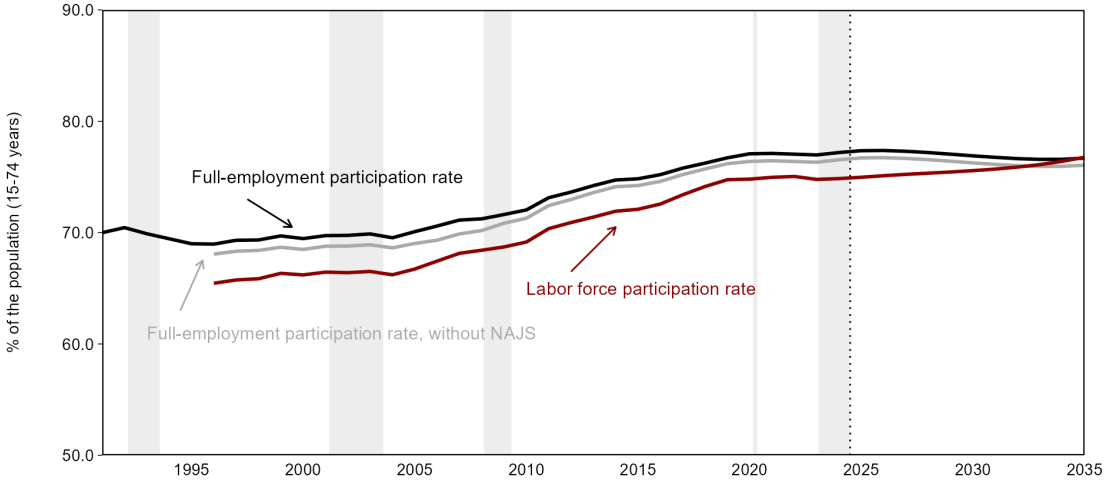

Notes: Gray rectangles in the background indicate recession periods according to SVR (2025) and based on more recent monthly GDP growth rates from Destatis (2025j). Author's own computations and illustration.

3.B.2 Alternative Calibration Procedure: Treating Remaining PCs as Zero

In the main text, we calibrate full-employment conditions by changing the first PC accordingly while fixing all other PCs at their observed values. Alternatively, we can fix all other PCs at zero. Here, we check whether those differences are quantitatively significant in our application.

To implement the alternative calibration procedure, we obtain $e^*_{s,a,t}$ and $u^*_{s,a,t}$ as in Equations (3.5) and (3.6), except for setting all other PCs, $f^*_{2,t}, \ldots, f^*_{40,t}$, to zero. Moreover, now the baseline to which we seek to compare $l^*_{s,a,t}$ is not $l_{s,a,t}$ but also a counterfactual measure, which we denote as $\bar{l}_{s,a,t}$. We derive $\bar{l}_{s,a,t}$ by plugging in the observed value for the first PC, but zero for all other factors, and proceed as in the main text by calculating

$$\bar{e}_{s,a,t} = \frac{exp\left(\sum_{k=1}^{1} \lambda^e_{k,s,a} f_{k,t} + e_{s,a,t-1}\right)}{1 + exp\left(\sum_{k=1}^{1} \lambda^e_{k,s,a} f_{k,t} + e_{s,a,t-1}\right)}, \tag{3A.5}$$

as well as, analogously, $\bar{u}_{s,a,t}$. Now, we derive the estimated HLFRs in this alternative calibration procedure by

$$\hat{h}_{s,a,t} = l^*_{s,a,t} - \bar{l}_{s,a,t} = \left(e^*_{s,a,t} + u^*_{s,a,t}\right) - \left(\bar{e}_{s,a,t} + \bar{u}_{s,a,t}\right). \tag{3A.6}$$

As before, this allows an interpretation of changes in labor market tightness. But now, $f_{1,t}$, with resulting $\bar{e}_{s,a,t}$ and $\bar{u}_{s,a,t}$, provide insights how employment and unemployment rates have changed *only* due to observed movements along the Beveridge curve, and $f^*_{1,t}$, with resulting $e^*_{s,a,t}$ and $u^*_{s,a,t}$, show how employment and unemployment rates would have changed if *only* labor market tightness had increased sufficiently strong to reach full-employment conditions. Again, the differences of both are the HLFRs.

In Figure 3A.8, the black dotted line indicates total HLF according to the baseline calibration procedure as in the main text and the red dotted line indicates the total HLF according to the alternative calibration procedure as just introduced. The differences between both lines are usually negligible. The only minor differences emerge around the year 2005, when employment and unemployment rates shifted strongly, which is not captured by setting all other PCs to zero. Overall, this comparison underlines that our results are not driven by the modeling choice for the remaining components.

Figure 3A.8: Estimated Hidden Labor Force, Baseline and Alternative Calibration Procedures, 1991–2024

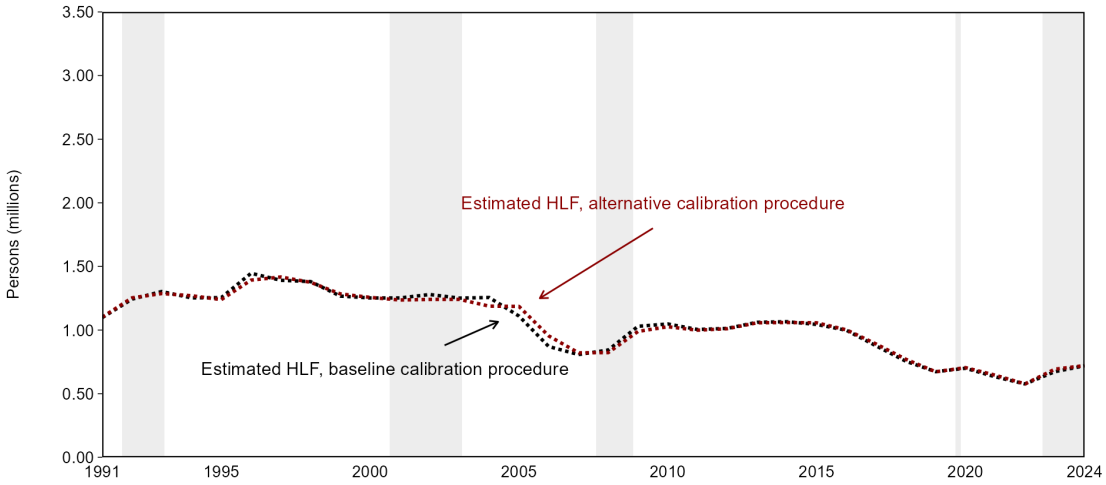

Notes: Gray rectangles in the background indicate recession periods according to SVR (2025) and based on more recent monthly GDP growth rates from Destatis (2025j). HLF = hidden labor force. See main and appendix text for detailed explanations of baseline and alternative calibration procedures. Author's own computations and illustration.

Chapter 4

Parsimonious Stochastic Forecasting of International and Internal Migration on the NUTS-3 Level

An Outlook of Regional Depopulation Trends in Germany

This chapter was published in the Vienna Yearbook of Population Research, volume 21, pages 361–415, under CC BY 4.0[1] *and is available from https://doi.org/10.1553/p-5pn2-fmn8. Minor adjustments have been made compared to the published version. These include correcting typing and notation errors, using title case instead of sentence case, as well as changes in section, equation, table, figure, and footnote numbering, text and table layout, and citation style, to ensure consistency throughout the thesis.*

4.1 Introduction

Regional differences in demographic trends related to population size and structure are well documented across countries (see, for example, BiB, 2021; De Beer et al., 2010; OECD, 2018, among others). Having precise knowledge of the quality and the quantity of those developments is crucial for regional infrastructure planning, such as for estimating the supply of childcare and schools needed, or for labor market planning (Wilson, 2015b; Zhang & Bryant, 2020). Similarly, the future demand for healthcare due to population aging (Vanella et al., 2020b), or for housing, depends on the future population size and structure (Gløersen et al., 2016; Vanella et al., 2020a). Therefore, both governments and

[1] https://creativecommons.org/licenses/by/4.0/ (accessed 1 April 2026)

enterprises have a strong interest in regional population forecasts that can provide them with a quantitative basis for decision-making (Wilson et al., 2021).

Notably, of the three components of demographic change — fertility, mortality, and migration — migration shapes regional populations the most over the short term (Deschermeier, 2011), while fertility and mortality trends are more important over the long term (Vanella et al., 2020a). Migration dynamics can have substantial effects on a region's population, and particularly in smaller areas, where outflows can have a large impact on both the size and the structure of the population (Deschermeier, 2011; Zhang & Bryant, 2020).

The causes and the consequences of migration are multi-faceted, and have been studied using a wide range of approaches across disciplines.[2] However, a pivotal distinction can be made between its two different, but nonetheless contiguous, components: internal and international flows.[3]

Discussions of internal migration frequently address issues such as persistent net outmigration from economically weaker regions, particularly among younger, more educated, and skilled sub-populations, which is likely to be driven by varying regional opportunities (Fratesi & Percoco, 2013; Sander, 2014). Regional heterogeneity in mobility, health services, shopping opportunities, housing, labor market opportunities, and education (Zhang & Bryant, 2020), or in attractiveness (Skirbekk et al., 2007), based on factors such as architecture and landscape, may drive internal migration, and can ultimately lead to the emergence of regional demographic disparities in larger countries (Eberhardt et al., 2014). Importantly, when a significant share of the younger population leaves a region, an echo effect can occur: i.e., as the population of reproductive age decreases, birth numbers decline, which, in turn, further accelerates depopulation trends.

By contrast, a wide range of factors, from crises and macroeconomic conditions (Vanella & Deschermeier, 2018) to environmental change (Black et al., 2011), can heavily affect international migration flows. In host countries, international flows are likely to affect different regions to varying degrees (see, for example, Heider et al., 2020, for the case of German regions). Moreover, there is evidence that the two components are closely intertwined (see King & Skeldon, 2010, for a comprehensive discussion): i.e., high levels of international immigration lead to further internal migration flows. For instance, the correlation coefficient between annual international immigration to Ger-

[2]Given the scope of this paper, we do not provide a comprehensive cross-disciplinary review of approaches to (regional) migration. However, suitable starting points for corresponding investigations may be recent contributions across disciplinary boundaries, such as in King (2011) or Pisarevskaya et al. (2020), among others.

[3]In this paper, the term *flow* generally refers to any migratory movement of people. Normally, the flows are documented as directional data, i.e., as migrations from certain origin regions to certain target regions.

many for the years 1994 to 2018 and the one-year delayed out-migration of the German districts (i.e., migration over district borders in 1995–2019) is 94.8% (own computation based on Destatis, 2021; Statistische Ämter des Bundes und der Länder, 2021).

Given the fundamental complexity of migration and its importance for regional demographic changes, and thus for regional planning in general, gaining a better understanding of future developments in regional migration is key to developing policies aimed at either counteracting regional depopulation and aging or mitigating the expected developments by, for example, adjusting infrastructure supply based on diminishing or changing regional demand (Iwanow & Gutting, 2020; Krüger, 2020). However, the existing approaches do not account for uncertainty in regional migration projections (e.g., Maretzke et al., 2021). By relying on deterministic assumptions, these projections are generally unable to quantify the probability that specific migration scenarios will occur, or the resulting migration flows. Given the importance of migration for regional population dynamics, these approaches clearly have significant shortcomings. At the same time, modeling migration is demanding, as it has a high degree of stochasticity; that is, migration tends to be volatile and sensitive to acute events (Vanella & Deschermeier, 2018). In the present paper, we evaluate potential approaches to incorporating stochasticity into small area migration forecasting, while simultaneously accounting for varying patterns and correlations across different age groups and regions. By incorporating both international and internal migration into a joint framework, we propose a novel, parsimonious stochastic forecasting approach.

The remainder of the paper is structured as follows. In the next section, we give a short overview of the state of research on migration projections, with an emphasis on regional migration, and discuss the features and limitations of existing (deterministic) approaches. In the third section, we introduce the data sources used and the properties of the best-performing model among a variety of models compared based on a backtest. Then, based on this model, we provide, in the fourth section, a stochastic forecast of age-specific future migration among German regions until 2040, indicating both the extent and the probabilities of migration-induced population declines. In the last section, we present our conclusions and a discussion of the results and the limitations of the study, while pointing out the need for more detailed data and further methodological advances.

4.2 (Regional) Migration Projections: An Illustrative Overview

Typically, population projections take into account three demographic components of population change: fertility, mortality, and migration. Those projections draw on a vari-

ety of methodological procedures at both the national[4] and the regional level.[5] Notably, of the three major components, migration is the most challenging to forecast (UN, 2022), largely due to data limitations caused by the under-detection of actual migrations in the reported data (Rogers et al., 2010), and to inconsistencies between different datasets and territorial changes, which can complicate the construction of consistent time series (Vanella & Deschermeier, 2018). Moreover, the sensitivity of migratory movements to political, social, economic, and environmental trends and events implies that such movements are characterized by high stochasticity and inherently limited predictability. This is because the phenomena underlying migration may themselves be difficult to predict (Vanella & Deschermeier, 2018, 2020), and can appear rather abruptly, as demonstrated by the war-related refugee flows from Syria and Iraq between 2014 and 2016 (Vanella et al., 2022), or, more recently, the refugee flows from Afghanistan (Heidelberg Institute for International Conflict Research, 2022) and Ukraine (UNHCR, 2022).

Given the wide range of challenges associated with migration forecasting, there is no consensus on "best practices". Approaches differ regarding what and how to forecast; that is, regarding which target variables should be used, e.g., what modeling flows or rates should be employed, and what degree of detail they should have. Moreover, there is no consensus on the overall modeling framework that should be used. The latter raises questions that are inevitably related to the incorporation of risk and uncertainty in the model, including questions ranging from what estimation strategy and what determinants should be used, to what cross- and autocorrelations should be considered, to what underlying assumptions about future migration should be included.

4.2.1 Flows, Rates and the Degree of Detail: Target Variables

Initially, migration forecasts depend primarily on the target variables to be modeled. While the approaches used by the statistical offices generally target gross or net migration flows, many authors, such as Bijak (2011) or Fuchs et al. (2021a), have argued against forecasting migration flows. Fuchs et al. (2021a) pointed to the "philosophical advantages" of forecasting migration rates instead of flows. Migration rates show relatively robust age patterns (Rogers & Castro, 1981), which implies that rates should be less volatile than flows. Migration rates are computed based on the population at risk of migrating. Consequently, forecasting rates rather than flows accounts for structural changes in the size and the age structure of the population, which can, in turn, significantly influence migration flows. Moreover, forecasts of migration flows using very small

[4]For a general overview, see Vanella et al. (2020a).
[5]A recent comprehensive survey is given by Wilson et al. (2021).

baseline populations, such as the oldest-old or the populations of sparsely populated regions, may lead to negative simulations for the end-of-period population. This combination may, in absolute values, result in net out-migration estimations that exceed the initial population base — which is obviously impossible (Fuchs et al., 2021a). Thus, particularly, albeit not exclusively, in regional forecasting contexts, estimating rates appears to have advantages compared to estimating flows.

Indeed, regional migration rate forecasts have a long tradition (see, e.g., Rogers & Castro 1981 or Rogers et al. 2010). However, one clear limitation of forecasting regional migration rates is that in-migration rates are difficult to define. Whereas out-migration rates from one region can be easily computed, at least in countries with adequate regional population and migration data, computing in-migration rates is not as straightforward since the baseline population is not well-defined. Calculating migration rates based on the regions of origin of the migrants is not feasible in many contexts, and especially in the case of international migration from countries with less reliable statistical documentation. While computing rates based on the corresponding population of the target region for the purposes of projection is an alternative approach, it is philosophically questionable, as we do not use the population at risk in the denominator, but instead approximate the gravity of more populous regions, in lieu of computing migration rates (Fuchs et al., 2021a).

In addition to the question of whether to model flows or rates, the question of what degree of detail is appropriate can arise when deciding whether to incorporate the target variable disaggregated by categories such as age, gender, or citizenship, as substantial differences in these categories have been documented. Raymer et al. (2011) estimated migrations by origin, destination, age, and gender for European countries, and found age- and gender-specific patterns across countries. Similarly, Van Mol & de Valk (2016) demonstrated that the age- and gender-structure of migrants differs depending on both their citizenship and their destination country.

4.2.2 Consistency in Forecasts of Internal and International Migration

On the regional level, migration comprises both international and internal flows. These flows affect and shape regions within a country quantitatively and qualitatively, and to different degrees (Fratesi & Percoco, 2013). In Germany, for example, distinct internal migration patterns have been observed in recent decades, as, following reunification, the number of people migrating from East Germany to West Germany greatly exceeded the number of people migrating in the opposite direction (see, as a recent example, Rosenbaum-Feldbrügge et al., 2022). While this demonstrates that both components

should be included in projections, it also suggests that the target variables should be further distinguished for this category as well. The latter point is again supported by empirical evidence. For example, in the case of Germany, scholars have shown that out-migration from East Germany is selective in terms of age and gender (Kröhnert & Vollmer, 2012; Leibert, 2016).

However, relying on highly disaggregated target variables along all these dimensions faces two limitations in empirical applications. First, detailed regional migration data[6] are usually sparse (Rowe et al., 2019; Wilson et al., 2021). Second, even when these data are available, the dimensionality increases drastically, particularly for approaches that include region-to-region flows, which may even be disaggregated by gender, age, and citizenship, as outlined above.

Migration projections that focus on the national level, such as those by UN (2022), do not cover the regional perspective and are, therefore, not necessarily compatible with regional projections for the same country. For the case of Germany, Maretzke et al. (2021) followed a hierarchical procedure that, first, assumed one of the variants suggested by Destatis (2019) for international migration between Germany and other countries, and, second, assumed internal migration rates in Germany based on a qualitative assessment and past data. While this approach has merit, it cannot capture changes in internal migration patterns after immigration shocks.[7] Moreover, due to its complex model structure, which is based on bi-directional internal migration, it is not feasible to sufficiently incorporate uncertainty into the projection, particularly given the high stochasticity in international migration (for more on that problem, see Section 4.2.4).

4.2.3 Modeling Migration Processes and Determinants

Closely connected to questions of which target variables should be selected is the decision about which general modeling framework should be used, e.g., which migration determinants should be included. A large body of literature has emphasized the importance of including determinants in analyses of migration patterns. Among the potential drivers of migration that have been discussed in the literature are economic reasons (e.g., Bertoli et al., 2013; Grogger & Hanson, 2011; Mayda, 2010), the impact of education (e.g., Bernard & Bell, 2018; Lutz & KC, 2011; Lutz, 2021), network effects (e.g., Beine et al., 2011; Pedersen et al., 2008), the institutional framework (e.g., Geis et al., 2013; Ortega

[6] Bell et al. (2015) present a comprehensive overview of internal migration data for the 193 UN member states.

[7] Even after internal and international migrations have been separated, there is still a variety of possible approaches to incorporating these flows. Interested readers may consult Rees et al. (2015), who discussed a variety of approaches to modeling international migration streams in subnational population projections.

& Peri, 2013), personal preferences (Mulliner et al. 2020; also amenity migration, e.g., Steinicke et al. 2012), and environmental causes (e.g., Beine & Parsons, 2015; Black et al., 2011; Cai et al., 2016).[8]

Notably, these scholars found that the observed migration patterns are usually explained by more than one of those drivers, or by interactions between them. For example, Leibert (2016) attributed the abovementioned internal migration in Germany, in which gender-selective out-migration plays a large role, to a combination of economic and context-specific institutional factors, including the labor market situation in East Germany after reunification, combined with high levels of labor force participation among East German women. Heider et al. (2020) found that the locational choices of international migrants across German regions are strongly driven by network effects, as well as by individual-level factors, such as educational considerations. Prenzel (2021), using German data, showed that regional population aging, fueled by the selective out-migration of younger individuals, may itself reinforce out-migration, and thus that polarization dynamics, in addition to the other discussed reasons, may be another explanatory factor in regional migration patterns.[9]

Just as a variety of migration determinants have been discussed across disciplines, a wide range of approaches have been used to forecast migration. While statistical offices (e.g., UN, 2022) tend to rely on rather simple models for migration computations, more sophisticated alternatives have been applied in the literature. For instance, Kubis & Schneider (2020) used an econometric panel model that predicted immigration and emigration by EU citizens in Germany, and included labor market and freedom-of-movement variables as predictors. Lipps & Betz (2005) suggested forecasting cumulative net migration to Germany using an ARIMA model. Vanella & Deschermeier (2018) proposed ARIMA forecasting of principal components derived from age-, gender-, and nationality-specific net migration to Germany. Moreover, migration forecasts between certain regions can also be performed based on directional models. Examples of studies that used this approach include Abel & Cohen (2019), and the sources cited therein. An example for forecasting bi-directional flows between Germany and Poland was provided by Bijak (2011).

Importantly, the methodological approach to migration forecasting may also vary depending on the extent to which cross-correlations between in-migration and out-migration, age and gender groups (which also model family migration indirectly), and different re-

[8] For further discussions, see, among others, Simpson (2022) or Van Hear et al. (2018). Interested readers may also refer to collections of interdisciplinary perspectives on migration, such as Brettell & Hollifield (2022).

[9] For a more detailed discussion of the drivers of migration between East and West Germany, see Rosenbaum-Feldbrügge et al. (2022).

gions are included in the model. Vanella & Deschermeier (2018), for example, covered these correlations on the national level by employing the abovementioned approach. From a regional perspective, simple (top-down) models do not sufficiently account for correlations in migration between regions. An illustrative example is that large inflows to a major city like Berlin will be highly correlated with migration flows to or from neighboring regions; in this case, Brandenburg. These correlations might be negative in the case of movements between Berlin and Brandenburg, or they may be positive if large inflows to Berlin are associated with large inflows to the neighboring regions because, for example, migrants are unable to find accommodation in Berlin due to a lack of available housing (Henger & Oberst, 2019b). At the same time, co-movement, such as family migration, will be observable in the data due to high positive correlations between corresponding age groups. This is a well-known phenomenon that has been investigated by Rogers & Castro (1981) and in later studies on the age schedule of migration.

4.2.4 Incorporating Risk and Uncertainty

Finally, migration projections, like demographic projections in general, differ in how they include risk and uncertainty. Migration projections are often categorized as either deterministic or stochastic approaches. While deterministic population projections were frequently employed in the past, as they were widely used by statistical agencies (Deschermeier, 2011; Vanella & Deschermeier, 2020), stochastic approaches have become increasingly popular in recent decades, at least on the national level.[10]

Deterministic approaches, which are often scenario-based (see, e.g., UN, 2022), seek to identify several realistic outcomes. Some authors use rather naïve assumptions: i.e., that the most recent observations form the basis for the most probable future scenarios. For instance, the United Nations Population Division relies on such an assumption in its projections of international non-refugee migration in the medium scenario of its World Population Prospects (UN, 2022). In cases in which the assumption that recent migration flows will continue in the future is not realistic, alternative values may be proposed, either for the near future (specifying a level), or for the medium to long term (specifying a full future trajectory). For instance, the national population projections for Germany proposed by Destatis (2019) assume that net migration will, in sum, converge to levels computed as the historical means over three varying periods. In this example, net migration to Germany is assumed to reach a level of between $111,000$ and $300,000$ in 2030.

[10] For a survey on Germany, see Vanella & Deschermeier (2020).

Among the reasons why deterministic approaches have been popular are that they can be computed quickly, and they can be easily used to compare a range of different policy scenarios and the corresponding effects (Vanella et al., 2020a). For example, Lomax et al. (2020) recently discussed a series of Brexit-dependent migration scenarios, and presented corresponding deterministic projections for each scenario. Lutz et al. (2019) developed several demographic scenarios for the European Union, in which they analyzed the impacts of fertility, mortality, migration, education, and labor force participation. They showed that projections of how many people, stratified by skill level, will be living and working in the European Union in 2060 differed depending on which assumptions were applied. Similarly, Marois et al. (2020) compared six scenarios for the EU-28 that differed depending on which assumptions regarding immigration volumes, the educational selectivity of migrants, and labor force integration and participation were used, and analyzed the corresponding impacts on various dependency ratios. De Beer et al. (2010), taking a smaller-scale perspective, compared four policy scenarios based on different assumptions for reducing socioeconomic inequalities and moderating climate change across European regions, and assessed the impact of these policies on demographic developments, such as (working-age) population growth and population aging.

However, despite being popular, deterministic approaches have major limitations, as they rely on scenario assumptions; that is, on fixing the relevant parameters at predefined values and then making a straightforward calculation of the corresponding future developments. As these approaches are unable to quantify the probability that the respective scenarios will occur (Vanella et al., 2020a), they do not reflect future uncertainty, but instead only present a rather small number of realistic scenarios. While these scenarios may be informative, the statistical probability that they will actually take place is close to zero (Keilman et al., 2002). By contrast, stochastic (population) projections overcome these limitations, as they quantify the probability that future trajectories will occur, by relying on statistical information and methods for both frequentist (e.g., Fuchs et al. 2018, or Vanella & Deschermeier 2020) and Bayesian (Azose et al., 2016) frameworks.

Despite having these favorable properties, the stochastic modeling of (international) migration has previously been performed for only a few individual countries (Azose et al., 2016), such as Germany (Vanella & Deschermeier, 2020), or for migration between countries, such as between Germany and Poland (Bijak, 2011). However, as was noted above, the quantification of prediction intervals instead of point forecasts is preferable, since it allows researchers to assign probabilities to the outcomes of the respective future migration trajectories (Vanella & Deschermeier, 2018). Nonetheless, given its volatile

nature, migration is particularly difficult to forecast, even when a stochastic framework is applied.[11]

Notably, in addition to stochastic approaches, there is also a series of approaches that combine both (scenario) assumptions and policy comparisons. For example, Lutz et al. (1998) suggested randomizing expert-based scenarios to derive stochastic, expert-based forecasts. Abel et al. (2016) incorporated future education pathways based upon the Sustainable Development Goals in a Bayesian framework. Marois et al. (2021) used a stochastic microsimulation model for China, with pre-defined parameter values, e.g., for the total fertility rate, to project adjusted old-age dependency ratios that factored in both educational attainment and labor force participation. Similarly, Bijak (2011) and Azose et al. (2016), among others, have recently suggested using Bayesian approaches to combine the information derived from the data with qualitative knowledge or assumptions regarding future migration. The use of such approaches is conceivable if the necessary data are not available or are erroneous, or if we believe that the past data are unlikely to reflect future developments in migration.

4.2.5 Migration Forecasts for German Regions

For the reasons outlined above, the approaches to modeling regional migration are, in practice, quite heterogeneous. However, deterministic approaches are used even more frequently for regional projections than for projections on the national level. This is illustrated by looking at various recent population projections for German regions, some of which have already been addressed. For example, Maretzke et al. (2021) provided comprehensive population estimates for German NUTS-3 regions until 2040. They modeled internal migration using high dimensional, region-to-region migration data from 2011–2017 and assuming constant mean outflow rates in the future, disaggregated by age and gender. Similarly, they modeled net international migration by applying a series of deterministic assumptions based on regional data from the observation period and assumptions about the overall level of migration to Germany in the future. Reinhold & Thomsen (2015) provided population projection results for NUTS-3 regions of the German federal state of Lower Saxony using an average of different projection techniques. While they relied on several deterministic assumptions about regional migration dynamics, such as constant inward to outward migration ratios or zero net migration, they did not differentiate between internal and international migration. Breidenbach et al. (2019) provided much more fine-grained estimates, projecting the total population in Germany

[11] Which additionally lowers the predictive value of selective (i.e., deterministic) scenarios, as the probability of an outcome is lower than it is for processes that are easier to predict, such as mortality improvements.

until 2050 using a 1 × 1-km grid. They did not take internal migration dynamics into account. Moreover, they assumed that net international migration to Germany will remain at constant levels and will be distributed across regions proportionally to the total population. Regional projections using the subnational data of other countries often relied on deterministic modeling as well (e.g., Eurostat, 2021; Raymer et al., 2006; Wilson, 2015b).

By contrast, fewer regional migration projections have taken uncertainty into account. Ballas et al. (2005) estimated the internal migration probabilities for regions in Ireland over the 1991–2002 period by using Monte Carlo sampling from individual census records. However, they excluded international migration from their analysis due to a lack of data. Bryant & Zhang (2016) estimated regional emigration rates, disaggregated by sex and age, in New Zealand over the 2014–2038 time interval using a complex Bayesian approach. Similarly, Zhang & Bryant (2020) used a sophisticated Bayesian model to project migration between Icelandic regions.

Thus, even though migration dynamics play a crucial role in the demographic development — and, consequently, in the overall economic and social development — of regions, most regional projection approaches do not rely on a consistent (including both international and internal migration) and accurate (stochastic) modeling strategy. Investigating either international or internal migration, but not both, fails to account for the interdependencies or regionally differing effects of these two migration components. Furthermore, as Fuchs et al. (2021a) demonstrated, in addition to relying on the sensitivity to the assumed parameter values, modeling migration deterministically implies a heavy dependence on a detailed approach for modeling in-migration and out-migration dynamics. This issue is of particular importance on the regional level, as Wilson & Bell (2004) showed for internal migration. In the same vein, Wilson et al. (2021) underlined the need for stochastic modeling of regional population changes in future research.

Therefore, given the state of the research and the respective implications and limitations of the prevailing deterministic methods outlined above, we propose in the upcoming section a comprehensive and parsimonious stochastic framework for forecasting migration on the regional level in Germany.

4.3 Data and Methods

Based on the literature, we can identify a series of potentially relevant characteristics of a model for forecasting migration between German regions. However, the incorporation of these factors is constrained by data availability, which we discuss below. Moreover, *ex-*

ante, there is ambiguity about which modeling approach performs the best. Therefore, the comparison of different specifications may be necessary.

Previous studies have evaluated a series of candidate models to find out which one performs the best. Reinhold & Thomsen (2015), using data for selected German regions, compared the accuracy of individual and model averaging forecasting techniques. Rayer (2008) compared the forecast error levels of different population forecasting techniques using data on U.S. counties. Wilson (2015a), building upon the findings of Rayer (2008) and others, compared the forecast accuracy of more than 200,000 simple to more complex averaged and composite model specifications for regions in Australia, England and Wales, and New Zealand.

In line with these examples, and based on both the relevant factors discussed in the review above and the available data for German regions, we identified eight models to be tested and compared to each other:

- a prediction of gross migration flows using naïve status quo assumptions,
- a prediction of gross migration flows using observed mean and median values,
- a prediction of net migration flows using Principal Component Analysis,
- a prediction of log-gross migration flows using Principal Component Analysis,
- a prediction of gross migration rates using naïve status quo assumptions,
- a prediction of gross migration rates using observed mean and median values,
- a prediction of net migration rates using Principal Component Analysis, and
- a prediction of log-gross migration rates using Principal Component Analysis.

Thus, our empirical strategy consisted of two major building blocks. First, we determined which of those eight competing models is most accurate by conducting a sequence of deterministic backtests (see, for instance, Vanella & Deschermeier, 2019). In doing so, we applied each model to each of the six available gender-age groups[12] by taking data for the years 1995–2014 as a baseline, while assuming no knowledge of the migration trends after that period. We then created in-sample forecasts for the years 2015–2019, and compared the corresponding *ex-post* errors. Interested readers can find details on the models that were tested, the measure of accuracy that was used (the symmetric mean absolute percentage error, see Chen et al., 2017), and the results for all other models in Appendix 4.A. Second, the best-performing model was used to conduct a stochastic

[12] 0–17; 18–24; 25–29; 30–49; 50–64; 65+ years.

NUTS-3-level migration forecast until 2040. By applying this two-step procedure, we addressed the discussions outlined in the literature review about which target variables (net versus gross, flows versus rates) and empirical strategies should be used (from naïve models to Principal Component Analysis), and how uncertainty should be incorporated.

4.3.1 Data: Sources and Preparation

We used publicly available small-area data on migration from and to NUTS-3 regions in Germany (*Kreise/Districts*) for the 1995–2019 period from the German Federal Statistical Office and the Statistical Offices of the Federal States (Statistische Ämter des Bundes und der Länder, 2022). As there were various changes in administrative territories over the baseline period, we redistributed the past migration flows[13] to districts based on their boundaries as of December 31, 2019. For the data of districts in which the boundaries changed[14] over time, and for which obtaining consistent time series was therefore not feasible, we created pseudo-districts. Appendix 4.B gives an overview of the territorial reforms since 1995, and of how we converted data with incompatible boundaries into consistent time series.

Although it would have been preferable to do so, as we discussed above, the available data did not allow us to distinguish between internal and international flows or citizenships. Furthermore, in 15 of the 16 federal states, the district-level data did not distinguish migrants by gender before 2002. We obtained gender-differenced time series for those 15 federal states by performing a backcast of the rates for males among all migrants across all age groups and districts. For this purpose, we computed the age-specific shares of males among all migrants for 2002–2019, and then performed PCA on the resulting 4,596 time series (in- and out-migration, six age groups, 383 districts). The obtained PCs were backcasted until 1995, and were then retransformed to male shares for all age groups and districts, and multiplied by the total migration data to obtain gender-specific flows.[15]

[13] In contrast to the general definition of migration flows as presented in Section 4.1, our model refers to the sum of either inflows or outflows during one-year periods from the perspective of a certain district. For instance, we consider each out-migration from Berlin as an outflow and each in-migration to Berlin as an inflow. Thus, our definition of flows is non-directional. For example, a person moving from Berlin to Wolfsburg in the year 2020 will appear as an outflow in the data for Berlin and as an inflow in the data for Wolfsburg.

[14] For instance, after reunification, some districts in East Germany were dissolved and redistributed to three or four new districts.

[15] We purposely keep the description of the backcast method rather short. For interested readers, more details are offered in Appendix 4.C.

4.3.2 Forecast Model

The highest forecast accuracy was achieved by the PCA model for log-gross migration flows. Using this model for our forecast, we first performed PCA on the covariance matrix of annual age- (six groups), gender- (binary), and district-specific (396 districts and pseudo-districts) log-migration flow time series for 1995–2019, which corresponds to a 25 (years) × 9,504 (variables) matrix. PCA performed singular value decomposition on this matrix, thereby transforming the original and highly correlated data into linear combinations of the original variables that were uncorrelated, so-called principal components. This allowed us to efficiently cover cross-correlations between the original variables in our forecast (Vanella, 2018). More technical details on the PCA model used for the specific case in this paper are given in Appendix 4.A.

The sign-reversed loadings (coefficients) of the district-, age- and gender-specific log-migration on Principal Component 1 (PC1)[16] are illustrated in Figures 4.1–4.4, whereby Figures 4.1 and 4.2 indicate loadings of age- and gender-specific in-migration and Figures 4.3 and 4.4 indicate loadings of age- and gender-specific out-migration. Darker colors are associated with higher correlations between PC1 and the respective log-migrations. Shades of green indicate negative loadings of the respective flows on PC1, while shades of purple indicate a positive connection.

For instance, the district of Göttingen (I) has a dark green color in Figure 4.1(a), which means that a decrease in the sign-reversed PC1 is, on average and *ceteris paribus* (c.p.), associated with relatively large *increases* in in-migration to Göttingen among males aged 0–17 years. Simultaneously, the dark purple of the district of Höxter (II) indicates that, for the same age-gender stratum, an increase in the sign-reversed PC1 is, on average and c.p., associated with rather large *increases* in in-migration to Höxter. Moreover, the district of Göttingen (I) has a dark green color in Figure 4.4(f) as well.

This implies that a decrease in the sign-reversed PC1 is associated not only with increases in *in-migration* to Göttingen among young people, but also with increases in *out-migration* from Göttingen among females aged 65+ (c.p.). These selected examples demonstrate that trends in PC1 cover migration dynamics that occur simultaneously across districts, age groups, and genders. Thus, as indicated by the literature review, we found that results relying on estimation by PCA accounted for the correlations and the interdependencies between regions and demographic groups reported in the historical data, such as the displacement of age groups due to overburdened local real estate markets.

[16]For ease of interpretation, the sign of the PC1 time series (and, thereby, its loadings) was reversed in Figures 4.1-4.5, such that an increase in PC1 is associated with c.p. increases in migration.

Figure 4.1: Loadings of the First Principal Component for Log-Inflows by Males

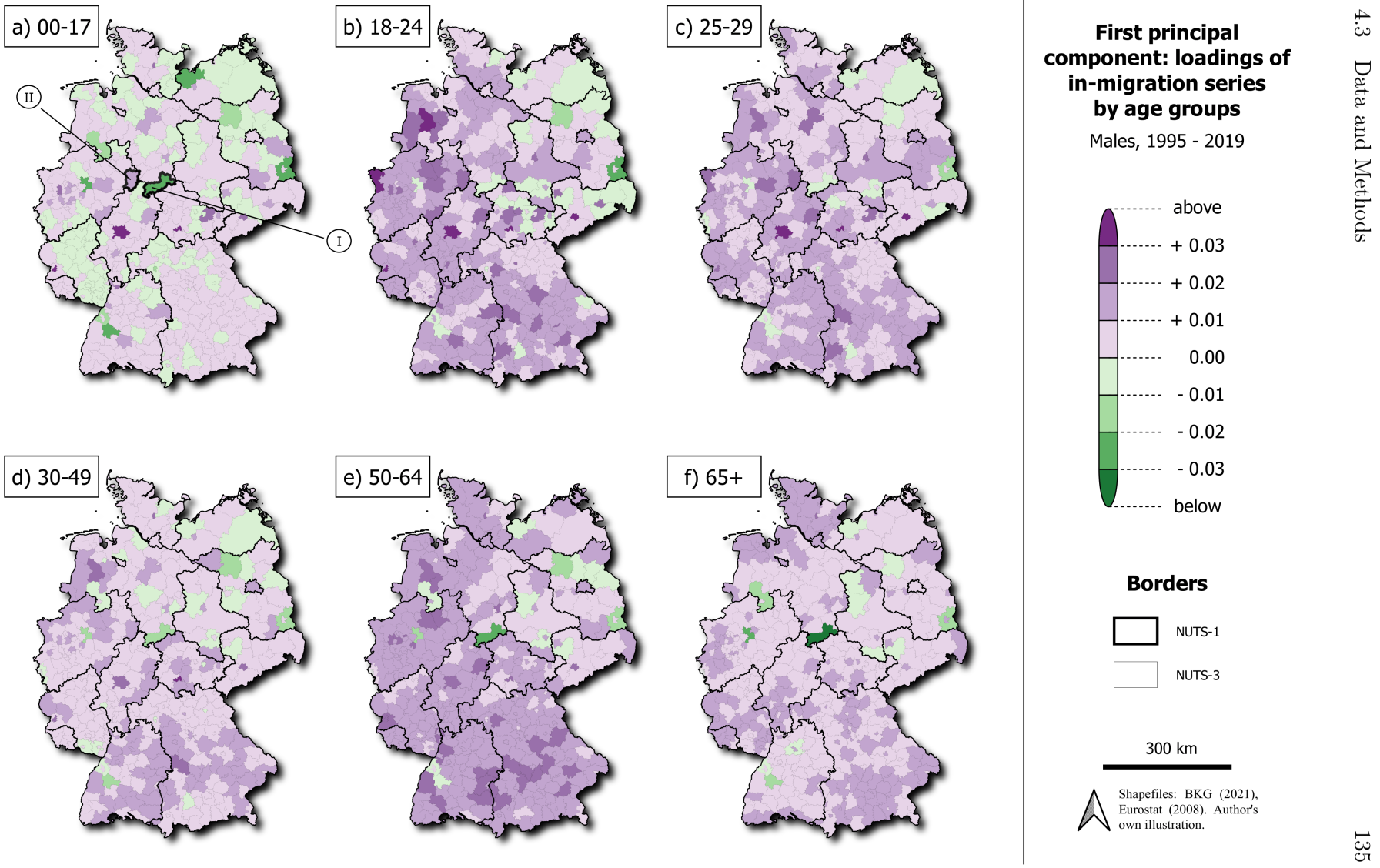

Source: Authors' computation and illustration. [Original source of figure: Vanella et al. (2023), see https://doi.org/10.1553/p-5pn2-fmn8]

Figure 4.2: Loadings of the First Principal Component for Log-Inflows by Females

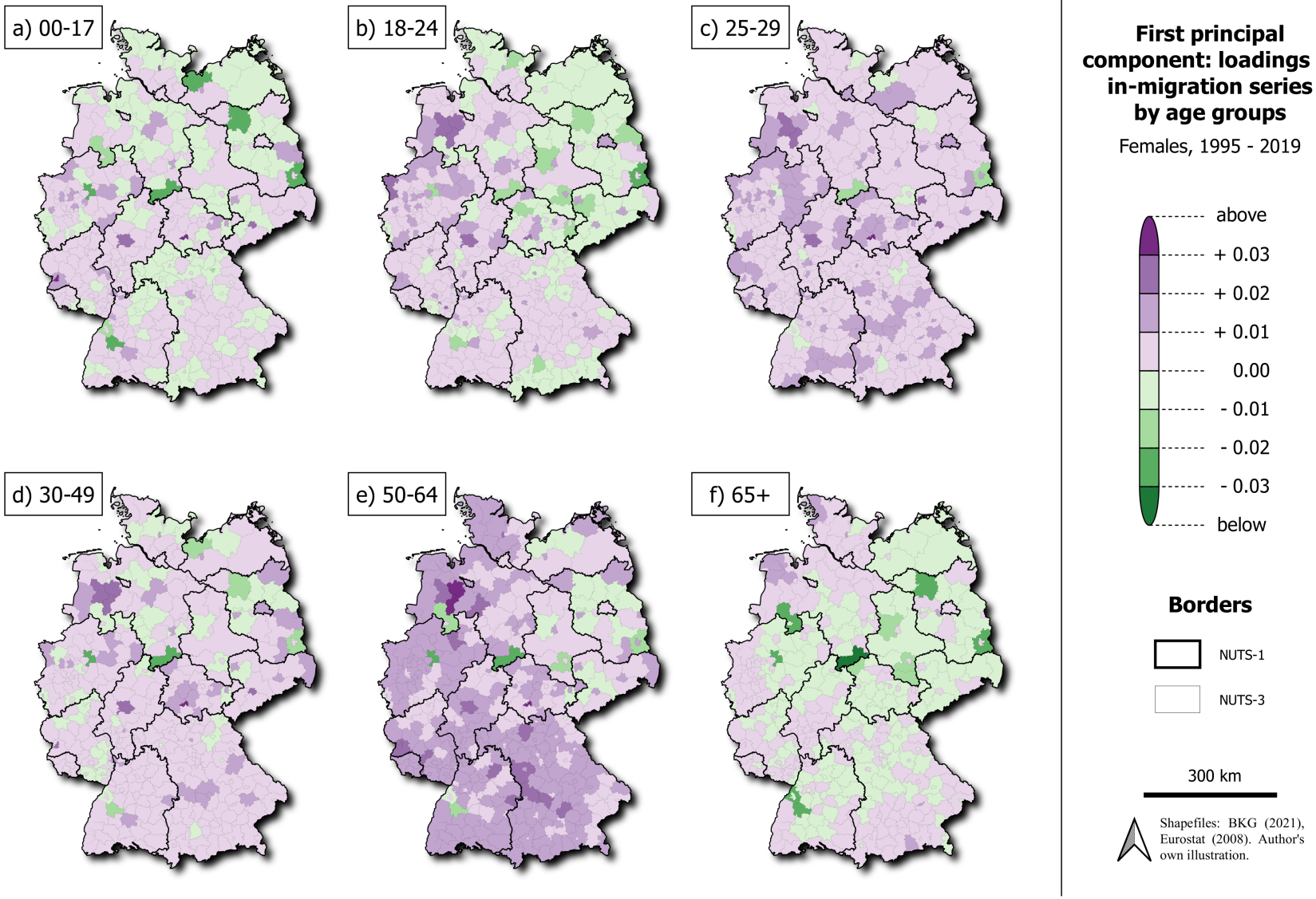

Notes: Authors' computation and illustration. [Original source of figure: Vanella et al. (2023), see https://doi.org/10.1553/p-5pn2-fmn8]

Figure 4.3: Loadings of the First Principal Component for Log-Outflows by Males

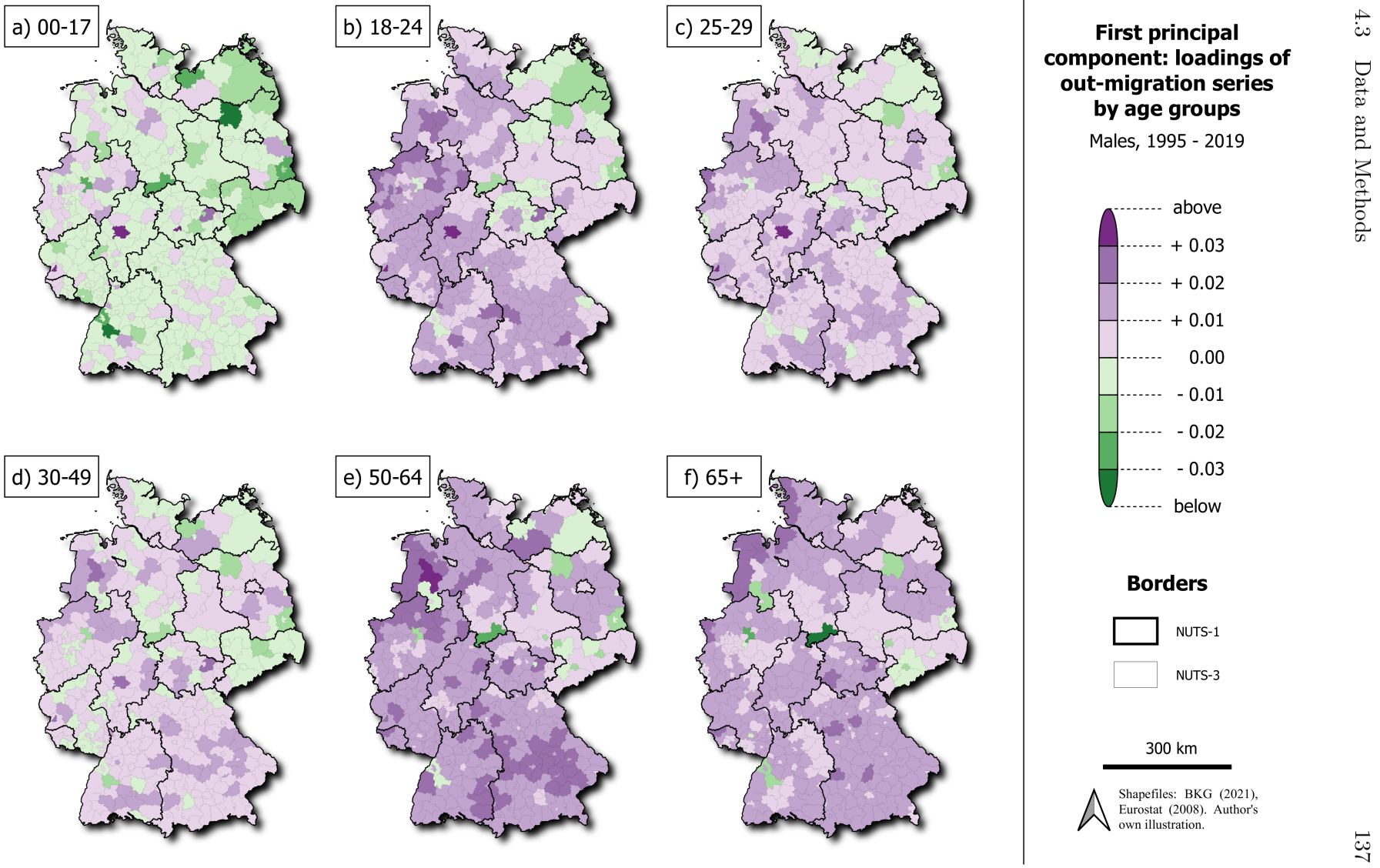

Source: Authors' computation and illustration. [Original source of figure: Vanella et al. (2023), see https://doi.org/10.1553/p-5pn2-fmn8]

Figure 4.4: Loadings of the First Principal Component for Log-Outflows by Females

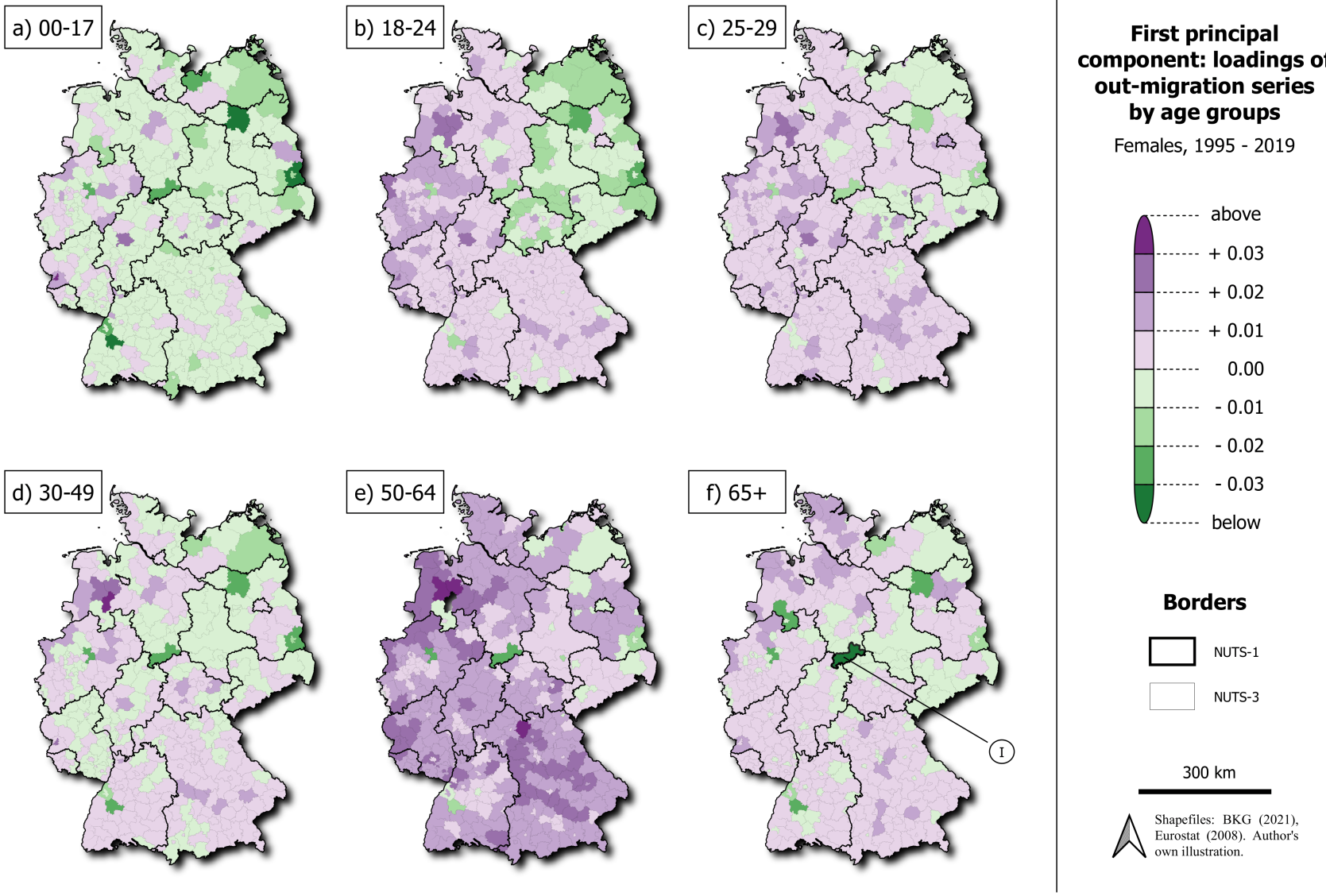

Source: Authors' computation and illustration. [Original source of figure: Vanella et al. (2023), see https://doi.org/10.1553/p-5pn2-fmn8]

Overall, PC1 explained more than 52% of the variance in the 9,504 variables throughout the 25-year period. Figure 4.5 illustrates its sign-reversed course over time, alongside a forecast that was derived using an approach explained in Appendix 4.A (see description of Model 4), including 95% prediction intervals (PIs) for illustrative purposes. Apart from the years 2015 and 2016, which were outliers due to the significant international refugee inflows and internal migration flows that occurred during that period (see Fuchs et al. 2021a, and Vanella et al. 2022), PC1 followed a mostly monotonous course: migration was increasing steadily, then slowed down in the late 2000s, and accelerated again in the wake of the so-called Arab Spring in 2011 (Vanella & Deschermeier, 2018). After the large inflow of refugees ended in 2016, a deceleration of the curve can be observed.

Therefore, the long-term trend of PC1 can be emulated quite well by fitting an inverse logistic trend function to the time series. The model's inflection point (the year 2011) was chosen such that the fit maximized the model's likelihood. Then, the model coefficients were estimated by ordinary least squares (OLS). The model generating the prediction in Figure 4.5 is given in (4.1).

$$E[P_{1,y}|P_{1,2019}] \approx -345.675 - 45.998\frac{exp(\frac{y-2011}{2.856})}{1+exp(\frac{y-2011}{2.856})} + r_{2019} \tag{4.1}$$

with

- $P_{1,y}$: value of PC1 in year y,
- y taking the values $2020, 2021, ..., 2040$,
- $r_{2019} \approx 3.478$: the residual between the observation for PC1 in 2019 and the trend function's prediction for 2019.

After visual inspection of the residuals' time series and their autocorrelation function (ACF) and partial autocorrelation function (PACF) (see, e.g., Shumway & Stoffer, 2017), we concluded that they were appropriately modeled by a random walk process.

4.4 Stochastic Forecast of Regional Migration Flows until 2040

Having estimated in-sample regional migration using the best-performing specification, we attempted to forecast future regional migration among German regions until 2040. However, as was outlined above, uncertainty about future migration was a major concern. To account for this uncertainty, we set up a stochastic version of (4.1), which is given in (4.2).

Figure 4.5: Time Series of Principal Component 1 (Sign-Reversed) with Forecast

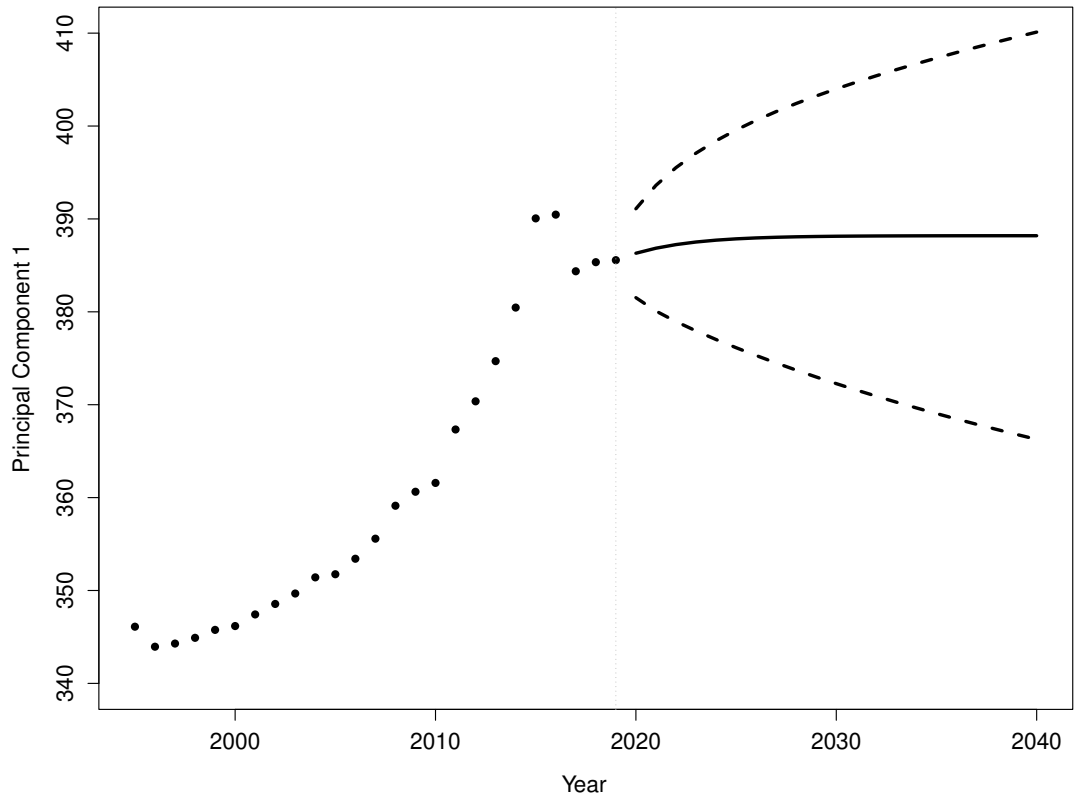

Source: Authors' computation and illustration. [Original source of figure: Vanella et al. (2023), see https://doi.org/10.1553/p-5pn2-fmn8]

Table 4.1: Explained Share of Variance by Principal Component

Principal component	**Individual share of explained variance [as %]**	**Cumulative share of explained variance [as %]**
1	52.4	52.4
2	25.7	78.1
3	4.9	83.0
4	3.9	86.9
5	2.1	89.0
6	1.8	90.7
7	1.1	91.8
8	1.0	92.8
9-9,504	< 1.0	100.0

$$P_{1,y} \approx -345.675 - 45.998 \frac{exp(\frac{y-2011}{2.856})}{1 + exp(\frac{y-2011}{2.856})} + r_y, \tag{4.2}$$

with r_y being a random walk process that can be written as:

$$r_y = r_{y-1} + \varepsilon_y = r_{y-2} + \varepsilon_{y-1} + \varepsilon_y = \ldots, \tag{4.3}$$

with ε_y being a stochastic white noise process:

$$\varepsilon_y \sim NIID(0, 0.149^2) \quad \forall\, y. \tag{4.4}$$

By drawing 1,000 times for each year over the forecast horizon, from (4.4), plugged into (4.3), and thus also in (4.2), we computed 1,000 trajectories for PC1 until 2040. The remaining PCs jointly explained less than half of the variance in all log-migration time series (see Table 4.1). Since they did not show clear trending behavior, we assumed that those PCs followed random walk processes, as in (4.3), and simulated 1,000 trajectories for each, which allowed us to consider the associated risk and to construct more realistic PIs, as suggested by Vanella & Deschermeier (2020). Using this approach, we obtained annual simulation matrices for all PCs that could be easily retransformed into annual simulation matrices of the log-migration, and, by exponentiation, of migration flows, as given in (4.5):

$$\Gamma_y = exp(\Pi_y \Lambda^{-1}), \tag{4.5}$$

with Π_y $(1,000 \times 9,504)$ being the simulation matrix of the PCs for year y, Λ^{-1} being the inverse of the loadings matrix $(9,504^2)$, and Γ_y being the simulation matrix of the migration flows for year y $(1,000 \times 9,504)$. Based on the quantiles of the 1,000 simulated

trajectories, we derived PIs for each district-, age-, gender-, and direction-specific time series.

Subsequently, we aggregated each individual trajectory over the forecast horizon, resulting in cumulative migration flows until 2040:

$$\Gamma = \sum_{y=2020}^{2040} \Gamma_y. \tag{4.6}$$

Having obtained migration flows over the forecast horizon, we were able to derive measures of migration-associated depopulation for each district, age, and gender. To this end, we subtracted, for each of the 1,000 trajectories, the forecasted outflows from the respective forecasted inflows. This yielded cumulative district-, age- and gender-specific net migration distributions through 2040. More formally, let $\gamma_{d,a,g,i,.,t}$ be the cumulative inflows to district d by individuals in age group a and of gender g in trajectory t for 2020–2040, and $\gamma_{d,a,g,0,.,t}$ be the corresponding outflow. Then, the net cumulative flow for the said district, age group, gender, and trajectory is

$$\gamma_{d,a,g,n,.,t} = \gamma_{d,a,g,i,.,t} - \gamma_{d,a,g,o,.,t}. \tag{4.7}$$

Thus, $\gamma_{d,a,g,n,.,t}$ indicates whether a district faces an increase or a decrease in the corresponding demographic stratum because of migration flows over the forecast horizon — importantly, in absolute numbers.

However, German districts differ in population size, which alters the relevance of flows as absolute numbers. For example, a population decline of $10,000$ is more severe in a district of 50,000 inhabitants than in a district of 1,000,000 inhabitants. To obtain a more realistic picture of the significance for each district of population decline due to negative net migration or population growth due to positive net migration, we computed the quotient of the cumulative net migration and the official population estimate as of December 31, 2019 ($B_{d,a,g,2019}$) for each stratum:

$$\frac{\gamma_{d,a,g,n,.,t}}{B_{d,a,g,2019}}. \tag{4.8}$$

Finally, we used our stochastic results to estimate the probability of migration-induced depopulation for each stratum. For instance, let $\Delta_{d,a,g,.}$ be a binary variable that takes the value of one if the cumulative net migration to d among individuals in age group a and of gender g during 2020–2040 is negative, and the value of zero otherwise:

$$\Delta_{d,a,g,t} \coloneqq \mathbb{1}(\gamma_{d,a,g,n,.,t} < 0). \tag{4.9}$$

Then, the estimated probability of migration-induced depopulation, based on our Monte Carlo simulation with 1,000 trajectories, for the said district, age group, and gender is

$$\hat{P}(D) = \frac{\sum_{t=1}^{1,000} \Delta_{d,a,g,t}}{1,000}. \tag{4.10}$$

We will present the results generated from (4.6), (4.8) and (4.10) by district and age in Section 4.5. Gender-specific results can be found in Online Supplementary File 1 (available at https://doi.org/10.1553/p-5pn2-fmn8). We discuss the limitations of our approach in Section 4.5.

4.5 Results

4.5.1 Future Migration Flows among German Regions

As the initial output of the model, given by (4.6), delivers migration flows, we visualize and compare the corresponding median of the forecasted flows in Figure 4.6. In this context, four distinct future migration patterns become visible.

First, there is strong evidence that for the 18–24 age group, migration-induced depopulation will occur in the majority of German regions by 2040, as indicated by the dark turquoise colors in Figure 4.6(b). Simultaneously, we observe scattered brown-colored districts on the map representing major cities, which indicates that high levels of positive net migration to these cities among this age group will occur over the forecast horizon. For instance, Berlin (III), Hamburg (IV), München (V), Köln (VI), and Hannover region (VII) are easily distinguishable from their respective neighboring regions. These results are very much in line with the observed internal migration patterns in the recent past, which were characterized by educational migration by young adults from rural areas to nearby cities with universities and more occupational training opportunities (Siedentop et al., 2014, and the sources cited in the literature review).

Second, as illustrated by Figure 4.6(c), the forecast indicates that for the 25–29 age group, there will be positive net migration in most German regions, particularly in large cities, and only slight decreases in others. A key explanatory factor in this result is that overall positive net international migration is predicted for this age group, due to both labor migration and, as implicitly included in the data, refugee migration (Vanella & Deschermeier, 2018; Vanella et al., 2022). The major cities and some of their surrounding areas will experience larger inflows since international migrants traditionally move to larger cities that are internationally known, and that frequently offer migrants a better network of co-patriates (Henger & Oberst, 2019a; Saa et al., 2020; Sharma & Das,

Figure 4.6: Median Cumulative Net Migration in 2020–2040 by NUTS-3 Region and Age Group

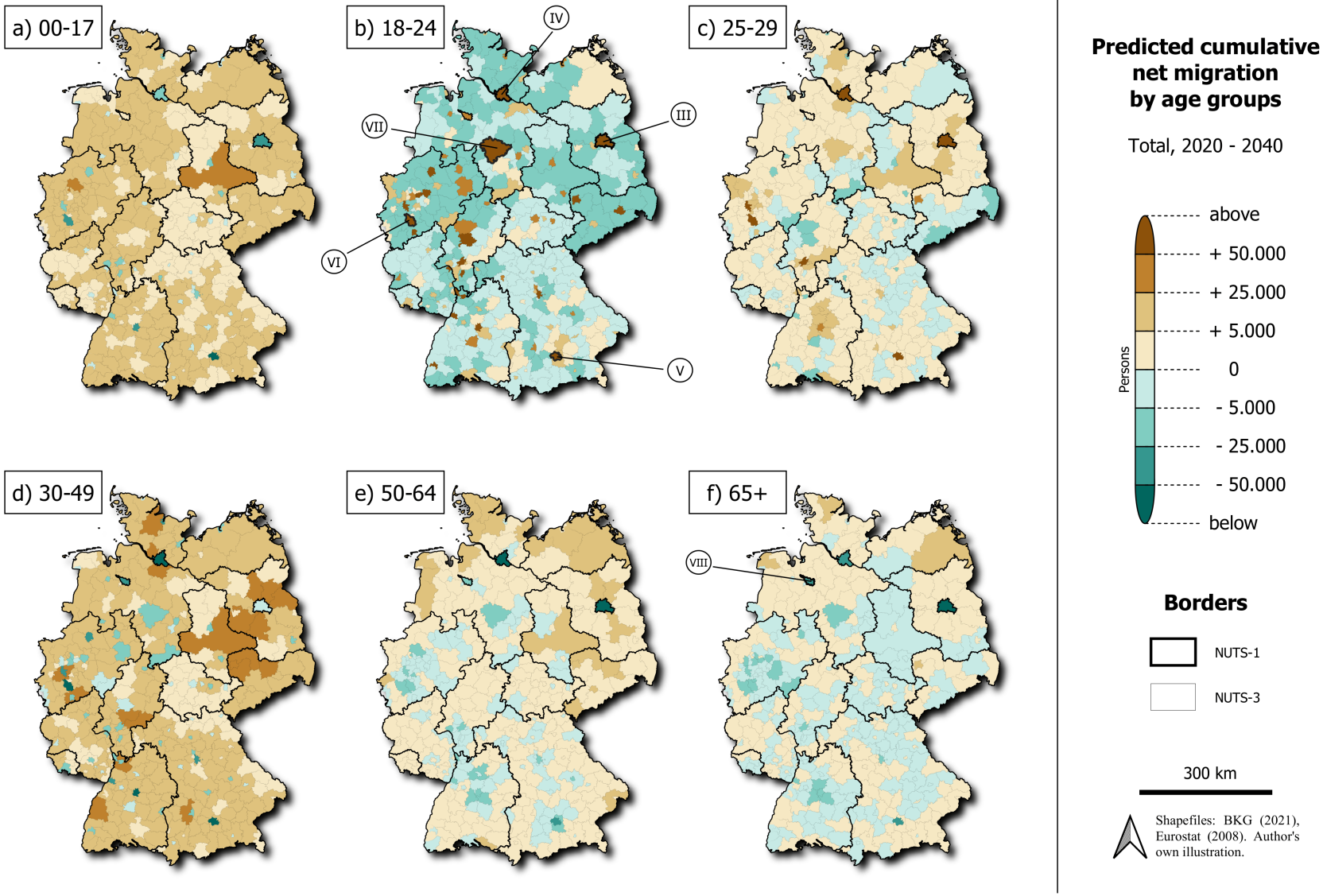

Source: Authors' computation and illustration. [Original source of figure: Vanella et al. (2023), see https://doi.org/10.1553/p-5pn2-fmn8]

2018, and the sources cited in the literature review) who can facilitate their orientation after they arrive in the destination country (Gans & Ritzinger, 2014; Martén et al., 2019). However, by construction, Figure 4.6(c) displays internal movements as well. Here, migration patterns may be explained by the overall regional economic situation; that is, by labor market opportunities. Wage differentials between West Germany and East Germany have persisted since reunification (Smolny & Kirbach, 2011). Moreover, employment growth remains higher in West Germany, and this trend is expected to continue (Heining et al., 2021). For instance, the district of Göttingen shows positive net migration for the 18–24 age group (Figure 4.6(b)) but negative net migration for the 25–29 age group. This can be explained by Göttingen having a highly respected university that attracts students from other regions, but also a relatively small labor market that does not offer enough qualified jobs to keep graduates from leaving the city after they have finished their studies (Buch et al., 2011).[17]

Third, Figures 4.6(a) (0–17 years) and 4.6(d) (30–49 years) show quite different patterns of regional migration flows, apart from the overall positive net international migration. According to the median forecast, there will be negative net migration to major cities among the 30–49 age group. Figure 4.6(a) echoes these trends, as it shows migration among children, who typically migrate with their parents, most of whom are in the 30–49 age group. This echo in the migration age schedule has been investigated for decades and was already observed by Rogers & Castro (1981), as was discussed above. The observed migration patterns can also be attributed to other factors identified in the literature, such as increased personal preferences for living in a quieter and more rural environment, and financial constraints that make it difficult to afford to live in a city (Günther, 2013). Young families are especially likely to search for housing on the outskirts of cities (Peter et al., 2022), as these areas tend to offer more safety and quiet and more affordable housing (Voigtländer & Sagner, 2020). Notably, as was discussed earlier, young families who leave cities often migrate to neighboring regions, as these areas typically offer good infrastructure and allow them to reach the city center relatively quickly (Peter et al., 2022). Moreover, the abovementioned gravity of major cities for internal and international migrants results in additional pressure on real estate markets, which can, in turn, lead to high levels of out-migration (e.g., Henger & Oberst, 2019b).

Fourth, Figures 4.6(e) and 4.6(f) illustrate that despite the large numbers of people in both groups, migration intensities generally decrease with age, as indicated by the

[17]Readers should, however, keep in mind that Figure 4.6 visualizes absolute net migration. Therefore, the color shades are naturally darker for larger districts. This somewhat explains the shades of the pseudo-district 150018285868991, which is merged from multiple rather rural districts in the federal state of Sachsen-Anhalt (see Appendix 4.A for more details). Simultaneously, the 25–29 age group is the smallest of the six included age groups; thus, by construction, it tends to yield smaller absolute numbers.

lighter shades. A notable exception to these decreasing dynamics is the finding that deurbanization trends accelerate with increasing age, and will continue to do so in the future, according to the forecast. In Figures 4.6(e) and 4.6(f), the dark turquoise colors in Berlin, Hamburg, Bremen (VIII), and München indicate that levels of net out-migration among older people are high in these regions. Simultaneously, migration gains among older age groups are expected to occur in some areas surrounding these major cities, and in some northern regions of Germany, particularly those bordering the North Sea and the Baltic Sea. Recalling the literature review, this finding can be attributed to amenity migration. It is well known that retirement is associated with local migration peaks (Rogers & Castro, 1981), as significant numbers of individuals migrate to regions or countries they find more attractive (Vanella & Deschermeier, 2018). In our forecast, the seaside regions are expected to experience net inflows of older age groups in the future.

4.5.2 Migration Flows along the Urban-Rural Continuum

The analysis of migration flows across regions according to the median forecast has shown that in-migration and out-migration exhibit distinct age-specific patterns that can be linked to a series of explanatory factors discussed in the literature. Those factors often result in migration along the urban-rural-continuum, as was outlined. However, relying on district-level data may blur this finding, given that districts do not have a uniform residential structure; that is, each district may contain both rural and urban areas. To substantiate the finding that future migration will run along the urban-rural continuum, we analyzed the forecasted migration figures with respect to the residential structure of a district.

An established classification for German regions is the RegioStaR typology by the Federal Ministry for Digital and Transport (BMVI). In a recent example, Heinsohn et al. (2022) suggested using the RegioStaR 7 specification to characterize regions in a study on regional COVID-19 infection dynamics in schools, as it provides a reasonable trade-off between enabling a sufficient differentiation of regions (seven) while still ensuring that the analysis is comprehensible. Since RegioStaR uses LAU nomenclature, Heinsohn et al. (2022) calculated the median category among all LAUs in each NUTS-3 region, with each LAU weighted by the corresponding population on December 31, 2019. The resulting figure is used as the representative RegioStaR category of the NUTS-3 region (district). We borrowed their approach in the present paper. The RegioStaR typology is provided online by the BMVI (2021), alongside population estimates. Based on the outlined procedure, we derived net migration forecasts by age group and type of region.

Table 4.2: Median Cumulative Net Migration 2020–2040 by Age Group and Type of Region [in Thousands]

RegioStaR category	**Age group**						**Cum.**
	0-17	**18-24**	**25-29**	**30-49**	**50-64**	**65+**	
71: metropolis in urban region	−198	+1,814	+999	−400	−236	−271	**+1,708**
72: regiopolis and large city in urban region	+58	+1,486	−36	−393	−52	−80	**+981**
73: medium-sized city, urban area in urban region	+888	−221	+202	+1,304	−69	−48	**+2,057**
74: small town area, village area in urban region	+369	−193	+63	+554	+57	+16	**+865**
75: central city in rural region	+106	+131	−32	+104	+39	+18	**+366**
76: medium-sized city, urban area in rural region	+520	−241	+40	+664	+170	+20	**+1,172**
77: small town area, village area in rural region	+373	−259	+54	+535	+187	+48	**+938**

Source: Author's computation and illustration.

The median values in thousands of individuals, cumulated over the forecast horizon, are given in Table 4.2. In the median, the model forecasted no overall migration-induced depopulation for any RegioStaR category due to positive international net migration. There was, however, support for the finding of age-specific regional depopulation due to age-specific migration patterns.

Heavily urban areas (71, 72) are expected to gain more than three million net migrants in the young adult age group (aged 18–24). Conversely, more rural areas to medium-sized cities (73, 74, 76, 77) are expected to face substantial declines in the population aged 18–24. This confirms the finding that internal migration from more rural to urban areas will occur among young people, most of whom are moving to pursue educational opportunities.

Simultaneously, these urban areas will face migration-induced declines among the 0–17 and 30–49 age groups. Again, more rural areas and medium-sized cities will experience the opposite trend: i.e., strong inflows of these age groups. This substantiates the finding that families are expected to migrate from heavily urban areas to smaller-sized cities or the countryside.

Similarly, cities are expected to lose population in the age groups close to or beyond retirement age, while more rural areas experience corresponding inflows. Again, this underlines the finding that amenity migration from urban areas to more rural regions will occur among people aged 50 and older.

4.5.3 Migration Flows Relative to District Population Size

All of the results presented up to this point rely on levels. On the one hand, this allows us to compare the districts and to track migration patterns across region types. On the other hand, absolute numbers may not capture the district-specific significance of migration, as the population sizes of districts vary greatly. Therefore, we computed the cumulative net migration over the forecast horizon relative to the 2019 end-of-year population, as given in (4.8). However, readers should keep in mind that this is a synthetic measure that should not be confused with a rate or a share. Again, Figure 4.7 illustrates the median results.

The displayed patterns demonstrate that focusing on levels of migration flows can blur the significance of migration flows for particular regions. For instance, Berlin and its neighboring regions are disproportionately affected by family migration, as shown by these regions having darker color shades compared to other regions across Germany in Figures 4.7(a) and 4.7(d). Moreover, as Figure 4.7(b) illustrates, the out-migration by young adults from more rural areas to cities is, proportional to the number of persons in this age group, even more pronounced than the results in terms of levels suggest. Particularly in the eastern part of Germany, Berlin and other university cities appear to attract significant shares of individuals aged 18–24 who are migrating for educational reasons. However, our results also suggest that this trend is at least partially offset by remigration after the completion of education. Finally, Figures 4.7(e) and 4.7(f) demonstrate that migration patterns among people aged 50 and older are less intense, proportional to the age group size, than the observed net flows in Figures 4.6(e) and 4.6(f) indicate.

4.5.4 Probabilities of Migration-Induced Regional Depopulation

The results presented above have demonstrated that until 2040, distinct age-specific migration patterns are likely to shape population dynamics across German regions.

However, migration patterns, and thus our findings, are subject to substantial uncertainty. To account for this uncertainty in our forecast, we present the probability of migration-induced depopulation, as derived via (4.9) and (4.10), through our Monte Carlo simulation in Figure 4.8. Again, we cumulated the results over the forecast horizon and present total rather than gender-specific findings. The latter can be found in Online Supplementary File 1.

First, among children, migration-induced depopulation[18] is highly unlikely to occur over the forecast horizon in the vast majority of German districts. We observe that

[18] Which does not rule out depopulation because of low fertility.

Figure 4.7: Median Cumulative Net Migration in 2020–2040 by NUTS-3 Region and Age Group Divided by the Corresponding Population on December 31, 2019

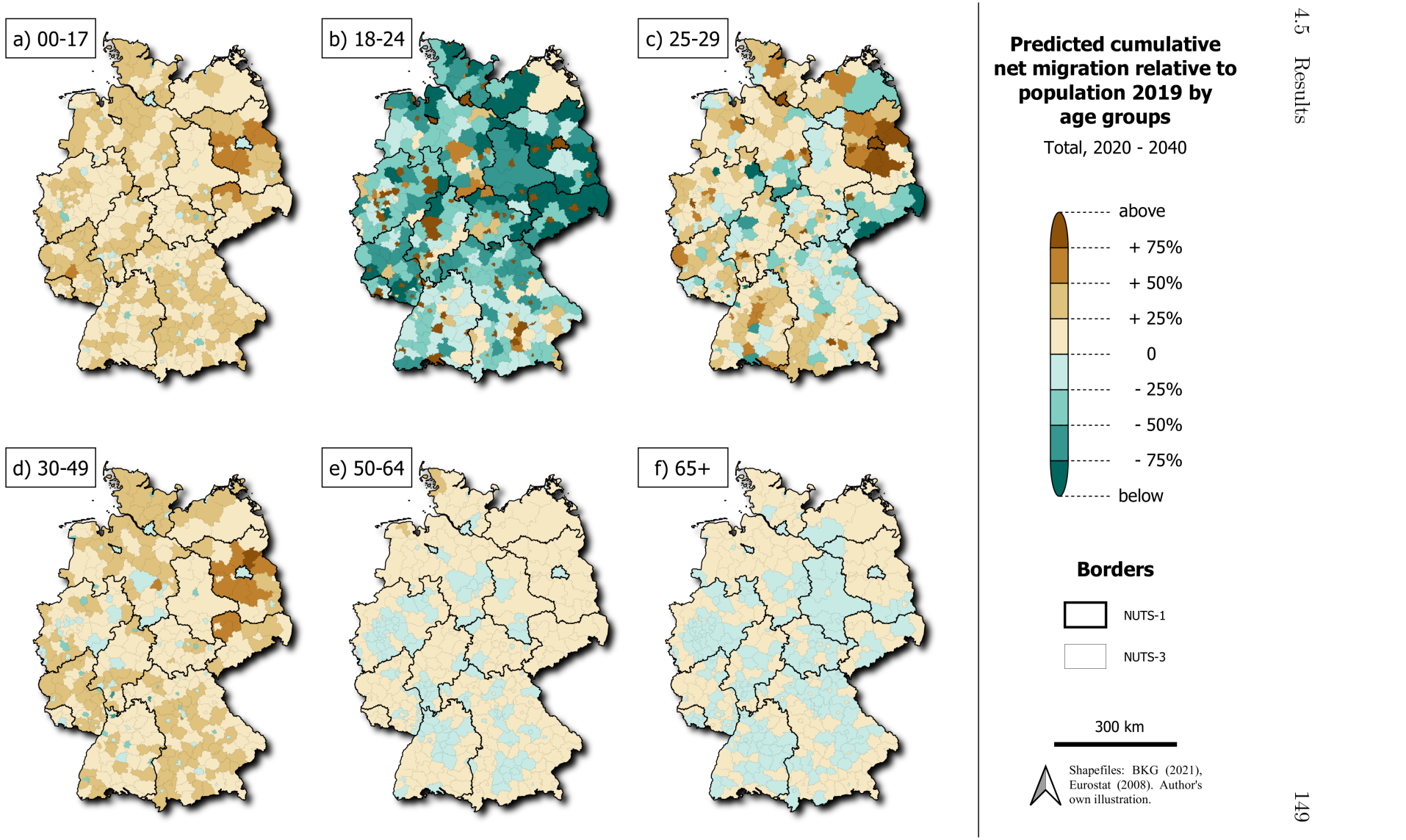

Source: Authors' computation and illustration. [Original source of figure: Vanella et al. (2023), see https://doi.org/10.1553/p-5pn2-fmn8]

Figure 4.8: Probability of Migration-Induced Depopulation Between 2019 and 2040 by District and Age Group

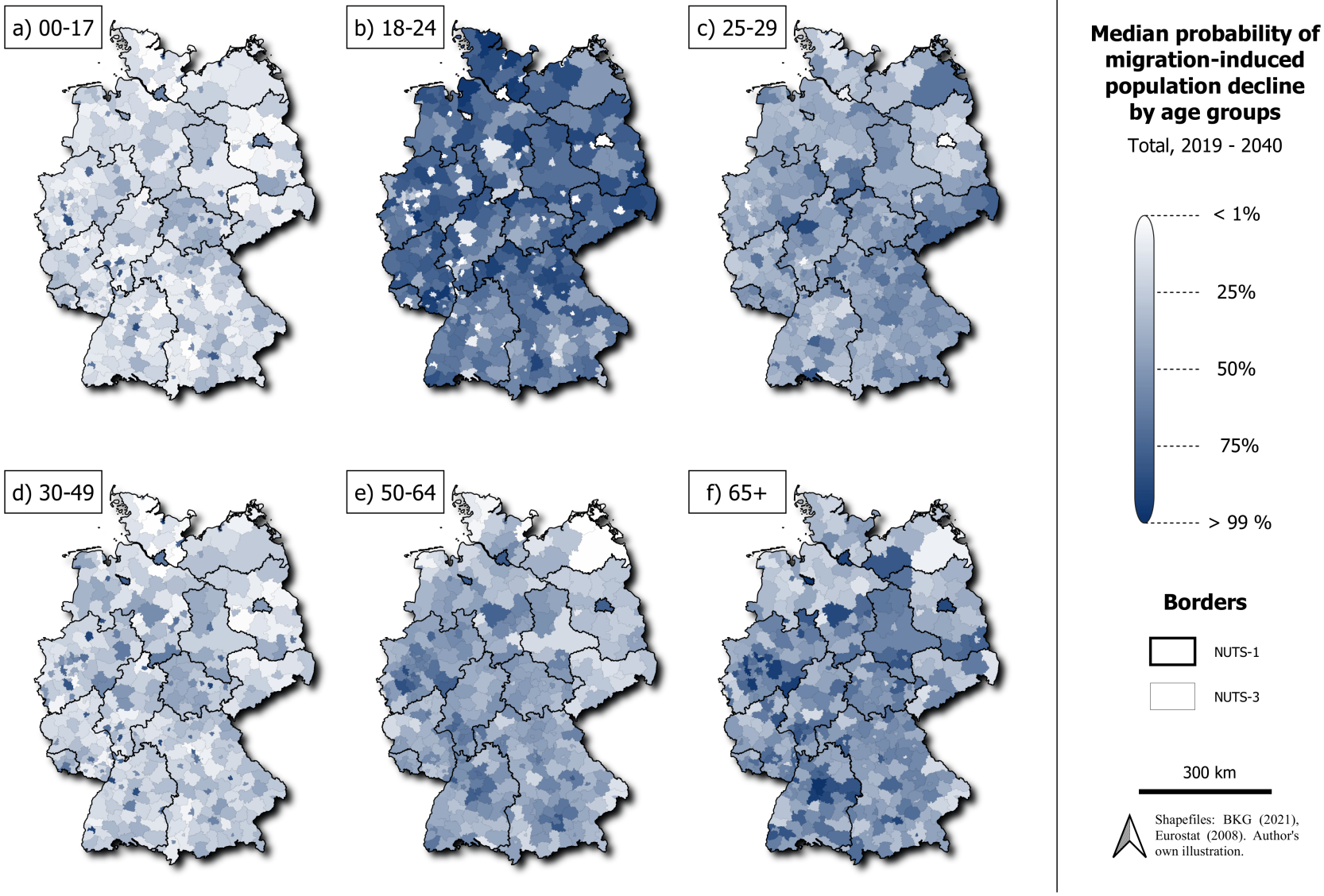

Source: Authors' computation and illustration. [Original source of figure: Vanella et al. (2023), see https://doi.org/10.1553/p-5pn2-fmn8]

only some major cities face an increased probability of migration-driven decreases in the youngest age group. This finding is substantiated by the model results for the 30–49 age group, for whom the decline probabilities, as well as the forecasted median flows, closely mirror those of the youngest age group.

Second, in most German districts, the probability that the population aged 18–24 will shrink due to net out-migration is high. At the same time, we see that large cities, depicted by white dots surrounded by dark blue areas in Figure 4.8, have very low probabilities of losing population in this age group. Thus, the forecasted median migration flows indicate not only that substantial migration-induced declines of the population aged 18–24 will take place in rural areas in both absolute and proportional terms, but also that these declines are highly likely to actually occur.

Third, for the 25–29 age group, no clear patterns in terms of decline probabilities can be derived. It is likely that the composite, mutually offsetting effects of different migration flows, such as international migration, remigration after education, or labor market-related migration, and the accompanying uncertainty, cause wide prediction intervals. Consequently, based upon the forecast presented in this paper, no clear statement regarding the probability of a migration-induced decline in the population aged 25–29, even in the regions exhibiting negative developments in the median forecast in Figures 4.6 and 4.7, can be made.

Fourth, median population changes due to migration among the population aged 50 and older will be quantitatively rather small, but are highly likely to take place in some districts. In other words, the model results shown in Figure 4.8 suggest that large cities are likely to face a decline in the population close to or beyond retirement age due to net outflows of people in this age group.

4.6 Discussion and Conclusion

This article presented a novel approach for joint stochastic forecasting of both international and internal migration on the NUTS-3 level in Germany. Relying on backtests, we found that a principal-component-based approach to estimating log-migration flows gave the best prediction. This approach simultaneously computed future trajectories of in-migration and out-migration flows by age group and gender, while accounting for correlations among in-migration and out-migration cross districts, age groups, and genders. Moreover, time trends in migration and autocorrelations were captured via time series analysis. Including stochasticity by using a Monte Carlo simulation, we derived both the regional depopulation probabilities and the median net migration by age group and type of region for the 2020–2040 period. Thus, given the state of research in regional

migration projections and forecasts, our modeling effort adds a novel approach to the existing literature.

Our findings provide evidence of strong heterogeneity in migration-induced regional depopulation patterns across German regions. This heterogeneity encompasses differences in both the quality and the quantity of migration by age group, gender, and region. The results indicate that among parents (aged 30–49) and their children (aged 0–17), the probability of migrating and the migration flows are increased only for migration from large cities to the countryside. By contrast, the model results point to a high probability of migrating and large migration flows of young adults (aged 18–24) from more rural regions to cities, presumably for reasons such as education. Similarly, the findings suggest that among people of early working ages (aged 25–29), the probability of migrating to economically stronger regions is high, which demonstrates the role labor market opportunities play in migration decisions. In contrast to the patterns observed among younger age groups, the results for people close to or beyond retirement age (aged 50 and older) indicate that they are more likely to migrate from urban areas and industrial centers, and that, while these migration patterns are quantitatively less distinct, they are still highly probable.

Compared to the official German regional population projection performed by Maretzke et al. (2021), our median forecast has qualitative similarities but quantitative differences. The latter stem from significant differences in the predicted net international migration levels. Whereas Maretzke et al. (2021) assumed that net migration to Germany will converge to a level of $200,000$ by 2026, and will remain at that level thereafter, our model predicts a cumulative net migration level of over eight million between 2020 and 2040, i.e., an annual average of $385,000$ over that period. While this estimate is within the range of scenarios deemed realistic by Destatis (2019), it is close to their high migration assumption. Notably, an advantage of our approach is that it is fully stochastic and covers all scenarios described by Destatis (2019), while quantifying their individual probabilities. However, our structural results are remarkably similar to those of Maretzke et al. (2021). Whereas both studies predicted positive net international migration for all types of regions, they also predicted that cities and their neighboring regions will gain population in the younger age groups, whereas the rural areas will lose population in these age groups due to internal migration to urban centers. Thus, the migration-induced increases in rural areas are attributable to in-migration by the older age groups, leading to the aging of the overall regional population. Therefore, both studies predicted that the increase in the heterogeneity of regional age structures, particularly between urban and rural areas, will continue in the future.

Nonetheless, the approach presented in this paper is subject to several limitations. First, due to data availability, the analysis was restricted to six pre-defined age groups. This may be a drawback for future research, since the inclusion of our findings into annual population forecasts will likely require migration forecasts for one-year age groups. We did not impose assumptions on the age structure of the migrants to circumvent this limitation, but instead relied on the information available in the raw data. Fitting age schedules to the data, which is a common practice in migration modeling, would lead to smooth curves, and, when plugged into a forecast model, narrower prediction intervals that underestimate the future risk (Vanella & Deschermeier, 2020). Our model can, however, be seen as a building block that may feed into hierarchical migration forecasts. For instance, we could use auxiliary data, such as information on the age structure at a higher level of geographical aggregation, such as federal states, to construct forecasts of within-age group distributions of migrants and multiply them by our age group-specific forecasts, which would result in one-year age group trajectories. Similarly, the availability of gender-specific migration data at this level of geographical disaggregation was restricted to the period from 2002 onward. Therefore, we needed to approximate the gender-specific time series before that point in time by predicting the gender shares through backcasting. Thus, having sufficiently detailed demographic input data would lead to more accurate age- and gender-specific migration forecasts.

Second, closely connected to the preceding limitation, the best-performing model in the backtests, which was used to perform the forecasting exercise, relied on migration flows. As was outlined in Section 4.2, several authors (Bijak, 2011; Fuchs et al., 2021a) noted the advantages of using migration rates rather than flows. However, as was also discussed in Section 4.2, calculating in-migration rates at the regional level is not straightforward. Thus, the reliance on pseudo-in-migration rates, with their accompanying disadvantages, in the model comparison procedure likely explains the underperformance of the models using migration rates compared to those using flows.

Third, given the volatile nature of migration dynamics in general, migration data are associated with high levels of uncertainty. In particular, international refugee migration is hardly predictable, since it is sensitive to unforeseeable shocks (Vanella et al., 2022). For prediction purposes, it is important to have a sound estimation of future international flows, including of refugee migration, as these processes also shape internal migration. This is a point that should be addressed in future research.

Fourth, the forecast can only be as good as the input data. Thus, trends not included in the historical data also cannot be predicted over the long term by an adequate stochastic approach.[19]

Fifth, closely connected to the preceding point, migration is influenced by a variety of factors, which, for illustrative purposes, and while acknowledging the vast diversity among underlying reasons for migration decisions across individuals and households, may be identified as either push or pull factors, with the first being those that induce out-migration from some region, and the latter being those that draw in-migration to some region (Lee, 1966). Both push and pull factors can be of an economic,[20] a political,[21] a social[22], or an environmental nature.[23] A truly holistic approach would forecast migration based on the future development of those predictors. Importantly, the latter would need to be predicted themselves, which would be far from straightforward and would greatly exceed the scope of this paper.

To conclude, our model addresses a significant shortcoming in the regional migration projection literature by comparing the performance of different modeling approaches and suggesting a stochastic strategy, thereby stimulating the improvement of the projection approaches commonly used by both researchers and statistical offices. In the bigger picture, by contributing to the accuracy of regional population projections in general, this paper also enhances the quality of the demographic base upon which decisions and actions in local and regional planning are taken.

[19]For example, the model is restricted to real estate market developments, as reflected in the past data. Regions, and especially cities, can only increase to the extent that the supply of housing and infrastructure (e.g., childcare, schools or mobility infrastructure) allows them to do so. Similarly, migration is only possible if the receiving region's real estate market offers the migrants room to live. A city that has received a large number of migrants in the past, but does not have living space available and is not building new housing projects, will not be able to generate further positive net migration in the future. However, this limitation appears to be mitigated by our model, as many of those trends — for instance, the trends for Berlin — are already included in the data for past periods, and are, therefore, implicitly included in the model.

[20]For example, income (differences) or unemployment rates (Kubis & Schneider, 2020).

[21]Such as forced migration because of armed conflicts (Heidelberg Institute for International Conflict Research, 2022) or migration induced by restrictions to freedom of speech in the country of origin (EASO, 2016).

[22]Such as migration to a more family-friendly region after the birth of a child, as shown in the paper.

[23]For instance, nutritional problems caused by droughts and associated crop failures (UNHCR, 2020).

4.A Appendix A: Model Selection

4.A.1 Model 1: Gross Migration Flows, Naïve Model

As a baseline, we assumed a naïve model that holds migration flows constant to their last observed levels, i.e., for each district, age group, and gender, the expected annual migration flows $M_{d,a,g,y}$ for the years 2015–2019 were assumed to equal the corresponding observation for 2014:

$$E[M_{d,a,g,y}] = M_{d,a,g,2014}, \qquad y = 2015, 2016, \ldots, 2019. \tag{4A.1}$$

4.A.2 Models 2A and 2B: Gross Migration Flows, Observed Mean and Median Values

As was discussed, several of the contemporaneous approaches in migration forecasting assume the convergence of migration flows to a prespecified level. Therefore, we tested two variants of models with target levels. Model 2A was inspired by the international migration assumption in Destatis (2019). Thus, we assumed that the migration flows for all strata will equal their respective historical means over the whole baseline period, i.e.

$$E[M_{d,a,g,y}] = \bar{M}_{d,a,g}, \qquad y = 2015, 2016, \ldots, 2019, \tag{4A.2}$$

with $\bar{M}_{d,a,g}$ being the annual mean of migration to or from district d for age group a and gender g for 1995–2014. As a second variant, Model 2B imposed the expected median, since Vanella & Deschermeier (2020) suggested assuming that crisis-induced migration converges toward its long-term median rather than the mean, as the mean is more sensitive to extreme migration, which may, for example, be caused by extraordinary refugee flows. Then, the expected annual migration flow from or to some district, by some age group of a certain gender, is

$$E[M_{d,a,g,y}] = \tilde{M}_{d,a,g}, \qquad y = 2015, 2016, \ldots, 2019, \tag{4A.3}$$

with $\tilde{M}_{d,a,g}$ being the median migration flow from or to district d for age group a and gender g for 1995–2014.

4.A.3 Model 3: Net Migration Flows, Principal Component Analysis

Model 3 is based on Vanella & Deschermeier (2018), applying PCA to the time series matrix of district-, age-, and gender-specific net migration flows, a $20 \times 4,752$ matrix.[24] As was outlined, PCA transforms the original variables into linear combinations that are correlated to all original variables, yet are uncorrelated among themselves. For the case of net migration flows, for instance, the value of the jth PC in year y can be written as:

$$P_{j,y} = \sum_{d=1}^{396} \sum_{a=1}^{6} \sum_{g=1}^{2} \lambda_{j,d,a,g} N_{d,a,g,y}, \tag{4A.4}$$

with $\lambda_{j,d,a,g}$ being called the loading (or coefficient) of net migration in district d, in age group a, and of gender g on PC j, and $N_{d,a,g,y}$ being the observed net migration in the said district of the said age group and gender in the said year. The loadings are computed by singular value decomposition.[25] Based on graphical analysis of the time series, the ACF, the PACF and maximum likelihood estimation, we fit a trend function with a linear and cosine trend to the time series of the first PC (which explained close to 55% of the variance in the 4,752 time series). The nuisance parameter was emulated by a random walk process:

$$E[P^3_{1,y}|P^3_{1,2014}] \approx 3,588 - 1,393(y - 1997) + 4,276 \cos\left(\frac{(y-1997)\pi}{3}\right) + r^3_{2014}, \quad y = 2015, 2016, \ldots, 2019, \tag{4A.5}$$

with r_{2014} being the residual between the value of the first PC and the predicted value by the trend function in 2014. The cosine had a periodicity of six years and was fitted as suggested by Vanella et al. (2021) for forecasting weekly mortality rates. The past values are illustrated with the predictions for 2015–2019 in Figure 4A.1, again sign-reversed as in the main text to facilitate interpretation.

The remaining 4,751 PCs were assumed to be constant for 2015–2019, similarly to 4A.1. The matrix of predicted PCs was then transformed back into predictions of net migration for each district, age group, and gender by inverting 4A.4 over the set of PC predictions. In matrix notation, the predicted annual net migrations 2015–2019 are

$$\hat{N} = \hat{P} \times \Lambda^{-1}, \tag{4A.6}$$

[24] 20 years of observations (1995–2014) in the rows, 2 genders × 6 age groups (≤17; 18–24; 25–29; 30–49; 50–64; ≥65) × 396 (pseudo) districts in the columns

[25] See, e.g., Vanella (2018) for more details on applied PCA in demographic forecasting.

Figure 4A.1: Time Series (Sign-Reversed) of Principal Component 1 of Net Migration Model with Forecast

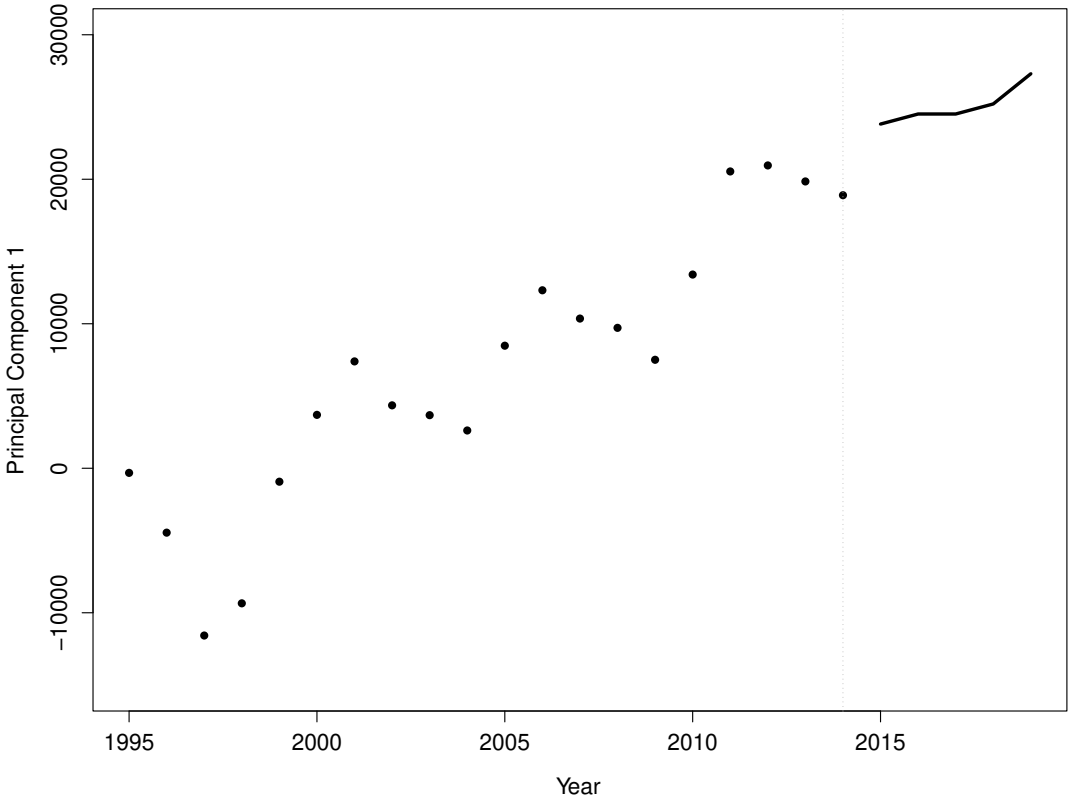

Source: Authors' computation and illustration. [Original source of figure: Vanella et al. (2023), see https://doi.org/10.1553/p-5pn2-fmn8]

with $\hat{P}(5 \times 4,752)$ being the predicted PCs for 2015–2019 and Λ^{-1} being the inverted loading matrix $(4,752^2)$.

4.A.4 Model 4: Log-Gross Migration Flows, Principal Component Analysis

For Model 4, the best-performing model used for the stochastic forecast in the main text, we pursued an estimation approach similar to that for Model 3. However, instead of using net migration flows, we applied PCA to a $20 \times 9,504$ matrix of the district-, age-, and gender-specific migration log-inflows and log-outflows:

$$Q_{j,y} = \sum_{d=1}^{396} \sum_{a=1}^{6} \sum_{g=1}^{2} \sum_{z=1}^{2} \lambda_{j,d,a,g,z} L_{d,a,g,z,y}, \tag{4A.7}$$

with $L_{d,a,g,z,y}$ being the log-migration in or from district d, among age group a, of gender g and of type z ($z = 1$: inflows; $z = 2$: outflows) in year y.

In doing so, we were able to cover trends of both in-migration and out-migration while simultaneously accounting for interdependencies between the two; a phenomenon that was also observed by, for example, Fuchs et al. (2021a). By construction, migration flows cannot take negative values. Thus, we included the natural logarithms of migration flows in the PCA. Here again, the first PC (which covered almost 57% of the variance in the 9,504 variables) was predicted in detail by fitting a trend function (in this case, an inverse logistic trend) to the data and modeling the nuisance as a random walk. The resulting forecast function was:

$$E[P^4_{1,y}|P^4_{1,2014}] \approx 3.646 - 41.803\frac{exp(\frac{y-2003}{2.908})}{1+exp(\frac{y-2003}{2.908})} + r^4_{2014}, \qquad y = 2015, 2016, \ldots, 2019. \tag{4A.8}$$

Figure 4A.2 shows the sign-reversed course of the first PC with its prediction for 2015–2019.

The remaining 9,503 PCs were assumed constant, as they did not exhibit clear trending behavior. Thus, the prediction of the PC matrix can be easily performed in a similar fashion as given in 4A.6.

4.A.5 Model 5: Gross Migration Rates, Naïve Model

Many authors have suggested forecasting migration rates instead of migration flows, as was discussed in the literature review. Fuchs et al. (2021a), for instance, showed for international migration in Germany that emigration rates are less volatile than emigration flows. Therefore, we tested models that were, in essence, similar to those already tested, but used migration rates instead of flows.

For instance, the out-migration rate of age group a of gender g from district d in year y is defined as the quotient of out-migration flows from that stratum, divided by the end-of-year population estimate of the said stratum at the end of the previous year:

$$e_{d,a,g,y} \coloneqq \frac{E_{d,a,g,y}}{B_{d,a,g,y-1}} \tag{4A.9}$$

Since it is not possible to derive immigration rates due to data restrictions (see Fuchs et al. 2021a and the discussion in Section 4.2), we defined the notion of pseudo-in-

Figure 4A.2: Time Series (Sign-Reversed) of Principal Component 1 of the Log-Migration Model with Forecast

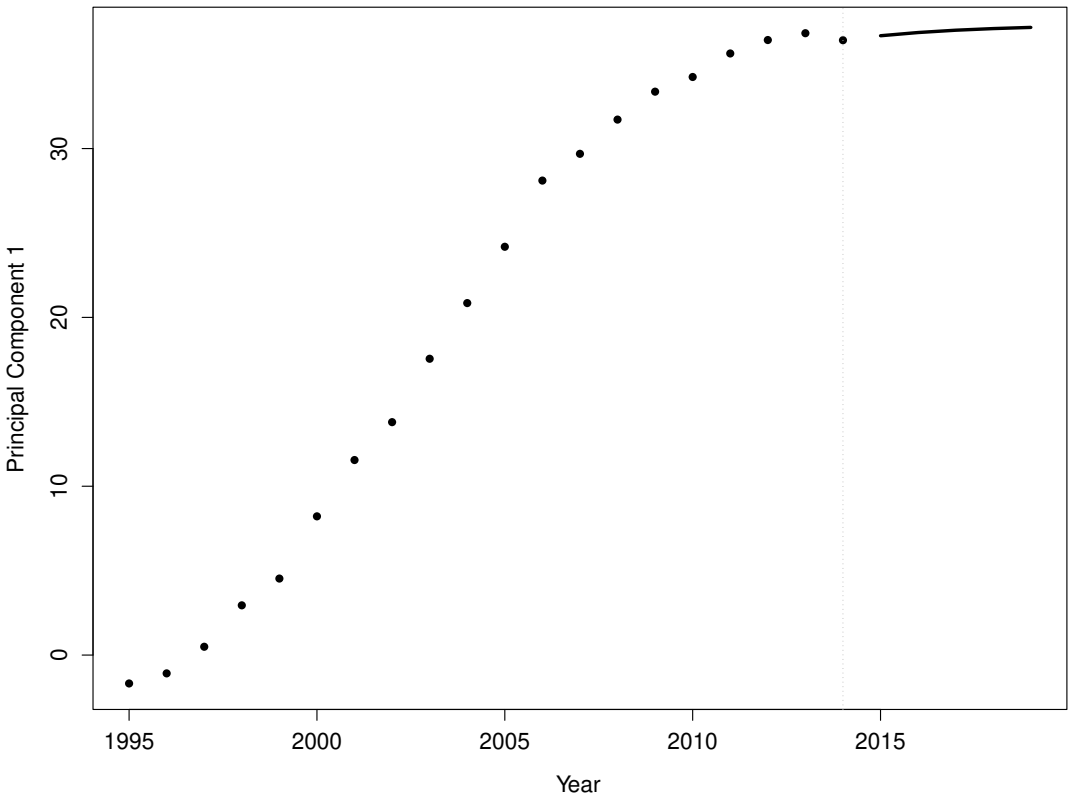

Source: Authors' computation and illustration. [Original source of figure: Vanella et al. (2023), see https://doi.org/10.1553/p-5pn2-fmn8]

migration rates, which relate the inflow to some districts to the population of the target region instead of the origin region:

$$i_{d,a,g,y} \coloneqq \frac{I_{d,a,g,y}}{B_{d,a,g,y-1}}. \tag{4A.10}$$

Although this is a highly hypothetical measure, it allowed for a standardization of in-migration according to out-migration that enabled us to consider the previously discussed correlations between in-migration and out-migration flows in our statistical analysis. Moreover, we indirectly included a higher gravity of migration by larger districts, and thus implicitly accounted for spatial dependence. Model 5 took a naïve prediction approach similar to that in Model 1, but with migration rates, which were held constant at their 2014 level:

$$E[m_{d,a,g,y}] = m_{d,a,g,2014}, \qquad y = 2015, 2016, \ldots, 2019. \tag{4A.11}$$

4.A.6 Models 6A and 6B: Gross Migration Rates, Observed Mean and Median Values

Like in Models 2A and 2B, in these models, we tested two scenarios for the migration rates, with Model 6A assuming the long-term means and Model 6B taking the long-term medians as asymptotes. Accordingly, Model 6A assumed

$$E[m_{d,a,g,y}] = \bar{m}_{d,a,g}, \qquad y = 2015, 2016, \ldots, 2019, \tag{4A.12}$$

with $\bar{m}_{d,a,g}$ being the mean of the district-, age-, and gender-specific migration rate over the 1996–2014 period.[26] Accordingly, Model 6B assumed

$$E[m_{d,a,g,y}] = \tilde{m}_{d,a,g}, \qquad y = 2015, 2016, \ldots, 2019, \tag{4A.13}$$

with $\tilde{m}_{d,a,g}$ being the median of the district-, age-, and gender-specific migration rate over the 1996–2014 period.

4.A.7 Model 7: Net Migration Rates, Principal Component Analysis

Corresponding to Model 3, we performed PCA on pseudo net migration rates for all strata. We defined the pseudo net migration rate in district d for age group a and gender g in year y as the difference between 4A.10 and 4A.9, given that migration projections

[26] Note that there is no observation for 1995 because the population data are not available in the needed format before December 31, 1995.

Figure 4A.3: Time Series (Sign-Reversed) of Principal Component 1 of the Log-Migration Rate Model with Forecast

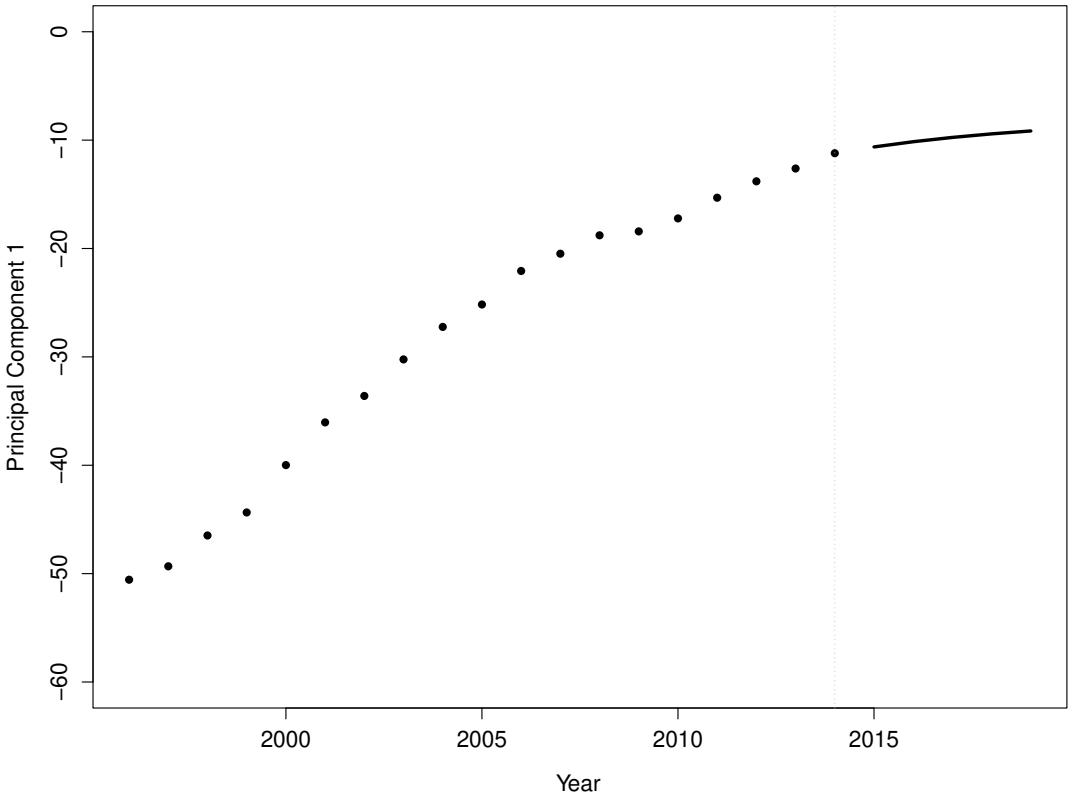

Source: Authors' computation and illustration. [Original source of figure: Vanella et al. (2023), see https://doi.org/10.1553/p-5pn2-fmn8]

based on net growth rates are the current standard in regional population projections in Germany (see Maretzke et al., 2021):

$$n_{d,a,g,y} \coloneqq i_{d,a,g,y} - e_{d,a,g,y}. \tag{4A.14}$$

However, in this case, PCA did not produce trending functions, and thus did not give insights useful for forecasting. As a result, the prediction of the PCs led to the same problem that arose when using the raw data: i.e., determining which target values should be pre-defined. Therefore, Model 7 was discarded.

4.A.8 Model 8: Log-Gross Migration Rates, Principal Component Analysis

Finally, we performed PCA on the compilation matrix of all log-pseudo in-migration and out-migration rate time series.[27] Like for the approaches explained earlier, a forecast model was fit to the time series of the first PC (which explained over 54% of the variance in the 9,504 variables over the 1996–2014 period). The past course and forecast are illustrated in Figure 4A.3.

The prediction was computed by the following forecast function:

$$E[P^8_{1,y}|P^8_{1,2014}] \approx 70.554 - 61.548\frac{exp(\frac{y-2000}{4.854})}{1+exp(\frac{y-2000}{4.854})} + r^8_{2014}, \qquad y = 2015, 2016, \ldots, 2019. \tag{4A.15}$$

The parameters are similar to the previously presented PC-based approaches. Here, again, the remaining PCs do not exhibit clear trending behavior, and are therefore expected to remain constant at their 2014 levels over the forecast horizon.

4.A.9 Comparison of the Forecast Performance of the Candidate Models

Since units and dimensions of the predictions depend on the underlying model (net versus gross migration, or flows versus rates), we applied a relative measure of forecast accuracy. Additionally, the dataset covered zero values of gross migration. To account for these specifics of the data, we compared the models via their ex-post *symmetric mean absolute percentage error* (SMAPE). Chen et al. (2017) defined the SMAPE as

$$SMAPE \coloneqq \frac{1}{n}\sum_t \frac{2|e_t|}{|Y_t| + |F_t|}, \tag{4A.16}$$

with Y_t being the observation for some variable Y at time t, F_t being its forecast based on some model for the same period, and e_t being the difference between Y_t and F_t. Using the SMAPE not only provides the desired properties, i.e., a relative measure that allows for zero values; it also avoids a high level of asymmetry among the forecast errors, which could appear for denominators close to zero (Chen et al., 2017).

Table 4A.1 gives a short presentation of the model approaches with their respective SMAPEs. The results of our backtests indicated a poor predictive performance of Model 3, which extrapolated past trends in net migration flows. PCA of pseudo net migration

[27] Again, we ensured non-negativity among eventual simulations in this way.

rates did not give additional insights compared to the rather simple models (1, 2A, 2B, 5, 6A, 6B) that were based on pre-stated assumptions about the development of migration. Notably, Models 2A, 2B, 6A and 6B performed significantly worse than the naïve Models 1 and 5, with the rate model having a slightly lower SMAPE than the flow model. According to our measure, the PC-based models that distinguished between in- and out-migration were superior, with Model 4 having the best forecast performance overall. Thus, Model 4 was used for the following forecast in the present study.

Table 4A.1: Model Summaries with Forecast Accuracies

Model	**Input variables**	**Dimensions**	**Target variables**	**Method**	**SMAPE**
1	Gross migration	396 Districts 6 Age groups 2 Genders In- and out-migration	Gross migration	Naïve prediction of all district-, age- and gender-specific migration flows	7.63%
2A	Gross migration	396 Districts 6 Age groups 2 Genders In- and out-migration	Gross migration	All district-, age- and gender-specific migration flows assumed to take their respective annual means from 1995–2019 in the forecast	14.23%
2B	Gross migration	396 Districts 6 Age groups 2 Genders In- and out-migration	Gross migration	All district-, age- and gender-specific migration flows assumed to take their respective annual medians from 1995–2019 in the forecast	15.16%
3	Net migration	396 Districts 6 Age groups 2 Genders Net migration	Principal components of net migration	PCA on covariance matrix of district-, age- and gender-specific net migration flow time series matrix. Forecast function fit for first PC; naïve prediction of remaining PCs.	44.88%
4	Log-gross migration	396 Districts 6 Age groups 2 Genders In- and out-migration	Principal components of log-gross migration	PCA on covariance matrix of logarithmized district-, age- and gender-specific gross migration flow time series matrix. Forecast function fit for first PC; naïve prediction of remaining PCs	1.27%
5	Gross migration rates	396 Districts 6 Age groups 2 Genders Pseudo in-migration rates and out-migration rates	Gross migration rates	Naïve prediction of all district-, age- and gender-specific (pseudo) migration rates	7.4%

Continued

Table 4A.1: Continued

Model	Input variables	Dimensions	Target variables	Method	SMAPE
6A	Gross migration rates	396 Districts 6 Age groups 2 Genders Pseudo in-migration rates and out-migration rates	Gross migration rates	All district-, age-, and gender-specific (pseudo) migration rates assumed to take their respective annual means from 1995–2019 in the forecast	14.06%
6B	Gross migration rates	396 Districts 6 Age groups 2 Genders Pseudo in-migration rates and out-migration rates	Gross migration rates	All district-, age-, and gender-specific (pseudo) migration rates assumed to take their respective annual medians from 1995–2019 in the forecast	14.73%
7	Pseudo net migration rates	396 Districts 6 Age groups 2 Genders Pseudo net migration rates	Principal components of pseudo-net migration rates	PCA on covariance matrix of district-, age- and gender-specific pseudo net migration rate time series matrix. Naïve prediction of all PCs.	Discarded due to lack of trends identified by PCA
8	Log-gross migration rates	396 Districts 6 Age groups 2 Genders Pseudo in-migration rates and out-migration rates	Principal components of log-gross migration rates	PCA on covariance matrix of logarithmized district-, age- and gender-specific pseudo migration rate time series matrix. Forecast function fit for first PC; naïve prediction of remaining PCs	2.96%

4.B Appendix B: Inclusion of Territorial Reforms and Lack of Data in Germany since 1995 in the Model

Table 4A.2: Inclusion of Territorial Reforms and Lack of Data in Germany since 1995 in the Model

Time	**Change in raw data**	**Data preparation**
1998	No data before 1998 available for Eisenach city (16056)	Computation of data before 1998 as differences between inter-district migration data for all Thüringen districts from totals for Thüringen.
1998	Kreisreform Sachsen: • Merging of various districts • Renaming of statistical regions: ◦ Chemnitz: 141 → 145 ◦ Dresden: 142 → 146 ◦ Leipzig: 143 → 147	All old district definitions discarded; district definitions since 1998 available for whole period in the raw data
2007	Redefinitions of Sachsen-Anhalt districts: • Halle city: 15202 → 15002 • Magdeburg city: 15303 → 15003 • Altmarkkreis Salzwedel: 15370 → 15081 • Landkreis Stendal: 15363 → 15090	Old definitions changed to new ones before 2007
2007	Mergers of Sachsen-Anhalt districts: • Bördekreis (15355) and Ohrekreis (15362) → Landkreis Börde (15083) • Kreis Mansfelder Land (15260) and Kreis Sangerhausen (15266) → Landkreis Mansfeld-Südharz (15087) • Kreis Merseburg-Querfurt (15261) and Saalkreis (15265) → Saalekreis (15088)	Aggregation of data before 2007 to new definitions
2007	• Redefinition of Burgenlandkreis: 15256 → 15084 • Integration of Landkreis Weißenfels (15268) into 15084	Aggregation of 15256 and 15268 before 2007 into 15084
2007	Mergers and separations of Sachsen-Anhalt districts: • Merger of Landkreis Bitterfeld (15154) and Landkreis Köthen (15159) → Landkreis Anhalt-Bitterfeld (15082) • Merger of Landkreis Halberstadt (15357), Landkreis Quedlinburg (15364), and Landkreis Wernigerode (15369) → Landkreis Harz (15085) • Merger of Kreis Bernburg (15153) and Kreis Schönebeck (15367) → Salzlandkreis (15089) • Landkreis Anhalt-Zerbst (15151) divided into Dessau-Roßlau city (15001), Landkreis Anhalt-Bitterfeld (15082), Landkreis Jerichower Land (15086), and Landkreis Wittenberg (15091) • Landkreis Aschersleben-Staßfurt (15352) divided into Landkreis Harz (15085) and Salzlandkreis (15089)	No one-to-one distribution to new borders possible; thus, aggregation of all districts to pseudo-district 150018285868991

Continued

Appendix B. Continued

Table 4A.2 continued

Time	Change in raw data	Data preparation
2008	Separate reporting of data of city of Hannover and Hannover region without Hannover city	Separate time series before 2008 cannot be constructed; thus, data since 2008 cumulated to total Hannover region, according to old definition
2009	Merger of Aachen city (05334002) and Kreis Aachen (05354) to Städteregion Aachen (05334)	Computation of data since 2009 to old definitions by subtracting 05334002 from 05334
2011	Mergers of Mecklenburg-Vorpommern districts: • Landkreis Bad Doberan (13051) and Landkreis Güstrow (13053) → Landkreis Rostock (13072) • Hansestadt Stralsund (13005), Landkreis Nordvorpommern (13057), and Landkreis Rügen (13061) → Landkreis Vorpommern-Rügen (13073) • Landkreis Ludwigslust (13054) and Landkreis Parchim (13060) → Landkreis Ludwigslist-Parchim (13076)	Aggregation of data before 2011 to new definitions
2011	• Redefinition of Landkreis Nordwestmecklenburg: 13058 → 13074 • Integration of Hansestadt Wismar (13006) into 13074	Aggregation of 13058 and 13074 before 2011 into 13074
2011	Mergers and separations of Mecklenburg-Vorpommern districts: • Hansestadt Greifswald (13001), partially Landkreis Demmin (13052), Landkreis Ostvorpommern (13059), and Landkreis Uecker-Randow (13062) → Landkreis Vorpommern-Greifswald (13075) • Neubrandenburg city (13002), partially Landkreis Demmin (13052), Landkreis Mecklenburg-Strelitz (13055), and Landkreis Müritz (13056) → Landkreis Mecklenburgische Seenplatte (13071)	No one-to-one distribution to new border possible; thus, aggregation of all districts to pseudo-district 1307175
2016	• Redefinition of Landkreis Göttingen: 03152 → 03159 • Integration of Landkreis Osterode am Harz (03156) into 03159	Aggregation of 03152 and 03156 before 2016 into 03159

4.B.1 Approaches to Boundary Change Incorporation

The table above gives a comprehensive overview of the boundary changes underlying the dataset used for the empirical analysis. We applied a rather simple method that sought to obtain consistent time series throughout the period under consideration (1995–2019) by either relying on outdated boundaries or merging districts. We acknowledge that there is an established literature offering a variety of approaches to obtaining missing year-district (or another level of geographical disaggregation) observations, which strongly depends on the corresponding use case. Interested readers may start with examples such as Martin et al. (2002), Norman et al. (2003), or Logan et al. (2021).

4.C Appendix C: Estimation of Age- and Sex-Specific Migration before 2002

As indicated in Section 4.3, for districts in 15 of the 16 federal states, age-specific but no gender-specific migration data are available in the pre-2002 data. To address this gap, we took annual age- and gender-specific data on district-level gross migration flows (Statistische Ämter des Bundes und der Länder, 2022) for 2002–2019. Based on these data, we constructed time series for migration flows by age group and gender for each district for in- and out-migration. To account for differences in the migration patterns between the genders and to retrieve the maximum of information from the data, we computed the annual shares of males among all migrants for each age-district stratum for 2002–2019:

$$s_{d,a,z,y} \coloneqq \frac{M_{d,a,m,z,y}}{M_{d,a,z,y}}, \tag{4A.17}$$

with $M_{d,a,m,z,y}$ being the number of male migrations from or to district d in age group a for migration type z in year y, and $M_{d,a,z,y}$ being the corresponding total migration number for both genders.

The data were highly dimensional (4,596 time series), and the time series were highly correlated. Again, we applied PCA to deal with both problems. Figures 4A.4 and 4A.5 show the time series of the first two PCs. Those time series explained 55.7% of the total variance in the male share time series.

The red lines show the backcasts derived from time series models that were constructed as linear combinations of a mathematical trend function (exponential trend between 2002 and 2015 for the first principal component, and the logistic trend between 2002 and 2010 for the second principal component) and a random walk model each. The remaining PCs did not show clear trending behavior, and were therefore assumed to be

Figure 4A.4: Time Series of Principal Component 1 of Male Shares in District Migration with Backcast

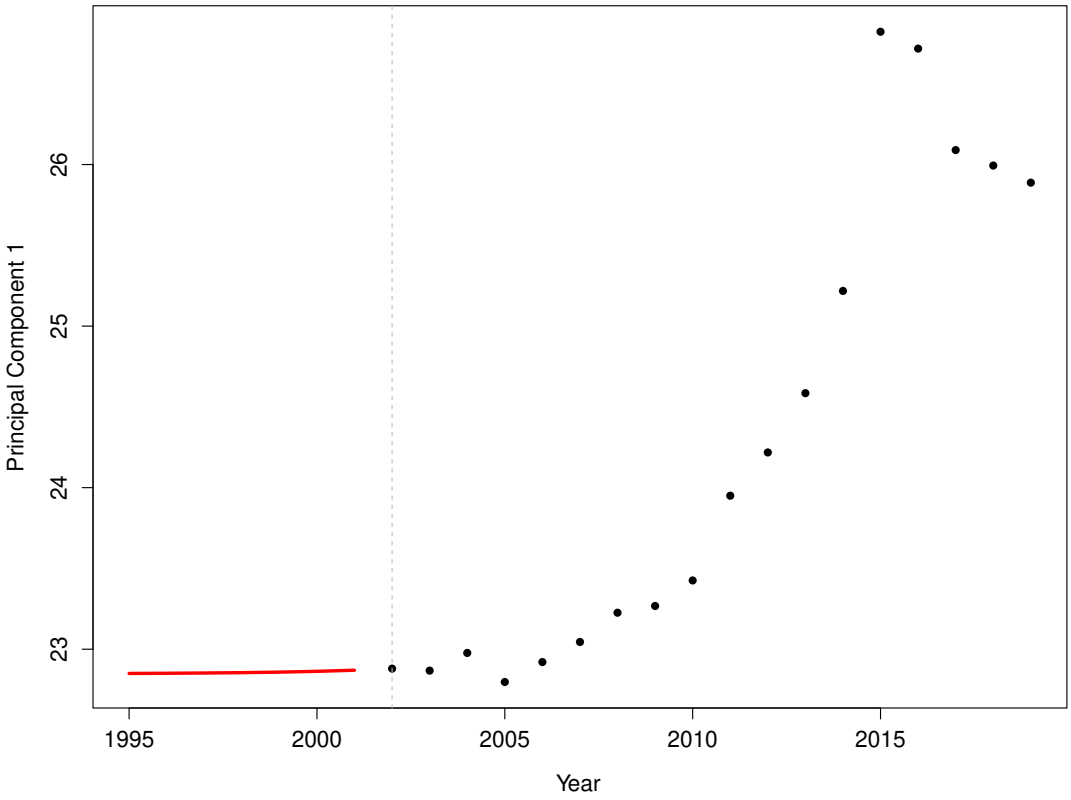

Source: Authors' computation and illustration. [Original source of figure: Vanella et al. (2023), see https://doi.org/10.1553/p-5pn2-fmn8]

random walks. The backcasts of the PCs were then retransformed into backcasts of the male migration shares for each age group and district. We derived the shares of men and women among all migrants per age-district stratum and year by multiplying the corresponding backcast of the male share, and its inverse, by the total migration for the given age-district stratum.

Supplementary Files S2 and S3 (available at https://doi.org/10.1553/p-5pn2-fmn8) offer the annual migration flows for the years 1995–2019 and the corresponding (pseudo) migration rates through 1996–2019, by age, gender, direction, and district, respectively, in matrix form for further use. The data before 2002 are our backcast estimates as described above.

Figure 4A.5: Time Series of Principal Component 2 of Male Shares in District Migration with Backcast

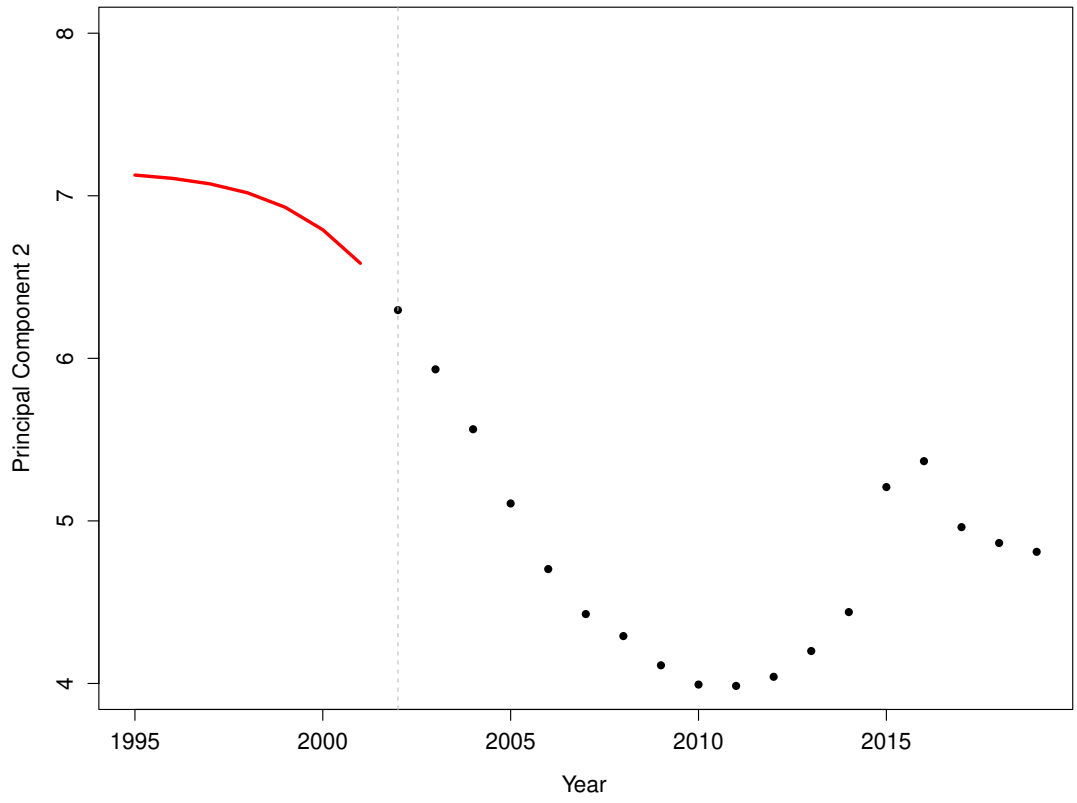

Source: Authors' computation and illustration. [Original source of figure: Vanella et al. (2023), see https://doi.org/10.1553/p-5pn2-fmn8]

Chapter 5

Conclusion

Population decline, in particular among those of working age, is impending or unfolding across many countries and regions, marking the reversal of a stylized fact. This thesis examines population decline and its implications from three perspectives.

In the second chapter, we exploit cross-country variation to uncover labor market adjustments to population decline. To this end, we compile a new historical dataset for 16 advanced economies, covering demographic and economic data for the period 1875–2019. We augment a panel VAR with a smooth-transition structure, thus allowing macroeconomic interdependencies to differ between times of population growth and times of population decline. Using external instruments, we identify population shocks in the reduced-form residuals and derive impulse response functions. The results provide novel insights: Population decline passes through to the labor market more quickly compared to population growth; subsequently, we observe regime-dependent adjustment processes. The results suggest that labor force participation increases stronger in times of population decline compared to the decrease in times of population growth. At the same time, we do not find any effect on the unemployment rate following a decline shock, but an increase following a growth shock. Moreover, in both regimes, we find that the capital-labor ratio changes — it increases in times of decline and decreases in times of growth.

In the third chapter, we provide a modeling framework for one of the main adjustment channels identified in the preceding chapter, that is, changes in labor force participation. More precisely, we examine to what extent the activation of the hidden labor force may contribute to mitigate the adverse effects of population decline on labor supply. To this end, we develop a parsimonious empirical framework and identify a labor market tightness factor from a matrix of employment and unemployment rates by sex and age for the period 1991–2024. Linking our approach to the literature on the full-employment level of the unemployment rate, we are able to simulate full-employment conditions by

calibrating the identified factor accordingly; this yields hidden labor force rates by sex and age. Applying our framework to the case of Germany, we find substantial activation potentials, and show that increases at the extensive margin — the labor market entry of the hidden labor force — could serve as an important building block to maintain the aggregate employment level in the upcoming years.

In the fourth chapter, we address the processes underlying population change itself, and thus the denominator of participation rates, specifically, the role of migration flows for regional population decline. We use migration data for German regions by sex and age groups for the period 1995–2019. After identifying the best-performing among various model specifications by comparing the corresponding pseudo-out-of-sample forecasts, we draw on a Monte Carlo simulation to present a stochastic forecast of regional migration flows in Germany until 2040. The results indicate that well-known migration patterns across regions are likely to persist. This leads to distinct differences for the probability of facing migration-induced population decline across regions and age groups.

By combining these three perspectives, the thesis offers a comprehensive account of population decline, analyzing not only the effects, but also investigating mitigation potentials and developing a stochastic forecasting framework for regional migration flows. These contributions provide novel insights and promising starting points for future research and applications; nevertheless, limitations apply.

While the second chapter provides evidence on (asymmetric) adjustments to population growth and population decline as well as a (partially) novel historical data compilation, both of which may serve as points of departure for future modeling and data collection approaches, the insights and conclusions are naturally subject to the limitations of the underlying data. This encompasses changes in definitions over time, as well as changes in macroeconomic interdependencies, both discussed in the corresponding subchapter. Moreover, the identified mechanisms mirror the adjustments observed in response to past shocks. Thus, although — from a policy perspective and particularly in light of the impending population decline in many countries — our findings appear promising, they should neither be understood as an automatism nor as a forecast of adjustments in the future, but rather as reference points for possible adjustment channels.

In the third chapter, we address the feasibility of one of these reference points — increases in labor force participation — by introducing an easily applicable and intuitive approach to estimate hidden labor force rates by sex and age, thus providing insights on activation potentials at the extensive margin. While we find considerable activation potentials that could contribute to maintain the aggregate employment level in Germany during the upcoming years, the approach neither accounts for activation potentials at

the intensive margin, nor provides insights into how full-employment conditions could be established. Both aspects provide natural starting points for future research — for example, by preparing and including information on part-time and full-time shares by sex and age. In a similar vein, an extension of the framework to include data disaggregated along further demographic categories could contribute to a more nuanced approximation of existing activation potentials. In view of earlier findings for Germany, this could encompass the preparation and inclusion of labor force participation rates by citizenship, but also an analysis using participation data for sub-national geographies could offer insights into regionally varying activation potentials beyond differences in population size and structure. However, such extensions likely encounter limited data availability.

Nonetheless, a thorough understanding of future population dynamics themselves is also crucial. The forecasting model for regional migration flows introduced in the fourth chapter addresses this issue, thereby offering advantages over existing approaches: On the one hand, it accounts for trends over time, rather than assuming constant migration rates in the future; on the other hand, it also accounts for the uncertainty inherent to the forecast. At the same time, however, a comparison with recent international net migration data for Germany suggests that the model's implied forecasts may have been too optimistic. This calls for a refinement of the presented approach in future research. Moreover, the model predicts migration flows rather than migration rates — yet, the differences in the pseudo-out-of-sample performance of both approaches are small. In view of the advantages of modeling migration rates — such as excluding a negative net migration that exceeds the size of the resident population in the region in question — this calls for a refinement in future approaches with a particular focus on modeling migration rates.

Bibliography

Abel, G. J., Barakat, B., KC, S., & Lutz, W. (2016). Meeting the Sustainable Development Goals leads to lower world population growth. *Proceedings of the National Academy of Sciences*, 113(50), 14294–14299.

Abel, G. J. & Cohen, J. E. (2019). Bilateral international migration flow estimates for 200 countries. *Scientific Data*, 6, article 82.

Abelshauser, W. (1975). *Wirtschaft in Westdeutschland 1945–1948: Rekonstruktion der Wachstumsbedingungen in der amerikanischen und britischen Zone*. Stuttgart: Dt. Verl.-Anst.

Abildgren, K. (2005). *Estimates of the Danish general government budget balance and the cyclical budget volatility 1875–2003*. Danmarks Nationalbank Working Paper 30.

Abildgren, K. (2017). A Chart & Data Book on the Monetary and Financial History of Denmark. Retrieved 12 June 2020 from https://sites.google.com/view/kim-abildgren/historical-statistics.

Abraham, K. G. & Kearney, M. S. (2020). Explaining the Decline in the US Employment-to-Population Ratio: A Review of the Evidence. *Journal of Economic Literature*, 58(3), 585–643.

ABS (1917). *Census of the Commonwealth of Australia. Part XII – Occupations*. Melbourne: McCarron, Bird & Co.

ABS (1925). *Census of the Commonwealth of Australia. Part XVII – Occupations*. Melbourne: H. J. Green, Government Printer.

ABS (1937). *Census of the Commonwealth of Australia. Part XXIII – Occupations*. Canberra: L. F. Johnston, Commonwealth Government Printer.

Acemoğlu, D. & Restrepo, P. (2017). Secular Stagnation? The Effect of Aging on Economic Growth in the Age of Automation. *American Economic Review*, 107(5), 174–179.

Acemoğlu, D. & Restrepo, P. (2022). Demographics and Automation. *The Review of Economic Studies*, 89(1), 1–44.

AKETR (2016). *Methodenhandbuch: Regionale Erwerbstätigenrechnung im Rahmen der Volkswirtschaftlichen Gesamtrechnung*. Wiesbaden: Hessisches Statistisches Landesamt.

Aksoy, Y., Basso, H. S., Smith, R. P., & Grasl, T. (2019). Demographic Structure and Macroeconomic Trends. *American Economic Journal: Macroeconomics*, 11(1), 193–222.

Allen, R. C. (2001). The Great Divergence in European Wages and Prices from the Middle Ages to the First World War. *Explorations in Economic History*, 38(4), 411–447.

AMECO (2026). AMECO database. Retrieved 26 January 2026 from https://ec.europa.eu/info/business-economy-euro/indicators-statistics/economic-databases/macro-economic-database-ameco/ameco-database_en.

Anderton, D. L., Barrett, R. E., & Bogue, D. J. (1997). *The Population of the United States*. New York, NY: The Free Press.

Antonakakis, N., Chatziantoniou, I., & Filis, G. (2017). Energy consumption, CO2 emissions, and economic growth: An ethical dilemma. *Renewable and Sustainable Energy Reviews*, 68,

808–824.

Armstrong, D. (1999). Hidden male unemployment in Northern Ireland. *Regional Studies*, 33(6), 499–511.

Arrow, K. J., Chenery, H. B., Minhas, B. S., & Solow, R. M. (1961). Capital-Labor Substitution and Economic Efficiency. *The Review of Economics and Statistics*, 43(3), 225–250.

Ashenfelter, O., Doran, K., & Schaller, B. (2010). A Shred of Credible Evidence on the Long-run Elasticity of Labour Supply. *Economica*, 77(308), 637–650.

Auerbach, A. J. & Gorodnichenko, Y. (2012). Measuring the Output Responses to Fiscal Policy. *American Economic Journal: Economic Policy*, 4(2), 1–27.

Autor, D., Goldin, C., & Katz, L. F. (2020). Extending the Race between Education and Technology. *AEA Papers and Proceedings*, 110, 346–351.

Azose, J. J., Ševčíková, H., & Raftery, A. E. (2016). Probabilistic population projections with migration uncertainty. *Proceedings of the National Academy of Sciences*, 113(23), 6460–6465.

BA (2020). Arbeitslosigkeit im Zeitverlauf: Entwicklung der Arbeitslosenquote (Jahreszahlen). Retrieved 22 June 2021 from www.statistik.arbeitsagentur.de.

Baffigi, A. (2011). *Italian National Accounts, 1861–2011*. Quaderni di storia economica / Economic History Working Papers 18.

Bai, J. & Ng, S. (2008). Large Dimensional Factor Analysis. *Foundations and Trends in Econometrics*, 3(2), 89–163.

Ballas, D., Clarke, G. P., & Wiemers, E. (2005). Building a dynamic spatial microsimulation model for Ireland. *Population, Space and Place*, 11(3), 157–172.

Bank of England (2017). A millennium of macroeconomic data: The Bank of England's collection of historical macroeconomic and financial statistics. Retrieved 12 June 2020 from https://www.bankofengland.co.uk/statistics/research-datasets.

Bargain, O., Orsini, K., & Peichl, A. (2014). Comparing Labor Supply Elasticities in Europe and the United States. *Journal of Human Resources*, 49(3), 723–838.

Bargain, O. & Peichl, A. (2016). Own-wage labor supply elasticities: variation across time and estimation methods. *IZA Journal of Labor Economics*, 5(1), article 10.

Barro, R. J. (1991). Economic Growth in a Cross Section of Countries. *The Quarterly Journal of Economics*, 106(2), 407–443.

Barro, R. J. (1998). *Determinants of Economic Growth: A Cross-Country Empirical Study*. Cambridge, MA: MIT Press.

Barro, R. J. & Lee, J.-W. (1994). Sources of economic growth. *Carnegie-Rochester Conference Series on Public Policy*, 40, 1–46.

Barro, R. J. & Lee, J. W. (2013). A new data set of educational attainment in the world, 1950–2010. *Journal of Development Economics*, 104, 184–198.

Bauer, A. (2024). Accounting for qualification in mismatch unemployment. *Journal for Labour Market Research*, 58, article 27.

BBSR (2026). Laufende Raumbeobachtung des BBSR - INKAR. Retrieved 01 May 2026 from https://www.inkar.de/.

Beine, M., Bertoli, S., & Fernández-Huertas Moraga, J. (2016). A Practitioners' Guide to Gravity Models of International Migration. *The World Economy*, 39(4), 496–512.

Beine, M., Docquier, F., & Özden, Ç. (2011). Diasporas. *Journal of Development Economics*, 95(1), 30–41.

Beine, M. & Parsons, C. (2015). Climatic factors as determinants of international migration. *The Scandinavian Journal of Economics*, 117(2), 723–767.

Bell, M., Charles-Edwards, E., Kupiszewska, D., Kupiszewski, M., Stillwell, J., & Zhu, Y. (2015). Internal Migration Data Around the World: Assessing Contemporary Practice. *Population, Space and Place*, 21(1), 1–17.

Bengtsson, E. & Molinder, J. (2017). The economic effects of the 1920 eight-hour working day reform in Sweden. *Scandinavian Economic History Review*, 65(2), 149–168.

Bergeaud, A., Cette, G., & Lecat, R. (2016). Productivity trends in advanced countries between 1890 and 2012. *Review of Income and Wealth*, 62(3), 420–444.

Berger, M. C. (1985). The Effect of Cohort Size on Earnings Growth: A Reexamination of the Evidence. *Journal of Political Economy*, 93(3), 561–573.

Bernard, A. & Bell, M. (2018). Educational selectivity of internal migrants: A global assessment. *Demographic Research*, 39, 835–854.

Bertoli, S., Fernández-Huertas Moraga, J., & Ortega, F. (2013). Crossing the border: Self-selection, earnings and individual migration decisions. *Journal of Development Economics*, 101, 75–91.

Beveridge, W. (1944). *Full Employment in a Free Society*. London: George Allen & Unwin.

BFS (2022). Bruttoinlandprodukt, lange Serie, 1948–2020. Retrieved 04 August 2022 from www.bfs.admin.ch/asset/de/23184196.

BFS (2023). Ständige Wohnbevölkerung nach Geschlecht und Alter, 1860–2020. Retrieved 01 July 2023 from https://www.bfs.admin.ch/asset/de/23284918.

BFS (2025). Grenzgängerstatistik (GGS). Retrieved 19 February 2025 from https://www.bfs.admin.ch/bfs/de/home/statistiken/arbeit-erwerb/erhebungen/ggs.html.

Biavaschi, C. (2013). The labor demand was downward sloping: Disentangling migrants' inflows and outflows, 1929–1957. *Economics Letters*, 118(3), 531–534.

BiB (2021). Demographic facts and trends in Germany, 2010–2020. Retrieved 10 May 2026 from https://www.bib.bund.de/Publikation/2021/Demographic-facts-and-trends-in-Germany-2010-2020.html.

BiB (2023). Zusammengefasste Geburtenziffer in Deutschland (1871–2021). Retrieved 07 August 2023 from https://www.bib.bund.de/Permalink.html?cms_permaid=1217838.

BiB (2026a). Zu- und Fortzüge über die Außengrenzen Deutschlands (1950-2024). Retrieved 01 May 2026 from https://www.bib.bund.de/DE/Fakten/Fakt/M01-Zuzuege-Fortzuege-Deutschland-ab-1950.html.

BiB (2026b). Zusammengefasste Geburtenziffer in Deutschland (1871–2023). Retrieved 10 February 2026 from https://www.bib.bund.de/DE/Fakten/Fakt/F08-Zusammengefasste-Geburtenziffer-ab-1871.html.

Bijak, J. (2011). *Forecasting International Migration in Europe: A Bayesian View*. Dordrecht: Springer.

BIS (2022). BIS long consumer prices database. Retrieved 04 August 2023 from www.bis.org/.

BKG (2026). Verwaltungsgebiete 1:5 000 000, Stand 31.12. (VG5000 31.12.). Retrieved 01 May 2026 from https://sgx.geodatenzentrum.de/web_public/gdz/datenquellen/datenquellen_vg_nuts.pdf.

Black, R., Adger, W. N., Arnell, N. W., Dercon, S., Geddes, A., & Thomas, D. (2011). The effect of environmental change on human migration. *Global Environmental Change*, 21(Supplement 1), S3–S11.

Blanc, G. & Wacziarg, R. (2025). *Malthusian Migrations*. Working paper.

Blanchard, O. & Diamond, P. (1989). The Beveridge curve. *Brookings Papers on Economic Activity*, 20(1), 1–76.

Blanchflower, D. G. & Oswald, A. J. (1995). An Introduction to the Wage Curve. *Journal of Economic Perspectives*, 9(3), 153–167.

Bloemen, H. G. (2005). Job search, search intensity, and labor market transitions: an empirical analysis. *Journal of Human Resources*, 40(1), 232–269.

Bloom, D. E. & Williamson, J. G. (1998). Demographic Transitions and Economic Miracles in Emerging Asia. *The World Bank Economic Review*, 12(3), 419–455.

Blundell, R., Bozio, A., & Laroque, G. (2013). Extensive and Intensive Margins of Labour Supply: Work and Working Hours in the US, the UK and France. *Fiscal Studies*, 34(1), 1–29.

Blundell, R., Ham, J., & Meghir, C. (1998). Unemployment, discouraged workers and female labour supply. *Research in Economics*, 52(2), 103–131.

BMA (1950). *Entwicklung und Ursachen der Arbeitslosigkeit in der Bundesrepublik Deutschland (1946–1950)*. Bonn.

BMAS (2012). *Statistisches Taschenbuch 2011*. Bonn.

BMVI (2021). Regionalstatistische Raumtypologie (RegioStaR). Retrieved 09 December 2021 from https://www.bmvi.de/SharedDocs/DE/Artikel/G/regionalstatistische-raumtypologie.html.

Bodnár, K. & Nerlich, C. (2022). *The macroeconomic and fiscal impact of population ageing*. European Central Bank, Occasional Paper Series 296.

Boikos, S., Bucci, A., & Sequeira, T. N. (2023). May human capital rescue the Empty Planet? *Economics Letters*, 232, article 111352.

Bolt, J. & van Zanden, J. L. (2020). *Maddison style estimates of the evolution of the world economy: A new 2020 update*. Working Paper WP-15.

Bongaarts, J. (2009). Human population growth and the demographic transition. *Philosophical Transactions of the Royal Society B*, 364(1532), 2985–2990.

Boserup, E. (1965). *The Conditions of Agricultural Growth: The Economics of Agrarian Change Under Population Pressure*. Abingdon: Routledge/Taylor & Francis.

Bossler, M., Gürtzgen, N., Kubis, A., Küfner, B., & Lochner, B. (2020). The IAB Job Vacancy Survey: Design and Research Potential. *Journal for Labour Market Research*, 54(13), 1–12.

Bossler, M. & Popp, M. (2026). Labor Demand on a Tight Leash. *ILR Review*, Online first.

Breidenbach, P., Kaeding, M., & Schaffner, S. (2019). Population Projection for Germany 2015–2050 on Grid Level (RWI-GEO-GRID-POP-Forecast). *Jahrbücher für Nationalökonomie und Statistik (Journal of Economics and Statistics)*, 239(4), 733–745.

Brettell, C. B. & Hollifield, J. F., Eds. (2022). *Migration Theory: Talking Across Disciplines*. New York, NY: Routledge.

Brida, J. & Accinelli, E. (2007). The Ramsey model with logistic population growth. *Economics Bulletin*, 3(15), 1–8.

Brunello, G. (2010). The effects of cohort size on European earnings. *Journal of Population Economics*, 23(1), 273–290.

Bryant, J. & Zhang, J. L. (2016). Bayesian forecasting of demographic rates for small areas: Emigration rates by age, sex, and region in New Zealand, 2014–2038. *Statistica Sinica*, 26(4), 1337–1363.

Bucci, A. (2023). Can a negative population growth rate sustain a positive economic growth rate in the long run? *Mathematical Social Sciences*, 122, 17–28.

Buch, T., Hamann, S., Meier, H., Niebuhr, A., Peters, C., & Puckelwald, J. (2011). *Analyse der Berücksichtigung eines Wanderungsindikators im Rahmen der Abgrenzung des GRW-Fördergebiets*. IAB-Forschungsbericht 4/2011.

Bundesbank (2020). Lange Zeitreihen: Zur Wirtschaftsentwicklung in Deutschland. Retrieved 23 June 2020 from https://www.bundesbank.de/de/statistiken/indikatorensaetze/lange-zeitreihen/lange-zeitreihen-zur-wirtschaftsentwicklung-in-deutschland-832406.

Bundesbank (2023). Lange Zeitreihen: Zur Wirtschaftsentwicklung in Deutschland. Aktualisierte Ausgabe. Retrieved 09 August 2023 from https://www.bundesbank.de/resource/blob/843330/54b834c4dbe9f8ce7d6d5fa7d733486d/mL/0-lange-zeitreihen-data.pdf.

Butlin, M. (1977). *A Preliminary Annual Database 1900/01 to 1973/74*. Source Papers in Economic History 22.

Butschek, F. (1974). Erwerbstätigkeit in Österreich 1961 bis 1980. *WIFO Monatsberichte*, 47(10), 479–490.

Butschek, F. (1992). *Der österreichische Arbeitsmarkt – von der Industrialisierung bis zur Gegenwart*. Wien and Stuttgart: Gustav-Fischer-Verlag.

Börsch-Supan, A. (2008). The Impact of Global Aging on Labor, Product, and Capital Markets. *Population and Development Review*, 34, 52–77.

Börsch-Supan, A. & Schnabel, R. (1998). Social Security and Declining Labor-Force Participation in Germany. *American Economic Review*, 88(2), 173–178.

Cai, R., Feng, S., Oppenheimer, M., & Pytlikova, M. (2016). Climate variability and international migration: The importance of the agricultural linkage. *Journal of Environmental Economics and Management*, 79, 135–151.

Canova, F. & Ciccarelli, M. (2013). Panel Vector Autoregressive Models: A Survey. In T. B. Fomby, L. Kilian, & A. Murphy (Eds.), *VAR Models in Macroeconomics – New Developments and Applications: Essays in Honor of Christopher A. Sims* (pp. 205–246). Bingley, U.K.: Emerald Group Publishing Limited.

Canova, F., Ciccarelli, M., & Ortega, E. (2007). Similarities and convergence in G-7 cycles. *Journal of Monetary Economics*, 54(3), 850–878.

Carbonero, F., Ernst, E., & Weber, E. (2020). *Robots Worldwide: The Impact of Automation on Employment and Trade*. IAB-Discussion Paper 07/2020.

Card, D., Kluve, J., & Weber, A. (2018). What Works? A Meta Analysis of Recent Active Labor Market Program Evaluations. *Journal of the European Economic Association*, 16(3), 894–931.

Cattell, R. B. (1966). The scree test for the number of factors. *Multivariate Behavioral Research*, 1(2), 245–276.

Causa, O., Soldani, E., Nguyen, M., & Tanaka, T. (2025). *Labour shortages and labour market inequalities: Evidence and policy implications*. OECD Economics Department Working Papers 1832.

CBS (2014). Labour force; 1800–2013 (12-hours threshold), series 71882eng. Retrieved 07 July 2020 from https://opendata.cbs.nl/statline/portal.html.

Central Bureau of Statistics of Norway (1966). *Langtidslinjer i norsk økonomi 1865–1960 (Trends in Norwegian Economy 1865–1960)*. Oslo: Statistisk Sentralbyrå.

Central Bureau of Statistics of Norway (1968). *Historisk Statistikk 1968 (Historical Statistics 1968)*. Oslo: Statistisk Sentralbyrå.

Cervellati, M., Sunde, U., & Zimmermann, K. F. (2017). Demographic dynamics and long-run development: insights for the secular stagnation debate. *Journal of Population Economics*, 30(2), 401–432.

Chen, C., Twycross, J., & Garibaldi, J. M. (2017). A new accuracy measure based on bounded relative error for time series forecasting. *PLoS One*, 12(3), e0174202.

Chetty, R. (2012). Bounds on Elasticities With Optimization Frictions: A Synthesis of Micro and Macro Evidence on Labor Supply. *Econometrica*, 80(3), 969–1018.

Christiaans, T. (2011). Semi-endogenous growth when population is decreasing. *Economics Bulletin*, 31(3), 2667–2673.

Cipollone, A., Patacchini, E., & Vallanti, G. (2014). Female labour market participation in Europe: novel evidence on trends and shaping factors. *IZA Journal of European Labor Studies*, 3(1), article 18.

Clark, C. (1957). *The Conditions of Economic Progress*. London: Macmillan.

Clark, M. G. (1983). The Swiss Experience with Foreign Workers: Lessons for the United States. *Industrial and Labor Relations Review*, 36(4), 603–623.

Coleman, D. (2008). The demographic effects of international migration in Europe. *Oxford Review of Economic Policy*, 24(3), 452–476.

Comunale, M. (2022). A panel VAR analysis of macro-financial imbalances in the EU. *Journal of International Money and Finance*, 121, article 102511.

Costa, D. L. (2000). From Mill Town to Board Room: The Rise of Women's Paid Labor. *Journal of Economic Perspectives*, 14(4), 101–122.

Crump, R., Eusepi, S., Giannoni, M., & Sahin, A. (2019). A unified approach to measuring u*. *Brookings Papers on Economic Activity*, 50(1), 143–238.

Cvrcek, T. (2013). Wages, Prices, and Living Standards in the Habsburg Empire, 1827–1910. *The Journal of Economic History*, 73(1), 1–37.

Dagsvik, J. K., Kornstad, T., & Skjerpen, T. (2013). Labor force participation and the discouraged worker effect. *Empirical Economics*, 45, 401–433.

Dagsvik, J. K., Kornstad, T., & Skjerpen, T. (2025). *Stochastic Modeling of Labor Supply and Discouraged Worker Behavior*. Working paper.

Davenport, R. (2021). Patterns of death, 1800-2020: Global rates and causes. In P. N. Stearns (Ed.), *The Routledge History of Death since 1800*, volume 1 (pp. 21–44). Abingdon, Oxon; New York, NY: Routledge, Taylor & Francis Group.

De Beer, J., Van der Gaag, N., Van der Erf, R., Bauer, R., Fassmann, H., Kupiszewska, D., Kupiszewski, M., Rees, P., Boden, P., Dennett, A., Jasińska, M., Stillwell, J., Wohland, P., De Jong, A., Ter Veer, M., Roto, J., Van Well, L., Heins, F., Bonifazi, C., & Gesano, G. (2010). *DEMIFER: Demographic and Migratory Flows Affecting European Regions and Cities*. Final report | version 30/09/2010.

de Zwart, P., van Leeuwen, B., & van Leeuwen-Li, J. (2014). Real wages since 1820. In J. L. van Zanden, J. Baten, M. Mira d'Ercole, A. Rijpma, & M. P. Timmer (Eds.), *How Was Life? Global Well-being since 1820* (pp. 83–86). Paris: OECD Publishing.

Deschermeier, P. (2011). Population development of the Rhine-Neckar metropolitan area: A stochastic population forecast on the basis of functional data analysis. *Comparative Population Studies*, 36(4), 769–806.

Destatis (1972). *Bevölkerung und Wirtschaft 1872–1972*. Stuttgart: W. Kohlhammer.

Destatis (2016). Fachserie 1: Bevölkerung und Erwerbstätigkeit, Reihe 4.1.1: Stand und Entwicklung der Erwerbstätigkeit in Deutschland. Retrieved 19 January 2026 from https://www.statistischebibliothek.de/mir/receive/DESerie_mods_00000004.

Destatis (2017). Kohortensterbetafeln für Deutschland. Ergebnisse aus den Modellrechnungen für Sterbetafeln nach Geburtsjahrgang. 1871–2017. Retrieved 06 June 2023 from https://www.statistischebibliothek.de/mir/receive/DEHeft_mods_00096629.

Destatis (2019). *Bevölkerung im Wandel: Annahmen und Ergebnisse der 14. koordinierten Bevölkerungsvorausberechnung*. Wiesbaden: Statistisches Bundesamt.

Destatis (2020). Erwerbspersonenvorausberechnung. Retrieved 20 March 2026 from https://www.destatis.de/DE/Themen/Arbeit/Arbeitsmarkt/Erwerbstaetigkeit/Erwerbspersonenvorausberechnung-2020.html.

Destatis (2021). Wanderungen zwischen Deutschland und dem Ausland: Deutschland, Jahre, Kontinente, Geschlecht. Retrieved 22 May 2021 from https://www-genesis.destatis.de/datenbank/online/.

Destatis (2023). 15. koordinierte Bevölkerungsvorausberechnung für Deutschland. Retrieved 11 July 2023 from https://service.destatis.de/bevoelkerungspyramide/.

Destatis (2025a). 3,1 Millionen Menschen 2024 in Stiller Reserve am Arbeitsmarkt. Retrieved 26 December 2025 from https://www.destatis.de/DE/Presse/Pressemitteilungen/2025/06/PD25_231_13.html.

Destatis (2025b). Abweichungen zwischen Erwerbstätigenrechnung und Mikrozensus bei der Zahl der Erwerbstätigen. Retrieved 15 January 2026 from https://www.destatis.de/DE/Themen/Arbeit/Arbeitsmarkt/Erwerbstaetigkeit/Methoden/Erlaeuterungen/erlaeuterungen-etr-zum-mz.html.

Destatis (2025c). Gründe für Nichtsuche 2024 (in %). Retrieved 19 January 2026 from https://www.destatis.de/DE/Themen/Arbeit/Arbeitsmarkt/Erwerbstaetigkeit/Tabellen/stille-reserve-2024-gruende-nichtsuche.html.

Destatis (2025d). Gründe für Nichtverfügbarkeit 2024 (in %). Retrieved 19 January 2026 from https://www.destatis.de/DE/Themen/Arbeit/Arbeitsmarkt/Erwerbstaetigkeit/Tabellen/stille-reserve-2024-gruende-nichtverfuegbarkeit.html.

Destatis (2025e). Number of persons in employment reaches new high in 2024. Retrieved 26 December 2025 from https://www.destatis.de/EN/Press/2025/01/PE25_001_13321.html.

Destatis (2025f). Redesigned microcensus as of 2020. Retrieved 19 January 2026 from https://www.destatis.de/EN/Themes/Society-Environment/Population/Households-Families/Methods/microcensus-2020.html.

Destatis (2025g). Statistischer Bericht: Personal des öffentlichen Dienstes – Stichtag 30.06.2024. Retrieved 15 January 2026 from https://www.destatis.de/DE/Themen/Staat/Oeffentlicher-Dienst/Publikationen/Downloads-Oeffentlicher-Dienst/statistischer-bericht-personalstand-oeffentlicher-dienst-2140600247005.xlsx.

Destatis (2025h). Statistischer Bericht: Rückgerechnete Bevölkerung auf Grundlage des Zensus 2022 (2011–2021). Retrieved 19 January 2026 from https://www.destatis.de/DE/Themen/Gesellschaft-Umwelt/Bevoelkerung/Bevoelkerungsstand/Publikationen/Downloads-Bevoelkerungsstand/statistischer-bericht-rueckgerechnete-bevoelkerung-zensus-5124105219005.html.

Destatis (2025i). Unfreiwillig Teilzeitbeschäftigte. Retrieved 21 February 2026 from https://www.destatis.de/DE/Themen/Arbeit/Arbeitsmarkt/Qualitaet-Arbeit/Dimension-3/unfreiwillig-teilzeitbeschaeftige.html.

Destatis (2025j). VGR des Bundes - Bruttowertschöpfung, Bruttoinlandsprodukt (nominal/preisbereinigt): Deutschland, Quartale, Original- und bereinigte Daten. Retrieved 03 November 2025 from https://www-genesis.destatis.de/datenbank/online/statistic/81000/table/81000-0002.

Destatis (2026a). National accounts - population, employment: Germany, years [table 81000-0011]. Retrieved 10 March 2026 from https://www-genesis.destatis.de/datenbank/online/statistic/81000/table/81000-0011.

Destatis (2026b). Sterbetafel (Periodensterbetafel): Deutschland, Jahre, Geschlecht, Vollendetes Alter. Retrieved 16 May 2026 from https://www-genesis.destatis.de/datenbank/online/statistic/12621/table/12621-0001.

Destatis (2026c). Unemployment. Retrieved 19 January 2026 from https://www.destatis.de/EN/Themes/Labour/Labour-Market/Employment/Methods/Unemployment.html.

Destatis (2026d). Wanderungen zwischen Deutschland und dem Ausland: Deutschland, Jahre, Nationalität, Geschlecht, Altersjahre. Retrieved 16 May 2026 from https://www-genesis.destatis.de/datenbank/online/statistic/12711/table/12711-0006.

Dinopoulos, E. & Thompson, P. (1999). Scale effects in Schumpeterian models of economic growth. *Journal of Evolutionary Economics*, 9(2), 157–185.

Doepke, M., Hazan, M., & Maoz, Y. D. (2015). The Baby Boom and World War II: A Macroeconomic Analysis. *The Review of Economic Studies*, 82(3), 1031–1073.

Dustmann, C., Frattini, T., & Rosso, A. (2015). The Effect of Emigration from Poland on Polish Wages. *The Scandinavian Journal of Economics*, 117(2), 522–564.

Duval, R. A., Ji, Y., Li, L., Oikonomou, M., Pizzinelli, C., Shibata, I., Sozzi, A., & Tavares, M. (2022). *Labor Market Tightness in Advanced Economies*. IMF Staff Discussion Notes 2022(001).

EASO (2016). *Significant push/pull factors for determining of asylum-related migration – A literature review*. Luxembourg: Publications Office of the European Union.

Easterlin, R. A. (1961). The American Baby Boom in Historical Perspective. *American Economic Review*, 51(5), 869–911.

Eberhardt, W., Pollermann, K., & Küpper, P. (2014). *Sicherung der Nahversorgung in ländlichen Räumen: Impulse für die Praxis*. Bonn: Bundesamt für Bauwesen und Raumordnung.

ECB (2006). *May 2006*. Monthly Bulletin 06/2006.

Ediev, D. & Gisser, R. (2007). Reconstruction of historical series of life tables and of age-sex structures for the Austrian population in the 19th and the first half of the 20th century. *Vienna Yearbook of Population Research*, 2007, 327–355.

Eggertsson, G. B., Lancastre, M., & Summers, L. H. (2019). Aging, Output Per Capita, and Secular Stagnation. *American Economic Review: Insights*, 1(3), 325–342.

Elgin, C. & Tumen, S. (2012). Can sustained economic growth and declining population coexist? *Economic Modelling*, 29(5), 1899–1908.

Elsby, M. W. L., Michaels, R., & Ratner, D. (2015). The Beveridge curve: A survey. *Journal of Economic Literature*, 53(3), 571–630.

Emerson, J. (2011). Unemployment and labor force participation in the United States. *Economics Letters*, 111(3), 203–206.

Escudero, V. (2018). Are active labour market policies effective in activating and integrating low-skilled individuals? An international comparison. *IZA Journal of Labor Policy*, 7(1), article 4.

European Commission (2024). *2024 Ageing Report: Economic & Budgetary Projections for the EU Member States (2022-2070)*. Institutional Paper 279.

Eurostat (2021). Population projections at regional level. Retrieved 30 November 2021 from https://ec.europa.eu/eurostat/statistics-explained/index.php?title=Population_projections_at_regional_level.

Eurostat (2025a). Employed persons commuting to work by country of work and NUTS 2 region [Table lfst_r_lfe2ecomm]. Retrieved 26 December 2025 from https://doi.org/10.2908/LFST_R_LFE2ECOMM.

Eurostat (2025b). Labour market slack – employment supply and demand mismatch. Retrieved 23 December 2025 from https://ec.europa.eu/eurostat/statistics-explained/index.php?title=Labour_market_slack_-_employment_supply_and_demand_mismatch.

Eurostat (2026a). GISCO Territorial units for statistics (NUTS). Retrieved 01 May 2026 from https://ec.europa.eu/eurostat/web/gisco/geodata/statistical-units/territorial-units-statistics.

Eurostat (2026b). Population on 1 January by age and sex. Retrieved 19 March 2026 from https://ec.europa.eu/eurostat/databrowser/view/demo_pjan__custom_20606712/default/table.

Eurostat (2026c). Supplementary indicators to unemployment (1992–2020) – annual data. Retrieved 19 March 2026 from https://ec.europa.eu/eurostat/databrowser/view/lfsi_sup_a_h__custom_20766768/default/table.

Evers, M., De Mooij, R., & Van Vuuren, D. (2008). The Wage Elasticity of Labour Supply: A Synthesis of Empirical Estimates. *De Economist*, 156(1), 25–43.

FEA (2025a). Arbeitslose und Arbeitslosenquoten – Deutschland und West/Ost (Zeitreihe ab 1950). Retrieved 19 January 2026 from https://statistik.arbeitsagentur.de/.

FEA (2025b). Gemeldete Arbeitsstellen – Deutschland und Westdeutschland (Zeitreihe ab 1950). Retrieved 19 January 2025 from https://statistik.arbeitsagentur.de/.

Feenstra, R. C., Inklaar, R., & Timmer, M. P. (2015). The Next Generation of the Penn World Table. *American Economic Review*, 105(10), 3150–3182.

Fehr, H., Kallweit, M., & Kindermann, F. (2012). Pension reform with variable retirement age: a simulation analysis for Germany. *Journal of Pension Economics & Finance*, 11(3), 389–417.

Fernández, R. (2013). Cultural Change as Learning: The Evolution of Female Labor Force Participation over a Century. *American Economic Review*, 103(1), 472–500.

Ferrie, J. S. & Hatton, T. J. (2015). Two Centuries of International Migration. In B. R. Chiswick & P. W. Miller (Eds.), *Handbook of the Economics of International Migration* (pp. 53–88). Amsterdam, Heidelberg: North-Holland.

Foote, C. (2007). *Space and time in macroeconomic panel data: young workers and state-level unemployment revisited*. Federal Reserve Bank of Boston Working Papers No. 07-10.

Franzmann, G. (2015). Histat-Datenkompilation: Bevölkerung nach Alter in Jahren und nach Geschlecht für das Deutsche Reich, die frühere Bundesrepublik und Deutschland, 1871–2010. GESIS Datenarchiv, Köln. Histat. Studiennummer 8617. Datenfile Version 1.0.0. Retrieved 23 November 2020 from https://doi.org/10.4232/1.12313.

Fratesi, U. & Percoco, M. (2013). Selective migration, regional growth and convergence: Evidence from Italy. *Regional Studies*, 48(10), 1650–1668.

Fuchs, J. (2015). Decomposing the Effect of Population Ageing on Labour Supply. *The Athens Journal of Social Sciences*, 2(2), 109–124.

Fuchs, J., Söhnlein, D., & Vanella, P. (2021a). Migration forecasting – significance and approaches. *Encyclopedia*, 1(3), 689–709.

Fuchs, J., Söhnlein, D., & Weber, B. (2021b). *Projektion des Erwerbspersonenpotenzials bis 2060: Demografische Entwicklung lässt das Arbeitskräfteangebot stark schrumpfen*. IAB-Kurzbericht 25/2021.

Fuchs, J., Söhnlein, D., Weber, B., & Weber, E. (2018). Stochastic forecasting of labor supply and population: An integrated model. *Population Research and Policy Review*, 37(1), 33–58.

Fuchs, J. & Weber, B. (2005). *Neuschätzung der Stillen Reserve und des Erwerbspersonenpotenzials für Westdeutschland (inkl. Berlin-West)*. IAB-Forschungsbericht 15/2005.

Fuchs, J. & Weber, B. (2010). *Umfang und Struktur der westdeutschen stillen Reserve: Aktualisierte Schätzungen*. IAB-Forschungsbericht 11/2010.

Fuchs, J. & Weber, B. (2021). *Neue Schätzungen für die Stille Reserve – erstmalig Anwendung des IAB-Konzepts auf Gesamtdeutschland*. IAB-Forschungsbericht 06/2021.

Fuchs, J. & Weber, E. (2013). A new look at the discouragement and the added worker hypotheses: Applying a trend-cycle decomposition to unemployment. *Applied Economics Letters*, 20(15), 1374–1378.

Fuchs, J. & Weber, E. (2017). Long-term unemployment and labour force participation. A decomposition of unemployment to test for the discouragement and added worker hypotheses. *Applied Economics*, 49(60), 5971–5982.

Fuà, G. (1976). *Occupazione e capacità produttive: la realtà italiana*. Bologna: Il Mulino.

Galenson, W. & Zellner, A. (1957). International comparison of unemployment rates. In Universities-National Bureau Committee for Economic Research (Ed.), *The Measurement and Behavior of Unemployment* (pp. 439–584). Princeton: NBER.

Galor, O. & Mountford, A. (2008). Trading population for productivity: Theory and evidence. *The Review of Economic Studies*, 75(4), 1143–1179.

Gans, P. & Ritzinger, A. (2014). Räumliche Auswirkungen der internationalen Migration – Einführung. In P. Gans (Ed.), *Räumliche Auswirkungen der internationalen Migration* (pp. 1–9). Hannover: Verlag der Akademie für Raumforschung und Landesplanung.

Gapminder (2015a). New births (total number, estimated). Retrieved 20 May 2020 from https://www.gapminder.org/data/.

Gapminder (2015b). Population, total. Retrieved 20 May 2020 from https://www.gapminder.org/data/.

Garloff, A., Pohl, C., & Schanne, N. (2013). Do small labor market entry cohorts reduce unemployment? *Demographic Research*, 29(15), 379–406.

Gehrke, B. & Hochmuth, B. (2021). Counteracting Unemployment in Crises: Non-Linear Effects of Short-Time Work Policy*. *The Scandinavian Journal of Economics*, 123(1), 144–183.

Geis, W., Übelmesser, S., & Werding, M. (2013). How do migrants choose their destination country? An analysis of institutional determinants. *Review of International Economics*, 21(5), 825–840.

Gertler, M. & Karadi, P. (2015). Monetary Policy Surprises, Credit Costs, and Economic Activity. *American Economic Journal: Macroeconomics*, 7(1), 44–76.

GESIS (2025). Series: Microcensus (MZ). Retrieved 19 January 2026 from https://www.gesis.org/en/missy/metadata/MZ.

Geyer, J., Haan, P., Hammerschmid, A., & Peters, M. (2020). Labor Market and Distributional Effects of an Increase in the Retirement Age. *Labour Economics*, 65, article 101817.

Gilmore, O. (2021). The working week in manufacturing since 1820. In OECD (Ed.), *How Was Life? Volume II: New Perspectives on Well-being and Global Inequality since 1820* (pp. 53–71). Paris: OECD Publishing.

Giordano, C. & Zollino, F. (2016). *A Historical Reconstruction of Capital and Labour in Italy, 1861–2013*. Quaderni di Storia economica (Economic History Working Papers) 37.

Gløersen, E., Drăgulin, M., Hans, S., Kaucic, J., Schuh, B., Keringer, F., & Celotti, P. (2016). *The impact of demographic change on European regions*. Luxembourg: Publications Office of the European Union.

Goldin, C. (1991). The Role of World War II in the Rise of Women's Employment. *American Economic Review*, 81(4), 741–756.

González, A., Teräsvirta, T., & van Dijk, D. (2005). *Panel smooth transition regression models*. SSE/EFI Working Paper Series in Economics and Finance 604.

Goossens, M., Peeters, S., & Pepermans, G. (1988). Interwar Unemployment in Belgium. In B. Eichengreen & T. J. Hatton (Eds.), *Interwar Unemployment in International Perspective* (pp. 289–324). Dordrecht: Springer.

Greasley, D. & Oxley, L. (2004). Globalization and real wages in new zealand, 1873–1913. *Explorations in Economic History*, 41(1), 26–47.

Grogger, J. & Hanson, G. H. (2011). Income maximization and the selection and sorting of international migrants. *Journal of Development Economics*, 95(1), 42–57.

Groote, P., Albers, R., & de Jong, H. (1996). *A standardised time series of the stock of fixed capital in the Netherlands*. Working paper.

Grytten, O. H. (1994). *En empirisk analyse av det norske arbeidsmarked 1918–1939: arbeidsledigheten i Norge i internasjonalt perspektiv*. Bergen: Norges Handelshøyskole.

Grytten, O. H. (2004). The gross domestic product for Norway 1830–2003. In Ø. Eitrheim, J. T. Klovland, & J. F. Qvigstad (Eds.), *Historical Monetary Statistics for Norway 1819–2003* (pp. 241–288). Oslo: Norges Bank.

Grytten, O. H. (2008). Why was the Great Depression not so Great in the Nordic Countries? Economic Policy and Unemployment. *The Journal of European Economic History*, 37(2/3), 369–384.

Guttman, L. (1954). Some necessary conditions for common-factor analysis. *Psychometrika*, 19(2), 149–161.

Günther, M. (2013). *Wohnen der Altersgruppe 65plus*. Report.

Hall, R. E. & Jones, C. I. (1999). Why do Some Countries Produce So Much More Output Per Worker than Others?*. *The Quarterly Journal of Economics*, 114(1), 83–116.

Hamermesh, D. S. (1993). *Labor Demand*. Princeton, NJ: Princeton Univ. Press.

Handler, H., Merth, E., & Morwind, K. (1968). *Kapitalstockschätzung für Österreich*. Forschungsbericht 18.

Hatton, T. J. & Williamson, J. G. (1998). *The Age of Mass Migration: Causes and Economic Impact*. New York: Oxford Univ. Press.

Headey, D. D. & Hodge, A. (2009). The Effect of Population Growth on Economic Growth: A Meta-Regression Analysis of the Macroeconomic Literature. *Population and Development Review*, 35(2), 221–248.

Heidelberg Institute for International Conflict Research (2022). *Conflict Barometer 2021*. Conflict Barometer No. 30.

Heider, B., Stroms, P., Koch, J., & Siedentop, S. (2020). Where do immigrants move in Germany? The role of international migration in regional disparities in population development. *Population, Space and Place*, 26(8), article e2363.

Heikkinen, S. (1997). *Labour and the market: workers, wages, and living standards in Finland, 1850–1913*. Helsinki: Finnish Academy of Science and Letters.

Heining, J., Jost, O., Rossen, A., Roth, D., & Weyh, A. (2021). *Regionale Arbeitsmarktprognose 2021/2022: Viele Regionen erreichen 2022 wieder Vorkrisenniveau*. IAB-Kurzbericht 21/2021.

Heinsohn, T., Lange, B., Vanella, P., Rodiah, I., Glöckner, S., Joachim, A., Becker, D., Brändle, T., Dhein, S., Ehehalt, S., Fries, M., Galante-Gottschalk, A., Jehnichen, S., Kolkmann, S., Kossow, A., Hellmich, M., Dötsch, J., & Krause, G. (2022). Infection and transmission risks of COVID-19 in schools and their contribution to population infections in Germany: A retrospective observational study using nationwide and regional health and education agency notification data. *PLoS Medicine*, 19(12), article e1003913.

Hellwagner, T., Söhnlein, D., & Weber, E. (2023). *Modeling Migration Dynamics in Stochastic Labor Supply Forecasting*. IAB-Discussion Paper 5/2023.

Hellwagner, T. & Weber, E. (2024). *Labor Market Adjustments to Population Decline: A Historical Macroeconomic Perspective, 1875–2019*. IAB-Discussion Paper 5/2024.

Henger, R. & Oberst, C. (2019a). *Alterung der Gesellschaft im Stadt-Land Vergleich*. IW-Kurzbericht 16/2019.

Henger, R. & Oberst, C. (2019b). *Immer mehr Menschen verlassen die Großstädte wegen Wohnungsknappheit*. IW-Kurzbericht 20/2019.

Herrendorf, B., Rogerson, R., & Valentinyi, A. (2014). Growth and Structural Transformation. In P. Aghion & S. Durlauf (Eds.), *Handbook of Economic Growth, Volume 2B* (pp. 855–941). London a.o.: Elsevier.

Hjerppe, R. (1989). *The Finnish economy 1860–1985: Growth and structural change*. Helsinki: Government Printing Centre.

HMD (2020). All statistics for HMD. University of California, Berkeley (USA), and Max Planck Institute for Demographic Research (Germany). Retrieved 08 July 2020 from www.mortality.org.

HMD (2023). All statistics for HMD. University of California, Berkeley (USA), and Max Planck Institute for Demographic Research (Germany). Retrieved 03 April 2023 from www.mortality.org.

Hobijn, B. (2024). Comment on '$u^* = \sqrt{uv}$: The Full-Employment Rate of Unemployment in the United States'. *Brookings Papers on Economic Activity*, 55(2), 408–419.

Hoffmann, W. G. (1965). *Das Wachstum der deutschen Wirtschaft seit der Mitte des 19. Jahrhunderts*. Berlin; Heidelberg: Springer.

Hohls, R. (1991). *Arbeit und Verdienst. Entwicklung und Struktur der Arbeitseinkommen im Deutschen Reich und in der Bundesrepublik*. Berlin: Dissertation, FU Berlin.

Holst, E. & Schupp, J. (2000). Hidden labour force in Germany. *DIW Weekly Report*, 9, 285–292.

Horn, J. (1965). A rationale and test for the number of factors in factor analysis. *Psychometrika*, 30, 179–185.

HSSO (2022a). Bruttoinlandsprodukt nach Verwendungsarten in Preisen von 1929 und nominal. Table Q.16a. Retrieved 04 August 2023 from https://hsso.ch/2012/q/16a.

HSSO (2022b). Erwerbstätige Ausländer (Total) nach Aufenthaltskategorien und Wirtschaftsklassen Ende August 1956–1972 und 1974–1987. Table F.17c. Retrieved 17 July 2022 from https://hsso.ch/2012/f/17c.

HSSO (2022c). Erwerbstätige, Wochen-, Jahresarbeitszeit 1890–2005. Wirtschaftsgeschichte der Schweiz im 20. Jahrhundert. Table F.29a. Retrieved 01 November 2021 from https://hsso.ch/2012/f/29a.

HSSO (2022d). Lebendgeborene nach Kantonen 1801–1866 und 1867–1995. Tables C.18 and C.19. Retrieved 23 March 2022 from https://hsso.ch/2012/c/18.

HSSO (2022e). Stadt Zürich: Stellensuchende Männer und Frauen, offene Stellen und Stellenbesetzungen 1901–1995. Table F.23a. Retrieved 17 July 2023 from https://hsso.ch/2012/f/23a.

HSSO (2022f). Stellensuchende und Arbeitslosenquote nach Geschlecht im Jahresmittel 1913–1995. Table F.18a. Retrieved 01 November 2021 from https://hsso.ch/2012/f/18a.

HSUS (2023). Historical Statistics of the United States, Millenial Edition. Retrieved 13 July 2023 from https://hsus.cambridge.org/HSUSWeb/HSUSEntryServlet.

Huberman, M. & Minns, C. (2007). The times they are not changin': Days and hours of work in old and new worlds, 1870–2000. *Explorations in Economic History*, 44(4), 538–567.

Hubmann, G., Jobst, C., & Maier, M. (2020). A new long-run consumer price index for Austria (1800–2018). *Monetary Policy & the Economy*, Q3/20, 61–88.

Humphries, J. & Sarasúa, C. (2012). Off the Record: Reconstructing Women's Labor Force Participation in the European Past. *Feminist Economics*, 18(4), 39–67.

Hyndman, R. (2017). R-package addb. Retrieved 13 June 2023 from https://github.com/robjhyndman/addb.

ILO (1952). *Yearbook of Labour Statistics*. Geneva: ILO.

ILO (1977a). *Labour Force Estimates and Projection. 1950-2000. Volume IV. Northern America, Europe, Oceania and USSR*. Geneva: ILO.

ILO (1977b). *Labour Force Estimates and Projection. 1950-2000. Volume V. World Summary*. Geneva: ILO.

ILO (2013). *Resolution concerning statistics of work, employment and labour underutilization*. Geneva: ILO.

ILO (2025). Definitions and metadata. Retrieved 23 December 2025 from https://weso-data.ilo.org/definitions-and-metadata/.

IMF (2021). IMF Investment and Capital Stock Dataset, 2021. Retrieved 21 July 2023 from https://data.imf.org.

Iwanow, I. & Gutting, R. (2020). Wanderungen als Herausforderung und zukunftsbestimmende Komponente kommunaler Prozesse. In P. Deschermeier, J. Fuchs, I. Iwanow, & C. B. Wilke (Eds.), *IAB-Bibliothek 372: Zur Relevanz von Bevölkerungsvorausberechnungen für Arbeitsmarkt-, Bildungs- und Regionalpolitik* (pp. 156–177). Bielefeld: wbv.

Jackman, R., Pissarides, C., & Savouri, S. (1990). Labour market policies and unemployment in the OECD. *Economic Policy*, 5(11), 449–490.

Jaimovich, N. & Siu, H. E. (2009). The Young, the Old, and the Restless: Demographics and Business Cycle Volatility. *American Economic Review*, 99(3), 804–826.

Jentsch, C. & Lunsford, K. (2022). Asymptotically Valid Bootstrap Inference for Proxy SVARs. *Journal of Business & Economic Statistics*, 40(4), 1876–1891.

Jolliffe, I. T. (2002). *Principal component analysis*. New York, NY: Springer.

Jones, C. I. (2022). The End of Economic Growth? Unintended Consequences of a Declining Population. *American Economic Review*, 112(11), 3489–3527.

Jones, C. I. & Romer, P. M. (2010). The New Kaldor Facts: Ideas, Institutions, Population, and Human Capital. *American Economic Journal: Macroeconomics*, 2(1), 224–245.

Jordà, O., Schularick, M., & Taylor, A. M. (2017). Macrofinancial History and the New Business Cycle Facts. *NBER macroeconomics annual*, 31(1), 213–263.

JSPS (2023). Long-Term Economic Statistics (LTES) database (Japan). Labor Force. Retrieved 10 August 2023 from https://d-infra.ier.hit-u.ac.jp/English/ltes/a000.html.

Kaiser, H. F. (1960). The application of electronic computers to factor analysis. *Educational and Psychological Measurement*, 20(1), 141–151.

Kajanovičová, V., Novotný, B., & Pospíšil, M. (2020). Ramsey model with non-constant population growth. *Mathematical Social Sciences*, 104, 40–46.

Kaldor, N. (1961). Capital Accumulation and Economic Growth. In F. A. Lutz & D. C. Hague (Eds.), *The Theory of Capital* (pp. 177–222). London; New York, NY: Palgrave Macmillan.

Kase, K. (2004). Unemployment Policy in Prewar Japan: How Progressive Was Japanese Social Policy? *Social Science Japan Journal*, 7(2), 199–221.

Kato, M. (2008). Hidden from View? The Measurement of Japanese Interwar Unemployment. *Annual Research Bulletin of Osaka Sangyo University*, 1, 77–103.

Keane, M. & Rogerson, R. (2012). Micro and Macro Labor Supply Elasticities: A Reassessment of Conventional Wisdom. *Journal of Economic Literature*, 50(2), 464–476.

Keilman, N., Dinh, P. Q., & Hetland, A. (2002). Why population forecasts should be probabilistic - illustrated by the case of Norway. *Demographic Research*, 6, 409–454.

Keyfitz, N. (1971). On the momentum of population growth. *Demography*, 8, 71–80.

Kindermann, F. & Püschel, V. (2024). *Women's Labor Supply Incentives and Old-Age Income Redistribution*. Working paper.

King, R. (2011). Geography and migration studies: Retrospect and prospect. *Population, Space and Place*, 18(2), 134–153.

King, R. & Skeldon, R. (2010). 'Mind the gap!' Integrating approaches to internal and international migration. *Journal of Ethnic and Migration Studies*, 36(10), 1619–1646.

K.K. Statistische Zentralkommission (1916). *3. Band. Berufsstatistik nach den Ergebnissen der Volkszählung vom 31. Dezember 1910*. Wien: Karl Gerold's Sohn.

Klinger, S. & Weber, E. (2016). Decomposing beveridge curve dynamics by correlated unobserved components. *Oxford Bulletin of Economics and Statistics*, 78(6), 877–894.

Klüsener, S., Grigoriev, P., Scholz, R., & Jdanov, D. (2018). Adjusting Inter-censal Population Estimates for Germany 1987–2011: Approaches and Impact on Demographic Indicators. *Comparative Population Studies*, 43, 31–64.

Koop, G., Pesaran, M. H., & Potter, S. M. (1996). Impulse response analysis in nonlinear multivariate models. *Journal of Econometrics*, 74(1), 119–147.

Kosche, E. & Bach, H. W. (1991). Beschäftigung, Arbeitslosigkeit und Arbeitsmarktpolitik in Deutschland seit Mitte des 19. Jahrhunderts: Ein Überblick. *Sozialer Fortschritt*, 40(5), 122–132.

Krantz, O. & Schön, L. (2007). *Swedish Historical National Accounts 1800–2000*. Lund studies in economic history 41.

Kröhnert, S. & Vollmer, S. (2012). Gender-specific migration from eastern to western Germany: Where have all the young women gone? *International Migration*, 50(5), 95–112.

Krüger, M. (2020). Siedlungsfokus-Wüstung. Umbau- und Rückbaustrategien am Beispiel von ländlichen Referenzkommunen. In P. Deschermeier, J. Fuchs, I. Iwanow, & C. B. Wilke (Eds.), *IAB-Bibliothek 372: Zur Relevanz von Bevölkerungsvorausberechnungen für Arbeitsmarkt-, Bildungs- und Regionalpolitik* (pp. 202–231). Bielefeld: wbv.

Kubis, A. & Schneider, L. (2020). Schätzung der Wanderungsströme von EU-Bürgern und EU-Bürgerinnen nach und aus Deutschland bis 2040. In P. Deschermeier, J. Fuchs, I. Iwanow, & C. B. Wilke (Eds.), *IAB-Bibliothek 372: Zur Relevanz von Bevölkerungsvorausberechnungen für Arbeitsmarkt-, Bildungs- und Regionalpolitik* (pp. 69–92). Bielefeld: wbv.

Kubis, A. & Schneider, L. (2024). *Zuwanderung und Arbeitsmarkt - eine Analyse für Deutschland und die Bundesländer*. Gütersloh: Bertelsmann Stiftung.

Kuczynski, J. (1962). *Die Geschichte der Lage der Arbeiter unter dem Kapitalismus. Bd. 3: 1871–1900*. Berlin: Akademie-Verlag.

Kuczynski, J. (1967). *Die Geschichte der Lage der Arbeiter unter dem Kapitalismus. Bd. 4: 1900–17/18*. Berlin: Akademie-Verlag.

Körner, T. & Marder-Puch, K. (2015). Der Mikrozensus im Vergleich mit anderen Arbeitsmarktstatistiken: Ergebnisunterschiede und Hintergründe seit 2011. *Wirtschaft und Statistik*, 4, 39–52.

Lee, E. S. (1966). A theory of migration. *Demography*, 3(1), 47–57.

Lee, G. & Parasnis, J. (2014). Discouraged workers in developed countries and added workers in developing countries? *Economic Modelling*, 41, 90–98.

Leibert, T. (2016). She leaves, he stays? Sex-selective migration in rural East Germany. *Journal of Rural Studies*, 43, 267–279.

Lianos, T. P., Pseiridis, A., & Tsounis, N. (2023). Declining population and GDP growth. *Humanities and Social Sciences Communications*, 10(1), article 725.

Lichtenberger, A., Heimberger, P., Arsenev, A., & Gökten, M. (2025). Full employment: A survey of theory, empirics and policies. *Kyklos*, 78, 1158–1184.

Lichter, A., Peichl, A., & Siegloch, S. (2015). The own-wage elasticity of labor demand: A meta-regression analysis. *European Economic Review*, 80, 94–119.

Lipps, O. & Betz, F. (2005). Stochastische Bevölkerungsprojektion für West- und Ostdeutschland. *Zeitschrift für Bevölkerungswissenschaft/Comparative Population Studies*, 30(1), 3–42.

Logan, J. R., Zhang, W., Stults, B. J., & Gardner, T. (2021). Improving estimates of neighborhood change with constant tract boundaries. *Applied Geography*, 132, article 102476.

Lomax, N., Wohland, P., Rees, P., & Norman, P. (2020). The impacts of international migration on the UK's ethnic populations. *Journal of Ethnic and Migration Studies*, 46(1), 177–199.

Long, C. (1953). Impact of Effective Demand on the Labor Supply. *American Economic Review*, 43(2), 458–467.

Long, C. (1958). *The Labor Force under Changing Income and Employment*. Princeton, NJ: Princeton University Press.

Lutz, W. (2021). *Advanced Introduction to Demography*. Cheltenham, UK; Northampton, MA, USA: Edward Elgar Publishing.

Lutz, W., Amran, G. A., Belanger, A., Conte, A., Gailey, N., Ghio, D., Grapsa, E., Jensen, K., Loichinger, E., Marois, G., Muttarak, R., Potančoková, M., Sabourin, P., & Stonawski, M. (2019). *Demographic scenarios for the EU*. Luxembourg: Publications Office of the European Union.

Lutz, W. & KC, S. (2011). Global human capital: Integrating education and population. *Science*, 333(6042), 587–592.

Lutz, W., Sanderson, W. C., & Scherbov, S. (1998). Expert-based probabilistic population projections. *Population and Development Review*, 24(Supplement: Frontiers of Population Forecasting), 139–155.

Lösch, A. (1936). *Bevölkerungswellen und Wechsellagen im Deutschen Reich von 1871 bis 1910*. Jena: Gustav-Fischer-Verlag.

Macunovich, D. J. (1999). The Fortunes of One's Birth: Relative Cohort Size and the Youth Labor Market in the United States. *Journal of Population Economics*, 12(2), 215–272.

Maddison, A. (1964). *Economic Growth in the West*. New York: Twentieth Century Fund.

Maddison, A. (1982). *Phases of capitalist development*. Oxford: Oxford University Press.

Maddison, A. (1994). *Standardised Estimates of Fixed Capital Stock: A Six Country Comparison*. Working paper.

Maestas, N., Mullen, K. J., & Powell, D. (2023). The Effect of Population Aging on Economic Growth, the Labor Force, and Productivity. *American Economic Journal: Macroeconomics*, 15(2), 306–332.

Malthus, T. R. (1798). *An Essay on the Principle of Population*. London: J. Johnson.

Maretzke, S., Hoymann, J., Schlömer, C., & Stelzer, A. (2021). *Raumordnungsprognose 2040*. BBSR-Analysen KOMPAKT 03/2021.

Marois, G., Bélanger, A., & Lutz, W. (2020). Population aging, migration, and productivity in Europe. *Proceedings of the National Academy of Sciences*, 117(14), 7690–7695.

Marois, G., Gietel-Basten, S., & Lutz, W. (2021). China's low fertility may not hinder future prosperity. *Proceedings of the National Academy of Sciences*, 118(40), article e2108900118.

Martin, D., Dorling, D., & Mitchell, R. (2002). Linking censuses through time: Problems and solutions. *Area*, 34(1), 82–91.

Martin, J. E. (1996). *Holding the Balance – A History of New Zealand's Department of Labour 1891–1995*. Christchurch: Canterbury University Press.

Martén, L., Hainmüller, J., & Hangartner, D. (2019). Ethnic networks can foster the economic integration of refugees. *Proceedings of the National Academy of Sciences*, 116(33), 16280–16285.

Maruani, M. & Meron, M. (2012). *Un siècle de travail des femmes en France*. Paris: La Découverte.

Mayda, A. M. (2010). International migration: A panel data analysis of the determinants of bilateral flows. *Journal of Population Economics*, 23, 1249–1274.

McCracken, M. & Ng, S. (2016). FRED-MD: A Monthly Database for Macroeconomic Research. *Journal of Business & Economic Statistics*, 34(4), 574–589.

Meinert, R. (1958). *Die Entwicklung der Arbeitszeit in der deutschen Industrie 1820–1956*. Münster: Dissertaion, Universität Münster.

Mertens, K. & Ravn, M. O. (2013). The Dynamic Effects of Personal and Corporate Income Tax Changes in the United States. *American Economic Review*, 103(4), 1212–1247.

Michaillat, P. & Saez, E. (2021). Beveridgean unemployment gap. *Journal of Public Economics Plus*, 2, article 100009.

Michaillat, P. & Saez, E. (2024a). *Beveridgean Phillips curve*. Working paper.

Michaillat, P. & Saez, E. (2024b). $u^* = \sqrt{uv}$: The Full-Employment Rate of Unemployment in the United States. *Brookings Papers on Economic Activity*, 55(2), 323–390.

Mitchell, B. R. (2013). *International Historical Statistics*. Basingstoke: Palgrave Macmillan.

Molinder, J. (2018). Swedish national unemployment rate according to available sources, 1911–2010, version 1.0, shlm database. Retrieved 18 December 2020 from https://jakobmolinderc om.wordpress.com/data/.

Mulliner, E., Riley, M., & Maliene, V. (2020). Older people's preferences for housing and environment characteristics. *Sustainability*, 12(14), article 5723.

NCHS (2023). Births and General Fertility Rates: United States. Retrieved 02 August 2023 from https://data.cdc.gov/NCHS/NCHS-Births-and-General-Fertility-Rates-United-Sta/e6fc-ccez/data.

Nickell, S., Nunziata, L., Ochel, W., & Quintini, G. (2003). The Beveridge curve, unemployment and wages in the OECD from the 1960s to the 1990s. In P. Aghion, R. Frydman, J. E. Stiglitz, & M. Woodford (Eds.), *Knowledge, Information, and Expectations in Modern Macroeconomics* (pp. 394–431). Princeton, NJ: Princeton University Press.

Norges Bank (2018). The gross domestic product for Norway. Retrieved 23 December 2020 from https://www.norges-bank.no/en/topics/Statistics/Historical-monetary-statistics.

Norman, P., Rees, P., & Boyle, P. (2003). Achieving data compatibility over space and time: Creating consistent geographical zones. *International Journal of Population Geography*, 9(5), 365–386.

NOS (1949). *Statistiske Oversikter 1948*. Oslo: Statistics Norway.

OECD (2005). Economic Outlook No. 77, January 2005. Retrieved 08 July 2020 from https://doi.org/10.1787/data-00089-en.

OECD (2016). Economic Outlook No. 100, November 2016. Retrieved 08 July 2020 from https://doi.org/10.1787/7fa317bf-en.

OECD (2018). Population dynamics and inclusiveness in regions: Regional population and changes over time. In OECD (Ed.), *OECD Regions and Cities at a Glance 2018* (pp. 68–73). Paris: OECD Publishing.

OECD (2019). Main Economic Indicators: Hourly Earnings: Manufacturing for Australia. Retrieved 15 January 2020 from https://doi.org/10.1787/data-00052-en.

OECD (2020). Main Economic Indicators: Consumer price indices (CPIs). Retrieved 27 March 2020 from https://doi.org/10.1787/data-00900-en.

OECD (2021). Average annual wages. Retrieved 28 March 2022 from https://stats.oecd.org/Index.aspx?DatasetCode=AV_AN_WAGE.

OECD (2022). Labour force participation rate. Retrieved 10 July 2022 from https://data.oecd.org/emp/labour-force-participation-rate.htm.

OECD (2022). *OECD Labour Force Statistics 2021.* Paris: OECD Publishing.

OECD (2022). Unemployment rate by age group. Retrieved 10 July 2022 from https://data.oecd.org/unemp/unemployment-rate-by-age-group.htm.

OECD (2024). Labour force participation rate. Retrieved 19 September 2024 from https://www.oecd.org/en/data/indicators/labour-force-participation-rate.html.

OECD (2024). *OECD Economic Outlook, Volume 2024 Issue 2.* Paris: OECD Publishing.

OECD (2025). Labour force participation rates of adults, by educational attainment, age group and gender. Retrieved 3 November 2025 from https://data-explorer.oecd.org/s/39j.

OECD (2025). *OECD Employment Outlook 2025: Can We Get Through the Demographic Crunch?* Paris: OECD Publishing.

Ortega, F. & Peri, G. (2013). The effect of income and immigration policies on international migration. *Migration Studies*, 1(1), 47–74.

Österholm, P. (2010). Unemployment and labour-force participation in Sweden. *Economics Letters*, 106(3), 205–208.

Parker, A. & Weber, E. (forth.). *The Nature of Labor Market Uncertainty.* IAB-Discussion Paper.

Pedersen, P. J., Pytlikova, M., & Smith, N. (2008). Selection and network effects—Migration flows into OECD countries 1990–2000. *European Economic Review*, 52(7), 1160–1186.

Pedroni, P. (1999). Critical Values for Cointegration Tests in Heterogeneous Panels with Multiple Regressors. *Oxford Bulletin of Economics and Statistics*, 61(S1), 653–670.

Peter, H., Tippel, C., & Steinführer, A. (2022). *Wohnstandortentscheidungen in einer wohnbiographischen Perspektive: Eine explorative Studie in ländlichen und großstädtischen Kontexten.* Thünen Report 93.

Petzina, D., Abelshauser, W., & Faust, A. (1978). *Sozialgeschichtliches Arbeitsbuch: Bd. III: Materialien zur Statistik des Deutschen Reiches 1914–1945.* München: Beck.

Pierenkemper, T. (1984). Die Vermarktung von Arbeitskraft in Deutschland. Begriffe, Tendenzen, Forschungsprobleme. In K. J. Bade (Ed.), *Auswanderer – Wanderarbeiter – Gastarbeiter* (pp. 139–178). Ostfildern: Scripta Manufacturae.

Pierenkemper, T. (1987). The standard of living and employment in germany, 1850–1980: An overview. *The Journal of European Economic History*, 16(1), 51–73.

Pilat, D. (2002). The Long-Term Performance of the Japanese Economy. In A. Maddison, D. S. Prasada, & W. Shepherd (Eds.), *The Asian Economies in the Twentieth Century* (pp. 180–225). Cheltenham, UK: Edward Elgar Publishing.

Piore, M. J. (1987). Historical Perspectives and the Interpretation of Unemployment. *Journal of Economic Literature*, 25(4), 1834–1850.

Pisarevskaya, A., Levy, N., Scholten, P., & Jansen, J. (2020). Mapping migration studies: An empirical analysis of the coming of age of a research field. *Migration Studies*, 8(3), 455–481.

Pissarides, C. (1985). Short-Run Equilibrium Dynamics of Unemployment, Vacancies and Real Wages. *American Economic Review*, 75(4), 676–690.

Prado, S. (2010). Nominal and real wages of manufacturing workers, 1860–2007. In R. Edvinsson, T. Jacobson, & D. Waldenström (Eds.), *Historical Monetary and Financial Statistics for Sweden, Volume I: Exchange rates, prices, and wages, 1277–2008* (pp. 479–527). Stockholm: Ekerlids Förlag.

Prenzel, P. (2021). Are old regions less attractive? Interregional labour migration in a context of population ageing. *Papers in Regional Science*, 100(6), 1429–1447.

Provenzano, S. (2017). The empirics of hidden labor force dynamics in Germany. *Jahrbücher für Nationalökonomie und Statistik (Journal of Economics and Statistics)*, 237(5), 373–406.

Rahlf, T. (2015). Zeitreihendatensatz für Deutschland, 1834–2012. Studiennummer 8603. GESIS Datenarchiv, histat. Köln. Retrieved 07 July 2020 from https://doi.org/10.4232/1.12202.

Ramey, V. A. & Francis, N. (2009). A Century of Work and Leisure. *American Economic Journal: Macroeconomics*, 1(2), 189–224.

Rankin, K. (1993). The New Zealand Workforce: 1950–2000. *New Zealand Journal of Industrial Relations*, 18(2), 214–235.

Rankin, K. (1994). Workforce and Employment Estimates: New Zealand 1921–1939. *Labour, Employment and Work in New Zealand*, 1994, 332–343.

Rayer, S. (2008). Population forecast errors: A primer for planners. *Journal of Planning Education and Research*, 27(4), 417–430.

Raymer, J., Bonaguidi, A., & Valentini, A. (2006). Describing and projecting the age and spatial structures of interregional migration in Italy. *Population, Space and Place*, 12(5), 371–388.

Raymer, J., de Beer, J., & van der Erf, R. (2011). Putting the pieces of the puzzle together: Age and sex-specific estimates of migration amongst countries in the EU/EFTA, 2002–2007. *European Journal of Population*, 27, 185–215.

RCISSS (2016). Long-Term Economic Statistics (LTES) Database. Retrieved 17 June 2020 from https://www.ier.hit-u.ac.jp/English/databases/ltes.html.

Rees, P., Wohland, P., Norman, P., & Lomax, N. (2015). *Sub-national projection methods for Scotland and Scottish areas: a review and recommendations*. Research report.

Reher, D. S. (2015). Baby booms, busts, and population ageing in the developed world. *Population Studies*, 69(sup1), S57–S68.

Reinhart, C. M. & Rogoff, K. S. (2014). Recovery from Financial Crises: Evidence from 100 Episodes. *American Economic Review*, 104(5), 50–55.

Reinhold, M. & Thomsen, S. L. (2015). Subnational population projections by age: An evaluation of combined forecast techniques. *Population Research and Policy Review*, 34(4), 593–613.

Rengers, M. (2004). Das international vereinbarte Labour-Force-Konzept. *Wirtschaft und Statistik*, 12/2004, 1369–1383.

Rengers, M., Bringmann, J., & Holst, E. (2017). Arbeitszeiten und Arbeitszeitwünsche: Unterschiede zwischen Mikrozensus und SOEP. *Wirtschaft und Statistik*, 4/2017, 11–43.

Rengers, M. & Fuchs, J. (2022). Stille Reserve in Deutschland: Gemeinsamkeiten und Unterschiede zweier Konzepte. *AStA Wirtschafts- und Sozialstatistisches Archiv*, 16, 189–230.

Riphahn, R. T. & Schrader, R. (2023). Reforms of an early retirement pathway in Germany and their labor market effects. *Journal of Pension Economics and Finance*, 22(3), 304–330.

Ritschl, A. (1985). On the stability of the steady state when population is decreasing. *Journal of Economics*, 45(2), 161–170.

Rōdō Undō Shiryō Iinkai (1959). *Nihon rōdō undō shiryō, 10th volume*. Tokyo: Rōdō Undō Shiryō Iinkai.

Rogers, A. & Castro, L. J. (1981). *Model migration schedules*. International Institute for Applied Systems Analysis, Research Report 81-30.

Rogers, A., Little, J., & Raymer, J. (2010). *The indirect estimation of migration: Methods for dealing with irregular, inadequate, and missing data*. Dordrecht: Springer Netherlands.

Romer, C. (1986a). Spurious Volatility in Historical Unemployment Data. *Journal of Political Economy*, 94(1), 1–37.

Romer, D. (2019). *Advanced Macroeconomics*. New York, NY: McGraw-Hill Education.

Romer, P. (1986b). Increasing Returns and Long-Run Growth. *Journal of Political Economy*, 94(5), 1002–1037.

Romer, P. (1990). Endogenous Technological Change. *Journal of Political Economy*, 98(5), 71–102.

Rosenbaum-Feldbrügge, M., Stawarz, N., & Sander, N. (2022). 30 Years of East-West Migration in Germany: A Synthesis of the Literature and Potential Directions for Future Research. *Comparative Population Studies*, 47, 185–210.

Rothenbacher, F. (2002). *The European Population, 1850–1945*. Basingstoke: Palgrave Macmillan.

Rowe, F., Bell, M., Bernard, A., Charles-Edwards, E., & Ueffing, P. (2019). Impact of Internal Migration on Population Redistribution in Europe: Urbanisation, Counterurbanisation or Spatial Equilibrium? *Comparative Population Studies*, 44, 201–234.

Saa, I. L., Novak, M., Morales, A. J., & Pentland, A. (2020). Looking for a better future: Modeling migrant mobility. *Applied Network Science*, 5, 70.

Sánchez-Romero, M., Schuster, P., & Prskawetz, A. (2024). Redistributive effects of pension reforms: who are the winners and losers? *Journal of Pension Economics & Finance*, 23(2), 294–320.

Sander, N. (2014). Internal migration in Germany, 1995–2010: New insights into east-west migration and re-urbanisation. *Comparative Population Studies*, 39(2), 217–246.

Sasaki, H. (2019). The Solow growth model with a CES production function and declining population. *Economics Bulletin*, 39(3), 1979–1988.

Sasaki, H. (2023). Growth with automation capital and declining population. *Economics Letters*, 222(C), article 110958.

Sasaki, H. & Hoshida, K. (2017). The effects of negative population growth: an analysis using a semiendogenous R&D growth model. *Macroeconomic Dynamics*, 21(7), 1545–1560.

Schmalz, D. (2025). The population growth discourse in the first decades of the United Nations: Interpretations of global economic inequality and the struggles for a just international legal order. *Leiden Journal of International Law*, 38(2), 131–147.

Schneemann, C., Bernardt, F., Kalinowski, M., Maier, T., Zika, G., & Wolter, M. I. (2025). *Auswirkungen des Strukturwandels auf die Arbeitsmarktregionen und Bundesländer in der langen Frist, Qualifikations- und Berufsprojektion bis 2040*. IAB-Forschungsbericht 03/2025.

Schröder, W. H. (1980). Die Entwicklung der Arbeitszeit im sekundären Sektor in Deutschland 1871–1913. *Technikgeschichte*, 47(3), 252–302.

Schulze, M.-S. (2005). *An Estimate of Imperial Austria's Gross Domestic Fixed Capital Stock, 1870–1913: Methods, Sources and Results*. LSE, Department of Economic History Working Papers No. 92/05.

Schön, L. & Krantz, O. (2012). *Swedish Historical National Accounts 1800–2000*. Lund papers in economic history 123.

Sensch, J. (2004). histat-Datenkompilation online: Geschichte der deutschen Bevölkerung seit 1815. Daten taken from GESIS Datenarchiv, Köln. Histat. Studiennummer 8171. Datenfile Version 1.0.0. Retrieved 01 September 2020 from https://search.gesis.org/research_data/ZA8171.

Sensch, J. (2012). histat-Datenkompilation online: Ausgewählte Zeitreihen aus Studien zur Entwicklung der Löhne/Gehälter und des Einkommens aus unselbständiger Arbeit in Deuschland, 1844–1990. GESIS Datenarchiv, Köln. Histat. Studiennummer 8177. Datenfile Version 2.0.0. Retrieved 01 September 2020 from https://search.gesis.org/research_data/ZA8177.

Sensch, J. (2014). histat-datenkompilation online: Arbeitslosigkeit von 1887 bis 2010 im internationalen vergleich. gesis datenarchiv, köln. histat. sudiennummer 8576. datenfile version 1.1.0. Retrieved 01 September 2020 from https://search.gesis.org/research_data/ZA8576.

Sensch, J. (2015). histat-Datenkompilation online: Zur Entwicklung der Arbeitszeit in Deutschland von der Industrialisierung bis zur Gegenwart. GESIS Datenarchiv, Köln, ZA8503. Datafile version 1.0.0. Retrieved 31 May 2022 from https://search.gesis.org/research_data/ZA8503.

Sensch, J. (2016). histat-Datenkompilation online: Entwicklung der Arbeitslosigkeit in Deutschland 1887–2000. GESIS Datenarchiv, Köln. Histat. Studiennummer 8218. Retrieved 01 September 2020 from https://search.gesis.org/research_data/ZA8218.

Sharma, A. & Das, M. (2018). Migrant networks in the urban labour market: Evidence from India. *The Journal of Development Studies*, 54(9), 1593–1611.

Shimer, R. (2001). The Impact of Young Workers on the Aggregate Labor Market. *The Quarterly Journal of Economics*, 116(3), 969–1007.

Shryock, H. S. & Siegel, J. S. (1976). *The methods and materials of demography*. New York, NY; London: Academic Press.

Shumway, R. H. & Stoffer, D. S. (2017). *Time series analysis and its applications: With R examples*. Springer International Publishing.

Siedentop, S., Junesch, R., Klein, M., Krumm, R., & Kleimann, R. (2014). *Wanderungsmotive im Ländlichen Raum*. Research report.

Simpson, N. B. (2022). Demographic and economic determinants of migration. *IZA World of Labor*, 2022, article 373.

Sims, C., Stock, J., & Watson, M. (1990). Inference in Linear Time Series Models with Some Unit Roots. *Econometrica*, 58(1), 113–144.

Siskova, M., Kuhn, M., Prettner, K., & Prskawetz, A. (2023). Does human capital compensate for population decline? *The Journal of the Economics of Ageing*, 26, article 100469.

Skirbekk, V., Prommer, I., KC, S., Terama, E., & Wilson, C. (2007). *PLUREL Report D1.2.1, Module 1: Driving forces and global trends (June 2007): Report on methods for demographic projections at multiple levels of aggregation*. Research report.

Smith, L. (2009). *The Australian Demographic Data Bank, 1901–2003: Populations [Computer File]*. Canberra: Australian Social Science Data Archive, The Australian National University.

Smits, J.-P., Horlings, E., & van Zanden, J. L. (2000). *Dutch GNP and its Components, 1800–1913*. Groningen: Groningen Growth and Development Centre.

Smolny, W. & Kirbach, M. (2011). Wage differentials between East and West Germany: Are they related to the location or to the people? *Applied Economics Letters*, 18(9), 873–879.

Sobotka, T., Skirbekk, V., & Philipov, D. (2011). Economic Recession and Fertility in the Developed World. *Population and Development Review*, 37(2), 267–306.

Sommariva, A. & Tullio, G. (1987). *German Macroeconomic History, 1880–1979: A Study of the Effects of Economic Policy on Inflation, Currency Depreciation and Growth*. London: Palgrave Macmillan.

SSB (1945). *Statistisk-økonomisk utsyn over krigsarene*. Oslo: Statistisk Sentralbyrå.

SSB (1950). *Økonomisk Utsyn overaret 1949*. Oslo: Statistisk Sentralbyrå.

SSB (2020). Sysselsatte personer etter nearing 1900–1969. 1000. Retrieved 01 November 2020 from https://www.ssb.no/.

Statistics Finland (2020). Population 31.12. by Year, Sex, Age and Information. Retrieved 18 January 2021 from https://pxdata.stat.fi.

Statistics Finland (2023). Live births by sex, 1751–2022. Table 12dj. Retrieved 13 July 2023 from https://pxdata.stat.fi.

Statistics Japan (2021). Population by Age (Single Year) and Sex (as of October 1 of Each Year) – Total population (from 1920 to 2000). Retrieved 15 August 2023 from www.e-stat.go.jp.

Statistics New Zealand (2002). *INFOS 3.0*. Wellington.

Statistische Ämter des Bundes und der Länder (2021). Zu- und Fortzüge (über Kreisgrenzen) nach Geschlecht und Nationalität – Jahressumme – regionale Tiefe: Kreise und krfr. Städte. Retrieved 17 December 2021 from https://www.regionalstatistik.de/.

Statistische Ämter des Bundes und der Länder (2022). Zu- und Fortzüge (über Kreisgrenzen) nach Geschlecht und Altersgruppen - Jahressumme - regionale Tiefe: Kreise und krfr. Städte. Retrieved 06 August 2022 from https://www.regionalstatistik.de/.

Steinicke, E., Čede, P., & Löffler, R. (2012). In-migration as a new process in demographic problem areas of the Alps. Ghost towns vs. amenity settlements in the alpine border area between Italy and Slovenia. *Erdkunde*, 66(4), 329–334.

Stock, J. & Watson, M. (2018). Identification and Estimation of Dynamic Causal Effects in Macroeconomics Using External Instruments. *The Economic Journal*, 128(610), 917–948.

Storesletten, K. (2000). Sustaining Fiscal Policy through Immigration. *Journal of Political Economy*, 108(2), 300–323.

Strulik, H. (2024). Long-run economic growth despite population decline. *Journal of Economic Dynamics and Control*, 168, 104943.

SVR (2024). *Frühjahrsgutachten 2024*. Wiesbaden.

SVR (2025). Business cycles of the german economy. Retrieved 22 January 2026 from https://www.sachverstaendigenrat-wirtschaft.de/en/topics/business-cycles-and-growth/konjunkturzyklus-datierung.html.

Sánchez-Barricarte, J. J. (2018). Measuring and explaining the baby boom in the developed world in the mid-20th century. *Demographic Research*, 38, 1189–1240.

Tiainen, P. (1994). *Taloudellisen kasvun tekijät Suomessa: työvoiman, pääoman ja kokonaistuottavuuden osuus vuosina 1900–90*. Helsinki: Dissertation, Finland.

Umemura, M. (1962). An analysis of employment structure in japan. *Hitotsubashi Journal of Economics*, 2(2), 16–29.

Umemura, M., Akasaka, K., Minami, R., Takamatsu, N., Arai, K., & Ito, S. (1988). *Rōdōryoku (Manpower)*. Tokyo: Tōyō Keizai Shinpōsha.

UN (1951). *Statistical Yearbook 1951, Third Issue*. New York: UN.

UN (2019). World Population Prospects 2019. Retrieved 20 May 2020 from https://population.un.org/wpp/.

UN (2022). *World Population Prospects 2022: Methodology of the United Nations population estimates and projections*. United Nations, Department of Economic and Social Affairs, Population Division: UN DESA/POP/2022/TR/NO. 4.

UN (2024). World Population Prospects 2024. Retrieved 01 May 2026 from https://population.un.org/wpp/.

UNHCR (2020). *Mid-year trends report 2020*. Report.

UNHCR (2022). *Ukraine situation*. Flash Update 26.

U.S. Bureau of the Census (1883). *Volume 1. Statistics of the Population of the United States*. Washington, D.C.: Government Printing Office.

U.S. Bureau of the Census (1895). *Volume 1. Report on Population of the United States*. Washington, D.C.: Government Printing Office.

U.S. Bureau of the Census (1975). *Historical Statistics of the United States: Colonial Times to 1970, Bicentennial Edition, Part 1*. Washington D.C.: Government Printing Office.

U.S. Bureau of the Census (2000). National intercensal tables: 1900–1990. Retrieved 14 July 2020 from https://www.census.gov/data/tables/time-series/demo/popest/pre-1980-national.html.

Van Hear, N., Bakewell, O., & Long, K. (2018). Push-pull plus: Reconsidering the drivers of migration. *Journal of Ethnic and Migration Studies*, 44(6), 927–944.

van Leeuwen, B. (2007). *Human Capital and Economic Growth in India, Indonesia, and Japan: A quantitative analysis, 1890–2000*. Utrecht: Dissertation.

van Meerten, M. (2003). *Capital formation in Belgium, 1900–1945*. Leuven: Leuven University Press.

Van Mol, C. & de Valk, H. (2016). Migration and immigrants in Europe: A historical and demographic perspective. In B. Garcés-Mascareñas & R. Penninx (Eds.), *Integration Processes and Policies in Europe* (pp. 31–55). Cham, CH: Springer.

Vanella, P. (2018). Stochastic forecasting of demographic components based on principal component. *Athens Journal of Sciences*, 5(3), 223–245.

Vanella, P. & Deschermeier, P. (2018). A stochastic forecasting model of international migration in Germany. In O. Kapella, N. F. Schneider, & H. Rost (Eds.), *Familie – Bildung – Migration. Familienforschung im Spannungsfeld zwischen Wissenschaft, Politik und Praxis. Tagungsband zum 5. Europäischen Fachkongress Familienforschung* (pp. 261–280). Opladen; Berlin; Toronto: Verlag Barbara Budrich.

Vanella, P. & Deschermeier, P. (2019). A principal component simulation of age-specific fertility – impacts of family and social policy on reproductive behavior in Germany. *Population Review: A Peer-Reviewed Journal of Sociological Demography*, 58(1), 78–109.

Vanella, P. & Deschermeier, P. (2020). A probabilistic cohort-component model for population forecasting – the case of Germany. *Journal of Population Ageing*, 13(4), 513–545.

Vanella, P., Deschermeier, P., & Wilke, C. B. (2020a). An overview of population projections—Methodological concepts, international data availability, and use cases. *Forecasting*, 2(3), 346–363.

Vanella, P., Hellwagner, T., & Deschermeier, P. (2022). Past and Future Trends in Refugee Migration on the Regional Level in Germany – An Analysis and Projection of Labor Market Effects. *Comparative Population Studies*, 47, 443–484.

Vanella, P., Hellwagner, T., & Deschermeier, P. (2023). Parsimonious stochastic forecasting of international and internal migration on the NUTS-3 level – an outlook of regional depopulation trends in Germany. *Vienna Yearbook of Population Research*, 21, 361–415.

Vanella, P., Heß, M., & Wilke, C. B. (2020b). A probabilistic projection of beneficiaries of long-term care insurance in Germany by severity of disability. *Quality & Quantity: International Journal of Methodology*, 54(3), 943–974.

Vernon, J. R. (1994). Unemployment rates in postbellum America: 1869–1899. *Journal of Macroeconomics*, 16(4), 701–714.

Villa, P. (1993). *Une analyse macroéconomique de la France au XXe siècle*. Paris: CNRS éditions.

Voigtländer, M. & Sagner, P. (2020). *Entwicklung von Löhnen und Mieten - dreigeteiltes Deutschland*. IW-Kurzbericht 4/2020.

Voigtländer, N. & Voth, H.-J. (2013). The Three Horsemen of Riches: Plague, War, and Urbanization in Early Modern Europe. *The Review of Economic Studies*, 80(2), 774–811.

Vollrath, D. (2024). The Elasticity of Aggregate Output with Respect to Capital and Labor. *American Economic Journal: Macroeconomics*, 16(4), 470–504.

Walwei, U. (2024). *Older workers in Germany: Employment potentials in international comparison*. IAB-Forschungsbericht 14/2024en.

Wanger, S., Hartl, T., & Zimmert, F. (2019). *Revision der IAB-Arbeitszeitrechnung 2019*. IAB-Forschungsbericht 07/2019.

Weber, E. (2014). *Das Ziel der Vollbeschäftigung in Deutschland: Fern, aber erreichbar*. IAB-Kurzbericht 15/2014.

Weber, E. (2026). The dovish turnaround: Germany's social benefit reform and job findings. *Journal of Policy Analysis and Management*, 45(1), article e22648.

Weber, E. & Weigand, R. (2018). Identifying macroeconomic effects of refugee migration to Germany. *Economics Bulletin*, 38(2), 852–862.

Weir, D. R. (1992). A Century of U.S. Unemployment, 1890–1990: Revised Estimates and Evidence for Stabilization. *Research in Economic History*, 14, 301–346.

WIFO (1958). Löhne, Gehälter und Masseneinkommen in Österreich 1950–1957. *Monatsberichte des Österreichischen Institutes für Wirtschaftsforschung*, XXXI. Jahrgang, Beilage Nr. 54.

WIFO (1965). Österreichs Volkseinkommen 1913 bis 1963. *Monatsberichte des Österreichischen Institutes für Wirtschaftsforschung*, 14. Sonderheft.

Williamson, J. G. (1995). The evolution of global labor markets since 1830: Background evidence and hypotheses. *Explorations in Economic History*, 32(2), 141–196.

Wilson, T. (2015a). New evaluations of simple models for small area population forecasts. *Population, Space and Place*, 21(4), 335–353.

Wilson, T. (2015b). Short-term forecast error of Australian local government area population projections. *Australasian Journal of Regional Studies*, 21(2), 253–275.

Wilson, T. & Bell, M. (2004). Comparative empirical evaluations of internal migration models in subnational population projections. *Journal of Population Research*, 21(2), 127–160.

Wilson, T., Grossman, I., Alexander, M., Rees, P., & Temple, J. (2021). Methods for small area population forecasts: State-of-the-art and research needs. *Population Research and Policy Review*, 41(3), 865–898.

Withers, G., Endres, T., & Perry, L. (1985). *Australian Historical Statistics: Labour Statistics*. Source Papers in Economic History 7.

World Bank (2025). Patent applications, residents. Retrieved 3 November 2025 from https://data.worldbank.org/indicator/IP.PAT.RESD.

Woytinsky, W. (1940). *Additional Workers and the Volume of Unemployment in the Depression*. Washington, DC: Social Science Research Council.

Xiao, Y., Amaglobeli, D., & Matsumoto, R. (2021). *IMF Investment and Capital Stock Dataset (ICSD) 2021: Manual & FAQ - Estimating Public, Private, and PPP Capital Stocks*. Companion Manual & FAQ.

Young, A. (2005). The Gift of the Dying: The Tragedy of AIDS and the Welfare of Future African Generations. *The Quarterly Journal of Economics*, 120(2), 423–466.

Zhang, J. L. & Bryant, J. (2020). Bayesian Disaggregated Forecasts: Internal Migration in Iceland. In S. Mazzuco & N. Keilman (Eds.), *Developments in Demographic Forecasting* (pp.

193–215). Cham, CH: Springer.

Zika, G., Kalinowski, M., Krinitz, J., Maier, T., Mönnig, A., Schneemann, C., Schroer, J. P., Wolter, M. I., & Zenk, J. (2025). *Fachkräftemonitoring für das BMAS - Mittelfristprognose bis 2029*. Forschungsbericht / Bundesministerium für Arbeit und Soziales 670.

Zimmermann, K. F. (1991). Ageing and the Labor Market: Age Structure, Cohort Size and Unemployment. *Journal of Population Economics*, 4(3), 177–200.

Zwick, W. & Velicer, W. (1986). Comparison of five rules for determining the number of components to retain. *Psychological Bulletin*, 99(3), 432–442.